Dynamics of Globular Clusters and Spiral Galaxies

Von der Universität Bayreuth
zur Erlangung des Grades eines
Doktors der Naturwissenschaften (Dr. rer. nat.)
genehmigte Abhandlung

von

Joachim Frenkler
geboren in Selb

1. Gutachter: Prof. Dr. Gerhard Rein
2. Gutachter: Prof. Dr. Håkan Andreasson

Tag der Einreichung: 08.08.2022
Tag des Kollogiums: 04.11.2022

Abstract

In Part I of this thesis we study the Vlasov-QUMOND system. This non-linear system of PDEs describes the time evolution of globular clusters in the context of the MOND theory. This theory proposes a modification of Newton's law of gravity that could be a solution for the missing mass problem in astrophysics. We use the QUMOND formulation of the MOND theory and develope a robust, mathematical fundament for this theory. We examine weak solutions of the initial value problem of the Vlasov-QUMOND system, prove conservation of energy for these solutions and prove the stability of a large class of stationary solutions.

Part II is devoted to the study of spiral galaxies. We develope a new technique to construct models for spiral galaxies with realistic and self-consistent dynamics. Using this technique we construct a flat, axisymmetric model for the Milky Way. We analyse the stability of this model numerically and describe two instabilities that can be active in our model. The first instability shows up as an exponential growth of the forces in tangential direction and is responsible for the formation of large scale spiral structures, which are very similar to the spiral structure of the real galaxy. The second instability is the Jeans instability, which has a disruptive nature. We discuss the implications these two instabilities have for the real galaxy and for the missing mass problem in astrophysics.

Zusammenfassung

In Teil I dieser Arbeit studieren wir das Vlasov-QUMOND-System. Dieses nichtlineare System von PDEs beschreibt die zeitlich Entwicklung von Kugelsternhaufen im Kontext der MOND-Theorie. Diese Theorie schlägt eine Modifizierung von Newtons Gravitationsgesetz vor, die eine mögliche Lösung für das Problem der fehlenden Massen in der Astrophysik ist. Wir benutzen die QUMOND Formulierung der MOND Theorie und entwickeln ein solides, mathematisches Fundament für diese Theorie. Wir studieren schwache Lösung des Anfangswertproblems des Vlasov-QUMOND-Systems, beweisen Energieerhaltung für diese Lösungen und beweisen die Stabilität einer großen Klasse von stationären Lösungen.

Teil II widmet sich dem Studium von Spiralgalaxien. Wir entwicklen eine neue Technik um Modelle für Spiralgalaxien zu konstruieren, in denen die Dynamiken sowohl realistisch als auch selbst-konsistent sind. Wir benutzen diese Technik und konstruieren ein flaches, axialsymmetrisches Modell für die Milchstraße. Wir analysieren die Stabilität diese Modells numerisch und beschreiben zwei Instabilitäten, die in unserem Modell aktiv sein können. Die erste Instabilität zeigt sich als ein exponentielles Wachstum der Kräfte in tangentialer Richtung und ist verantwortlich für die Bildung großflächiger Spiralstrukturen, die den Spiralstrukturen der realen Galaxie sehr ähnlich sind. Die zweite Instabilität ist die Jeans Instabilität, die eine zerstörerische Natur hat. Wir diskutieren die Implikationen, die diese beiden Instabilitäten für die reale Galaxie und für das Problem der fehlenden Massen in der Astrophysik haben.

Contents

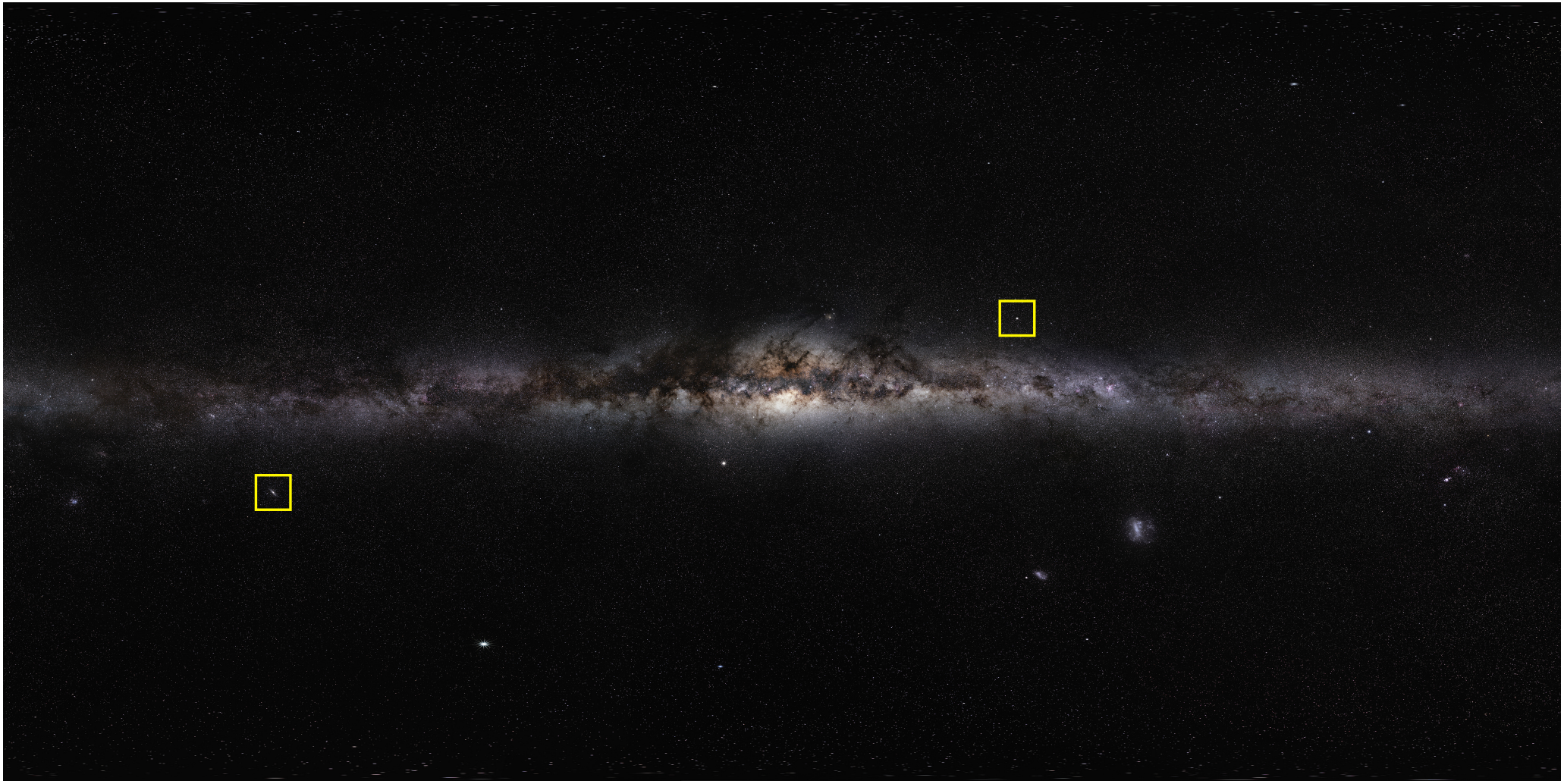

Figure 1: This panoramic image shows the entire night sky around the sun like we could see it, if we turned off all electric lighting for a moment. Prominent from left to right stretches the band of the Milky Way - the disc like, spiral galaxy we are living in. Due to our position inside the disc the Milky Way appears in this image as a horizontal line. The disc is made up of stars and gas. In the centre we see the luminous bulge that dominates the Milky Way's central parts. Left below the Milky Way's band we find the Andromeda galaxy (Figure 2) and right above the globular cluster Omega Centauri (Figure 3). Both are marked with a yellow square. **Credit:** ESO/S. Brunier

Figure 2: The Andromeda galaxy is our nearest large neighbour. Like the Milky Way it is a disc like, spiral galaxy. Its structure is similar to the Milky Way's. **Credit:** 2002 R. Gendler, Photo by R. Gendler

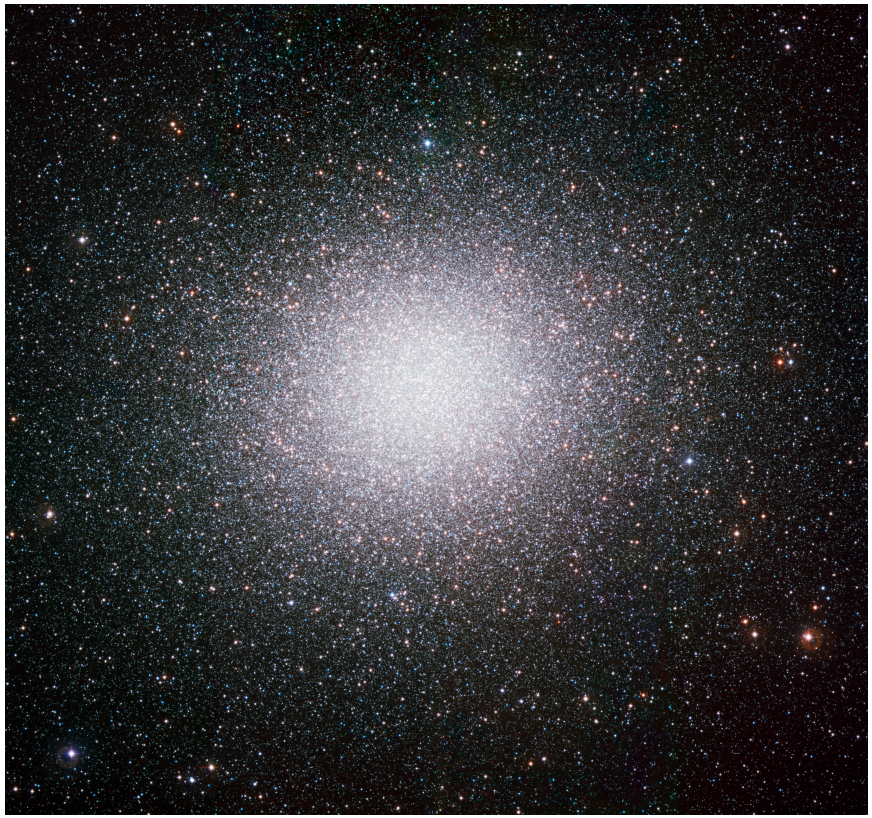

Figure 3: Omage Centauri is a globular cluster. It is an almost spherically symmetric, dense huddle of several Million stars that are bound together by their own gravity. There are about 150 globular clusters that belong to the Milky Way. **Credit:** ESO

1 Introduction

1.1 Globular clusters

Right above the Milky Way's band in Figure 1 we find the globular Omega Centauri (Figure 3). There are about 150 globular clusters that belong to the Milky Way. Globular clusters are almost spherically symmetric, dense huddles of stars. Therefore their pictorial German name is "Kugelsternhaufen". In Part I of this thesis we study the Vlasov-QUMOND system. This a non-linear system of PDEs that describes the dynamical evolution of globular clusters in the context of the MOND-Theory. This theory was proposed by Milgrom in 1983. The acronym MOND stands for MOdified Newtonian Dynamics. Our motivation is a mathematical one: We examine solutions to the initial value problem, conservation of energy and stability of stationary solutions.

There are two main mathematical problems that one has to deal with in the Vlasov-QUMOND system. First a square root enters the first derivative of the gravitational potential. Therefore the second derivatives of this potential are not well behaved and do not provide a good control for time dependent solutions. Second the potential energy in MOND is not finite. One can only study energy differences. It is difficult to control these differences efficiently, but this is necessary when we prove stability of stationary solutions.

In Part I of this thesis we prove that spherically symmetric, weak solutions to the initial value problem have a Lagrangian structure, despite the difficulties with the second derivates of the gravitational potential. We prove conservation of energy for Lagrangian solutions and we prove that a large class of stationary solutions is stable against spherically symmetric perturbations.

1.2 Spiral Galaxies

The band of the Milky Way stretches prominent from left to right in Figure 1. The Milky Way is the disc-like, spiral galaxy in which we are living. Due to our position inside the disc, the Milky Way appears as a horizontal line in Figure 1. Countless stars and nebulae make the Milky Way glow. Left below the Milky Way's band we see the Andromeda galaxy (Figure 2). Like the Milky Way it is a disc like, spiral galaxy and its structure is similar to the Milky Way's. Part II of this thesis is devoted to the study of spiral galaxies. Our motivation is both a mathematical and a physical one: How can we construct good dynamical models for spiral galaxies and which implications does the structure and stability of these models have for real galaxies.

Constructing a good, dynamical model for a spiral galaxy is a challenging, mathematical task. We want to achieve three points: First, like in the real galaxy all mass should be on almost circular orbits. Second, we want that the dynamics in our model are self-consistent. There the 'almost' makes things difficult; how to implement it in a self-consistent model? Third, we search for a reasonable stable model. Therefore we cannot ignore the 'almost' because without it the model becomes severely unstable.

In Part II of this thesis we develop an algorithm that allows us to construct a galaxy model that succeeds in all three aspects. We use this technique to construct a model for the Milky Way. We analyse this model and address two interesting questions from astrophysics that are still unresolved: How do the spiral arms in spiral galaxies form and why is the velocity dispersion in all spiral galaxies higher than one would expect from thermal considerations?

1.3 The missing mass problem

The underlying motivation for both parts of this thesis is the missing mass problem in astrophysics: It became apparent that astrophysics faced (and still faces) a problem when Rubin et al. (1980) and Bosma (1981) managed for the first time to measure the distribution and dynamics of atomic hydrogen (HI) in the outer parts of spiral galaxies. In spiral galaxies most mass is moving on almost circular orbits around the galactic centre. Originally they expected that at large radii r the circular velocity curve $v_c(r)$, i.e., the velocity with which the mass is rotating around the galactic centre, would show a Keplerian falloff $v_c(r) \propto r^{-1/2}$. But what they observed were almost flat circular velocity curves $v_c(r) \approx constant$. We describe this conflict and three possible solutions to it at the example of the Milky Way:

Based on observational data Binney & Tremaine (2008) constructed a model for the Milky Way consisting of a bulge, a stellar disc[1] and a gaseous disc. In Figure 5 we calculate the circular velocity curve for this model and compared it to the Milky Way's observed circular velocity curve (Eilers et al.,

[1] Binney & Tremaine (2008) included two stellar discs in their model. But these discs have similar properties and we consider only one disc with averaged parameters.

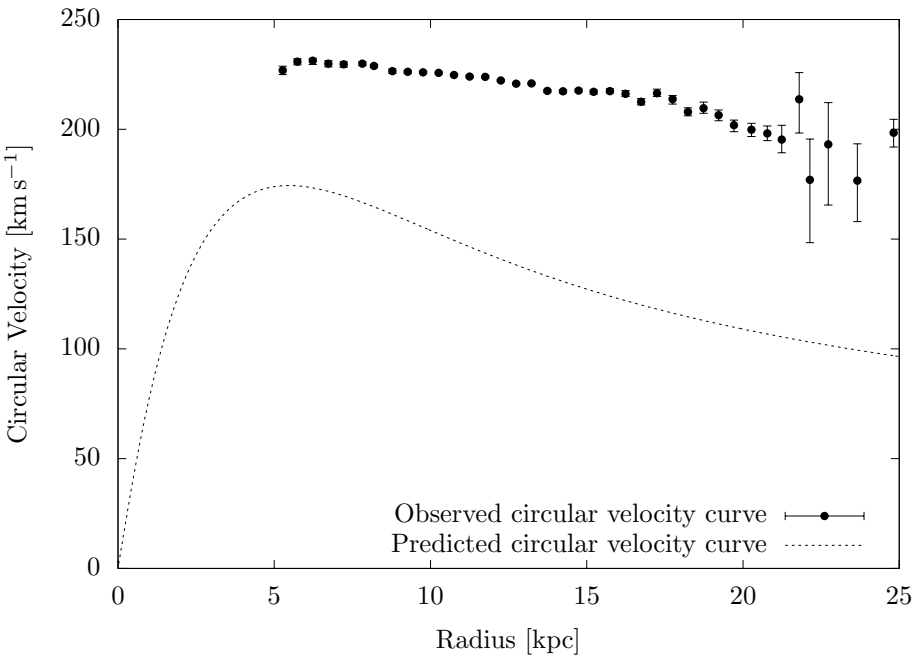

Figure 4: The circular velocity curve of the Milky Way measured by Eilers et al. (2019) (thick dots). We compare this curve with the predicted circular velocity curve that belongs to the stars and gases in Model I in Binney & Tremaine (2008) (dashed line). There is a large gap between the prediction from the model and the observation. This is a typical example for the missing mass problem.

2019). There is a large discrepancy between the predicted circular velocity curve from the model and the observed curve. Hence there is too few mass observed to explain the Milky Way's circular velocity curve using Newton's law of gravity. This is a typical example for the missing mass problem.

To resolve this problem Binney & Tremaine assume that the Milky Way is embedded in a large, almost spherically symmetric halo of non-baryonic, dark matter. This assumption is made by most astrophysicists nowadays. With the aid of this halo their model describes the Milky Way's circular velocity curve much better (Figure 5). There is still a gap between the observation and the prediction from the model, but this should not surprise because the available observational data concerning the Milky Way's circular velocity curve has largely improved within the last couple of years. Binney & Tremaine worked with older, less accurate data.

By assuming that there exists non-baryonic, dark matter many problematic observations in astrophysics can be explained very well and so most astrophysicists are content with this assumption. But recent measurements of the Hubble constant are in strong conflict with predictions from the standard model of cosmology, the ΛCDM model, where dark matter plays an important role. Nobel laureate Adam Riess comments on this new conflict: "We just need to follow the evidence. If our theories are incorrect, than so be it. It may be the case that the universe is more clever than we are now. And a better idea will come along later." (Deutscher Rundfunk, 2021). It is thus reasonable to look also for alternatives to the dark matter hypothesis that can provide solutions to the missing mass problem – and the present thesis will focus on these alternatives.

Another possible explanation for the missing mass problem was proposed by Milgrom (1983) and is called MOdified Newtonian Dynamics, in short MOND. Milgrom postulates that for small forces Newton's law of gravity must be modified. If a force is small, than according to his theory the real force would actually be proportional to the square root of the Newtonian force. This theory very effectively explains the circular velocity curves of many spiral galaxies (Gentile et al., 2011). Also if we simply take the baryonic model for the Milky Way from above and modify the circular velocity curve according to the MOND theory, observation and prediction match together reasonable well without any further adjustment (Figure 5).

A third possible way to explain the circular velocity curves of spiral galaxies was first noticed by Bosma (1981) and elaborated, e.g., in more detail by Hessman & Ziebart (2011). Bosma noticed that by scaling the densities of the stars and the gas he could explain his observed circular velocity curves. This

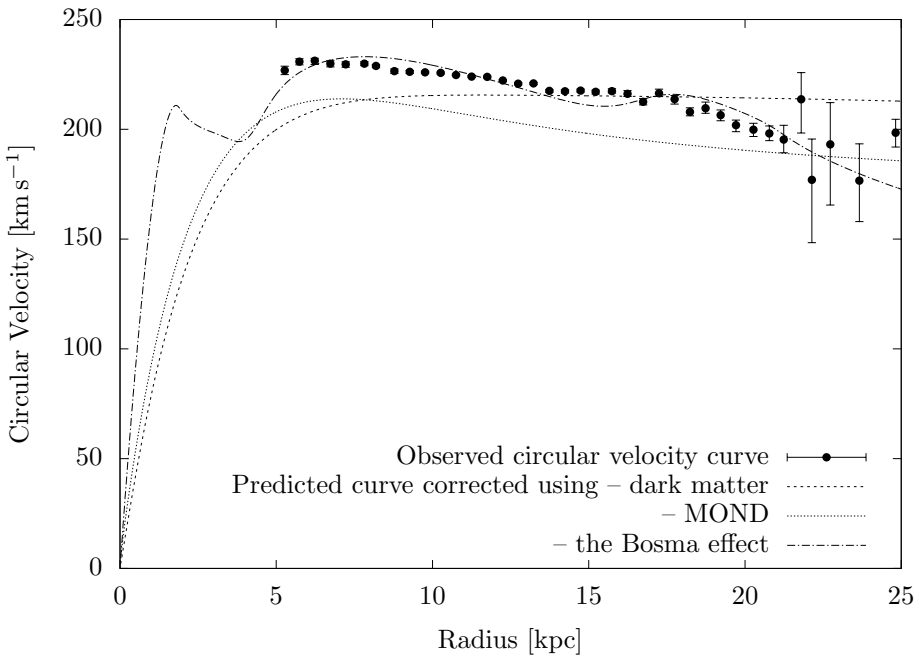

Figure 5: The thick dots mark again the Milky Way's circular velocity curve measured by Eilers et al. (2019). Further the circular velocity curves of three possible solutions to the missing mass problem in the Milky Way are presented. First: Model I in Binney & Tremaine (2008) uses non-baryonic, dark matter (dashed curve). Second: We corrected the predicted circular velocity curve from Figure 4 using MOND (dotted line). Third: We made use of the Bosma effect and scaled the baryonic components of Model II in Binney & Tremaine (2008) by factors between three and five (dashed dotted line); compare Sections 9.1 and 9.2.

phenomenon is called the Bosma effect. Making use of the Bosma effect Hessman & Ziebart managed to explain the circular velocity curves of many spiral galaxies very well. They interpret their scaled densities as proxies for baryonic mass components that reside in the disc but that have not been found yet. In Part II we construct a dynamical model for the Milky Way that explains the Milky Way's circular velocity curve by using the Bosma effect. The corresponding circular velocity curve is also shown in Figure 5.

Part I: The Vlasov-QUMOND System (VQMS)

"Since [globular clusters] are some of the simplest-looking structures in the Universe, [they] also provide a useful test-bed for theories of stellar dynamics: if we cannot explain the properties of these objects, what hope do we have of understanding any of the more complex structures in the Cosmos?" (Binney & Merrifield, 1998, §6.1).

In Part I of this thesis we undertake a rigorous, mathematical study of the equations that govern the evolution of globular clusters in the context of the MOND-theory.

2 Introduction Part I

Omega Centauri (Figure 3) is the most luminous of the Milky Way's about 150 globular clusters (Binney & Merrifield, 1998, §6.1). A typical globular cluster is approximately spherically symmetric, contains about 10^4 to 10^6 stars but no gas, dust or young stars. The stars in a globular cluster interact only gravitationally (Binney & Tremaine, 2008, §1.1.4). Since it is not practical to follow the trajectory of each single star, we describe a globular cluster by a distribution function $f = f(t, x, v)$ that evolves on position-velocity space; $t \geq 0$ is the time, $x \in \mathbb{R}^3$ is the position and $v \in \mathbb{R}^3$ is the velocity. The density $\rho_f(t, x)$ on position space that corresponds to f is given by integrating f over the velocities

$$\rho_f(t, x) = \int f(t, x, v)\, \mathrm{d}v. \tag{2.1}$$

The Newtonian gravitational potential $U_f^N(t, x)$ that is created by ρ_f is given by

$$U_f^N(t, x) = -G \int \frac{\rho_f(t, y)}{|x - y|}\, \mathrm{d}y \tag{2.2}$$

provided the convolution integral exists[2]. We want to study the evolution of a globular cluster not in Newtonian but in Mondian physics. Thus we have to transform the Newtonian potential into a Mondian one. In Mondian physics we want to replace $\partial_x U_f^N$ by

$$\partial_x U_f^N + \lambda(|\partial_x U_f^N|)\partial_x U_f^N$$

where $\lambda(\tau) \approx \sqrt{(a_0/\tau)}$ describes the deviation of Mondian physics from Newtonian[3]. However, the mere replacement of $\partial_x U_f^N$ with the above formula causes several problems like non-conservation of momentum (Famaey & McGaugh, 2012, §6). To avoid these problems we make use of the QUMOND theory[4], which was first proposed by Milgrom (2010), and set

$$\partial_x U_f^M \text{ is the irrotational part of } \partial_x U_f^N + \lambda(|\partial_x U_f^N|)\partial_x U_f^N. \tag{2.3}$$

How the irrotational part of the vector field is extracted and why $\partial_x U_f^M$ is indeed the gradient of some potential will be studied in Section 3.2 below. Consider now a test particle that is moving in the field $\partial_x U_f^M$. Its orbit $(x(t), v(t))$ is a solution of the ODE

$$\begin{aligned} \dot{x}(t) &= v(t), \\ \dot{v}(t) &= -\partial_x U_f^M(t, x(t)). \end{aligned}$$

Using the notation $z = (x, v)$, $b(t, z) = (v, -\partial_x U_f^M(t, x))$ this ODE can be written as

$$\dot{z}(t) = b(t, z(t)).$$

Since $\mathrm{div}_z\, b = 0$, the characteristic flow

$$Z = Z(t, s, z), \quad t, s \geq 0,\ z \in \mathbb{R}^6,$$

[2] In Part I of this thesis we set the gravitational constant G to unity since it does not affect our analysis.

[3] $a_0 \approx 1.2 \times 10^{-10}\,\mathrm{m\,s^{-2}}$ is the critical acceleration below that MOND effects dominate physics. As with the gravitational constant the concrete value of a_0 does not affect our analysis and we set $a_0 = 1$.

[4] QUMOND = QUasi linear formulation of MOND. The name originates from the fact that for calculating $\partial_x U_f^M$ we have to perform two linear and one non-linear, algebraic step. First we calculate U_f^N from ρ_f (first linear step). Then we calculate the field $\partial_x U_f^N + \lambda(|\partial_x U_f^N|)\partial_x U_f^N$ (the non-linear, algebraic step). Last we extract from this field its irrotational part (second linear step)

that belongs to this ODE preserves measure (DiPerna & Lions, 1989b). The distribution function f evolves along the characteristics. Since the total mass $\int f(t)\,\mathrm{d}z$, $t \geq 0$, must be constant, f must be constant along every characteristic. This guarantees that the mass

$$\int f(t,z)\,\mathrm{d}z = \int f(t,Z(t,0,z))\,\mathrm{d}z = \int f(0,z)\,\mathrm{d}z$$

is constant; the first equality uses that Z preserves measure, the second one that f is constant along characteristics. That f is constant along every characteristic $Z(t,0,z) = Z(t) = (X(t),V(t))$ means

$$\frac{\mathrm{d}}{\mathrm{d}t} f(t,X(t),V(t)) = 0.$$

Thus f must solve the Vlasov equation

$$\partial f + v \cdot \partial_x f - \partial_x U_f^M \cdot \partial_v f = 0. \tag{2.4}$$

We call f a solution of the Vlasov-QUMOND system (VQMS) if it solves (2.1) - (2.4). In Part I of this thesis we study weak solutions of the (VQMS) and we will introduce the precise notion of weak solution in Section 4.1. Note that the (VQMS) is a non-linear system of PDEs: We can write equation (2.2) also in the equivalent form

$$\Delta U_f^N = 4\pi G \rho_f, \quad \lim_{|x|\to\infty} U_f^N(x) = 0$$

(see Lemma 3.1.3 below) and equation 2.3 can alternatively be written as

$$\Delta U_f^M = \Delta U^N + \operatorname{div}\left(\lambda(|\nabla U_f^N|)\nabla U_f^N\right)$$

plus suitable boundary conditions (compare Lemma 3.2.3 below). The system is non-linear since the term $\partial_x U_f^N \cdot \partial_v f$ appearing in the Vlasov equation (2.4) is quadratic in f.

Keller (2016) proved the existence of spherically symmetric, global, weak solution of the initial value problem of the (VQMS). In Section 4 we prove conservation of energy for such solutions and study in detail the link between Eulerian and Lagrangian solutions.

Rein (2015) proved the existence of a large class of spherically symmetric, stationary solutions of the (VQMS). In Section 5 we prove for a somewhat smaller class of such stationary solutions that they are stable against spherically symmetric perturbations.

Spherically symmetric, stationary solutions of the (VQMS) are good models for globular clusters (Binney & Tremaine, 2008, §4.3). For example in the vivid discussion, whether the globular cluster NGC 2419 contradicts MOND or not, models are used that are of the type we consider here in this thesis (Ibata et al., 2011; Sanders, 2012).

3 Preliminaries

3.1 Newtonian potentials

In this thesis the Newtonian potential will play an important role in two different ways. On the one hand when we have a certain mass distribution with density ρ then U_ρ^N is the Newtonian gravitational potential that belongs to the density ρ. On the other hand in the QUMOND theory we must know how to decompose a vector field v in its irrotational and its solenoidal part. Here the Newtonian potentials of the three components v_i of the vector field play an important role. This we treat in Section 3.2 below.

For $\epsilon > 0$, $i,j = 1,2,3$ and a measurable function $g : \mathbb{R}^3 \to \mathbb{R}$ we define

$$T_{ij}^\epsilon g(x) := -\int_{|x-y|>\epsilon} \left[3\frac{(x_i-y_i)(x_j-y_j)}{|x-y|^5} - \frac{\delta_{ij}}{|x-y|^3}\right] g(y)\,\mathrm{d}y, \quad x \in \mathbb{R}^3,$$

provided that the convolution integral on the right hand side exists. Since

$$\partial_{x_i}\partial_{x_j}\frac{1}{|x|} = 3\frac{x_i x_j}{|x|^5} - \frac{\delta_{ij}}{|x|^3},$$

the limit of $T_{ij}^\epsilon g$ for $\epsilon \to 0$ plays an important in understanding the second derivatives of the Newtonian potential U_g^N. In the following two propositions we study this limit.

Proposition 3.1.1. *For every $\epsilon > 0$ and $g \in C_c^1(\mathbb{R}^3)$*

$$T_{ij}^\epsilon g \in C(\mathbb{R}^3)$$

and the limit

$$T_{ij} g := \lim_{\epsilon \to 0} T_{ij}^\epsilon g$$

exists in $L^\infty(\mathbb{R}^3)$. In particular

$$T_{ij} g \in C(\mathbb{R}^3).$$

Proposition 3.1.2. *Let $1 < p < \infty$. There is a $C_p > 0$ such that for every $\epsilon > 0$ and $g \in L^p(\mathbb{R}^3)$*

$$\|T_{ij}^\epsilon g\|_p \leq C_p \|g\|_p$$

and the limit

$$T_{ij} g := \lim_{\epsilon \to 0} T_{ij}^\epsilon g$$

exists in $L^p(\mathbb{R}^3)$ with

$$\|T_{ij} g\|_p \leq C_p \|g\|_p.$$

Proof of Proposition 3.1.1 and 3.1.2. The statements follow quite directly from the literature. To apply the results from the literature, we have to verify that

$$\Omega_{ij}(x) := 3\frac{x_i x_j}{|x|^2} - \delta_{ij}, \quad x \in \mathbb{R}^3, x \neq 0,$$

satisfies the following four assumptions:

1. Ω_{ij} must be homogeneous of degree 0, i.e., $\Omega_{ij}(\delta x) = \Omega_{ij}(x)$ for all $\delta > 0$, $x \neq 0$. This is obviously true.

2. Ω_{ij} must satisfy the cancellation property

$$\int_{|x|=1} \Omega_{ij}(x) \, \mathrm{dS}(x) = 0.$$

   If $i \neq j$, this is obviously true. If $i = j$ this is also true, since

$$\begin{aligned} \int_{|x|=1} \Omega_{ii}(x) \, \mathrm{dS}(x) &= 3 \int_{|x|=1} x_i^2 \, \mathrm{dS}(x) - 4\pi \\ &= \int_{|x|=1} |x|^2 \, \mathrm{dS}(x) - 4\pi = 0. \end{aligned}$$

3. Ω_{ij} must be bounded on $\{|x| = 1\}$. This is obviously true since Ω_{ij} is continuous on $\mathbb{R}^3 \backslash \{0\}$.

4. Ω_{ij} must satisfy the following smoothness property: For

$$w(\delta) := \sup_{\substack{|x-x'|<\delta \\ |x|=|x'|=1}} |\Omega_{ij}(x) - \Omega_{ij}(x')|$$

   must hold

$$\int_0^1 \frac{w(\delta)}{\delta} \, \mathrm{d}\delta < \infty.$$

   This is true since for $x, x' \in \mathbb{R}^3$ with $|x| = |x'| = 1$ and $|x - x'| < \delta$ we have

$$|\Omega_{ij}(x) - \Omega_{ij}(x')| = 3|x_i x_j - x_i' x_j'| \leq 3|x_i||x_j - x_j'| + 3|x_j'||x_i - x_i'| \leq 6\delta.$$

Now Proposition 3.1.2 follows directly from (Stein, 1970, Chapter II, Theorem 3) and Proposition 3.1.1 follows from (Dietz, 2001, Satz 2.2). In the formulation of her theorem Dietz does not mention the continuity of the $T_{ij}^\epsilon g$, but studying her proof carefully one sees that she has proven the Hölder continuity of $T_{ij}^\epsilon g$ under the assumption that $\operatorname{supp} g \subset B_1$. This holds obviously also for every $g \in C_c^1(\mathbb{R}^3)$. If however one is interested solely in the continuity of $T_{ij}^\epsilon g$, like we here in this thesis, one could also simply apply the transformation $y \mapsto x - y$ in the definition of $T_{ij}^\epsilon g$ and use standard results to deduce that $T_{ij}^\epsilon g$ is continuous.

□

Next we formulate regularity results for the Newtonian potential. Note that we have set the gravitational constant G to unity.

Lemma 3.1.3. *Let $g \in C_c^{1+n}(\mathbb{R}^3)$, $n \in \mathbb{N}_0$. Then the following holds*

a) The Newtonian potential $U_g^N \in C^{2+n}(\mathbb{R}^3)$. Its first derivative is given by

$$\partial_{x_i} U_g^N = U_{\partial_{y_i} g}^N, \quad i = 1, 2, 3,$$

which, using integration by parts, can be written as

$$\nabla U_g^N(x) = \int \frac{x-y}{|x-y|^3} g(y) \, \mathrm{d}y, \quad x \in \mathbb{R}^3.$$

The second derivative of U_g^N is given by

$$\partial_{x_i} \partial_{x_j} U_g^N = T_{ij} g + \delta_{ij} \frac{4\pi}{3} g,$$

where $i, j = 1, 2, 3$.

b) For every $R > 0$ there is a $C > 0$ such that

$$\|U_g^N\|_\infty + \|\nabla U_g^N\|_\infty \leq C \|g\|_\infty.$$

and

$$\|D^2 U_g^N\|_\infty \leq C(\|g\|_\infty + \|\nabla g\|_\infty)$$

provided $\operatorname{supp} g \subset B_R$.

c) U_g^N is the unique solution of

$$\Delta U_g^N = 4\pi g, \quad \lim_{|x| \to \infty} U_g^N(x) = 0.$$

in $C^2(\mathbb{R}^3)$

Proof. It is proven in (Rein, 2007, Lemma P1) that $U_g^N \in C^2(\mathbb{R}^3)$ if $g \in C_c^1(\mathbb{R}^3)$ and that the formulae for the first derivatives hold. If $g \in C_c^{1+n}(\mathbb{R}^3)$ with $n \geq 1$, it follows directly from

$$\partial_{x_i} U_g^N = U_{\partial_{y_i} g}^N$$

that $U_g^N \in C^{2+n}(\mathbb{R}^3)$. To prove a) it remains to verify the formula for the second derivatives. For every $x \in \mathbb{R}^3$ we have

$$\begin{aligned} \partial_{x_i} \partial_{x_j} U_g^N(x) = \partial_{x_i} U_{\partial_{y_j} g}^N(x) &= \int \frac{x_i - y_i}{|x-y|^3} \partial_{y_j} g(y) \, \mathrm{d}y = \\ &= -\int \frac{y_i}{|y|^3} \partial_{y_j}(g(x-y)) \, \mathrm{d}y = \int \partial_{y_i}(|y|^{-1}) \partial_{y_j}(g(x-y)) \, \mathrm{d}y. \end{aligned}$$

Dominated convergences and integration by parts then yield

$$\begin{aligned} \partial_{x_i} \partial_{x_j} U_g^N(x) &= \lim_{\epsilon \to 0} \int_{|y| > \epsilon} \partial_{y_i}(|y|^{-1}) \partial_{y_j}(g(x-y)) \, \mathrm{d}y \\ &= \lim_{\epsilon \to 0} \left(T_{ij}^\epsilon g(x) + \int_{|y| = \epsilon} \frac{y_i y_j}{|y|^4} g(x-y) \, \mathrm{dS}(y) \right); \end{aligned}$$

observe that the normal on $\{|y| = \epsilon\}$ is pointing inward and that there is no border term at infinity due to the compact support of g. $T_{ij}^\epsilon g$ converges uniformly to $T_{ij} g$ after Proposition 3.1.1. If $i \neq j$ then

$$\left| \int_{|y| = \epsilon} \frac{y_i y_j}{|y|^4} g(x-y) \, \mathrm{dS}(y) \right| = \left| \int_{|y| = \epsilon} \frac{y_i y_j}{|y|^4} (g(x-y) - g(x)) \, \mathrm{dS}(y) \right| \leq 4\pi \|\nabla g\|_\infty \epsilon.$$

Hence the border term vanishes. If $i = j$ then

$$\int_{|y|=\epsilon} \frac{y_i^2}{|y|^4} g(x-y)\,\mathrm{dS}(y) = \int_{|y|=\epsilon} \frac{y_i^2}{|y|^4}(g(x-y)-g(x))\,\mathrm{dS}(y) + g(x)\int_{|y|=\epsilon} \frac{y_i^2}{|y|^4}\,\mathrm{dS}(y).$$

As above the first term vanishes, however, the second one evaluates to $4\pi g(x)/3$. In total we get

$$\partial_{x_i}\partial_{x_j} U_g^N(x) = T_{ij} g(x) + \delta_{ij}\frac{4\pi}{3} g(x).$$

Let us turn to b). Since $\operatorname{supp} g \subset B_R$ and g is bounded one sees directly that

$$\|U_g^N\|_\infty + \|\nabla U_g^N\|_\infty \le C\|g\|_\infty.$$

That

$$\|D^2 U_g^N\|_\infty \le C(\|g\|_\infty + \|\nabla g\|_\infty),$$

is proven in (Rein, 2007, Lemma P1).

It remains to show c). It is stated in (Rein, 2007, Lemma P1) that U_g^N is the unique solution of

$$\Delta U_g^N = 4\pi g, \quad \lim_{|x|\to\infty} U_g^N(x) = 0,$$

however the proof is omitted. So let us briefly summarize the proof of this well known fact. Since

$$\sum_{i=1}^3 \left(3\frac{x_i^2}{|x|^5} - \frac{1}{|x|^3}\right) = 0,$$

we have

$$\sum_{i=1}^3 T_{ii} g = 0.$$

Thus´

$$\Delta U_g^N = \sum_{i=1}^3 \partial_{x_i}^2 U_g^N = \sum_{i=1}^3 \left(T_{ii} g + \frac{4\pi}{3} g\right) = 4\pi g.$$

The asymptotic behaviour of $U_g^N(x)$ for $|x| \to \infty$ follows from the compact support of g. That g is the unique solution of the above PDE follows from the strong maximum principle (Gilbarg & Trudinger, 1977, Theorem 2.2.). □

Lemma 3.1.4. *Let $g \in L^1 \cap L^p(\mathbb{R}^3)$ for a $1 < p < \infty$. Then $U_g^N \in L^1_{loc}(\mathbb{R}^3)$ exists, is twice weakly differentiable and the formulae for ∇U_g^N and $\partial_{x_i}\partial_{x_j} U_g^N$ from Lemma 3.1.3 and the following estimates hold*

a) If $1 < p < \frac{3}{2}$ and $3 < r < \infty$ with $\frac{1}{3} + \frac{1}{p} = 1 + \frac{1}{r}$ then

$$\|U_g^N\|_r \le C_{p,r}\|g\|_p.$$

b) If $1 < p < 3$ and $\frac{3}{2} < s < \infty$ with $\frac{2}{3} + \frac{1}{p} = 1 + \frac{1}{s}$ then

$$\|\nabla U_g^N\|_s \le C_{p,s}\|g\|_p.$$

c) For every $1 < p < \infty$

$$\|D^2 U_g^N\|_p \le C_p\|g\|_p.$$

Proof. With the formula for ∇U_g^N as in Lemma 3.1.3 we have

$$U_g^N = -\frac{1}{|\cdot|} * g \quad \text{and} \quad \nabla U_g^N = \frac{\cdot}{|\cdot|^3} * g.$$

$1/|\cdot|$ and $\cdot/|\cdot|^3$ are in the so called weak L^q-space with $q = 3$ and $q = \frac{3}{2}$ respectively since

$$\sup_{\alpha>0} \alpha\mathcal{L}\left(\left\{x : \frac{1}{|x|} > \alpha\right\}\right)^{1/3} = (4\pi/3)^{1/3} < \infty$$

and

$$\sup_{\alpha>0} \alpha \mathcal{L}\left(\left\{x : \frac{1}{|x|^2} > \alpha\right\}\right)^{2/3} = (4\pi/3)^{2/3} < \infty;$$

with $\mathcal{L}(\Omega)$ we denote the Lebesgue measure of a measurable set $\Omega \subset \mathbb{R}^n$, $n \in \mathbb{N}$. Thus (Lieb & Loss, 2010, Remark 4.3(2)) implies that $U_g^N \in L^r$ and $\nabla U_g^N \in L^s$ with the desired estimates provided $p < 3/2$ and $p < 3$ respectively. If $p \geq 3/2$, $U_\rho^N \in L^r(\mathbb{R}^3)$ for every $3 < r < \infty$ since $\rho \in L^1 \cap L^p(\mathbb{R}^3) \subset L^q(\mathbb{R}^3)$ for every $1 < q < 3/2$. The same argumentation holds for ∇U_ρ^N if $p \geq 3$.

We have to check that ∇U_g^N is indeed the weak derivative of U_g^N. For this take $\phi \in C_c^\infty(\mathbb{R}^3)$. The Hardy-Littlewood-Sobolev inequality (Lieb & Loss, 2010, Theorem 4.3) allows us to use Fubini:

$$\int U_g^N(x)\partial_{x_i}\phi(x)\,\mathrm{d}x = -\iint \frac{g(y)\partial_{x_i}\phi(x)}{|x-y|}\,\mathrm{d}x\,\mathrm{d}y.$$

Now Lemma 3.1.3 implies

$$\begin{aligned}
\int U_g^N(x)\partial_{x_i}\phi(x)\,\mathrm{d}x &= \int g(y) U_{\partial_{x_i}\phi}^N(y)\,\mathrm{d}y = \int g(y)\partial_{y_i} U_\phi^N(y)\,\mathrm{d}y \\
&= \iint g(y)\frac{y_i - x_i}{|y-x|^3}\phi(x)\,\mathrm{d}x\,\mathrm{d}y \\
&= -\int \left(\int \frac{x_i - y_i}{|x-y|} g(y)\,\mathrm{d}y\right)\phi(x)\,\mathrm{d}x \\
&= -\int \nabla U_g^N(x)\phi(x)\,\mathrm{d}x.
\end{aligned}$$

So the weak gradient of U_g^N is given by the formula for ∇U_g^N from Lemma 3.1.3.

Let $1 < p < \infty$. We study the second derivatives and take $(g_k) \subset C_c^1(\mathbb{R}^3)$ such that

$$g_k \to g \quad \text{in } L^p(\mathbb{R}^3) \text{ for } k \to \infty.$$

Then Hölder, integration by parts and Lemma 3.1.3 give

$$\begin{aligned}
\int U_g^N \partial_{x_i}\partial_{x_j}\phi\,\mathrm{d}x &= \lim_{k\to\infty} \int U_{g_k}^N \partial_{x_i}\partial_{x_j}\phi\,\mathrm{d}x \\
&= \lim_{k\to\infty} \int (T_{ij} g_k + \delta_{ij}\frac{4\pi}{3} g_k)\phi\,\mathrm{d}x \\
&= \int (T_{ij} g + \delta_{ij}\frac{4\pi}{3} g)\phi\,\mathrm{d}x.
\end{aligned}$$

Thus the weak second derivatives of U_g^N are given by the same formula as in Lemma 3.1.3. The desired estimate for $\partial_{x_i}\partial_{x_j} U_g^N$ follows from Proposition 3.1.2.

□

We will often need ∇U_ρ^N for a spherically symmetric density ρ.

Lemma 3.1.5. *Let $1 < p < 3$ and $\rho \in L^1 \cap L^p(\mathbb{R}^3)$, ≥ 0 be spherically symmetric. Then*

$$\nabla U_\rho^N(x) = \frac{M(r)}{r^2}\frac{x}{r}$$

for a.e. $x \in \mathbb{R}^3$ with $r = |x|$ and

$$M(r) := \int_{B_r} \rho(x)\,\mathrm{d}x = 4\pi \int_0^r s^2 \rho(s)\,\mathrm{d}s$$

denoting the mass inside the ball with radius r.

Proof. Assume that ρ would be continuous and compactly supported. Then $M \in C^1([0,\infty))$ with

$$M'(r) = 4\pi r^2 \rho(r), \quad r \geq 0.$$

Further

$$|M(r)| \leq \|\rho\|_1$$

and

$$|M(r)| \le \frac{4\pi}{3}\|\rho\|_\infty r^3$$

for $r \ge 0$. For $x \in \mathbb{R}^3$ and $r = |x|$

$$U(x) := -\int_r^\infty \frac{M(s)}{s^2}\,\mathrm{d}s$$

is well defined. If $r = |x| > 0$, U is continuously differentiable with

$$\nabla U(x) = \frac{M(r)}{r^2}\frac{x}{r}.$$

Since

$$|\nabla U(x)| \le \frac{4\pi}{3}\|\rho\|_\infty r$$

we have

$$\nabla U \in C(\mathbb{R}^3).$$

Further

$$\partial_{x_i}\partial_{x_j}U(x) = 4\pi\rho(r)\frac{x_i x_j}{r^2} - 3M(r)\frac{x_i x_j}{r^5} + \frac{M(r)}{r^3}\delta_{ij}, \quad r > 0.$$

Since ρ is continuous,

$$\frac{M(r)}{r^3} = \frac{4\pi}{3}\frac{1}{\mathcal{L}(B_r)}\int_{B_r}\rho\,\mathrm{d}x \to \frac{4\pi}{3}\rho(0)$$

and

$$\left|4\pi\rho(r) - \frac{3M(r)}{r^3}\right| = 4\pi\left|\rho(r) - \frac{1}{\mathcal{L}(B_r)}\int_{B_r}\rho\,\mathrm{d}x\right| \to 0$$

for $r \to 0$. Hence

$$D^2U \in C(\mathbb{R}^3).$$

Thus

$$U \in C^2(\mathbb{R}^3).$$

Further

$$\Delta U = 4\pi\rho$$

and

$$\lim_{|x|\to\infty}|U(x)| \le \lim_{|x|\to\infty}\frac{\|\rho\|_1}{|x|} = 0.$$

Since by Lemma 3.1.3 U_ρ^N is a solution of this PDE, too, and this solutions is unique

$$U_\rho^N = U$$

and

$$\nabla U_\rho^N(x) = \nabla U(x) = \frac{M(r)}{r^2}\frac{x}{r}, \quad x \in \mathbb{R}^3. \tag{3.1}$$

If now $\rho \in L^1 \cap L^p(\mathbb{R}^3)$, we take a sequence $(\rho_n) \subset C_c(\mathbb{R}^3)$ of spherically symmetric densities such that

$$\rho_n \to \rho \quad \text{in } L^p(\mathbb{R}^3) \text{ for } n \to \infty.$$

By Lemma 3.1.4

$$\nabla U_{\rho_n}^N \to \nabla U_\rho^N \quad \text{in } L^s(\mathbb{R}^3) \text{ for } n \to \infty \tag{3.2}$$

where $s > 3/2$ with $1/p + 2/3 = 1 + 1/s$. Set

$$M_n(r) := \int_{B_r}\rho_n\,\mathrm{d}x, \quad r \ge 0.$$

Then for every $r \ge 0$

$$|M_n(r) - M(r)| \le \|\rho_n - \rho\|_p\|1_{B_r}\|_{p/(p-1)}.$$

Hence for all $0 < S < R$

$$M_n \to M \quad \text{uniformly on } B_R \text{ for } n \to \infty$$

and

$$\frac{M_n(r)}{r^2}\frac{x}{r} \to \frac{M(r)}{r^2}\frac{x}{r} \text{ uniformly on } \{S < |x| < R\} \text{ for } n \to \infty.$$

Together with (3.1) and (3.2) this implies that for a.e. $x \in \mathbb{R}^3$

$$\nabla U_\rho^N(x) = \frac{M(r)}{r^2}\frac{x}{r}.$$

□

Later on in this thesis we will make regularly use of the following statement.

Lemma 3.1.6. *If $\rho, \sigma \in L^{6/5}(\mathbb{R}^3)$ then*

$$-\frac{1}{8\pi}\int \nabla U_\rho^N \cdot \nabla U_\sigma^N \,\mathrm{d}x = \frac{1}{2}\int U_\rho^N \sigma \,\mathrm{d}x = -\frac{1}{2}\iint \frac{\rho(y)\sigma(x)}{|x-y|}\,\mathrm{d}x\,\mathrm{d}y.$$

Proof. $\nabla U_\rho^N, \nabla U_\sigma^N \in L^2(\mathbb{R}^3)$ and $U_\rho^N \in L^6(\mathbb{R}^3)$ according to Lemma 3.1.4. Thus the first two integrals are well defined. By the Hardy-Littlewood-Sobolev inequality (Lieb & Loss, 2010, Theorem 4.3) also the third integral is well defined. If $\rho, \sigma \in C_c^\infty(\mathbb{R}^3)$, integration by parts and $\Delta U_\sigma^N = 4\pi\sigma$ give the above equalities of the integrals. Since $C_c^\infty(\mathbb{R}^3) \subset L^{6/5}(\mathbb{R}^3)$ is dense and all three integrals above are continuous maps from $L^{6/5} \times L^{6/5} \to \mathbb{R}$, the above equalities hold for all $\sigma, \rho \in L^{6/5}(\mathbb{R}^3)$. □

3.2 Irrotational vector fields

The basic MOND principle states that given a Newtonian gravitational potential U^N then the acceleration of a particle at position x is given by

$$\nabla U^N(x) + \lambda(|\nabla U^N(x)|)\nabla U^N(x).$$

However, as discussed before, this leads to physics without nice conservation laws. In the QUMOND theory this problem is overcome by making use of the Helmholtz-Weyl decomposition. This theorem states that the above vector field can - in a unique way - be decomposed into an irrotational vector field, which is the gradient of some potential, plus a solenoidal vector field. In the QUMOND theory we define now

$$\nabla U^M \text{ is the irrotational part of } \nabla U^N + \lambda(|\nabla U^N|)\nabla U^N$$

and the acceleration of a particle at position x is given by

$$\nabla U^M(x).$$

With this trick the equations of motions in the QUMOND theory can be derived from the Hamiltonian $\mathcal{H}(x,v) = \frac{1}{2}|v|^2 + U^M(x)$ overcoming the problems with conservation laws. In particular, we will be able to prove conservation of energy for solutions of the Vlasov-QUMOND-System. In this section we specify what we mean with the 'irrotational part of a vector field'.

Definition 3.2.1. Let $1 < p < \infty$ and $v \in L^p(\mathbb{R}^3)$ be a vector field. For $i = 1, 2, 3$ we define

$$H_i v := \frac{1}{4\pi}\sum_{j=1}^{3} T_{ij} v_j + \frac{1}{3} v_i.$$

We call the vector field $Hv \in L^p(\mathbb{R}^3)$ the irrotational part of v.

We will see below that Hv is indeed the irrotational part of v in the sense of the the Helmholtz-Weyl decomposition.

Theorem 3.2.2 (Helmholtz-Weyl decomposition)**.** *For every vector field $v \in L^p(\mathbb{R}^3)$, $1 < p < \infty$, exist uniquely determined $v_1 \in L^p_{irr}(\mathbb{R}^3)$ and $v_2 \in L^p_{sol}(\mathbb{R}^3)$ such that*

$$v = v_1 + v_2,$$

where the two subspaces $L^p_{irr}(\mathbb{R}^3)$ and $L^p_{sol}(\mathbb{R}^3)$ of $L^p(\mathbb{R}^3)$ are defined as follows:

$$L^p_{irr}(\mathbb{R}^3) := \left\{ w \in L^p(\mathbb{R}^3) \text{ such that } U \in W^{1,p}_{loc}(\mathbb{R}^3) \text{ exists with } w = \nabla U \right\},$$
$$L^p_{sol}(\mathbb{R}^3) := \left\{ w \in L^p(\mathbb{R}^3) \text{ such that } \operatorname{div} w = 0 \text{ weakly} \right\}.$$

Proof. In (Galdi, 2011, Theorem III.1.2) it is proven that the Helmholtz-Weyl decomposition in the sense of (Galdi, 2011, equation (III.1.5)) holds. This form of the theorem makes use of a different definition of the space L^p_{sol}. However, in (Galdi, 2011, Theorem III.2.3) it is proven that our definition here coincides with the definition used in (Galdi, 2011, Theorem III.1.2). □

Let us study how the Helmholtz-Weyl decomposition looks like for smooth vector fields with compact support.

Lemma 3.2.3. *Let $v \in C^2_c(\mathbb{R}^3)$. For every $1 < p < \infty$*

$$Hv = \frac{1}{4\pi}\nabla\left(\sum_{j=1}^{3} \partial_{x_j} U^N_{v_j}\right) \in C^1 \cap L^p_{irr}(\mathbb{R}^3)$$

is the uniquely determined, irrotational part of the vector field v according to the Helmholtz-Weyl decomposition. Further

$$\operatorname{div} Hv = \operatorname{div} v \text{ and } \operatorname{rot} Hv = 0.$$

Proof. By Proposition 3.1.2 $Hv \in L^p(\mathbb{R}^3)$ for every $1 < p < \infty$. Since by Lemma 3.1.3

$$U^N_{v_j} \in C^3(\mathbb{R}^3), \quad j = 1, 2, 3,$$

we have also

$$Hv = \frac{1}{4\pi}\nabla\left(\sum_{j=1}^{3} \partial_{x_j} U^N_{v_j}\right) \in C^1(\mathbb{R}^3).$$

In particular $Hv \in L^p_{irr}(\mathbb{R}^3)$. Since Hv is a gradient, its rotation is zero. For the divergence we have with Lemma 3.1.3

$$\operatorname{div} Hv = \frac{1}{4\pi}\sum_{j=1}^{3} \Delta U^N_{\partial_{y_j} v_j} = \sum_{j=1}^{3} \partial_{x_j} v_j = \operatorname{div} v.$$

Further we get

$$v_2 := v - Hv \in C^1 \cap L^p(\mathbb{R}^3)$$

for every $1 < p < \infty$ with $\operatorname{div}(v_2) = 0$ classically. Hence $v_2 \in L^p_{sol}(\mathbb{R}^3)$. □

We are particularly interested in the Helmholtz-Weyl decomposition of vector fields $v \in L^p(\mathbb{R}^3)$. If $p < 3$, we can show that $\partial_{x_j} U^N_{v_j}$ exists and, using the same formula as in Lemma 3.2.3, it is easy to deduct that in this situation, too, the Helmholtz-Weyl decomposition of v is given by $Hv + (v - Hv)$. If $p \geq 3$ however (and this is the case of special interest in Mondian physics), the integral

$$\partial_{x_j} U^N_{v_j} = \int \frac{x_j - y_j}{|x - y|^3} v_j(y)\,\mathrm{d}y$$

does not necessarily converge. Nevertheless, also in this situation the Helmholtz-Weyl decomposition of v is given by $Hv + (v - Hv)$ but we can no longer make use of the formula from Lemma 3.2.3. The key ingredients to prove this explicit form of the Helmholtz-Weyl decomposition for $v \in L^p(\mathbb{R}^3)$ are the following proposition and corollary[5] , which are based on Poincaré's inequality.

Proposition 3.2.4. *Let $1 < p < \infty$, $R > 0$, $v \in L^p(B_R)$ and $(U_k) \subset W^{1,p}(B_R)$ be such that*

$$\int_{B_R} U_k \,\mathrm{d}x = 0$$

and

$$\nabla U_k \to v \quad \text{in } L^p(B_R) \text{ for } k \to \infty$$

Then there is a $U \in W^{1,p}(B_R)$ such that

$$U_k \to U \quad \text{in } W^{1,p}(B_R) \text{ for } k \to \infty$$

and $\nabla U = v$.

[5]The important observation is that $L^p_{irr}(\mathbb{R}^3)$ and $L^p_{sol}(\mathbb{R}^3)$ are closed subsets of $L^p(\mathbb{R}^3)$. For $L^p_{sol}(\mathbb{R}^3)$ this is proved in Galdi (2011). For $L^p_{irr}(\mathbb{R}^3)$ Galdi leaves this as an exercise to the reader (Exercise III.1.2). Corollary 3.2.5 gives a solution to this exercise.

Proof. By Poincaré's inequality (Lieb & Loss, 2010, Theorem 8.11) and since (∇U_k) is a convergent sequence in $L^p(B_R)$

$$\|U_k - U_l\|_{L^p(B_R)} \leq C\|\nabla U_k - \nabla U_l\|_{L^p(B_R)} \to 0 \quad \text{for } k, l \to \infty.$$

Hence $(U_k) \subset L^p(B_R)$ is a Cauchy sequence. Thus

$$U := \lim_{k\to\infty} U_k \in L^p(B_R)$$

exists. In particular $v = \nabla U$. □

Corollary 3.2.5. *Let $1 < p < \infty$, $v \in L^p(\mathbb{R}^3)$ and $(U_k) \subset W^{1,p}_{loc}(\mathbb{R}^3)$ be such that*

$$\nabla U_k \to v \quad \text{in } L^p(\mathbb{R}^3) \text{ for } k \to \infty.$$

Then there exists $U \in W^{1,p}_{loc}(\mathbb{R}^3)$ such that $\nabla U = v$. In particular $L^p_{irr}(\mathbb{R}^3)$ is a closed subset of $L^p(\mathbb{R}^3)$.

Proof. For $n, k \in \mathbb{N}$ set

$$U_k^{(n)} := U_k - \frac{3}{4\pi n^3} \int_{B_n} U_k \,\mathrm{d}x.$$

Then

$$\int_{B_n} U_k^{(n)} \,\mathrm{d}x = 0$$

and by Proposition 3.2.4 there exists for every $n \in \mathbb{N}$

$$U^{(n)} := \lim_{k\to\infty} U_k^{(n)} \in L^p(B_n)$$

and

$$\nabla U^{(n)} = v.$$

Since $\nabla U^{(n)} = \nabla U^{(1)}$ on B_1, there exists for every $n \in \mathbb{N}$ a $c^{(n)} \in \mathbb{R}$ such that

$$\tilde{U}^{(n)} := U^{(n)} + c^{(n)} = U^{(1)}$$

on B_1. In particular $\tilde{U}^{(n)} = \tilde{U}^{(m)}$ on B_n for every $m, n \in \mathbb{N}$ with $n < m$. Hence there exists $U \in W^{1,p}_{loc}(\mathbb{R}^3)$ such that $\nabla U = v$.

This implies that $L^p_{irr}(\mathbb{R}^3)$ is a closed subset of $L^p(\mathbb{R}^3)$: Take $(v_k) \subset L^p_{irr}(\mathbb{R}^3)$ with $v_k \to v$ in $L^p(\mathbb{R}^3)$. By the definition of L^p_{irr} there exists $U_k \in W^{1,p}_{loc}(\mathbb{R}^3)$ such that $\nabla U_k = v_k$ and $\nabla U_k \to v$ in $L^p(\mathbb{R}^3)$. From what we have just proven follows that there exists $U \in W^{1,p}_{loc}(\mathbb{R}^3)$ such that $v = \nabla U$. Hence $v \in L^p_{irr}(\mathbb{R}^3)$. □

Theorem 3.2.6 (Explicit Helmholtz-Weyl decomposition)**.** *Let $1 < p < \infty$ and $v \in L^p(\mathbb{R}^3)$ be a vector field. Then the uniquely determined Helmholtz-Weyl decomposition of v is given by*

$$v = Hv + (v - Hv)$$

with

$$Hv \in L^p_{irr}(\mathbb{R}^3) \quad \text{and} \quad v - Hv \in L^p_{sol}(\mathbb{R}^3).$$

Proof. We can approximate $v \in L^p(\mathbb{R}^3)$ with a sequence $(v_k) \subset C^2_c(\mathbb{R}^3)$. By Lemma 3.2.3 the Helmholtz-Weyl decomposition of v_k is given by

$$v_k = Hv_k + (v_k - Hv_k)$$

with

$$Hv_k \in L^p_{irr}(\mathbb{R}^3) \quad \text{and} \quad v_k - Hv_k \in L^p_{sol}(\mathbb{R}^3).$$

By Corollary 3.2.5 $L^p_{irr}(\mathbb{R}^3)$ is a closed subset of $L^p(\mathbb{R}^3)$. By (Galdi, 2011, Theorem III.2.3) $L^p_{sol}(\mathbb{R}^3)$ is the closure of the set

$$\{v \in C^\infty_c(\mathbb{R}^3) \text{ with } \operatorname{div} v = 0\}$$

with respect to the L^p-norm on $\mathbb{R}^3$. Hence L^p_{sol} is a closed subset of $L^p(\mathbb{R}^3)$. Since $v_k \to v$ and $Hv_k \to Hv$ in $L^p(\mathbb{R}^3)$ for $k \to \infty$

$$Hv \in L^p_{irr}(\mathbb{R}^3) \quad \text{and} \quad v - Hv \in L^p_{sol}(\mathbb{R}^3)$$

and

$$v = Hv + (v - Hv)$$

is the uniquely determined Helmholtz-Weyl decomposition of v. □

For spherically symmetric vector fields the Helmholtz-Weyl decomposition is trivial.

Lemma 3.2.7. *Let $1 < p < \infty$. Then for every spherically symmetric vector field $v \in L^p(\mathbb{R}^3)$*

$$Hv = v.$$

Proof. Let $v \in L^p(\mathbb{R}^3)$ be a spherically symmetric vector field. There exists a sequence $(v_k) \subset C_c^\infty(\mathbb{R}^3)$ of spherically symmetric vector fields with

$$v_k \to v \quad \text{in } L^p(\mathbb{R}^3) \text{ for } k \to \infty.$$

Since the v_k are spherically symmetric

$$\operatorname{rot} v_k = 0.$$

Hence, by standard results for vector calculus, there exist potentials $(U_k) \subset C^\infty(\mathbb{R}^3)$ such that for every $k \in \mathbb{N}$

$$v_k = \nabla U_k,$$

in particular $v_k \in L^p_{irr}(\mathbb{R}^3)$ and the uniqueness of the Helmholtz-Weyl decomposition implies

$$Hv_k = v_k.$$

Since $H : L^p(\mathbb{R}^3) \to L^p(\mathbb{R}^3)$ is continuous

$$Hv = v.$$

□

Last in this chapter we want to prove one useful Lemma.

Lemma 3.2.8. *Let $1 < p, q < \infty$ with $\frac{1}{p} + \frac{1}{q} = 1$, and let $v \in L^p(\mathbb{R}^3)$, $w \in L^q(\mathbb{R}^3)$ be vector fields. Then*

$$\int v \cdot Hw \,\mathrm{d}x = \int Hv \cdot w \,\mathrm{d}x.$$

Proof. Assume that $v \in L^1 \cap L^p(\mathbb{R}^3)$ and $w \in L^1 \cap L^q(\mathbb{R}^3)$. Since $v, w \in L^1(\mathbb{R}^3)$ we can apply Fubini and get that for every $\epsilon > 0$ and $i, j = 1, 2, 3$

$$\begin{aligned}
\int T_{ij}^\epsilon v_j \, w_i \,\mathrm{d}x &= -\iint_{|x-y|>\epsilon} \partial_{x_i}\partial_{x_j} \left(\frac{1}{|x-y|}\right) v_j(y) \,\mathrm{d}y \, w_i(x) \,\mathrm{d}x \\
&= -\int v_j(y) \int_{|x-y|>\epsilon} \partial_{y_i}\partial_{y_j} \left(\frac{1}{|x-y|}\right) w_i(x) \,\mathrm{d}x \,\mathrm{d}y \\
&= \int v_j \, T_{ij}^\epsilon w_i \,\mathrm{d}y.
\end{aligned}$$

Hence by Hölder

$$\begin{aligned}
\int Hv \cdot w \,\mathrm{d}x &= \frac{1}{4\pi} \sum_{i,j=1}^3 \lim_{\epsilon\to 0} \int T_{ij}^\epsilon v_j \, w_i \,\mathrm{d}x + \frac{1}{3} \sum_{i=1}^3 \int v_i w_i \,\mathrm{d}x \\
&= \frac{1}{4\pi} \sum_{i,j=1}^3 \lim_{\epsilon\to 0} \int v_j \, T_{ij}^\epsilon w_i \,\mathrm{d}x + \frac{1}{3} \sum_{i=1}^3 \int v_i w_i \,\mathrm{d}x \\
&= \int v \cdot Hw \,\mathrm{d}x.
\end{aligned}$$

Since $L^1 \cap L^p(\mathbb{R}^3) \subset L^p(\mathbb{R}^3)$ and $L^1 \cap L^q(\mathbb{R}^3) \subset L^q(\mathbb{R}^3)$ are dense, and H is continuous, it follows that for every $v \in L^p(\mathbb{R}^3)$ and $w \in L^q(\mathbb{R}^3)$

$$\int Hv \cdot w \,\mathrm{d}x = \int v \cdot Hw \,\mathrm{d}x.$$

□

3.3 Mondian potentials

In the MOND theory we want to take the gradient of the Newtonian potential ∇U^N and add to it the correction term

$$\lambda(|\nabla U^N|)\nabla U^N.$$

This is the basic MOND paradigm. In this thesis we make use of the QUMOND-Theory (Milgrom, 2010) and add only the irrotational part

$$H(\lambda(|\nabla U^N|)\nabla U^N)$$

of the correction term to ∇U^N. This leads to the following, formal definition:

$$\nabla U^M := H(\nabla U^N + \lambda(|\nabla U^N|)\nabla U^N) \tag{3.3}$$

$$= \nabla U^N + H(\lambda(|\nabla U^N|)\nabla U^N). \tag{3.4}$$

The theory of the previous chapter ensures that ∇U^M is indeed the gradient of a potential.

In each of the following sections we make some of the following three assumptions on the measurable function

$$\lambda : (0,\infty) \to (0,\infty).$$

($\Lambda 1$) There is $\Lambda_1 > 0$ such that $\lambda(\sigma) \geq \Lambda_1/\sqrt{\sigma}$, for $\sigma > 0$ small,

($\Lambda 2$) There is $\Lambda_2 > 0$ such that $\lambda(\sigma) \leq \Lambda_2/\sqrt{\sigma}$, for every $\sigma > 0$,

($\Lambda 3$) $\lambda \in C^1((0,\infty))$, $\lambda(\sigma) \to 0$ as $\sigma \to \infty$ and there is $\Lambda_2 > 0$ such that $-\Lambda_2/(2\sigma^{3/2}) \leq \lambda'(\sigma) \leq 0$, for $\sigma > 0$.

Let us discuss the impact the various assumptions on λ have:

As a result of ($\Lambda 1$) the MONDian force becomes much stronger than its Newtonian counterpart if the absolute value of the force is low. This is the difference between Mondian and Newtonian physics that enables MOND to predict correctly flat circular velocity curves in spiral galaxies without having to rely on dark matter (see for example Gentile et al. (2011)). Further this property guarantees that MOND forces confine mass more effectively than Newtonian forces. This even simplifies the proof of the existence of minimizers of the variational problem studied in Section 5.2. Assumption ($\Lambda 2$) in contrast takes care that the MOND force does not get arbitrarily strong and remains in its physically motivated regime. Assumption ($\Lambda 3$) is a stronger version of ($\Lambda 2$) and grants more regularity of λ.

In the next Lemma we show that ($\Lambda 3$) implies ($\Lambda 2$) and the Hölder continuity of the function $\lambda(|u|)u$, $u \in \mathbb{R}^3$.

Lemma 3.3.1. *If $\lambda : (0,\infty) \to (0,\infty)$ satisfies ($\Lambda 3$) then it satisfies also ($\Lambda 2$) and there is a $C > 0$ such that for all $u, v \in \mathbb{R}^3$*

$$|\lambda(|u|)u - \lambda(|v|)v| \leq C|u - v|^{1/2}$$

with $\lambda(|u|)u = 0$ if $u = 0$.

Proof. Let $\sigma > 0$, then

$$\lambda(\sigma) = -\int_\sigma^\infty \lambda'(s)\,\mathrm{d}s \leq \frac{\Lambda_2}{2}\int_\sigma^\infty \frac{\mathrm{d}s}{s^{3/2}} = \frac{\Lambda_2}{\sqrt{\sigma}}.$$

Thus λ satisfies ($\Lambda 2$). Further, the function $\lambda(|u|)u$ is continuously differentiable on $\mathbb{R}^3\backslash\{0\}$, and for $u \in \mathbb{R}^3$, $u \neq 0$, holds

$$D(\lambda(|u|)u) = \lambda(|u|)E_3 + \lambda'(|u|)\frac{uu^T}{|u|}$$

where E_3 denotes the identity matrix of dimension 3. Since λ satisfies ($\Lambda 2$) and ($\Lambda 3$), we have

$$|D(\lambda(|u|)u)| \leq \frac{C}{\sqrt{|u|}}.$$

Let now $u, v \in \mathbb{R}^3$ be such that for all $t \in [0,1]$

$$w_t := v + t(u - v)$$

is different from zero. Then

$$|\lambda(|u|)u - \lambda(|v|)v| \leq \int_0^1 \left| \frac{\mathrm{d}}{\mathrm{d}t}(\lambda(|w_t|)w_t) \right| \mathrm{d}t \leq C \int_0^1 \frac{|u-v|^{1/2}}{|w_t|^{1/2}} \, \mathrm{d}t |u-v|^{1/2}.$$

Set

$$a := \frac{v}{|u-v|} \quad \text{and} \quad b := \frac{u-v}{|u-v|}$$

then $|b| = 1$ and we have

$$\int_0^1 \frac{|u-v|^{1/2}}{|w_t|^{1/2}} \, \mathrm{d}t = \int_0^1 \frac{\mathrm{d}t}{|a+tb|^{1/2}} \leq 2 \int_0^{1/2} \frac{\mathrm{d}s}{\sqrt{s}} < \infty.$$

Thus for a.e. $u, v \in \mathbb{R}^3 \backslash \{0\}$

$$|\lambda(|u|)u - \lambda(|v|)v| \leq C|u-v|^{1/2}.$$

By continuity this holds for all $u, v \neq 0$ and due to the Hölder continuity this holds for all $u, v \in \mathbb{R}^3$. □

In this thesis we use the QUMOND formulation of MOND. In her master thesis Keller (2016) used the AQUAL[6] formulation of MOND. Keller proved under the assumption of spherical symmetry that there exist global, weak solutions to the initial value problem for the Vlasov-AQUAL system. In spherical symmetry AQUAL and QUMOND are equivalent because in both formulations the Mondian field ∇U^M and the Newtonian field ∇U^N are connected via

$$\nabla U^M = \nabla U^N + \lambda(|\nabla U^N|)\nabla U^N$$

and no further corrections have to be made. However, Keller used a slightly different formulation of the above relation between ∇U^M and ∇U^N. Instead of using a function λ on the right side of the equation, she used a function μ on the left side of the equation. The above equation becomes then

$$\mu(|\nabla U^M|)\nabla U^M = \nabla U^N.$$

Keller made several assumption on the function μ. Since we want to use her existence result in this thesis, the following lemma shows how λ and μ are connected and which assumptions we have to make on λ such that the corresponding μ satisfies the assumptions made in Keller (2016)

Lemma 3.3.2. *Let $a_1^* < 1 < a_2^*$ and λ be continuously differentiable on $(0, \infty)$ with*

$$\lambda(\sigma) = \begin{cases} 1/\sqrt{\sigma} - 1 & , \sigma \leq (a_1^*)^2 \\ 0 & , \sigma \geq a_2^* \end{cases}$$

and

$$-\frac{1+\lambda(\sigma)}{\sigma} < \lambda'(\sigma) < 0$$

for $(a_1^*)^2 < \sigma < a_2^*$. This λ satisfies (Λ1) - (Λ3). Further

$$\tilde{\nu}(\sigma) := \sigma(1+\lambda(\sigma))$$

is strictly increasing for $\sigma > 0$, $\tilde{\mu} := \tilde{\nu}^{-1}$ exists and $\mu(\tau) := \tilde{\mu}(\tau)/\tau$ is continuously differentiable on $[0, \infty)$ with

$$\mu(\tau) = \begin{cases} \tau & , \tau \leq a_1^* \\ 1 & , \tau \geq a_2^* \end{cases}$$

and

$$\mu'(\tau) > 0$$

for $a_1^* < \tau < a_2^*$. So μ satisfies all assumptions from Keller (2016).

[6] The theory is called AQUAL because the field equation derives from an aquadratic Lagrangian (Famaey & McGaugh, 2012). The theory was introduced by Bekenstein & Milgrom (1984).

Proof. From the explicit form of λ and its C^1-regularity it follows directly that λ satisfies (Λ1) - (Λ3) Since

$$\tilde{\nu}'(\sigma) = 1 + \lambda(\sigma) + \sigma\lambda'(\sigma) > 0, \quad \sigma > 0,$$

$\tilde{\nu}$ is strictly increasing and both $\tilde{\mu} := \tilde{\nu}^{-1}$ and $\mu(\tau) := \tilde{\mu}(\tau)/\tau$, $\tau > 0$ exist. The formulae for $\mu(\tau)$ for τ small and τ large follow directly from the respective formulae for $\lambda(\sigma)$. It is also clear that μ is continuously differentiable on $[0, \infty)$. It remains to prove the monotonicity of μ. The monotonicity of λ implies

$$\tilde{\nu}'(\sigma) < 1 + \lambda(\sigma) = \frac{\tilde{\nu}(\sigma)}{\sigma}, \quad \text{for } 0 < \sigma < a_2^*.$$

Since

$$\tilde{\nu}'(\sigma) = (\tilde{\mu}^{-1})'(\sigma) = \frac{1}{\tilde{\mu}'(\tilde{\nu}(\sigma))},$$

the above inequality translates into

$$\tilde{\mu}'(\tau) > \frac{\tilde{\mu}(\tau)}{\tau},$$

where we have replaced $\tau = \tilde{\nu}(\sigma) \in (0, a_2^*)$. This implies the monotonicity of μ since

$$\tau\mu'(\tau) = (\tau\mu(\tau))' - \mu(\tau) = \tilde{\mu}'(\tau) - \frac{\tilde{\mu}(\tau)}{\tau} > 0.$$

□

In Section 4 it will be sufficient to work with the definition (3.3). We will derive the regularity of the field ∇U^M using the assumption (Λ2) and the regularity of the field ∇U^N. We do not need the Mondian potential U^M explicitly. In Section 5 however we study a variational problem. And for proving that the Euler-Lagrange equation holds, which belongs to this problem, it is important to have an explicit form of the potential U^M. In Lemma 3.2.3 we have seen that for a vector field

$$v \in C_c^2(\mathbb{R}^3)$$

Hv is the gradient of

$$\frac{1}{4\pi}\sum_{j=1}^{3} \partial_{x_j} U_{v_j}^N.$$

But if $\rho \in L^1 \cap L^p(\mathbb{R}^3)$ for a $1 < p < 3$,

$$\nabla U_\rho^N \in L^q(\mathbb{R}^3)$$

for a $3/2 < q < \infty$ and

$$v := \lambda\left(|\nabla U_\rho^N|\right) \nabla U_\rho^N \in L^{2q}(\mathbb{R}^3)$$

provided (Λ2) holds. But then $\partial_{x_j} U_{v_j}^N$ is not well defined. However we can still recover a slight variation of Lemma 3.2.3.

Lemma 3.3.3. *Assume that (Λ2) holds and let $\rho \in L^1 \cap L^p(\mathbb{R}^3)$ for a $1 < p < 3$ and let $3/2 < q < \infty$ with $2/3 + 1/p = 1 + 1/q$. Set*

$$U_\rho^\lambda(x) := \frac{1}{4\pi}\int \lambda\left(|\nabla U_\rho^N(y)|\right) \nabla U_\rho^N(y) \cdot \left(\frac{x-y}{|x-y|^3} + \frac{y}{|y|^3}\right) \mathrm{d}y, \quad x \in \mathbb{R}^3.$$

Then

$$U_\rho^\lambda \in W_{loc}^{1,2q}(\mathbb{R}^3)$$

and

$$\nabla U_\rho^\lambda = H\left(\lambda\left(|\nabla U_\rho^N|\right) \nabla U_\rho^N\right) \in L^{2q}(\mathbb{R}^3).$$

Further

$$U_\rho^M := U_\rho^N + U_\rho^\lambda \in W_{loc}^{1,q}(\mathbb{R}^3) + W_{loc}^{1,2q}(\mathbb{R}^3)$$

with weak derivative

$$\nabla U_\rho^M = \nabla U_\rho^N + H\left(\lambda\left(|\nabla U_\rho^N|\right) \nabla U_\rho^N\right) \in L^q(\mathbb{R}^3) + L^{2q}(\mathbb{R}^3).$$

Proof. Let $R > 0$. First we prove that for

$$I(x,y) := \lambda\left(|\nabla U_\rho^N(y)|\right)\nabla U_\rho^N(y)\cdot\left(\frac{x-y}{|x-y|^3}+\frac{y}{|y|^3}\right),\quad x,y\in\mathbb{R}^3,$$

holds

$$\iint_{|x|\le R}|I(x,y)|\,\mathrm{d}x\,\mathrm{d}y<\infty. \tag{3.5}$$

Let p,q be as stated above and let r be the dual exponent of $2q$. Since $3<2q<\infty$,

$$1<r<\frac{3}{2}.$$

Then

$$\begin{aligned}\iint_{|x|\le R,|y|\le 2R}|I(x,y)|\,\mathrm{d}x\,\mathrm{d}y &\le \Lambda_2\iint_{|x|\le R,|y|\le 2R}|\nabla U_\rho^N(y)|^{1/2}\left(\frac{1}{|x-y|^2}+\frac{1}{|y|^2}\right)\mathrm{d}x\,\mathrm{d}y\\ &\le 2\Lambda_2\mathcal{L}(B_R)\|\nabla U_\rho^N\|_q^{1/2}\left\|\frac{1}{|y|^2}\right\|_{L^r(B_{3R})}<\infty.\end{aligned}$$

Next observe that for all $y\in\mathbb{R}^3\backslash\{0\}$, $i,j=1,2,3$

$$\left|\partial_{y_i}\frac{y_j}{|y|^3}\right| = \left|\frac{\delta_{ij}}{|y|^3}-3\frac{y_iy_j}{|y|^5}\right|\le\frac{4}{|y|^3}.$$

Thus for $x,y\in\mathbb{R}^3$ with $|x|\le R$, $|y|>2R$ holds

$$\left|\frac{x_j-y_j}{|x-y|^3}-\frac{y_j}{|y|^3}\right| = \left|\int_0^1\frac{\mathrm{d}}{\mathrm{d}s}\frac{y_j-sx_j}{|y-sx|^3}\,\mathrm{d}s\right|\le R\int_0^1\frac{\mathrm{d}s}{|y-sx|^3}.$$

Since for all $0\le s\le 1$

$$|y-sx|\ge\frac{|y|}{2},$$

we estimate further

$$\left|\frac{x_j-y_j}{|x-y|^3}-\frac{y_j}{|y|^3}\right|\le\frac{8R}{|y|^3}.$$

Hence

$$\begin{aligned}\iint_{|x|\le R,|y|>2R}|I(x,y)|\,\mathrm{d}x\,\mathrm{d}y &\le C\iint_{|x|\le R,|y|>2R}|\nabla U_\rho^N(y)|^{1/2}\frac{1}{|y|^3}\,\mathrm{d}y\\ &\le C\mathcal{L}(B_R)\|\nabla U_\rho^N\|_q^{1/2}\left\|\frac{1}{|y|^3}\right\|_{L^r(\{|y|>2R\})}\\ &<\infty.\end{aligned}$$

Thus (3.5) holds. Fubini then implies that

$$U_\rho^\lambda\in L^1_{loc}(\mathbb{R}^3).$$

It remains to prove that

$$\nabla U_\rho^\lambda = H\left(\lambda\left(|\nabla U_\rho^N|\right)\nabla U_\rho^N\right).$$

We write shortly

$$v := \frac{1}{4\pi}\lambda\left(|\nabla U_\rho^N|\right)\nabla U_\rho^N\in L^{2q}(\mathbb{R}^3).$$

Let $\phi\in C_c^\infty(\mathbb{R}^3)$. Then

$$\int U_\rho^\lambda\partial_{x_i}\phi\,\mathrm{d}x = \iint v(y)\cdot\left(\frac{x-y}{|x-y|^3}+\frac{y}{|y|^3}\right)\partial_{x_i}\phi(x)\,\mathrm{d}y\,\mathrm{d}x.$$

Thanks to (3.5) we can apply Fubini and, since

$$\int\partial_{x_i}\phi(x)\,\mathrm{d}x = 0,$$

we have

$$\int U_\rho^\lambda \partial_{x_i}\phi \,\mathrm{d}x = -\int v\cdot\nabla U^N_{\partial_{x_i}\phi}\,\mathrm{d}y = -\sum_{j=1}^3 \int v_j \partial_{y_i}\partial_{y_j} U_\phi^N \,\mathrm{d}y.$$

Lemma 3.1.3 and Proposition 3.1.2 imply

$$\int U_\rho^\lambda \partial_{x_i}\phi \,\mathrm{d}x = -\sum_{j=1}^3 \lim_{\epsilon\to 0}\int v_j \left(T_{ij}^\epsilon \phi + \delta_{ij}\frac{4\pi}{3}\phi\right)\mathrm{d}y.$$

As in the proof of Lemma 3.2.8 we have

$$\int v_j\, T_{ij}^\epsilon \phi \,\mathrm{d}y = \int T_{ij}^\epsilon v_j\, \phi \,\mathrm{d}y.$$

Hence

$$\begin{aligned}\int U_\rho^\lambda \partial_{x_i}\phi \,\mathrm{d}x &= -4\pi \int \left(\sum_{j=1}^3 T_{ij}v_j + \frac{1}{3}v_i\right)\phi \,\mathrm{d}y \\ &= -4\pi \int H_i v\, \phi \,\mathrm{d}y.\end{aligned}$$

Thus

$$\nabla U_\rho^\lambda = 4\pi H v = H\left(\lambda\left(|\nabla U_\rho^N|\right)\nabla U_\rho^N\right).$$

In particular, the Helmholtz-Weyl decomposition Theorem 3.2.6 implies

$$U_\rho^\lambda \in W^{1,2q}_{loc}(\mathbb{R}^3).$$

As in the proof of Lemma 3.1.4 we see that $U_\rho^N \in L^{q'}(\mathbb{R}^3)$ for some $q' > q$. Thus

$$U_\rho^N \in W^{1,q}_{loc}(\mathbb{R}^3)$$

with

$$\nabla U_\rho^N \in L^q(\mathbb{R}^3).$$

So we have

$$U_\rho^M := U_\rho^N + U_\rho^\lambda \in W^{1,q}_{loc}(\mathbb{R}^3) + W^{1,2q}_{loc}(\mathbb{R}^3)$$

□

When we deal with a spherically symmetric density ρ, the following lemma holds

Lemma 3.3.4. *Assume that (Λ3) holds and let $1 < p < 3$. If $\rho \in L^1 \cap L^p(\mathbb{R}^3)$ is spherically symmetric,*

$$U_\rho^N,\, U_\rho^\lambda \in C^1(\mathbb{R}^3\backslash\{0\})$$

and for $x \in \mathbb{R}^3\backslash\{0\}$, $r = |x|$ holds

$$U_\rho^M(r) = U_\rho^M(1) + \int_1^r \left(1 + \lambda\left(\frac{M(s)}{s^2}\right)\right)\frac{M(s)}{s^2}\,\mathrm{d}s$$

under a slight abuse of notation.

Proof. Lemma 3.1.5 tells us that

$$\nabla U_\rho^N(x) = \frac{M(r)}{r^2}\frac{x}{r}, \quad x \in \mathbb{R}^3\backslash\{0\},\ r = |x|.$$

Since $\rho \in L^1(\mathbb{R}^3)$

$$M(r) \in C([0,\infty)).$$

Hence

$$\nabla U_\rho^N \in C(\mathbb{R}^3\backslash\{0\}).$$

Since (Λ3) holds, the map

$$\mathbb{R}^3 \ni u \mapsto \lambda(|u|)u$$

is continuous (Lemma 3.3.1). Since by Lemma 3.2.7

$$\nabla U_\rho^\lambda = H\left(\lambda\left(|\nabla U_\rho^N|\right)\nabla U_\rho^N\right) = \lambda\left(|\nabla U_\rho^N|\right)\nabla U_\rho^N,$$

if follows

$$\nabla U_\rho^\lambda \in C(\mathbb{R}^3\backslash\{0\}).$$

Hence

$$U_\rho^\lambda,\, U_\rho^N \in C^1(\mathbb{R}^3\backslash\{0\})$$

and by the fundamental theorem of calculus

$$U_\rho^M(r) = U_\rho^N(r) + U_\rho^\lambda(r) = U_\rho^M(1) + \int_1^r \left(1 + \lambda\left(\frac{M(s)}{s^2}\right)\right)\frac{M(s)}{s^2}\,\mathrm{d}s.$$

□

3.4 Absolutely continuous functions

In Section 4 we examine weak Eulerian and weak Lagrangian solutions of the (VQMS). The Lagrangian solutions will only have absolutely continuous characteristics. Therefore we devote this small section to the topic of absolutely continuous functions.

Definition 3.4.1. A point-wise defined function $h : [0,T] \to \mathbb{R}$, $T > 0$, is absolutely continuous iff there is a function $h' \in L^1((0,T))$ such that for all $t \in [0,T]$

$$h(t) = h(0) + \int_0^t h'(s)\,\mathrm{d}s.$$

Obviously every absolutely continuous function is also continuous. Further the following characterization of absolutely continuous functions is important.

Lemma 3.4.2. *A function h is absolutely continuous on $[0,T]$ iff $h \in W^{1,1}((0,T))$. h' from Definition 3.4.1 and the weak derivative of $h \in W^{1,1}((0,T))$ are identical.*

Proof. Let h be absolutely continuous with

$$h(t) = h(0) + \int_0^t h'(s)\,\mathrm{d}s, \quad 0 \le t \le T,$$

and take $\phi \in C_c^\infty((0,T))$. Then

$$\begin{aligned}\int_0^T h(t)\phi'(t)\,\mathrm{d}t &= \int_0^T \left(h(0) + \int_0^t h'(s)\,\mathrm{d}s\right)\phi'(t)\,\mathrm{d}t \\ &= \int_0^T h'(s)\int_s^T \phi'(t)\,\mathrm{d}t\,\mathrm{d}s \\ &= -\int_0^T h'(s)\phi(s)\,\mathrm{d}s.\end{aligned}$$

Thus $h \in W^{1,1}((0,T))$ with weak derivative h'.

Let now be $h \in W^{1,1}((0,T))$ and denote by h' the weak derivative of h. We define the absolutely continuous function

$$\tilde{h}(t) := \int_0^t h'(s)\,\mathrm{d}s, \quad 0 \le t \le T.$$

Then we know that $\tilde{h} \in W^{1,1}((0,T))$, too, and both h and $\tilde{h}$ have the same weak derivative. Hence h and $\tilde{h}$ defer only by a constant (Lieb & Loss, 2010, Theorems 6.10. and 6.11.). In particular h is continuous, too, and, since

$$\tilde{h}(0) = 0,$$

we have for all $0 \le t \le T$

$$h(t) = h(0) + \tilde{h}(t) = h(0) + \int_0^t h'(s)\,\mathrm{d}s.$$

Thus h is absolutely continuous. □

It is know that the chain rule holds for functions in $W^{1,1}((0,T))$. Let us transfer this result to absolutely continuos functions.

Lemma 3.4.3 (Chain rule)**.** *Let $G \in C^1(\mathbb{R}^n;\mathbb{R})$, $n \in \mathbb{N}$, and let $h : [0,T] \to \mathbb{R}^n$ be absolutely continuous. Then $G \circ h$ is absolutely continuous on $[0,T]$ and the chain rule holds, i.e.,*

$$(G \circ h)'(t) = \nabla G(h(t)) \cdot h'(t), \quad 0 \le t \le T.$$

Proof. Theorem 6.16 of Lieb & Loss (2010) states that the lemma holds, provided ∇G is bounded. Since h is continuous, $h([0,T])$ is a bounded subset of $\mathbb{R}^n$ and

$$h([0,T]) \subset B_R$$

for an $R > 0$ large enough. Let us now replace G by a function $\tilde{G} \in C_c^1(\mathbb{R}^n)$ such that $\tilde{G} = G$ on B_R. Then $\nabla\tilde{G}$ is bounded and the statement of the lemma holds for $\tilde{G} \circ h$. Since $\tilde{G} \circ h(t) = G \circ h(t)$ and $\nabla\tilde{G}(h(t)) = \nabla G(h(t))$ for all $t \in [0,T]$, the statement of the lemma holds for $G \circ h$, too. □

Last in this chapter let us take a look on integration by parts for absolutely continuous functions.

Lemma 3.4.4 (Integration by parts)**.** *Let g, h be absolutely continuous on $[0,T]$, $T > 0$. Then for all $0 \le t_1 \le t_2 \le T$*

$$\int_{t_1}^{t_2} g'(s)h(s)\,\mathrm{d}s = g(t_2)h(t_2) - g(t_1)h(t_1) - \int_{t_1}^{t_2} g(s)h'(s)\,\mathrm{d}s.$$

Proof. Using the definition of absolutely continuous functions we get

$$\begin{aligned}\int_{t_1}^{t_2} g'(s)h(s)\,\mathrm{d}s &= \int_{t_1}^{t_2} g'(s)\left(h(t_1) + \int_{t_1}^{s} h'(\sigma)\,\mathrm{d}\sigma\right)\mathrm{d}s \\ &= (g(t_2) - g(t_1))h(t_1) + \int_{t_1}^{t_2}\int_{\sigma}^{t_2} g'(s)\,\mathrm{d}s\, h'(\sigma)\,\mathrm{d}\sigma \\ &= g(t_2)h(t2) - g(t_1)h(t_1) - \int_{t_1}^{t_2} g(\sigma)h'(\sigma)\,\mathrm{d}\sigma.\end{aligned}$$

□

3.5 Weak flow of $\dot{z} = b(s,z)$

Consider a test particle that is at time $t \ge 0$ at position $x \in \mathbb{R}^3$ and has velocity $v \in \mathbb{R}^3$. If this particle moves in a gravitational field $F(s,x)$, $s \ge 0$, its trajectory $(X(s), V(s))$ is a solution of the ODE

$$\begin{aligned}\dot{X} &= V, \\ \dot{V} &= F(s,X)\end{aligned} \tag{3.6}$$

with initial condition $X(t) = x$, $V(t) = v$. Alternatively – introducing the notation $z = (x,v)$, $Z = (X,V)$ and $b(s,z) = (v, F(s,x))$ – we can say the trajectory is a solution of

$$\dot{Z} = b(s,Z) \tag{3.7}$$

with initial condition $Z(t) = z$. If b is continuous and Lipschitz continuous with respect to z, the Cauchy-Lipschitz theorem provides global solutions to the ODE (3.7), which have many nice properties. However, in Mondian physics $|F|$ behaves like a square root when $|F|$ is close to zero. Thus, at most, we can expect b to be Hölder continuous with respect to z, but not Lipschitz, and the Cauchy-Lipschitz theorem will not help us any further. Fortunately, DiPerna & Lions (1989b) generalized the classical Cauchy-Lipschitz theory and provide solutions to the ODE (3.7) – sharing almost the same nice properties as the classical solutions – under much weaker assumptions. The major change in their theory is that they replace the assumption

$$b(s,\cdot) \text{ must be Lipschitz}$$

by

$$b(s,\cdot) \in W^{1,1}_{loc}(\mathbb{R}^3).$$

In this chapter we study the flow of the above ODE in the context of the DiPerna-Lions theory.

Definition 3.5.1. Let $b : [0,T] \times \mathbb{R}^6 \to \mathbb{R}^6$ and $Z : [0,T] \times [0,T] \times \mathbb{R}^6 \to \mathbb{R}^6$ be measurable. We call Z a weak, measure preserving flow of the ODE (3.7) iff Z satisfies (Z1) - (Z3).

(Z1) For all $t \in [0,T]$ and for a.e. $z \in \mathbb{R}^6$

$$b(\cdot, Z(\cdot,t,z)) \in L^1([0,T])$$

and $Z(\cdot,t,z)$ is absolutely continuous on $[0,T]$ with

$$Z(s,t,z) = z + \int_t^s b(\sigma, Z(\sigma,t,z))\,\mathrm{d}\sigma$$

for all $s \in [0,T]$.

(Z2) For all $t_1, t_2, t_3 \in [0,T]$

$$Z(t_1,t_2,Z(t_2,t_3,z)) = Z(t_1,t_2,z)$$

for a.e. $z \in \mathbb{R}^3$.

(Z3) For all $s,t \in [0,T]$ and $\Omega \subset \mathbb{R}^6$ measurable

$$\mathcal{L}(Z(s,t,\Omega)) = \mathcal{L}(\Omega)$$

The definition of a flow that preserves measure makes only sense if $\mathrm{div}_z\, b = 0$ like it is the case in the ODE 3.6, in which we are interested. This becomes clear in the proof of Theorem 3.5.4.

The following lemma lists two important properties of a weak, measure preserving flow.

Lemma 3.5.2. *Let $b : [0,T] \times \mathbb{R}^6 \to \mathbb{R}^6$ be measurable, $T > 0$, and Z be a weak, measure preserving flow of* (3.7)*. Then (Z4) and (Z5) hold:*

(Z4) For all $s,t \in [0,T]$

$$Z(s,t,Z(t,s,z)) = z$$

for a.e. $z \in \mathbb{R}^3$.

(Z5) For all $s,t \in [0,T]$ and $g \in L^1(\mathbb{R}^6)$

$$\int g(z)\,\mathrm{d}z = \int g(Z(s,t,z))\,\mathrm{d}z.$$

Proof. (Z4) follows directly from (Z1) and (Z2): Let $z \in \mathbb{R}^6$ be such that $Z(s,t,Z(t,s,z)) = Z(s,s,z)$ and such that $Z(\cdot,s,z)$ is absolutely continuous with weak derivative $b(\cdot, Z(\cdot,s,z))$. This holds for a.e. $z \in \mathbb{R}^6$. Then

$$Z(s,t,Z(t,s,z)) = Z(s,s,z) = z + \int_s^s b(\sigma, Z(\sigma,s,z))\,\mathrm{d}\sigma = z.$$

(Z5) follows from (Z4) and (Z3): W.l.g. $g \geq 0$. Then

$$\begin{aligned}\int g(z)\,\mathrm{d}z &= \int_0^\infty \mathcal{L}(\{g > \alpha\})\,\mathrm{d}\alpha = \int_0^\infty \mathcal{L}(Z(t,s,\{g>\alpha\}))\,\mathrm{d}\alpha = \\ &= \int_0^\infty \mathcal{L}(\{g \circ Z(s,t,\cdot) > \alpha\})\,\mathrm{d}\alpha = \int g(Z(s,t,z))\,\mathrm{d}z,\end{aligned}$$

which is the desired statement. Only the argument

$$\mathcal{L}(Z(t,s,\{g>\alpha\})) = \mathcal{L}(\{g \circ Z(s,t,\cdot) > \alpha\}), \quad \text{for } \alpha > 0,$$

deserves still some more attention. This would be clear if $Z(t,s,\cdot)$ would be a bijective function with inverse $Z(s,t,\cdot)$, however, according to (Z2), it is only bijective on $\mathbb{R}^6$ up to a set of measure zero. Set therefore

$$\begin{aligned}N &:= \{z \in \mathbb{R}^6 | Z(s,t,Z(t,s,z)) \neq z\},\\ M &:= \{\zeta \in \mathbb{R}^6 | Z(t,s,Z(s,t,\zeta)) \neq \zeta\}.\end{aligned}$$

Then $\mathcal{L}(N) = \mathcal{L}(M) = 0$ and

$$Z(t, s, \cdot) : \mathbb{R}^6 \backslash N \to \mathbb{R}^6 \backslash M$$

is bijective with inverse $Z(s, t, \cdot)$: That $Z(t, s, \cdot)$ is injective is clear from the definition of N. To see that it is also surjective take $\zeta \in \mathbb{R}^6 \backslash M$ and set $z := Z(s, t, \zeta)$. Then

$$Z(t, s, z) = Z(t, s, Z(s, t, \zeta)) = \zeta.$$

$z \in \mathbb{R}^6 \backslash N$ since

$$Z(s, t, Z(t, s, z)) = Z(s, t, Z(t, s, Z(s, t, \zeta))) = Z(s, t, \zeta) = z.$$

Thus $Z(t, s, \cdot)$ is surjective, hence it is bijective. This implies that

$$Z(t, s, \{g > \alpha\} \backslash N) = \{g \circ Z(s, t, \cdot) > \alpha\} \backslash M.$$

Since the flow is measure preserving it maps sets of measure zero onto sets of measure zero and we get

$$\begin{aligned} \mathcal{L}(Z(t, s, \{g > \alpha\})) &= \mathcal{L}(Z(t, s, \{g > \alpha\} \backslash N)) \\ &= \mathcal{L}(\{g \circ Z(s, t, \cdot) > \alpha\} \backslash M) \\ &= \mathcal{L}(\{g \circ Z(s, t, \cdot) > \alpha\}). \end{aligned}$$

□

Notation 3.5.3. Let $T > 0$, $1 \leq p, q \leq \infty$, $n \in \mathbb{N}$, $\Omega \subseteq \mathbb{R}^n$ measurable and $U \subseteq \mathbb{R}^n$ open. By

$$L^q(0, T; L^p(\Omega))$$

and

$$L^q(0, T; W^{1,p}(U))$$

we denote the usual Bochner spaces. We use further the two spaces

$$L^q(0, T; L^p_{loc}(\mathbb{R}^n))$$

and

$$L^q(0, T; W^{1,p}_{loc}(\mathbb{R}^n))$$

where a function

$$f : [0, T] \to L^p_{loc}(\mathbb{R}^n)$$

belongs to the space $L^q(0, T; L^p_{loc}(\mathbb{R}^n))$ iff for every $R > 0$ the function

$$f : [0, T] \to L^p(B_R), t \mapsto f(t)|_{B_R}$$

is in $L^q(0, T; L^p(B_R))$; the definition of the space $L^q(0, T; W^{1,p}_{loc}(\mathbb{R}^n))$ is analogue.

Theorem 3.5.4 (DiPerna-Lions)**.** *Let $F \in L^1(0, T; W^{1,1}_{loc}(\mathbb{R}^3)) \cap L^\infty(0, T; L^\infty(\mathbb{R}^3))$, $T > 0$. Then there exists a weak, measure preserving flow $Z = (X, V)$ of the ODE* (3.6) *that has the property that for every $R > 0$ there exists an $R' > 0$ such that for a.e. $z \in B_R$ and every $s \in [0, T]$*

$$|Z(s, 0, z)| \leq R'.$$

Remark 3.5.5. DiPerna & Lions (1989b) also prove uniqueness of the flow Z, but since we will not make use of the uniqueness statement, we skip its treatment.

Proof. We want to apply Theorem III.3[7] on page 539 of DiPerna & Lions (1989b). When in this proof we use a page number or a reference to an equation, we mean always the respective page or equation in the paper DiPerna & Lions (1989b).

First we have to verify that the right hand side of our ODE satisfies $(*)$ and $(**)$ on page 520. This is trivial since $(v, F(s, x))$ is obviously divergence free and the assumptions on F guarantee that

$$(v, F(s, x)) \in L^1(0, T; W^{1,1}_{loc}(\mathbb{R}^6))$$

[7] Observe that there is an error of numbering in DiPerna & Lions (1989b). Theorem III.2 exists twice: One time on page 537 and a second time on page 539. We need the second theorem and we will refer to it as Theorem III.3 throughout this thesis.

and

$$\frac{|v| + |F(s,x)|}{1 + |x| + |v|} \in L^1(0,T; L^\infty(\mathbb{R}^6)).$$

Define

$$L := \{\phi : \mathbb{R}^6 \to \mathbb{R} \text{ measureable with } |\phi| < \infty \text{ a.e.}\}$$

like on page 532. Then there exists by Theorem III.3 of DiPerna & Lions (1989b) a

$$Z = (X, V) : [0,T] \times [0,T] \to L^N$$

that is a solution of the initial value problem for the ODE 3.6 in the sense of (77). This Z satisfies (Z2) and (Z3); to see (Z3) one has to combine equation (74) with (75) and use that the divergence of $b(s,z) = (v, F(s,x))$ vanishes. Since we assumed that $F \in L^\infty(0,T; L^\infty(\mathbb{R}^3))$, Theorem III.3 of DiPerna & Lions (1989b) implies further that

$$Z \in C\left([0 \le t \le T]; L^\infty_{loc}(\mathbb{R}^6; C([0 \le s \le T]))\right)^{8}.$$

In particular $Z : [0,T] \times [0,T] \times \mathbb{R}^6 \to \mathbb{R}^6$ is measurable and for every $R > 0$ exists an $R' > 0$ such that for a.e. $z \in B_R$ and every $s \in [0,T]$ holds

$$|Z(s,0,z)| \le R'.$$

It remains to prove (Z1). We use the notation

$$b(s,z) = (v, F(s,x)), \quad s \in [0,T], z = (x,v) \in \mathbb{R}^6.$$

Then equation (80) implies that for all $t \in [0,T]$ and almost every $z \in \mathbb{R}^6$ holds:

$$Z(\cdot, t, z) \in W^{1,1}((0,T))$$

with weak derivative

$$\partial_s Z(s,t,z) = b(s, Z(s,t,z)), \quad s \in (0,T).$$

Thus Lemma 3.4.2 implies that $Z(\cdot,t,z)$ is absolutely continuous with

$$Z(s,t,z) = Z(t,t,z) + \int_t^s b(\sigma, Z(\sigma,t,z))\,\mathrm{d}\sigma, \quad s \in [0,T].$$

Fix an arbitrary $t \in [0,T]$. It remains to prove that $Z(t,t,z) = z$ for a.e. $z \in \mathbb{R}^6$. Below we will write shortly

$$Z(s) = Z(s,t,z).$$

Let $\beta \in C_c^\infty(\mathbb{R}^6)$ be a vector field, then for a.e. $z \in \mathbb{R}^6$ the chain rule for absolutely continuous functions (Lemma 3.4.3) implies that $\beta_i \circ Z(\cdot,t,z)$ is absolutely continuos, too, with weak derivative

$$\partial_s \beta_i(Z(s)) = \nabla \beta_i(Z(s)) \cdot b(s, Z(s)), \quad s \in [0,T]$$

for each $i = 1, \dots, 6$. Hence for every $\phi \in C_c^\infty([t,T) \times \mathbb{R}^6)$ integration by parts (Lemma 3.4.4) yields

$$\begin{aligned}\int\int_t^T \nabla\beta_i(Z(s)) \cdot b(s,Z(s))\phi(s,z)\,\mathrm{d}s\,\mathrm{d}z = \\ = -\int \beta_i(Z(t))\phi(t,z)\,\mathrm{d}z - \int\int_t^T \beta_i(Z(s))\partial_s\phi(s,z)\,\mathrm{d}s\,\mathrm{d}z.\end{aligned}$$

Now we exploit that Z is a solution of the initial value problem for the ODE (3.7) in the sense of (77). Observe that β is an admissible function as defined on page 532. That (77) holds in distributions sense, means

$$\begin{aligned}\int\int_t^T \nabla\beta_i(Z(s)) \cdot b(s,Z(s))\phi(s,z)\,\mathrm{d}s\,\mathrm{d}z = \\ = -\int \beta_i(z)\phi(t,z)\,\mathrm{d}z - \int\int_t^T \beta_i(Z(s))\partial_s\phi(s,z)\,\mathrm{d}s\,\mathrm{d}z;\end{aligned}$$

[8] Observe that there is one excess bracket in (DiPerna & Lions, 1989b, Theorem III.3). The statement $L^p_{loc}(\mathbb{R}^N); C([0 \le s < \infty)))$ should be $L^p_{loc}(\mathbb{R}^N; C([0 \le s < \infty)))$

for the notion of solution in distributions sense compare page 514. Since we can choose ϕ of the form

$$\phi(s,z) = w(z)\psi(s,z), \quad s \in [t,T],\ z \in \mathbb{R}^6,$$

where $w \in C_c^\infty(\mathbb{R}^6)$ is arbitrary and $\psi \in C_c^\infty((-\infty,T)\times\mathbb{R}^6)$ is such that $\psi = 1$ on $\{t\}\times \operatorname{supp} w$, the lemma of du Bois-Reymond implies that

$$\beta_i(Z(t,t,z)) = \beta_i(z) \tag{3.8}$$

for a.e. $z \in \mathbb{R}^6$. Assume that

$$N := \{z \in \mathbb{R}^6 | Z(t,t,z) \neq z\}$$

has positive measure. Then there is an $R > 0$ such that

$$N_R := \{z \in B_R | Z(t,t,z) \neq z\}$$

has positive measure. Since Z preserves measure there is an $R' > R$ such that

$$Z(t,t,N_R) \cap B_{R'}$$

has positive measure. Let $\beta \in C_c^\infty(\mathbb{R}^6)$ be such that $\beta(z) = z$ on $B_{R'}$. Then

$$\beta_i(Z(t,t,z)) \neq \beta_i(z)$$

for all $z \in N_R$ with $Z(t,t,z) \in B_{R'}$. But this set has positive measure contradicting (3.8). This shows that (Z1) holds.

□

4 Time dependent solutions of the (VQMS)

As stated in the introduction we search distribution functions $f = f(t,x,v)$ that are solutions of the Vlasov-QUMOND system (VQMS):

$$\begin{aligned}
&\partial_t f + v\cdot\partial_x f - \partial_x U_f^M \cdot \partial_v f = 0,\\
&\partial_x U_f^M = \partial_x U_f^N + H\left(\lambda(|\partial_x U_f^N|)\partial_x U_f^N\right),\\
&U_f^N(t,x) = -\int \frac{\rho_f(t,y)}{|x-y|}\,\mathrm{d}y,\\
&\rho_f(t,x) = \int f(t,x,v)\,\mathrm{d}v.
\end{aligned}$$

The term $H(\lambda(|\partial_x U_f^N|)\partial_x U_f^N)$ makes the difference between the Vlasov-QUMOND system studied here in this thesis and the Vlasov-Poisson system that is, e.g., studied extensively in Rein (2007). The term $\lambda(|\partial_x U_f^N|)\partial_x U_f^N$ is the MOND-correction and H extracts the irrotational part of it thus taking care that $\partial_x U_f^M$ is indeed the gradient of some potential.

Now we introduce the notion of weak solutions for the initial value problem of the (VQMS). We distinguish between Eulerian and Lagrangian solutions.

4.1 Weak Eulerian and weak Lagrangian solutions

We assume throughout this section that $T > 0$ and $1 < p,q < \infty$ with

$$\frac{1}{p} + \frac{1}{q} = 1.$$

Further we assume that $\mathring{f} \in L^p(\mathbb{R}^6)$, ≥ 0. We do not make explicit assumptions on λ. We admit any λ that is sufficiently regular such that

$$\partial_x U_f^M \in L^1(0,T;L^q_{loc}(\mathbb{R}^3))$$

exists (The subscript f refers to the weak Eulerian and weak Lagrangian solutions defined next).

Definition 4.1.1. We call a function

$$f : [0,T] \times \mathbb{R}^6 \to \mathbb{R}$$

a weak Eulerian solution of the (VQMS) with initial condition $\mathring{f}$ iff

$$f \in L^\infty(0,T; L^p_+(\mathbb{R}^6)),$$

it exists

$$\partial_x U_f^M \in L^1(0,T; L^q_{loc}(\mathbb{R}^3))$$

and for all $\phi \in C_c^\infty([0,T) \times \mathbb{R}^6)$ holds

$$\int_0^T \int f(\partial_t \phi + v \cdot \partial_x \phi - \partial_x U_f^M \cdot \partial_v \phi) \,\mathrm{d}z \,\mathrm{d}t + \int \mathring{f}\phi(0,z) \,\mathrm{d}z = 0.$$

Definition 4.1.2. We call a function

$$f : [0,T] \times \mathbb{R}^6 \to \mathbb{R}$$

a weak Lagrangian solution of the (VQMS) with initial condition $\mathring{f}$ iff there exists both

$$\partial_x U_f^M \in L^1(0,T; L^q_{loc}(\mathbb{R}^3))$$

and a weak flow $Z = (X, V)$ of the ODE

$$\begin{aligned} \dot{X} &= V, \\ \dot{V} &= -\partial_x U_f^M(s, X) \end{aligned}$$

such that

$$f(t,z) = \mathring{f}(Z(0,t,z))$$

for every $t \in [0,T]$ and $z \in \mathbb{R}^6$.

We prove the useful fact that Lagrangian solutions preserve L^p-norms of f.

Lemma 4.1.3. *Let f be a weak Lagrangian solution with initial condition $\mathring{f}$. Then*

$$f \in L^\infty(0,T; L^p(\mathbb{R}^6))$$

and for all $t \in [0,T]$

$$\|f(t)\|_p = \|\mathring{f}\|_p.$$

If further $\mathring{f} \in L^p \cap L^s(\mathbb{R}^6)$ for a $1 \le s \le \infty$, then we have additionally that for every $t \in [0,T]$

$$\|f(t)\|_s = \|\mathring{f}\|_s.$$

Proof. Let $t \in [0,T]$. Since Z is a weak flow, (Z5) implies

$$\|f(t)\|_p^p = \int f(t,z)^p \,\mathrm{d}z = \int \mathring{f}(Z(0,t,z))^p \,\mathrm{d}z = \int \mathring{f}(z)^p \,\mathrm{d}z = \|\mathring{f}\|_p^p. \tag{4.1}$$

Hence

$$\int_0^T \int f(t,z)^p \,\mathrm{d}z \,\mathrm{d}t = \int_0^T \|\mathring{f}\|_p^p \,\mathrm{d}t = T\|\mathring{f}\|_p^p$$

and $f \in L^p([0,T] \times \mathbb{R}^6)$. Since

$$L^p([0,T] \times \mathbb{R}^6) = L^p(0,T; L^p(\mathbb{R}^6))$$

(Knopf, 2017, Lemma 4),

$$f : [0,T] \to L^p(\mathbb{R}^6)$$

is Borel-measurable. Together with (4.1) this implies

$$f \in L^\infty(0,T; L^p(\mathbb{R}^6)).$$

If now $\mathring{f} \in L^p \cap L^s(\mathbb{R}^6)$ for a $1 \le s < \infty$, then (4.1) implies that also

$$\|f(t)\|_s = \|\mathring{f}\|_s$$

for all $t \in [0,T]$. If $s = \infty$ this statement follows from the fact that Z preserves measure (Z3).

□

We want to understand how Eulerian and Lagrangian solutions of the (VQMS) are connected. One connection can easily be seen.

Theorem 4.1.4. *Every weak Lagrangian solution of the (VQMS) with initial condition $\mathring{f}$ is also a weak Eulerian one.*

Proof. Let f be a weak Lagrangian solution. Obviously $f \geq 0$ a.e.. Further Lemma 4.1.3 implies that $f \in L^\infty(0,T;L^p(\mathbb{R}^6))$. Now take $\phi \in C_c^\infty([0,T)\times\mathbb{R}^6)$. Then the chain rule for absolutely continuous functions (Lemma 3.4.3) implies that $\phi(\cdot, Z(\cdot,0,z))$ is absolutely continuous on $[0,T]$ for a.e. $z \in \mathbb{R}^6$. For brevity we use in the following the notations

$$b(t,z) = (v, -\partial_x U_f^M(t,x))$$

and

$$Z(t) = Z(t,0,z)$$

for $t \in [0,T]$, $z = (x,v) \in \mathbb{R}^6$. Then

$$\begin{aligned}
&\int_0^T \int f(t,z)(\partial_t\phi(t,z) + b(t,z)\cdot\partial_z\phi(t,z))\,\mathrm{d}z\,\mathrm{d}t = \\
&\quad = \int_0^T \int \mathring{f}(z)(\partial_t\phi(t,Z(t)) + b(t,Z(t))\cdot\partial_z\phi(t,Z(t)))\,\mathrm{d}z\,\mathrm{d}t \\
&\quad = \int \mathring{f}(z)\int_0^T \frac{\mathrm{d}}{\mathrm{d}t}\phi(t,Z(t))\,\mathrm{d}t\,\mathrm{d}z \\
&\quad = -\int \mathring{f}(z)\phi(0,Z(0))\,\mathrm{d}z = -\int \mathring{f}(z)\phi(0,z)\,\mathrm{d}z;
\end{aligned}$$

in the last equality we used (Z4). Thus f is also a weak Eulerian solution. □

The other way around - to prove that an Eulerian solution is also a Lagrangian one - is more difficult. An answer to this question is given by DiPerna & Lions. Here the assumption

$$\partial_x U_f^M \in L^1(0,T;W^{1,q}_{loc}(\mathbb{R}^3)),$$

is essential.

Theorem 4.1.5. *Every weak Eulerian solution f of the (VQMS) with initial condition $\mathring{f}$ is - after modifying it on a set of measure zero - also a weak Lagrangian solution provided*

$$\partial_x U_f^M \in L^1(0,T;W^{1,q}_{loc}(\mathbb{R}^3)) \cap L^\infty(0,T;L^\infty(\mathbb{R}^3)).$$

Proof. In Theorem 3.5.4, which is based on Theorem III.3 of DiPerna & Lions (1989b), we have already shown that with the above regularity of $\partial_x U_f^M$ there exits a weak flow $Z = (X,V)$ of

$$\begin{aligned}
\dot{X} &= V, \\
\dot{V} &= -\partial_x U_f^M(s,X).
\end{aligned}$$

Set

$$\tilde{f}(t,z) := \mathring{f}(Z(0,t,z)), \quad t \in [0,T],\ z \in \mathbb{R}^6.$$

As in Lemma 4.1.3 one proves that

$$\tilde{f} \in L^\infty(0,T;L^p(\mathbb{R}^6))$$

and as in Theorem 4.1.4 one proves that $\tilde{f}$ is a weak Eulerian solutions with initial condition $\mathring{f}$ of the PDE

$$\partial_t\tilde{f} + v\cdot\partial_x\tilde{f} - \partial_x U_f^M\cdot\partial_v\tilde{f} = 0;$$

here it should be pointed out that $\partial_x U_f^M$ is independent of $\tilde{f}$. According to Corollary II.1 in DiPerna & Lions (1989b) the solution of this PDE is unique. Hence $f = \tilde{f}$ a.e. and $\tilde{f}$ is a weak Lagrangian solution of the (VQMS) with initial condition $\mathring{f}$. □

4.2 Existence of weak Eulerian solutions

Keller (2016) proved the existence of global, spherically symmetric solutions to the initial value problem of the (VQMS). We transfer her results into the notion of this thesis.

Remark. In the following theorem $\mathring{f}$ and f are said to be spherically symmetric. This means that for all $A \in SO(3)$, $t \in [0,\infty)$ and a.e. $x, v \in \mathbb{R}^3$

$$\begin{aligned} \mathring{f}(Ax, Av) &= \mathring{f}(x, v), \\ f(t, Ax, Av) &= f(t, x, v). \end{aligned}$$

Theorem 4.2.1 (Keller)**.** *Let λ be as in Lemma 3.3.2 and $\mathring{f} \in C_c^1(\mathbb{R}^6)$, ≥ 0 and spherically symmetric. Then there exists*

$$f : [0,\infty) \times \mathbb{R}^6 \to [0,\infty)$$

spherically symmetric such that for every $1 \leq p < \infty$ and $T > 0$

$$\begin{aligned} f &\in L^\infty(0,T; L^p(\mathbb{R}^6)), \\ \rho_f &\in L^\infty(0,T; L^p(\mathbb{R}^3)), \\ \partial_x U_f^M &\in L^\infty(0,T; L^\infty(\mathbb{R}^3)), \end{aligned}$$

and for all $\phi \in C_c^\infty([0,T) \times \mathbb{R}^6)$ holds

$$\int_0^T \int f(\partial_t \phi + v \cdot \partial_x \phi - \partial_x U_f^M \cdot \partial_v \phi) \,\mathrm{d}z \,\mathrm{d}t + \int \mathring{f} \phi(0,z) \,\mathrm{d}z = 0.$$

In particular f is a weak Eulerian solution of the (VQMS) with initial condition $\mathring{f}$. Further we have that for every $T > 0$ there is an $R > 0$ such that

$$\begin{aligned} \operatorname{supp} f|_{[0,T]\times\mathbb{R}^3\times\mathbb{R}^3} &\subset [0,T] \times B_R \times B_R, \\ \operatorname{supp} \rho|_{[0,T]\times\mathbb{R}^3} &\subset [0,T] \times B_R. \end{aligned}$$

Proof. When in this proof we use a reference to a theorem (germ. 'Satz') or chapter we refer to the respective theorem or chapter in Keller (2016).

Keller first studies a regularized version of the (VQMS) where $\partial_x U_f^M$ gets replaced by a regularized field $\partial_x U_k^M$. The regularization is made such that it vanishes for $k \to \infty$ (see the introduction to Chapter 4). Satz 3.10 implies that for every $k \in \mathbb{N}$ there are

$$\begin{aligned} f_k &\in C^1([0,\infty) \times \mathbb{R}^6), \\ \rho_k &\in C^1([0,\infty)) \times \mathbb{R}^3), \\ \partial_x U_k^M &\in C^{0,1}([0,\infty) \times \mathbb{R}^3) \end{aligned}$$

such that $f_k(0) = \mathring{f}$ and

$$\begin{aligned} &\partial_t f_k + v \cdot \partial_x f_k - \partial_x U_k^M \cdot \partial_v f_k = 0 && \text{on } [0,\infty) \times \mathbb{R}^6, \\ &\rho_k(t,x) = \int f_k(t,x,v) \,\mathrm{d}v && t \in [0,\infty),\ x \in \mathbb{R}^3, \end{aligned}$$

and

$$\partial_x U_k^M$$

is the regularized Mondian force corresponding to ρ_k. Further there exist

$$R, P : [0,\infty) \to [0,\infty)$$

monotonic increasing such that for all $t \in [0,\infty)$, $k \in \mathbb{N}$

$$\begin{aligned} \operatorname{supp} f_k(t) &\subset B_{R(t)} \times B_{P(t)}, \\ \operatorname{supp} \rho_k(t) &\subset B_{R(t)}. \end{aligned}$$

Satz 4.2, 4.4 and 4.10 imply that (after selecting a suitable subsequence that again is denoted by f_k, etc.) for every $T > 0$, $R' > 0$

$$\begin{aligned} f_k &\rightharpoonup f && \text{weakly in } L^2([0,T]\times\mathbb{R}^6),\\ \rho_k &\rightharpoonup \rho_f && \text{weakly in } L^2([0,T]\times\mathbb{R}^3),\\ \partial_x U_k^M &\to \partial_x U_f^M && \text{strongly in } L^2([0,T]\times B_{R'}) \end{aligned}$$

for $k \to \infty$. In particular

$$\begin{aligned} \operatorname{supp} f &\subset [0,T]\times B_{R(T)}\times B_{P(T)},\\ \operatorname{supp}\rho &\subset [0,T]\times B_{R(T)}. \end{aligned} \tag{4.2}$$

Now integration by parts gives that for every $\phi \in C_c^\infty([0,T)\times\mathbb{R}^6)$

$$\begin{aligned} 0 &= -\int_0^T\int (\partial_t f_k + v\cdot\partial_x f_k - \partial_x U_k^M\cdot\partial_v f_k)\phi \,\mathrm{d}z\,\mathrm{d}t\\ &= \int_0^T\int f_k(\partial_t\phi + v\cdot\partial_x\phi - \partial_x U_k^M\cdot\partial_v\phi)\,\mathrm{d}z\,\mathrm{d}t + \int \mathring{f}(z)\phi(0,z)\,\mathrm{d}z\\ &\to \int_0^T\int f(\partial_t\phi + v\cdot\partial_x\phi - \partial_x U_f^M\cdot\partial_v\phi)\,\mathrm{d}z\,\mathrm{d}t + \int \mathring{f}(z)\phi(0,z)\,\mathrm{d}z \end{aligned}$$

for $k\to\infty$. Satz 4.2 states further that $f \in L^\infty([0,\infty)\times\mathbb{R}^6)$. Thanks to (4.2) this implies that

$$f \in L^p([0,T]\times\mathbb{R}^6) = L^p(0,T;L^p(\mathbb{R}^6))$$

for every $1 \le p < \infty$. Further for every measurable set $I \subset [0,T]$

$$\begin{aligned} \int_I \|f(t)\|_p^p\,\mathrm{d}t &= \int_I \iiint_{\{|x|<R(t),|y|<P(t)\}} f^p\,\mathrm{d}v\,\mathrm{d}x\,\mathrm{d}t\\ &\le \|f\|_\infty^p \mathcal{L}(B_{R(T)}\times B_{P(T)})\mathcal{L}(I). \end{aligned}$$

Thus the map

$$[0,T]\ni t\mapsto \|f(t)\|_p^p$$

is bounded. In particular the map

$$[0,T]\ni t\mapsto \|f(t)\|_p$$

is bounded, too, and hence

$$f \in L^\infty(0,T;L^p(\mathbb{R}^6)).$$

In particular f is a weak Eulerian solution of the (VQMS) with initial condition $\mathring{f}$. Analogous as for f one proves

$$\rho_f \in L^\infty(0,T;L^p(\mathbb{R}^3)).$$

Consequently there is a sequence of spherically symmetric, simple functions

$$\rho^n : [0,T]\to L^p(\mathbb{R}^3),\quad n\in\mathbb{N},$$

such that for a.e. $t\in[0,T]$

$$\rho^n(t)\to\rho(t)\quad \text{strongly in } L^p(\mathbb{R}^3) \text{ for } n\to\infty.$$

W.l.g. we may assume $\operatorname{supp}\rho^n \subset [0,T]\times B_{R(T)}$. Let $p>3$ and $1<q<\frac{3}{2}$ with $1/p+1/q=1$, then

$$\begin{aligned} \|\partial_x U_f^N(t) - \partial_x U_{\rho^n}^N(t)\|_\infty &\le \sup_{x\in\mathbb{R}^3}\int_{|y|<R(T)} \frac{|\rho_f(t,y)-\rho^n(t,y)|}{|x-y|^2}\,\mathrm{d}y\\ &\le \|\rho_f(t)-\rho^n(t)\|_p \left(\int_{|y|<R(T)}\frac{\mathrm{d}y}{|y|^{2q}}\right)^{1/q}\\ &\le C\|\rho_f(t)-\rho^n(t)\|_p. \end{aligned}$$

By Lemma 3.3.2 λ obeys ($\Lambda 3$) and hence λ is by Lemma 3.3.1 Hölder continuous. Thus

$$\|\lambda(|\partial_x U_f^N(t)|)\partial_x U_f^N(t) - \lambda(|\partial_x U_{\rho^n}^N(t)|)\partial_x U_{\rho^n}^N(t)\|_\infty \leq \|\partial_x U_f^N(t) - \partial_x U_{\rho^n}^N(t)\|_\infty^{1/2}.$$

Since $\partial_x U_f^N$ is a spherically symmetric vector field, Lemma 3.2.7 implies

$$\partial_x U_f^M = \partial_x U_f^N + H(\lambda(|\partial_x U_f^N|)\partial_x U_f^N) = \partial_x U_f^N + \lambda(|\partial_x U_f^N|)\partial_x U_f^N.$$

The same holds for $\partial_x U_{\rho^n}^N$. Thus the above inequalities imply

$$\|\partial_x U_f^M - \partial_x U_{\rho^n}^M\|_\infty \leq C\left(\|\rho_f(t) - \rho^n(t)\|_p + \|\rho_f(t) - \rho^n(t)\|_p^{1/2}\right).$$

Since the $(\partial_x U_{\rho^n}^N + \lambda(|\partial_x U_{\rho^n}^N|)\partial_x U_{\rho^n}^N)_n$ are a sequence of simple functions and $\rho^n(t) \to \rho_f(t)$ in $L^p(\mathbb{R}^3)$ for a.e. $t \in [0,T]$,

$$\partial_x U_f^M \in L^\infty(0,T;L^\infty(\mathbb{R}^3)).$$

□

4.3 The link between weak Eulerian and weak Lagrangian solutions

In the previous section we studied the existence of weak Eulerian solutions. Now we ask whether these solutions are also Lagrangian ones? If we want to give a positive answer to this question, then in view of Theorem 4.1.5 we have to prove the existence of weak derivatives of $\partial_x U_f^M$ with respect to the position variable $x \in \mathbb{R}^3$.

Let us summarize what we know already about weak Eulerian solutions. Theorem 4.2.1 states that there exists a spherically symmetric, weak Eulerian solution f of the (VQMS) with initial condition $\mathring{f} \in C_c^1(\mathbb{R}^3)$. For these solutions

$$\rho_f \in L^\infty(0,T;L^p(\mathbb{R}^3))$$

for every $1 \leq p < \infty$ and $T > 0$. Then Lemma 3.1.4 gives that also

$$D^2 U_f^N \in L^\infty(0,T;L^p(\mathbb{R}^3))$$

for every $1 < p < \infty$. Therefore

$$\partial_x U_f^N \in L^\infty(0,T;C^{0,\alpha}(\mathbb{R}^3))$$

for all $0 < \alpha < 1$ by Morrey's inequality. Assuming that ($\Lambda 3$) holds Lemma 3.3.1 implies that

$$\partial_x U_f^M \in L^\infty(0,T;C^{0,\beta}(\mathbb{R}^3))$$

for all $0 < \beta < \frac{1}{2}$. Taking a second look on Morrey's inequality one could now expect that

$$D^2 U_f^M \in L^\infty(0,T;L^p(\mathbb{R}^3))$$

for all $1 < p < 6$. But this expectation proves deceptive. Why? Let us remain in the situation of spherical symmetry and for $\rho = \rho(x)$ spherically symmetric study the divergence of

$$\nabla U_\rho^M = \nabla U_\rho^N + \lambda(|\nabla U_\rho^N|)\nabla U_\rho^N.$$

In view of Lemma 3.1.5

$$\lambda(|\nabla U_\rho^N(x)|)\nabla U_\rho^N(x) = \frac{\sqrt{M(r)}}{r}\frac{x}{r}, \quad r = |x|,$$

where for convenience we assumed $\lambda(\sigma) = 1/\sqrt{\sigma}$, $\sigma > 0$. So

$$\begin{aligned}\operatorname{div}(\nabla U_\rho^M(x)) &= \Delta U_\rho^N(x) + \frac{1}{r^2}(r\sqrt{M(r)})' \\ &= 4\pi\rho(r) + \frac{\sqrt{M(r)}}{r^2} + \frac{\sqrt{M(r)}'}{r}.\end{aligned}$$

ρ is just fine, the second term can be controlled as expected above, but the third one will cause problems. We prove the following

Proposition 4.3.1. *Let $R > 0$, $1 < p, q < \infty$ and $\rho \in C^1 \cap L^p(\mathbb{R}^3)$, ≥ 0, spherically symmetric. Then*

$$\left\| \frac{\sqrt{M(r)}}{r^2} \right\|_{L^q(B_R)} \leq C \|\rho\|_p^{1/2}$$

if $1 < q < 6$ and $p > 3q/(6-q)$ with $C = C(p, q, R) > 0$, and

$$\left\| \frac{\sqrt{M(r)}'}{r} \right\|_{L^q(B_R)} \leq C \|\rho\|_p^{1/2}$$

if $1 < q < 2$ and $p > q/(2-q) + q$ with $C = C(p, q, R) > 0$. With $\sqrt{M(r)}'$ we denote the function

$$\sqrt{M(r)}' := \begin{cases} \frac{2\pi r^2 \rho(r)}{\sqrt{M(r)}} & , \text{ if } M(r) > 0 \\ 0 & , \text{ if } M(r) = 0 \end{cases}.$$

Proof. Let $1 < q < 6$ and $1 < p < \infty$ with $p > 3q/(6-q)$. For $r \geq 0$

$$M(r) = \int_{B_r} \rho(x) \, \mathrm{d}x \leq \|\rho\|_p \|1_{B_r}\|_{p/(p-1)} \leq C \|\rho\|_p r^{3-3/p}.$$

Thus

$$\left\| \frac{\sqrt{M(r)}}{r^2} \right\|_{L^q(B_R)}^q = \int_{B_R} M(r)^{q/2} r^{-2q} \, \mathrm{d}x \leq C \|\rho\|_p^{q/2} \int_{B_R} r^{\frac{3q}{2} - \frac{3q}{2p} - 2q} \, \mathrm{d}x.$$

Since

$$\frac{3q}{2} - \frac{3q}{2p} - 2q > -3 \Leftrightarrow 3 - \frac{q}{2} > \frac{3q}{2p} \Leftrightarrow p > \frac{3q}{6-q}$$

we have

$$\left\| \frac{\sqrt{M(r)}}{r^2} \right\|_{L^q(B_R)} \leq C \|\rho\|_p^{1/2}.$$

Now we turn to the second estimate. Let $1 < q < 2$, $p > q/(2-q) + q$ and $r_0 \geq 0$ be such that $M(r_0) = 0$ and $M(r) > 0$ for all $r > r_0$. Since $\rho \in C^1(\mathbb{R}^3)$, $M(r) \in C^1([0, \infty))$ with

$$M'(r) = \frac{\mathrm{d}}{\mathrm{d}r} 4\pi \int_0^r s^2 \rho(s) \, \mathrm{d}s = 4\pi r^2 \rho(r).$$

Hence $\sqrt{(M(r))} \in C^1((r_0, \infty))$ with

$$\sqrt{M(r)}' = \frac{2\pi r^2 \rho(r)}{\sqrt{M(r)}}, \quad r > r_0.$$

Assume that $R > r_0$, then

$$\begin{aligned} \left\| \frac{\sqrt{M(r)}'}{r} \right\|_{L^q(B_R \setminus B_{r_0})}^q &= \int_{B_R \setminus B_{r_0}} \left(\frac{2\pi r \rho(r)}{\sqrt{M(r)}} \right)^q \mathrm{d}x \\ &\leq (2\pi R)^q \int_{B_R \setminus B_{r_0}} \rho(r)^\alpha \frac{\rho(r)^{q-\alpha}}{M(r)^{q/2}} \, \mathrm{d}x \end{aligned}$$

with

$$\alpha := \frac{p}{p-1}(q-1).$$

Obviously $\alpha > 0$, and further $\alpha < q$ since

$$\alpha = \frac{p}{p-1}(q-1) < q \Leftrightarrow 1 - \frac{1}{q} < 1 - \frac{1}{p} \Leftrightarrow q < p.$$

Now we apply Hölder's inequality and get

$$\left\| \frac{\sqrt{M(r)}'}{r} \right\|^q_{L^q(B_R \setminus B_{r_0})} \leq C\|\rho\|_p^\alpha \left\| \frac{\rho(r)^{q-\alpha}}{M(r)^{q/2}} \right\|_{L^{p/(p-\alpha)}(B_R \setminus B_{r_0})};$$

note that $0 < \alpha < q < p$. Since

$$(q-\alpha)\frac{p}{p-\alpha} = 1 \Leftrightarrow q - \alpha = 1 - \frac{\alpha}{p} \Leftrightarrow q - 1 = \alpha\left(1 - \frac{1}{p}\right) \Leftrightarrow \alpha = \frac{p}{p-1}(q-1),$$

we have

$$\begin{aligned}\left\| \frac{\rho(r)^{q-\alpha}}{M(r)^{q/2}} \right\|_{L^{p/(p-\alpha)}(B_R \setminus B_{r_0})} &= \left(\int_{B_R \setminus B_{r_0}} \rho(r) M(r)^{-pq/(2p-2\alpha)} \, \mathrm{d}x \right)^{(p-\alpha)/p} \\ &= C\left[\int_{r_0}^R \left(M(r)^{1-pq/(2p-2\alpha)} \right)' \mathrm{d}r \right]^{(p-\alpha)/p};\end{aligned}$$

here we have used that $pq/(2p-2\alpha) < 1$ since

$$\begin{aligned}\frac{pq}{2p-2\alpha} < 1 &\Leftrightarrow \frac{q}{2} < 1 - \frac{\alpha}{p} = 1 - \frac{q-1}{p-1} \\ &\Leftrightarrow \frac{2-q}{2} > \frac{q-1}{p-1} \\ &\Leftrightarrow p > 1 + \frac{2(q-1)}{2-q} = \frac{2-q+2q-2}{2-q} = \frac{q}{2-q}.\end{aligned}$$

Thus

$$\left\| \frac{\sqrt{M(r)}'}{r} \right\|^q_{L^q(B_R \setminus B_{r_0})} \leq C\|\rho\|_p^\alpha \|\rho\|_{L^1(B_R)}^{(p-\alpha)/p - q/2}.$$

Since

$$\|\rho\|_{L^1(B_R)} \leq C\|\rho\|_p$$

and

$$\begin{aligned}\frac{1}{q}\left(\alpha + \frac{p-\alpha}{p} - \frac{q}{2}\right) &= \frac{q-1}{q}\frac{p}{p-1} + \frac{1}{q}\left(1 - \frac{q-1}{p-1}\right) - \frac{1}{2} \\ &= \frac{(q-1)p + (p-q)}{q(p-1)} - \frac{1}{2} \\ &= \frac{pq-q}{q(p-1)} - \frac{1}{2} \\ &= \frac{1}{2},\end{aligned}$$

we finally have

$$\left\| \frac{\sqrt{M(r)}'}{r} \right\|_{L^q(B_R \setminus B_{r_0})} \leq C\|\rho\|_q^{1/2}.$$

□

Using the proposition we can control L^q-norms of the derivatives of the Mondian part

$$\lambda(|\nabla U_\rho^N|)\nabla U_\rho^N$$

of the force field provided $1 < q < 2$ and ρ is spherically symmetric.

Lemma 4.3.2. *Let $1 < q < 2$, $p > \frac{q}{2-q} + q$, $R > 0$ and $\rho \in L^1 \cap L^p(\mathbb{R}^3)$, ≥ 0, spherically symmetric. If (Λ3) holds,*

$$\lambda(|\nabla U_\rho^N|)\nabla U_\rho^N \in W^{1,q}_{loc}(\mathbb{R}^3)$$

with

$$\left\| \nabla\left[\lambda(|\nabla U_\rho^N|)\nabla U_\rho^N\right] \right\|_{L^q(B_R)} \leq C\|\rho\|_p^{1/2}$$

where $C = C(p, q, R) > 0$.

Proof. Since we are in spherical symmetry, Lemma 3.1.5 gives

$$\lambda(|\nabla U_\rho^N|)\nabla U_\rho^N = \lambda\left(\frac{M(r)}{r^2}\right)\frac{M(r)}{r^2}\frac{x}{r}, \quad x \in \mathbb{R}^3,\, r = |x|;$$

for better readability we suppress the x-argument on the left side. Using the abbreviation

$$\tilde{\lambda}(\sigma) = \lambda(\sigma)\sigma, \quad \sigma \geq 0,$$

we have

$$\lambda(|\nabla U_\rho^N|)\nabla U_\rho^N = \tilde{\lambda}\left(\frac{M(r)}{r^2}\right)\frac{x}{r}.$$

Thanks to Lemma 3.3.1

$$|\tilde{\lambda}(\sigma) - \tilde{\lambda}(\tau)| \leq C|\sigma - \tau|^{1/2}, \quad \sigma, \tau \geq 0, \tag{4.3}$$

for a $C > 0$ where

$$\tilde{\lambda}(0) = 0.$$

This Lemma states also that ($\Lambda 2$) holds, so

$$0 \leq \tilde{\lambda}(\sigma) \leq \Lambda_2\sqrt{\sigma}, \quad \sigma \geq 0. \tag{4.4}$$

Still using ($\Lambda 3$) we get

$$|\tilde{\lambda}'(\sigma)| \leq |\lambda'(\sigma)|\sigma + \lambda(\sigma) \leq \frac{C}{\sqrt{\sigma}}, \quad \sigma > 0, \tag{4.5}$$

for a $C > 0$. Thanks to (4.4), for every $R > 0$ holds

$$\left\|\lambda(|\nabla U_\rho^N|)\nabla U_\rho^N\right\|_{L^q(B_R)}^q \leq \Lambda_2^q \int_{B_R}\left(\frac{\sqrt{M(r)}}{r}\right)^q \mathrm{d}x \leq C\|\rho\|_1^{q/2}.$$

Next we approximate ρ by smooth densities ρ_n and study the (weak) derivatives of $\lambda(|\nabla U_{\rho_n}^N|)\nabla U_{\rho_n}^N$. Let $(\rho_n) \subset C_c^1(\mathbb{R}^3)$ be a sequence of spherically symmetric densities such that

$$\rho_n \to \rho \quad \text{strongly in } L^1(\mathbb{R}^3) \text{ and } L^p(\mathbb{R}^3) \text{ for } n \to \infty.$$

As above $\lambda(|\nabla U_{\rho_n}^N|)\nabla U_{\rho_n}^N \in L_{loc}^q(\mathbb{R}^3)$. Denote by

$$M_n(r) = \int_{B_r} \rho_n \,\mathrm{d}x, \quad r \geq 0,$$

the mass of ρ_n inside the ball with radius r. Then $M_n \in C^1(\mathbb{R}^3)$ with

$$\nabla(M_n(r)) = M_n'(r)\frac{x}{r} = 4\pi\rho_n(r)rx.$$

Let $r_n \geq 0$ be such that $M_n(r_n) = 0$ and $M_n(r) > 0$ for all $r > r_n$. Then

$$\lambda(|\nabla U_{\rho_n}^N|)\nabla U_{\rho_n}^N \in C^1(\mathbb{R}^3 \backslash \{|x| = r_n\})$$

with

$$\partial_{x_i}\left[\lambda(|\nabla U_{\rho_n}^N|)\partial_{x_j}U_{\rho_n}^N\right] = 0 \tag{4.6}$$

if $|x| < r_n$, and

$$\begin{aligned}
\partial_{x_i}\left[\lambda(|\nabla U_{\rho_n}^N|)\partial_{x_j}U_{\rho_n}^N\right] &= \partial_{x_i}\left(\tilde{\lambda}\left(\frac{M_n(r)}{r^2}\right)\frac{x_j}{r}\right) \\
&= \tilde{\lambda}'\left(\frac{M_n(r)}{r^2}\right)M_n'(r)\frac{x_i x_j}{r^4} \\
&\quad - 2\tilde{\lambda}'\left(\frac{M_n(r)}{r^2}\right)M_n(r)\frac{x_i x_j}{r^5} \\
&\quad + \tilde{\lambda}\left(\frac{M_n(r)}{r^2}\right)\left(\frac{\delta_{ij}}{r} - \frac{x_i x_j}{r^3}\right)
\end{aligned} \tag{4.7}$$

if $|x| > r_n$ and $i, j = 1, 2, 3$. Denote by

$$\partial_{x_i}\left[\lambda(|\nabla U^N_{\rho_n}|)\partial_{x_j}U^N_{\rho_n}\right]$$

the functions that are pointwise a.e. defined by (4.6) and (4.7). Using (4.4) and (4.5) we get for $|x| > r_n$

$$\begin{aligned}\left|\partial_{x_i}\left[\lambda(|\nabla U^N_{\rho_n}|)\partial_{x_j}U^N_{\rho_n}\right]\right| &\le C\left(\frac{M_n'(r)}{2\sqrt{M_n(r)}}\frac{1}{r} + \frac{\sqrt{M_n(r)}}{r^2}\right)\\ &= C\left(\frac{\sqrt{M_n(r)}'}{r} + \frac{\sqrt{M_n(r)}}{r^2}\right).\end{aligned}$$

Since $p > q/(2-q) + q$ and

$$\frac{q}{2-q} = \frac{3q}{6-3q} > \frac{3q}{6-q},$$

we can apply Proposition 4.3.1 and get for every $R > 0$

$$\left\|\partial_{x_i}\left[\lambda(|\nabla U^N_{\rho_n}|)\partial_{x_j}U^N_{\rho_n}\right]\right\|_{L^q(B_R)} \le C\|\rho_n\|_p^{1/2}. \tag{4.8}$$

Now we prove that the functions given by (4.6) and (4.7) are indeed the weak derivatives of $\lambda(|\nabla U^N_{\rho_n}|)\nabla U^N_{\rho_n}$. For every $\phi \in C_c^\infty(\mathbb{R}^3)$

$$\begin{aligned}\int \lambda(|\nabla U^N_{\rho_n}|)\partial_{x_j}U^N_{\rho_n}\partial_{x_i}\phi\,\mathrm{d}x &= \lim_{s\searrow r_n}\int_{\{|x|\ge s\}}\lambda(|\nabla U^N_{\rho_n}|)\partial_{x_j}U^N_{\rho_n}\partial_{x_i}\phi\,\mathrm{d}x\\ &= -\int\partial_{x_i}\left(\lambda(|\nabla U^N_{\rho_n}|)\partial_{x_j}U^N_{\rho_n}\right)\phi\,\mathrm{d}x\\ &\quad + \lim_{s\searrow r_n}\int_{\{|x|=s\}}\lambda(|\nabla U^N_{\rho_n}|)\partial_{x_j}U^N_{\rho_n}\phi\frac{x_i}{|x|}\,\mathrm{dS}(x).\end{aligned}$$

If $r_n = 0$, we use

$$\left|\lambda(|\nabla U^N_{\rho_n}|)\nabla U^N_{\rho_n}\right| \le \frac{\Lambda_2\sqrt{M_n(r)}}{r} \le \frac{\Lambda_2\|\rho\|_1^{1/2}}{r}$$

and get

$$\left|\int_{\{|x|=s\}}\lambda(|\nabla U^N_{\rho_n}|)\partial_{x_j}U^N_{\rho_n}\phi\frac{x_i}{|x|}\,\mathrm{dS}(x)\right| \le Cs \to 0 \quad \text{for } s\to 0.$$

If $r_n > 0$, we use

$$\left|\lambda(|\nabla U^N_{\rho_n}|)\nabla U^N_{\rho_n}\right| \le \frac{\Lambda_2}{r_n}\left(\int_{r_n<|x|<s}\rho_n\,\mathrm{d}x\right)^{1/2} \to 0 \quad \text{for } s\to r_n,$$

and get, too, that the border term in the above integration by parts vanishes. Hence the by (4.6) and (4.7) pointwise a.e. defined functions are indeed the weak derivatives of

$$\lambda(|\nabla U^N_{\rho_n}|)\nabla U^N_{\rho_n} \in W^{1,q}_{loc}(\mathbb{R}^3).$$

It remains to prove that

$$\lambda(|\nabla U^N_{\rho}|)\partial_{x_j}U^N_{\rho} \in W^{1,q}_{loc}(\mathbb{R}^3)$$

and that the estimate (4.8) holds with ρ_n replaced by ρ. Using (4.3) and Hölder we have for $R > 0$

$$\begin{aligned}\left\|\lambda(|\nabla U^N_{\rho_n}|)\nabla U^N_{\rho_n} - \lambda(|\nabla U^N_{\rho}|)\partial_{x_j}U^N_{\rho}\right\|_{L^1(B_R)} &= \int_{B_R}\left|\tilde\lambda\left(\frac{M(r)}{r^2}\right) - \tilde\lambda\left(\frac{M_n(r)}{r^2}\right)\right|\mathrm{d}x\\ &\le C\int_{B_R}\frac{|M(r)-M_n(r)|^{1/2}}{r}\,\mathrm{d}x\\ &\le C\left(\int_{B_R}|M_n(r)-M(r)|\,\mathrm{d}x\right)^{1/2}\\ &\le C\|\rho_n-\rho\|_1^{1/2}.\end{aligned}$$

Thus

$$\lambda(|\nabla U^N_{\rho_n}|)\nabla U^N_{\rho_n} \to \lambda(|\nabla U^N_{\rho}|)\partial_{x_j} U^N_{\rho} \quad \text{strongly in } L^1(B_R) \text{ for } n \to \infty.$$

Since

$$\|\rho_n\|_p \leq C$$

independent of $n \in \mathbb{N}$, (4.8) implies that there is a subsequence (again denoted by (ρ_n)) such that

$$\partial_{x_i}\left[\lambda(|\nabla U^N_{\rho_n}|)\partial_{x_j} U^N_{\rho_n}\right] \rightharpoonup V \quad \text{weakly in } L^q(\mathbb{R}^3) \text{ for } n \to \infty.$$

V is the weak derivative of

$$\lambda(|\nabla U^N_{\rho}|)\partial_{x_j} U^N_{\rho}$$

with respect to x_i and hence

$$\lambda(|\nabla U^N_{\rho}|)\nabla U^N_{\rho} \in W^{1,q}_{loc}(\mathbb{R}^3).$$

Since the L^q-norm is weakly lower semi-continuous, (4.8) implies

$$\begin{aligned}
\|V\|_{L^q(B_R)} &\leq \liminf_{n\to\infty} \left\|\partial_{x_i}\left[\lambda(|\nabla U^N_{\rho_n}|)\partial_{x_j} U^N_{\rho_n}\right]\right\|_{L^q(B_R)} \\
&\leq C \lim_{n\to\infty} \|\rho_n\|_p^{1/2} \\
&= C\|\rho\|_p^{1/2}.
\end{aligned}$$

□

The existence of weak derivatives of ∇U^M_ρ grants a Lagrangian description of the spherically symmetric solutions from Theorem 4.2.1.

Theorem 4.3.3. *Let λ be as in Lemma 3.3.2 and $\mathring{f} \in C^1_c(\mathbb{R}^3)$, ≥ 0 and spherically symmetric. Then the weak Eulerian solution f of the (VQMS) with initial condition $\mathring{f}$ from Theorem 4.2.1 is a weak Lagrangian one.*

Proof. Let $T > 0$, $R > 0$. We prove

$$\partial_x U^M_f \in L^1(0, T; W^{1,5/4}(B_R)).$$

Then Theorem 4.1.5 implies that f is also a weak Lagrangian solution. In the following proof we write shortly $\rho = \rho_f$.

Let $p > 3$. Since

$$\rho \in L^\infty(0, T; L^p(\mathbb{R}^3)),$$

there is a sequence of spherically symmetric, simple functions (ρ_n) such that for a.e. $t \in [0, T]$

$$\rho_n(t) \to \rho(t) \quad \text{in } L^p(\mathbb{R}^3) \text{ for } n \to \infty.$$

Since $\operatorname{supp}\rho \subset [0, T] \times B_{R'}$ for an $R' > 0$, we can choose the ρ_n such that

$$\operatorname{supp}\rho_n \subset [0, T] \times B_{R'}.$$

As in the proof of Theorem 4.2.1, we get

$$\|\partial_x U^M_{\rho_n}(t) - \partial_x U^M_{\rho}(t)\|_\infty \leq C\left(\|\rho_n(t) - \rho(t)\|_p + \|\rho_n(t) - \rho(t)\|_p^{1/2}\right).$$

Since $(\partial_x U^M_{\rho_n})$ is a sequence of simple functions, this implies

$$\partial_x U^M_\rho \in L^\infty(0, T; L^{5/4}(B_R)).$$

The compact support of the ρ_n implies that for a.e. $t \in [0, T]$ also

$$\rho_n(t) \to \rho(t) \quad \text{in } L^{5/4}(\mathbb{R}^3) \text{ for } n \to \infty.$$

Let $t \in [0, T]$ such that $\rho_n(t)$ converges in $L^p(\mathbb{R}^3)$ and in $L^{5/4}(\mathbb{R}^3)$ to $\rho(t)$ and take an arbitrary subsequence (ρ'_n) of (ρ_n). Lemma 3.1.4 and Lemma 4.3.2 imply that

$$\begin{aligned}
&\left\|\partial_x^2 U^N_{\rho'_n}(t)\right\|_{5/4} \leq C\|\rho'_n(t)\|_{5/4}, \\
&\left\|\partial_x\left(\lambda\left(|\partial_x U^N_{\rho'_n}(t)|\right)\partial_x U^N_{\rho'_n}(t)\right)\right\|_{L^{5/4}(B_R)} \leq C\|\rho'_n(t)\|_p;
\end{aligned}$$

observe that

$$\frac{5/4}{2-5/4}+\frac{5}{4}=\frac{5}{3}+\frac{5}{4}=\frac{35}{12}<3<p.$$

Since $\rho_n'(t)$ converges in both L^p and $L^{5/4}$, there is a $C>0$ such that

$$\left\|\partial_x^2 U^M_{\rho_n'}(t)\right\|_{L^{5/4}(B_R)}\leq C.$$

Hence there is a further sub-subsequence (ρ_n'') such that

$$\partial_x^2 U^M_{\rho_n''}(t)\rightharpoonup \partial_x^2 U^M_{\rho}(t)\quad \text{weakly in } L^{5/4}(B_R) \text{ for } n\to\infty.$$

We can repeat this argument for every subsequence of (ρ_n) and for every $t\in[0,T]$ such that $\rho_n(t)$ is convergent to $\rho(t)$. Thus for a.e. $t\in[0,T]$

$$\partial_x^2 U^M_{\rho_n}(t)\rightharpoonup \partial_x^2 U^M_{\rho}(t)\quad \text{weakly in } L^{5/4}(B_R) \text{ for } n\to\infty.$$

Let now $g\in L^5(B_R)$, then for a.e. $t\in[0,T]$

$$\int_{B_R} g\,\partial_x^2 U^M_{\rho_n}(t)\,\mathrm{d}x\to\int_{B_R} g\,\partial_x^2 U^M_{\rho}(t)\,\mathrm{d}x\quad \text{for } n\to\infty.$$

Thus the map

$$[0,T]\ni t\mapsto \int_{B_R} g\,\partial_x^2 U^M_{\rho}(t)\,\mathrm{d}x$$

is measurable as the pointwise limit of measurable functions. Thus the theorem of Pettis implies that also the map

$$[0,T]\ni t\mapsto \partial_x^2 U^M_{\rho}(t)\in L^{5/4}(B_R)$$

is measurable. Since for a.e. $t\in[0,T]$

$$\left\|\partial_x^2 U^M_{\rho}(t)\right\|_{L^{5/4}(B_R)}\leq C\left(\|\rho(t)\|_{5/4}+\|\rho(t)\|_p\right),$$

this map is also bounded. Hence

$$\partial_x U^M_{\rho}\in L^\infty(0,T;W^{1,5/4}(B_R)).$$

□

Thus in spherical symmetry a weak Eulerian solution is also a weak Lagrangian solution. As we argue in Section 6 it will not be difficult to prove Theorem 4.2.1 also without the assumption of spherical symmetry – at least on small time intervals. This way one can construct symmetry free weak Eulerian solutions. Will these solutions still be Lagrangian ones?

As we have argued in the introduction to this section one might expect from a naive argumentation that

$$D^2U^M_\rho\in L^q(\mathbb{R}^3)$$

for $1<q<6$ if

$$\rho\in L^1\cap L^\infty(\mathbb{R}^3).$$

However in Lemma 4.3.2 we were only able to prove an estimate of the type

$$\|D^2U^M_\rho\|_q\leq C\|\rho\|_p^{1/2}$$

if $1<q<2$. In the following Lemma we show that this estimate is indeed optimal; there is no such estimate if $q>2$. Further the subsequent Lemma will show that it is unlikely that any such estimate can be proven if we drop the assumption of spherical symmetry.

Lemma 4.3.4. *Let $\lambda(\sigma)=1/\sqrt{\sigma}$, $\sigma>0$. Then there is a sequence of spherically symmetric densities $(\rho_n)\subset L^1\cap L^\infty(\mathbb{R}^3)$ such that for all $n\in\mathbb{N}$ $\rho_n\geq 0$, $\operatorname{supp}\rho_n\subset B_2$ and $\|\rho_n\|_\infty\leq 1$, but*

$$\|D^2U^M_{\rho_n}\|_q\to\infty\quad \textit{for } n\to\infty$$

if $2<q<6$.

Remark 4.3.5. The Idea behind the proof of Lemma 4.3.4 is the following: In ΔU_ρ^M appears the term

$$\frac{\sqrt{M(r)}'}{r} = \frac{2\pi r\rho(r)}{\sqrt{M(r)}} = \frac{2\pi\rho(r)}{\sqrt{N(r)}}\frac{1}{\sqrt{r}}$$

where we have introduced the notion

$$N(r) := \frac{1}{r^3}M(r) = \frac{1}{r^3}\int_{B_r}\rho(x)\,\mathrm{d}x.$$

(Rudin, 1999, Satz 7.7) implies that for a.e. $y \in \mathbb{R}^3$

$$\frac{1}{r^3}\int_{B_r(y)}\rho(x)\,\mathrm{d}x \to \frac{4\pi}{3}\rho(y) \quad \text{for } r \to 0.$$

So we could expect that

$$\frac{\sqrt{M(r)}'}{r} \approx \frac{\sqrt{3\pi}\rho(r)}{\sqrt{\rho(0)}}\frac{1}{\sqrt{r}} \quad \text{for } r > 0 \text{ small.}$$

Assuming for the moment that $\rho(0) > 0$ and that $\|\rho\|_\infty < \infty$ this would guarantee that $\|\sqrt{M(r)}'/r\|_q$ is bounded for all $1 < q < 6$. Together with Proposition 4.3.1 this would give us a bound for $\|D^2U_\rho^M\|_q$ for all $1 < q < 6$. However, the pointwise representation of an L^p-function ρ is tricky:

Lets take an open set $\Omega_n \subset [0,2]$ such that for all $\epsilon > 0$

$$\mathcal{L}(\Omega_n \cap [0,\epsilon]) \approx \frac{\epsilon}{n}$$

and set

$$\rho_n(r) := 1_{\Omega_n}(r).$$

Then there is no well defined value of $\rho(0)$ and we get

$$N(r) \approx \frac{C}{n} \quad \text{for } r > 0 \text{ small}$$

with a constant $C > 0$ independent of n. Thus

$$\frac{\sqrt{M(r)}'}{r} \approx \frac{2\pi}{\sqrt{C}}\sqrt{n}1_{\Omega_n}(r)\frac{1}{\sqrt{r}} \quad \text{for } r > 0 \text{ small,}$$

and when we send $n \to \infty$ this is unbounded in L^q for $2 < q < 6$.

Proof of Lemma 4.3.4. For $n \in \mathbb{N}$ set

$$\Omega_n := \bigcup_{i=0}^{\infty}\left[2^{-i}, \left(1+\frac{1}{n}\right)2^{-i}\right)$$

and define

$$\rho_n(r) := \frac{1}{4\pi}1_{\Omega_n}(r), \quad r \geq 0.$$

Denote by

$$M_n(r) := \int_{B_r}\rho_n\,\mathrm{d}x$$

the mass of ρ_n inside the ball with radius $r \geq 0$. Let $n, j \in \mathbb{N}$, then

$$\begin{aligned} M_n(2^{-j+1}) &= \sum_{i=j}^{\infty}\int_{2^{-i}}^{(1+1/n)2^{-i}} r^2\,\mathrm{d}r \leq \sum_{i=j}^{\infty}\frac{1}{n}2^{-i}(2^{-i+1})^2 = \frac{4}{n}\sum_{i=j}^{\infty}\left(\frac{1}{8}\right)^i \\ &= \frac{4}{n}\left(\frac{1}{1-1/8} - \frac{1-(1/8)^j}{1-1/8}\right) = \frac{4}{n}\left(\frac{1}{8}\right)^j\frac{8}{7} = \frac{C_0}{n}(2^{-j})^3. \end{aligned}$$

Let $r \in [2^{-j}, 2^{-j+1})$ for a $j \geq 0$. Then

$$M_n(r) \leq M_n(2^{-j+1}) \leq \frac{C_0}{n}(2^{-j})^3 \leq \frac{C_0}{n} r^3.$$

Thus

$$N_n(r) := \frac{1}{r^3} M_n(r) \leq \frac{C_0}{n}$$

and

$$\frac{\rho_n(r)}{\sqrt{N_n(r)}} \geq \frac{\sqrt{n}}{4\pi\sqrt{C_0}} 1_{\Omega_n}(r). \tag{4.9}$$

Let now $2 < q < 6$, then

$$\|D^2 U^M_{\rho_n}\|_q \geq C \|\Delta U^M_{\rho_n}\|_q = C \left\| 4\pi\rho_n(r) + \frac{\sqrt{M_n(r)}}{r^2} + \frac{\sqrt{M_n(r)}'}{r} \right\|_q .$$

Since $\rho_n, M_n \geq 0$ and M_n is monotonic increasing

$$\|D^2 U^M_{\rho_n}\|_q \geq C \left\| \frac{\sqrt{M_n(r)}'}{r} \right\|_q = C \left\| \frac{r\rho_n(r)}{\sqrt{M_n(r)}} \right\|_q = C \left\| \frac{\rho_n(r)}{\sqrt{N_n(r)}} r^{-1/2} \right\|_q .$$

Now we use the estimate (4.9) and get

$$\begin{aligned} \|D^2 U^M_{\rho_n}\|_q &\geq C\sqrt{n} \left\| r^{-1/2} 1_{\Omega_n}(r) \right\|_q \\ &= C\sqrt{n} \left(\int_{\Omega_n} r^{2-q/2} \, \mathrm{d}r \right)^{1/q} \\ &= C\sqrt{n} \left(\sum_{i=0}^{\infty} \int_{2^{-i}}^{(1+1/n)2^{-i}} r^{2-q/2} \, \mathrm{d}r \right)^{1/q} . \end{aligned}$$

For $2 < q \leq 4$ we have

$$\sum_{i=0}^{\infty} \int_{2^{-i}}^{(1+1/n)2^{-i}} r^{2-q/2} \, \mathrm{d}r \geq \sum_{i=0}^{\infty} \frac{1}{n} 2^{-i} (2^{-i})^{2-q/2} = \frac{1}{n} \sum_{i=0}^{\infty} (2^{-3+q/2})^i$$

and for $4 < q < 6$

$$\sum_{i=0}^{\infty} \int_{2^{-i}}^{(1+1/n)2^{-i}} r^{2-q/2} \, \mathrm{d}r \geq \sum_{i=0}^{\infty} \frac{1}{n} 2^{-i} (2^{-i+1})^{2-q/2} = \frac{1}{n} 2^{2-q/2} \sum_{i=0}^{\infty} (2^{-3+q/2})^i .$$

Hence

$$\|D^2 U^M_{\rho_n}\|_q \geq C n^{1/2-1/q},$$

and this is divergent if $q > 2$.

□

So it is not possible for any $q > 2$ to prove an estimate of the form

$$\|D^2 U^M_{\rho}\|_{L^q(B_R)} \leq C \|\rho\|_p^{1/2}$$

even if ρ is spherically symmetric (and non-negative). Will the situation get even worse if we leave spherical symmetry?

Let us look at the difficulties that one can encounter. $D^2 U^M_\rho$ causes difficulties when $\nabla U^N_\rho(x) = 0$ for an $x \in \mathbb{R}^3$ because then

$$\lambda\left(\left|\nabla U^N_\rho(x+y)\right|\right) \left|\nabla U^N_\rho(x+y)\right| = \left|\nabla U^N_\rho(x+y)\right|^{1/2} \approx C\sqrt{y}$$

if $|y|$ is small and $\lambda(\sigma) = 1/\sigma$ for $\sigma > 0$. Consider now the following, symmetry free situation: For every $n \in \mathbb{N}$ place a point mass at position

$$x_n = (1 - 1/n, 0, 0) .$$

Then for every $n \in \mathbb{N}$ there is $0 < \alpha_n < 1$ such that for

$$y_n = \alpha_n x_n + (1 - \alpha_n) x_{i+1}$$

we have

$$\nabla U^N(y_n) = 0;$$

U^N denotes the Newtonian gravitational potential created by all the masses at the points x_n. So for every $n \in \mathbb{N}$ $D^2 U^N(y_n)$ will cause difficulties.

The exact treatment of such a non-symmetric situation is difficult. Can we perhaps mimic the above difficulties in spherical symmetry? The answer is yes, if we do not demand that ρ has to be non-negative. Then the next lemma shows that it is no more possible for any $1 \leq p, q \leq \infty$ to prove an estimate of the form

$$\|D^2 U_\rho^M\|_{L^q(B_R)} \leq C \|\rho\|_p^{1/2}.$$

Lemma 4.3.6. *Let $\lambda(\sigma) = 1/\sqrt{\sigma}$, $\sigma > 0$. Then there exists a $\rho \in L^1 \cap L^\infty(\mathbb{R}^3)$, spherically symmetric, which takes positive and negative values, such that*

$$\nabla U_\rho^M \notin W_{loc}^{1,1}(\mathbb{R}^3).$$

Proof. For $n \in \mathbb{N}$ set

$$a_n := \sum_{i=1}^{n} \frac{2}{i^2}$$

and let m_n be the center between a_n and a_{n+1}, i.e.,

$$m_n := a_n + \frac{1}{(n+1)^2}.$$

Then $a_1 = 2$ and

$$a_n \to \frac{\pi^2}{3} < 4 \quad \text{for } n \to \infty.$$

Set $M(r) := 0$ if $r \in [0, 2)$ or $r \in [\pi^2/3, \infty)$. If $r \in [2, \pi^2/3)$ set

$$M(r) := \begin{cases} \alpha & \text{if } r \in [a_n, m_n) \text{ and } r = a_n + \alpha \\ 1/(n+1)^2 - \alpha & \text{if } r \in [m_n, a_{n+1}) \text{ and } r = m_n + \alpha \end{cases}.$$

Then M is continuous and

$$\begin{aligned} M(a_n) &= 0, \\ M(m_n) &= \frac{1}{(n+1)^2}. \end{aligned} \tag{4.10}$$

Set $\rho(r) := 0$ if $r \in [0, 2)$ or $r \in [\pi^2/3, \infty)$. If $r \in [2, \pi^2/3)$ set

$$\rho(r) := \begin{cases} 1/(4\pi r^2) & \text{if } r \in [a_n, m_n) \\ -1/(4\pi r^2) & \text{if } r \in [m_n, a_{n+1}) \end{cases}.$$

Then $\rho \in L^1 \cap L^\infty(\mathbb{R}^3)$. Further for $r \geq 0$

$$M'(r) = 4\pi r^2 \rho(r)$$

and thus

$$M(r) = \int_0^r 4\pi s^2 \rho(s)\, \mathrm{d}s = \int_{B_r} \rho \, \mathrm{d}x.$$

In view of (4.10)

$$\nabla U_\rho^N(x) = \frac{M(r)}{r^2} \frac{x}{r}$$

will have a zero for all $x = (a_n, 0, 0)$, $n \in \mathbb{N}$. Let us see how this troubles the second derivatives of the Mondian potential:

As in the introduction to this section we have

$$\operatorname{div}(\nabla U_\rho^M(x)) = \rho(x) + \frac{1}{r^2}(r\sqrt{M(r)})'$$

for $r = |x| > 0$. But

$$\frac{1}{r^2}(r\sqrt{M(r)})' \notin L^1(B_4)$$

since

$$\begin{aligned}\int_{B_4} \left|\frac{1}{r^2}(r\sqrt{M(r)})'\right| \mathrm{d}x &= 4\pi \int_0^4 \left|(r\sqrt{M(r)})'\right| \mathrm{d}r \\ &= 4\pi \sum_{i=1}^{\infty} \left[\int_{a_n}^{m_n} (r\sqrt{M(r)})' \,\mathrm{d}r - \int_{m_n}^{a_{n+1}} (r\sqrt{M(r)})' \,\mathrm{d}r\right] \\ &= 8\pi \sum_{i=1}^{\infty} m_n \sqrt{M(m_n)} \geq 8\pi \sum_{i=1}^{\infty} \frac{1}{n+1} = \infty.\end{aligned}$$

Hence

$$\operatorname{div}(\nabla U_\rho^M) \notin L^1(B_4)$$

and

$$\nabla U_\rho^M \notin W^{1,1}_{loc}(\mathbb{R}^3).$$

□

Since the density ρ constructed in Lemma 4.3.6 mimics the difficulties that one can encounter in a situation without symmetry assumptions, we suspect that it is impossible to prove the existence of weak, integrable derivatives of ∇U_ρ^M for general $\rho \in L^1 \cap L^\infty(\mathbb{R}^3)$, ≥ 0. Thus the assumption of spherical symmetry in Theorem 4.3.3 seems indeed to be necessary - at least if one wants to rely on Theorem III.3 of DiPerna & Lions (1989b).

4.4 Conservation of energy

In this section we prove that weak Lagrangian solutions f of the (VQMS) conserve energy as long as the support of f remains bounded. Since we have already proven that the spherically symmetric, weak Eulerian solutions from Theorem 4.2.1 are also Lagrangian ones (Theorem 4.3.3) this yields conservation of energy for these solutions. In Section 6 we show how the result from this section can be used to prove also conservation of energy for symmetry free, weak Eulerian solutions even if we cannot prove that these solutions are Lagrangian ones.

General assumptions. *Throughout this section we assume that ($\Lambda 3$) holds.*

First a technical proposition that will be important to prove the finiteness of the potential energy.

Proposition 4.4.1. *Let $p > 1$, $R > 0$ and $\rho \in L^1 \cap L^p(\mathbb{R}^3), \geq 0$ with $\operatorname{supp}\rho \subset B_R$. Then*

$$\sqrt{1 - \frac{R^2}{|x|^2}}\,\frac{\|\rho\|_1}{(|x|+R)^2} \leq \left|\nabla U_\rho^N(x)\right| \leq \frac{\|\rho\|_1}{(|x|-R)^2}$$

for a.e. $x \in \mathbb{R}^3$ with $|x| > R$.

Proof. Let $x, y \in \mathbb{R}^3$ with $|y| < R < |x|$, then $|x-y| \geq |x| - R$, and hence

$$\left|\nabla U_\rho^N(x)\right| \leq \int \frac{\rho(y')}{(|x|-R)^2}\,\mathrm{d}y' = \frac{\|\rho\|_1}{(|x|-R)^2}.$$

Let α be the angle between the vectors x and $x-y$. With α_0 as in the following sketch

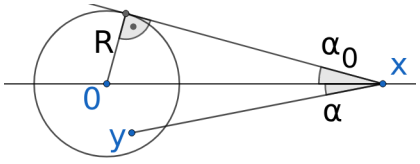

we have

$$|\alpha| \leq \alpha_0 \leq \frac{\pi}{2}$$

and

$$\cos\alpha \geq \cos\alpha_0 = \sqrt{1-\sin^2\alpha_0} = \sqrt{1-\frac{R^2}{|x|^2}}.$$

Together with the estimate $|x-y| \leq |x|+R$, this yields

$$\left|\nabla U_\rho^N(x)\right| \geq \left|\nabla U_\rho^N(x)\cdot\frac{x}{|x|}\right| = \left|\int \frac{\cos\alpha}{|x-y'|^2}\rho(y')\,\mathrm{d}y'\right| \geq \sqrt{1-\frac{R}{|x|^2}}\,\frac{\|\rho\|_1}{(|x|+R)^2}.$$

□

Next we introduce the function $\mathcal{Q}$, which is of importance in defining the potential energy.

Definition and Lemma 4.4.2. *Set*

$$\mathcal{Q}(v) := \int_0^v \lambda(u)u\,\mathrm{d}u, \quad v \in [0,\infty).$$

Then $\mathcal{Q} \in C^1([0,\infty))$, it is monotonic increasing and for all $v_1, v_2 \geq 0$

$$|\mathcal{Q}(v_2)-\mathcal{Q}(v_1)| \leq \frac{3}{2}\Lambda_2|v_2^{3/2}-v_1^{3/2}|.$$

Proof. First we observe that Lemma 3.3.1 implies

$$\mathcal{Q} \in C^1([0,\infty)).$$

Since $\lambda \geq 0$ we also see directly that $\mathcal{Q}$ is monotonic. Further with the transformation $u = w^{2/3}$ we have

$$\mathcal{Q}(v) = \frac{2}{3}\int_0^{v^{3/2}} \lambda(w^{2/3})w^{1/3}\,\mathrm{d}w.$$

Since (Λ3) implies (Λ2) (Lemma 3.3.1), we have

$$\lambda(w^{2/3})w^{1/3} \leq \Lambda_2.$$

Hence for $v_2 \geq v_1 \geq 0$

$$\mathcal{Q}(v_2)-\mathcal{Q}(v_1) \leq \frac{2}{3}\Lambda_2|v_2^{3/2}-v_1^{3/2}|. \tag{4.11}$$

□

Further we will need the following first order Taylor expansion of $\mathcal{Q}$:

Lemma 4.4.3. *There is a $C > 0$ such that for all $u, v \in \mathbb{R}^3$*

$$|\mathcal{Q}(|u|)-\mathcal{Q}(|v|)-\lambda(|v|)v\cdot(u-v)| \leq C|u-v|^{3/2}.$$

Proof. Let $u, v \in \mathbb{R}^3$ such that

$$w_t := v + t(u-v) \neq 0$$

for all $t \in [0,1]$. Set

$$q(t) := \mathcal{Q}(|w_t|).$$

Then

$$q \in C^2([0,1])$$

with

$$q'(t) = \mathcal{Q}'(|w_t|)\frac{w_t}{|w_t|}\cdot(u-v) = \lambda(|w_t|)w_t\cdot(u-v)$$

and

$$q''(t) = \lambda'(|w_t|)\frac{[w_t\cdot(u-v)]^2}{|w_t|} + \lambda(|w_t|)|u-v|^2.$$

We have

$$\begin{aligned} q(1) - q(0) &= \int_0^1 q'(s)\,\mathrm{d}s = \int_0^1 \left(q'(0) + \int_0^s q''(t)\,\mathrm{d}t \right) \mathrm{d}s \\ &= q'(0) + \int_0^1 \int_t^1 \mathrm{d}s\, q''(t)\,\mathrm{d}t \\ &= q'(0) + \int_0^1 (1-t) q''(t)\,\mathrm{d}t. \end{aligned}$$

Hence

$$\mathcal{Q}(|u|) - \mathcal{Q}(|v|) - \lambda(|v|)v \cdot (u-v) = \int_0^1 (1-t) q''(t)\,\mathrm{d}t.$$

By ($\Lambda 2$) and ($\Lambda 3$)

$$|q''(t)| \leq C \frac{|u-v|^2}{|w_t|^{1/2}}.$$

Hence

$$\left| \int_0^1 (1-t) q''(t)\,\mathrm{d}t \right| \leq C|u-v|^2 \int_0^1 \frac{\mathrm{d}t}{|w_t|^{1/2}}.$$

The integral on the right side becomes maximal if w_t would be zero for $t = 1/2$. Hence

$$\begin{aligned} \int_0^1 \frac{\mathrm{d}t}{|w_t|^{1/2}} &\leq \int_0^1 \frac{\mathrm{d}t}{\left| -\frac{1}{2}|u-v| + t|u-v| \right|^{1/2}} \\ &= |u-v|^{-1/2} \int_0^1 \frac{\mathrm{d}t}{|t-1/2|^{1/2}} \\ &= 2\sqrt{2}|u-v|^{-1/2}. \end{aligned}$$

Thus

$$|\mathcal{Q}(|u|) - \mathcal{Q}(|v|) - \lambda(|v|)v \cdot (u-v)| \leq C|u-v|^{3/2}.$$

□

In Mondian physics one can formally derive that the potential energy corresponding to a density $\rho(x)$ is given by

$$\tilde{E}_{pot}(\rho) = -\frac{1}{8\pi} \int \left| \nabla U_\rho^N \right|^2 \mathrm{d}x - \frac{1}{4\pi} \int \mathcal{Q}\left(\left| \nabla U_\rho^N \right| \right) \mathrm{d}x$$

(Milgrom, 2010). However the second integral is in general not finite. If we choose for example a compactly supported density ρ then

$$\nabla U_\rho^N(x) = O(|x|^{-2})$$

for $|x| \to \infty$ (Proposition 4.4.1). If we choose further $\lambda(v) = 1/\sqrt{v}$, then

$$\mathcal{Q}(v) = \frac{2}{3} v^{3/2}, \quad v \geq 0,$$

and

$$\mathcal{Q}(\nabla U_\rho^N(x)) = O(|x|^{-3})$$

and this is not integrable. Nevertheless we can study the difference between the potential energies of two densities ρ and $\bar{\rho}$.

Lemma 4.4.4. *Let $p > 3$ and $\rho, \bar{\rho} \in L^1 \cap L^p(\mathbb{R}^3)$, ≥ 0 with compact support and $\|\rho\|_1 = \|\bar{\rho}\|_1$, then*

$$\int \left| \mathcal{Q}\left(\left| \nabla U_\rho^N \right| \right) - \mathcal{Q}\left(\left| \nabla U_{\bar{\rho}}^N \right| \right) \right| \mathrm{d}x < \infty$$

and hence

$$\begin{aligned} \tilde{E}_{pot}(\rho) - \tilde{E}_{pot}(\bar{\rho}) = &- \frac{1}{8\pi} \int \left(\left| \nabla U_\rho^N \right|^2 - \left| \nabla U_{\bar{\rho}}^N \right|^2 \right) \mathrm{d}x \\ &- \frac{1}{4\pi} \int \left(\mathcal{Q}\left(\left| \nabla U_\rho^N \right| \right) - \mathcal{Q}\left(\left| \nabla U_{\bar{\rho}}^N \right| \right) \right) \mathrm{d}x \end{aligned}$$

is finite.

Proof. Lemma 3.1.4 implies that $D^2U_\rho^N, D^2U_{\bar\rho}^N \in L^p(\mathbb{R}^3)$. Since $p > 3$, Morrey's inequality (Evans, 2010, Section 5.6. Theorem 5) implies that there is a $C > 0$ such that for every $x \in \mathbb{R}^3$

$$\|\nabla U_\rho^N\|_{L^\infty(B_1(x))},\ \|\nabla U_{\bar\rho}^N\|_{L^\infty(B_1(x))} < C.$$

Hence

$$\nabla U_\rho^N,\ \nabla U_{\bar\rho}^N \in L^\infty(\mathbb{R}^3).$$

Hence for $R > 0$

$$\int_{|x|<2R} \left|\mathcal{Q}\left(\left|\nabla U_\rho^N\right|\right) - \mathcal{Q}\left(\left|\nabla U_{\bar\rho}^N\right|\right)\right| \mathrm{d}x < \infty.$$

Fix $R > 0$ such that $\operatorname{supp}\rho, \operatorname{supp}\bar\rho \subset B_R$. Using Lemma 4.4.2 we can estimate

$$\int_{|x|\geq 2R} \left|\mathcal{Q}\left(\left|\nabla U_\rho^N\right|\right) - \mathcal{Q}\left(\left|\nabla U_{\bar\rho}^N\right|\right)\right| \mathrm{d}x \leq C \int_{|x|\geq 2R} \left(\left|\nabla U_\rho^N\right|^{3/2} - \left|\nabla U_{\bar\rho}^N\right|^{3/2}\right).$$

Using Proposition 4.4.1 we can estimate further

$$\begin{aligned}
&\int_{|x|\geq 2R} \left|\mathcal{Q}\left(\left|\nabla U_\rho^N\right|\right) - \mathcal{Q}\left(\left|\nabla U_{\bar\rho}^N\right|\right)\right| \mathrm{d}x \\
&\quad\leq C\|\rho\|_1^{3/2} \int_{|x|\geq 2R} \left(\frac{1}{(|x|-R)^3} - \left(1 - \frac{R^2}{|x|^2}\right)^{3/4} \frac{1}{(|x|+R)^3}\right) \mathrm{d}x \\
&\quad\leq C \int_{|x|\geq 2R} \left(\frac{1}{(|x|-R)^3} - \frac{1}{(|x|+R)^3}\right) \mathrm{d}x \\
&\qquad + C \int_{|x|\geq 2R} \frac{1}{(|x|+R)^3} \left(1 - \left(1 - \frac{R^2}{|x|^2}\right)^{3/4}\right) \mathrm{d}x \\
&\quad\leq C \int_{|x|\geq 2R} \frac{6R}{(|x|-R)^4} \,\mathrm{d}x + C \int_{|x|\geq 2R} \frac{1}{(|x|+R)^3} \frac{R^{3/2}}{|x|^{3/2}} \,\mathrm{d}x < \infty.
\end{aligned}$$

So

$$\int \left|\mathcal{Q}\left(\left|\nabla U_\rho^N\right|\right) - \mathcal{Q}\left(\left|\nabla U_{\bar\rho}^N\right|\right)\right| \mathrm{d}x < \infty.$$

In particular this implies that the second integral in the difference of the potential energies exists. Further Lemma 3.1.4 implies that the first integral exists. So

$$\tilde E_{pot}(\rho) - \tilde E_{pot}(\bar\rho)$$

is well defined and finite. □

In this thesis we are interested in 'the' energy of one specific distribution function f on position-velocity space. But for the potential energy it makes only sense to study differences of potential energies as we have just seen. Therefore we always fix a reference density $\bar\rho$ on position space that has the same mass as f and study the difference between the potential energies of ρ_f and $\bar\rho$. However the (finite) term $\int |\nabla U_{\bar\rho}^N|^2 \,\mathrm{d}x$ in the previous Lemma added only a negligible constant. Hence we drop it and work in the sequential with the following

Definition 4.4.5. Let both $f \in L^\infty(\mathbb{R}^6)$ and $\bar\rho \in C(\mathbb{R}^3)$ be non-negative and compactly supported with

$$\iint f \,\mathrm{d}v \,\mathrm{d}x = \int \bar\rho \,\mathrm{d}x.$$

Then both the kinetic energy of f

$$E_{kin}(f) := \frac{1}{2} \iint |v|^2 f \,\mathrm{d}v \,\mathrm{d}x$$

and the potential energy of f (w.r.t the reference density $\bar\rho$)

$$\begin{aligned}
E_{pot}(f) := E_{pot}(\rho_f) := &- \frac{1}{8\pi} \int \left|\nabla U_{\rho_f}^N\right|^2 \mathrm{d}x \\
&- \frac{1}{4\pi} \int \left(\mathcal{Q}\left(\left|\nabla U_{\rho_f}^N\right|\right) - \mathcal{Q}\left(\left|\nabla U_{\bar\rho}^N\right|\right)\right) \mathrm{d}x
\end{aligned}$$

are finite and we define the total energy of f as

$$E(f) := E_{kin}(f) + E_{pot}(f).$$

We can prove conservation of energy for weak Lagrangian solutions as long as the characteristics do not escape to infinity.

Theorem 4.4.6. *Let $T > 0$ and $\mathring{f} \in L^\infty(\mathbb{R}^6)$, ≥ 0 with compact support. Let*

$$f(t,z) = \mathring{f}(Z(0,t,z)), \quad t \in [0,T],\ z \in \mathbb{R}^6$$

be a weak Lagrangian solution of the (VQMS) with initial condition $\mathring{f}$. If there is an $R > 0$ such that for a.e. $z \in \operatorname{supp} \mathring{f}$ holds

$$|Z(s,0,z)| \leq R, \quad s \in [0,T],$$

then the total energy

$$E(f(t)) = E_{kin}(f(t)) + E_{pot}(f(t)), \quad t \in [0,T],$$

is constant.

For the solution of the (VQMS) from Theorem 4.2.1 the following form of the above theorem holds.

Theorem 4.4.7. *Let λ be as in Lemma 3.3.2 and $\mathring{f} \in C_c^1(\mathbb{R}^3)$, ≥ 0 and spherically symmetric. Then the solution f of the (VQMS) with initial condition $\mathring{f}$ from Theorem 4.2.1 conserves energy.*

Proof. According to Theorem 4.3.3 the solution f of the (VQMS) from Theorem 4.2.1 is a Lagrangian solution with flow $Z = (X, V)$. Theorem 4.3.3 relies on Theorem 3.5.4 to prove the existence of the flow Z. This theorem states further that there is an $R > 0$ such that for a.e. $z \in \operatorname{supp} \mathring{f}$ and for all $s \in [0,T]$

$$|Z(s,0,z)| \leq R.$$

Hence Theorem 4.4.6 implies that the energy is conserved. □

For the rest of this chapter the assumptions of Theorem 4.4.6 shall hold. The proof of Theorem 4.4.6 is split into several small steps. First we look at the kinetic energy.

Lemma 4.4.8. *The kinetic energy of f is absolutely continuous and*

$$\frac{\mathrm{d}}{\mathrm{d}t} E_{kin}(f(t)) = -\int j_f(t,x) \cdot \partial_x U_f^M(t,x)\,\mathrm{d}x, \quad t \in [0,T]$$

where

$$j_f(t,x) := \int v f(t,x,v)\,\mathrm{d}v, \quad t \in [0,T],\ x \in \mathbb{R}^3.$$

Proof. Shortly we write

$$X(t) = X(t,0,x,v),$$
$$V(t) = V(t,0,x,v),$$

for $t \in [0,T]$ and $x, v \in \mathbb{R}^3$. $V(t)$ is absolutely continuous with

$$\frac{\mathrm{d}}{\mathrm{d}t} V(t) = -\partial_x U_f^M(t, X(t))$$

and hence, by Lemma 3.4.3, $|V(t)|^2$ is absolutely continuous with

$$\frac{\mathrm{d}}{\mathrm{d}t} |V(t)|^2 = -2V(t) \cdot \partial_x U_f^M(t, X(t)).$$

Hence

$$\begin{aligned} E_{kin}(f(t)) - E_{kin}(f(0)) &= \frac{1}{2} \iint |v|^2 f(t,x,v)\,\mathrm{d}v\,\mathrm{d}x - \frac{1}{2} \iint |v|^2 \mathring{f}(x,v)\,\mathrm{d}v\,\mathrm{d}x \\ &= \frac{1}{2} \iint (|V(t)|^2 - |V(0)|^2) \mathring{f}(x,v)\,\mathrm{d}v\,\mathrm{d}x \\ &= -\iint \int_0^t V(s) \cdot \partial_x U_f^M(s, X(s)) \mathring{f}(x,v)\,\mathrm{d}s\,\mathrm{d}v\,\mathrm{d}x. \end{aligned}$$

Applying Fubini and again the transformation formula

$$E_{kin}(f(t)) - E_{kin}(f(0)) = -\int_0^t \iint v \cdot \partial_x U_f^M(s,x) f(s,x,v) \,\mathrm{d}v \,\mathrm{d}x \,\mathrm{d}s$$
$$= -\int_0^t \int j_f(t,x) \cdot \partial_x U_f^M(t,x) \,\mathrm{d}x \,\mathrm{d}s;$$

it was legitimate to use Fubini since there are $1 < p, q < \infty$ with $1/p + 1/q = 1$ such that $\partial_x U_f^M \in L^1(0,T; L^q_{loc}(\mathbb{R}^3))$ and $f \in L^\infty(0,T; L^p(\mathbb{R}^3))$ with $\operatorname{supp} f(t) \subset B_R$, and hence

$$\int_0^t \iint \left| v \cdot \partial_x U_f^M(s,x) f(s,x,v) \right| \mathrm{d}v \,\mathrm{d}x \,\mathrm{d}s$$
$$\leq R \int_0^t \|f(s)\|_p \left\| \partial_x U_f^M(s) \right\|_{L^q(B_R)} \mathrm{d}s < \infty.$$

Thus $E_{kin}(f(t))$ is absolutely continuous with

$$\frac{\mathrm{d}}{\mathrm{d}t} E_{kin}(f(t)) = -\int j_f(t,x) \cdot \partial_x U_f^M(t,x) \,\mathrm{d}x.$$

□

When studying the time derivative of E_{pot} in the sequential, it is convenient to regularize f. For $\epsilon > 0$ and $w \in C_c^\infty(\mathbb{R}^3)$, ≥ 0, $\int w \,\mathrm{d}x = 1$ we set

$$w_\epsilon(x) := \frac{1}{\epsilon^3} w\left(\frac{x}{\epsilon}\right)$$

and

$$f_\epsilon(t,x,v) := \int f(t,y,v) w_\epsilon(x-y) \,\mathrm{d}y,$$
$$\rho_\epsilon(t,x) := \rho_{f_\epsilon}(t,x),$$
$$j_\epsilon(t,x) := j_{f_\epsilon}(t,x);$$

$t \in [0,T]$, $x, v \in \mathbb{R}^3$.

First we look at spatial derivatives of $U^N_{\rho_\epsilon}$ and $U^N_{j_\epsilon}$.

Proposition 4.4.9. *We have*

$$\rho_\epsilon, j_\epsilon \in C([0,T]; C_b^1(\mathbb{R}^3))$$

and

$$U^N_{\rho_\epsilon}, U^N_{j_{\epsilon,i}} \in C([0,T]; C_b^2(\mathbb{R}^3)),$$

$i = 1,2,3$. *Further for all $t \in [0,T]$ and for $\epsilon > 0$ small enough*

$$\operatorname{supp} \rho_\epsilon(t), \operatorname{supp} j_\epsilon(t) \subset B_R$$

and

$$\|\rho_\epsilon(t)\|_\infty, \|j_\epsilon(t)\|_\infty \leq C$$

for a $C > 0$.

Remark. $C_b(\mathbb{R}^3)$ denotes the space of continuous and bounded functions on $\mathbb{R}^3$ equipped with the uniform norm $\|\cdot\|_\infty$. $C_b^k(\mathbb{R}^3)$, $k \in \mathbb{N}$, denotes the space of k times continuously differentiable functions on $\mathbb{R}^3$ that are bounded and whose partial derivatives up to k-th order are bounded, too. The norm of $f \in C_b^k(\mathbb{R}^3)$ is given by the uniform norm of f plus the uniform norms of all partial derivatives of f up to k-th order.

Proof. Since $\|\mathring{f}\|_\infty < \infty$ and the characteristics $Z(t,0,z)$ with $z \in \operatorname{supp} \mathring{f}$ are bounded, it follows that for $\epsilon > 0$ small the support and the L^∞-norm of ρ_ϵ and j_ϵ are bounded as stated. Let $\epsilon > 0$ be small such that these bounds hold. We have

$$j_\epsilon(t,x) = \int v f_\epsilon(t,x,v) \,\mathrm{d}v = \iint v w_\epsilon(x-y) f(t,y,v) \,\mathrm{d}y \,\mathrm{d}v =$$
$$= \iint V(t) w_\epsilon(x - X(t)) \mathring{f}(y,v) \,\mathrm{d}y \,\mathrm{d}v$$

for $t \in [0,T]$, $x \in \mathbb{R}^3$ where we wrote shortly

$$X(t) = X(t,0,y,v),$$
$$V(t) = V(t,0,y,v).$$

For a.e. $(y,v) \in \mathbb{R}^6$ the integrand is continuous with respect to $(t,x) \in [0,T] \times \mathbb{R}^3$ and it is bounded by $R\|w_\epsilon\|_\infty \|\mathring{f}\|_\infty 1_{\{|z| \le R\}}$. Hence

$$j_\epsilon \in C([0,T] \times \mathbb{R}^3).$$

Since $\operatorname{supp} j_\epsilon(t) \subset B_R$ for all $t \in [0,T]$, j_ϵ is uniformly continuous and in particular

$$j_\epsilon \in C([0,T]; C_b(\mathbb{R}^3)).$$

We can differentiate under the integral sign and get that

$$\partial_x j_\epsilon(t,x) = \iint V(t) \nabla(w_\epsilon)(x - X(t)) \mathring{f}(y,v) \,\mathrm{d}y \,\mathrm{d}v$$

is continuous on $[0,T] \times \mathbb{R}^3$. j_ϵ still is compactly supported, hence

$$j_\epsilon \in C([0,T]; C_b^1(\mathbb{R}^3)).$$

Since the map

$$C_c^1(B_R) \ni g \mapsto U_g^N \in C_b^2(\mathbb{R}^3)$$

is continuous (Lemma 3.1.3), we have that

$$U_{j_{\epsilon,i}}^N \in C([0,T]; C_b^2(\mathbb{R}^3)).$$

The proof for ρ_ϵ is completely analogous. □

Now we differentiate $\nabla U_{\rho_\epsilon}^N$ with respect to the time variable.

Lemma 4.4.10. *The partial derivative*

$$\partial_t \partial_x U_{\rho_\epsilon}^N \in C([0,T] \times \mathbb{R}^3).$$

exists with

$$\partial_t \partial_x U_{\rho_\epsilon}^N = -4\pi H(j_\epsilon).$$

Proof. For matter of simplicity we calculate first $\partial_t U_{\rho_\epsilon}^N$ instead of directly $\partial_t \partial_x U_{\rho_\epsilon}^N$. Let $\psi \in C^1(\mathbb{R})$ with $0 \le \psi \le 1$, $0 \le \psi' \le 2$, $\psi(s) = 0$ if $s \le 1$ and $\psi(s) = 1$ if $s \ge 2$. For $\delta > 0$ we define

$$\begin{aligned} U_\delta(t,x) &:= -\int \frac{\rho_\epsilon(t,y')}{|x-y'|} \psi\left(\frac{|x-y'|}{\delta}\right) \mathrm{d}y' = \\ &= -\iiint \frac{f(t,\xi',v') w_\epsilon(y'-\xi')}{|x-y'|} \psi\left(\frac{|x-y'|}{\delta}\right) \mathrm{d}\xi' \,\mathrm{d}v' \,\mathrm{d}y'. \end{aligned}$$

With the transformations

$$y' = x + \xi' - y$$

and

$$(\xi', v') = (X(t,0,\xi,v), V(t,0,\xi,v)) =: (X(t), V(t))$$

we have

$$\begin{aligned} U_\delta(t,x) &= -\iiint \frac{f(t,\xi',v') w_\epsilon(x-y)}{|y-\xi'|} \psi\left(\frac{|y-\xi'|}{\delta}\right) \mathrm{d}\xi' \,\mathrm{d}v' \,\mathrm{d}y = \\ &= -\iiint \frac{\mathring{f}(\xi,v) w_\epsilon(x-y)}{|y-X(t)|} \psi\left(\frac{|y-X(t)|}{\delta}\right) \mathrm{d}\xi \,\mathrm{d}v \,\mathrm{d}y. \end{aligned}$$

Since both $X(t)$ and $V(t)$ are absolutely continuous for a.e. $(\xi,v) \in \mathbb{R}^6$ and

$$\frac{\mathrm{d}}{\mathrm{d}t} X(t) = V(t)$$

we have

$$X \in C^1([0,T])$$

for a.e. $(\xi, v) \in \mathbb{R}^6$. Hence

$$U_\delta,\, \partial_t U_\delta \in C([0,T] \times \mathbb{R}^3)$$

with

$$\begin{aligned}\partial_t U_\delta(t,x) = -\iiint \mathring{f}(\xi,v) w_\epsilon(x-y) \\ \left[\frac{y-X(t)}{|y-X(t)|^3} \cdot V(t) \psi\left(\frac{|y-X(t)|}{\delta}\right)\right. \\ \left. -\frac{1}{\delta}\frac{y-X(t)}{|y-X(t)|^2} \cdot V(t) \psi'\left(\frac{|y-X(t)|}{\delta}\right)\right] \mathrm{d}\xi\, \mathrm{d}v\, \mathrm{d}y.\end{aligned}$$

Since for $t \in [0,T]$, $x \in \mathbb{R}^3$

$$\left|U^N_{\rho_\epsilon}(t,x) - U_\delta(t,x)\right| \le \int_{|x-y'|\le 2\delta} \frac{\rho_\epsilon(t,y')}{|x-y'|}\, \mathrm{d}y' \le C\delta^2,$$

U_δ converges uniformly to $U^N_{\rho_\epsilon}$ on $[0,T] \times \mathbb{R}^3$ when $\delta \to 0$. For $t \in [0,T]$, $x \in \mathbb{R}^3$ set

$$\begin{aligned}V(t,x) &:= -\iiint \mathring{f}(\xi,v) w_\epsilon(x-y) \frac{y-X(t)}{|y-X(t)|^3} \cdot V(t)\, \mathrm{d}\xi\, \mathrm{d}v\, \mathrm{d}y \\ &= -\iiint f(t,\xi',v') w_\epsilon(y'-\xi') \frac{x-y'}{|x-y'|^3} \cdot v'\, \mathrm{d}\xi'\, \mathrm{d}v'\, \mathrm{d}y' \\ &= -\int j_\epsilon(t,y') \cdot \frac{x-y'}{|x-y'|^3}\, \mathrm{d}y' \\ &= -\sum_{i=1}^3 \partial_{x_i} U^N_{j_{\epsilon,i}}.\end{aligned}$$

Using that the characteristics $Z(t,0,z)$ with $z \in \operatorname{supp} \mathring{f}$ are bounded and that $1-\psi(s) = \psi'(s) = 0$ for $s \ge 2$, we get

$$\begin{aligned}&|\partial_t U_\delta(t,x) - V(t,x)| \\ &\le \iiint_{|y-X(t)|\le 2\delta} \mathring{f}(\xi,v) w_\epsilon(x-y) \left(\frac{R}{|y-X(t)|^2} + \frac{1}{\delta}\frac{2R}{|y-X(t)|}\right) \mathrm{d}\xi\, \mathrm{d}v\, \mathrm{d}y \\ &\le 5R \iiint_{|x-y'|\le 2\delta} \frac{f(t,\xi',v') w_\epsilon(y'-\xi')}{|x-y'|^2}\, \mathrm{d}\xi'\, \mathrm{d}v'\, \mathrm{d}y' \\ &= 5R \int_{|x-y'|\le 2\delta} \frac{\rho_\epsilon(t,y')}{|x-y'|^2}\, \mathrm{d}y' \le C\delta.\end{aligned}$$

Hence $\partial_t U_\delta$ converges uniformly to V on $[0,T] \times \mathbb{R}^3$ when $\delta \to 0$. Thus

$$\partial_t U^N_{\rho_\epsilon} = V = -\sum_{i=1}^3 \partial_{x_i} U^N_{j_{\epsilon,i}} \in C([0,T] \times \mathbb{R}^3)$$

exists. Further both $\partial_x U^N_{\rho_\epsilon}$ and $\partial_x \partial_t U^N_{\rho_\epsilon}$ exist and are continuous. The Theorem of Schwartz then implies that

$$\partial_t \partial_x U^N_{\rho_\epsilon} = \partial_x \partial_t U^N_{\rho_\epsilon} = -\sum_{i=1}^3 \partial_x \partial_{x_i} U^N_{j_{\epsilon,i}} \in C([0,T] \times \mathbb{R}^3)$$

exists, too[9]. Using the formula from Lemma 3.2.3 this can be written as

$$\partial_t \partial_x U^N_{\rho_\epsilon} = -4\pi H(j_\epsilon).$$

□

[9]The Theorem of Schwartz in this form was first proved by Peano (1890) and in this form can also be found in (Rudin, 1976, Theorem 9.41)

Now that we have the time derivative of $\partial_x U^N_{\rho_\epsilon}$, we can differentiate $E_{pot}(\rho_\epsilon(t))$, too.

Lemma 4.4.11.

$$E_{pot}(\rho_\epsilon) \in C^1([0,T])$$

with

$$\frac{\mathrm{d}}{\mathrm{d}t} E_{pot}(\rho_\epsilon(t)) = \int \left(\partial_x U^N_{\rho_\epsilon} + \lambda\left(\left|\partial_x U^N_{\rho_\epsilon}\right|\right) \partial_x U^N_{\rho_\epsilon}\right) \cdot H(j_\epsilon)\,\mathrm{d}x.$$

Proof. Differentiation under the integral sign gives the desired formula. We only have to justify this calculation by finding an integrable function $g = g(x)$ such that

$$\left|\partial_x U^N_{\rho_\epsilon}(t) + \lambda\left(\left|\partial_x U^N_{\rho_\epsilon}\right|\right) \partial_x U^N_{\rho_\epsilon}\right| |H(j_\epsilon)| \leq g$$

on $[0,T] \times \mathbb{R}^3$. From Proposition 4.4.9 follows that for $\epsilon > 0$ fixed

$$\|\rho_\epsilon(t)\|_\infty,\ \|j_\epsilon(t)\|_\infty,\ \|\partial_x j_\epsilon(t)\|_\infty \leq C, \quad t \in [0,T],$$

for a $C > 0$.With Lemma 3.1.3

$$\|\partial_x U^N_{\rho_\epsilon}(t)\|_\infty,\ \|\partial_x^2 U^N_{j_\epsilon}(t)\|_\infty \leq C, \quad t \in [0,T].$$

With the formula from Lemma 3.2.3 for $H(j_\epsilon)$

$$|H(j_\epsilon)(t,x)| \leq C|\partial_x^2 U^N_{j_\epsilon}(t,x)|,$$

hence

$$\|H(j_\epsilon)(t)\|_\infty \leq C, \quad t \in [0,T].$$

Further Proposition 4.4.1 implies that for $t \in [0,T]$, $|x| \geq 2R$

$$|\partial_x U^N_{\rho_\epsilon}(t,x)| \leq \frac{C}{|x|^2}.$$

Similarly one proves

$$|H(j_\epsilon)(t,x)| \leq \frac{C}{|x|^3}.$$

Combining the above estimates and using that $\lambda(u) \leq \Lambda_2/\sqrt{u}$, $u > 0$, gives g. Hence

$$E_{pot}(\rho_\epsilon) \in C^1([0,T]).$$

□

Sending $\epsilon \to 0$ yields conservation of energy.

Lemma 4.4.12. *$E_{pot}(f)$ is absolutely continuous on $[0,T]$ with*

$$\frac{\mathrm{d}}{\mathrm{d}t} E_{pot}(f(t)) = -\frac{\mathrm{d}}{\mathrm{d}t} E_{kin}(f(t)), \quad t \in [0,T].$$

In particular, the total energy is conserved.

Proof. First we show that $E_{pot}(\rho_\epsilon)$ converges pointwise to $E_{pot}(\rho_f)$ on $[0,T]$. For every $1 \leq p < \infty$ and $t \in [0,T]$ we have

$$\rho_\epsilon(t) \to \rho(t) \quad \text{in } L^p(\mathbb{R}^3) \text{ for } \epsilon \to 0$$

and thus by Lemma 3.1.4 for every $\frac{3}{2} < q < \infty$

$$\partial_x U^N_{\rho_\epsilon}(t) \to \partial_x U^N_{\rho_f}(t) \quad \text{in } L^q(\mathbb{R}^3) \text{ for } \epsilon \to 0.$$

in particular for every $R' > 0$

$$\partial_x U^N_{\rho_\epsilon}(t) \to \partial_x U^N_{\rho_f}(t) \quad \text{in } L^{3/2}(B_{R'}) \text{ for } \epsilon \to 0.$$

Since $\|\rho_\epsilon\|_1 = \|\rho_f\|_1 = \|\mathring{f}\|_1$, Proposition 4.4.1 gives for $t \in [0,T]$ and $|x| \geq 2R$

$$\begin{aligned}
&|\partial_x U^N_{\rho_\epsilon}(t,x)|^{3/2} - |\nabla U^N_{\rho_f}(t,x)|^{3/2} \\
&\quad \leq \|\mathring{f}\|_1^{3/2} \left(\frac{1}{(|x|-R)^3} - \frac{1}{(|x|+R)^3} + \frac{1}{(|x|+R)^3} \left(1 - \left(1 - \frac{R^2}{|x|^2} \right)^{3/4} \right) \right) \\
&\quad \leq C \left(\frac{1}{(|x|-R)^4} + \frac{1}{(|x|+R)^3} \frac{R^{3/2}}{|x|^{3/2}} \right) \leq \frac{C}{|x|^4}.
\end{aligned}$$

Let $\delta > 0$ and choose $R' > 2R$ such that

$$\int_{|x|>R'} \frac{\mathrm{d}x}{|x|^4} < \delta,$$

then Lemma 4.4.2 implies

$$\begin{aligned}
&|E_{pot}(\rho_\epsilon(t)) - E_{pot}(\rho_f(t))| \\
&\qquad \leq C \left(\left| \|\partial_x U^N_{\rho_\epsilon}(t)\|_2^2 - \|\partial_x U^N_{\rho_f}(t)\|_2^2 \right| + \int_{B_{R'}} \left| \mathcal{Q}(|\partial_x U^N_{\rho_\epsilon}|) - \mathcal{Q}(|\partial_x U^N_{\rho_f}|) \right| \mathrm{d}x + \delta \right). \qquad (4.12)
\end{aligned}$$

Lemma 4.4.3 implies

$$\begin{aligned}
&\int_{B_{R'}} \left| \mathcal{Q}(|\partial_x U^N_{\rho_\epsilon}|) - \mathcal{Q}(|\partial_x U^N_{\rho_f}|) \right| \mathrm{d}x \\
&\quad \leq C \int_{B_{R'}} |\partial_x U^N_{\rho_\epsilon} - \partial_x U^N_f|^{3/2} \,\mathrm{d}x + C \int \lambda(|\partial_x U^N_f|) |\partial_x U^N_f| \left| \partial_x U^N_{\rho_\epsilon} - \partial_x U^N_f \right| \mathrm{d}x \\
&\quad \leq C \int_{B_{R'}} |\partial_x U^N_{\rho_\epsilon} - \partial_x U^N_f|^{3/2} \,\mathrm{d}x + C\Lambda_2 \|\partial_x U^N_f\|^{1/2}_{L^{3/2}(B_{R'})} \|\partial_x U^N_{\rho_\epsilon} - \partial_x U^N_f\|_{L^{3/2}(B_{R'})} \\
&\quad \leq C \left(\|\partial_x U^N_{\rho_\epsilon} - \partial_x U^N_f\|^{3/2}_{L^{3/2}(B_{R'})} + \|\partial_x U^N_{\rho_\epsilon} - \partial_x U^N_f\|_{L^{3/2}(B_{R'})} \right)
\end{aligned}$$

Thus the right side of inequality (4.12) converges to a value below $C\delta$ as $\epsilon \to 0$. Since $\delta > 0$ was arbitrary,

$$E_{pot}(\rho_\epsilon) \to E_{pot}(\rho_f) \qquad (4.13)$$

pointwise on $[0,T]$ for $\epsilon \to 0$.

Next we show that the derivative of $E_{pot}(\rho_\epsilon)$ converges, too. Lemma 3.3.1 implies that

$$\begin{aligned}
&\|\lambda(|\partial_x U^N_{\rho_\epsilon}|)\partial_x U^N_{\rho_\epsilon} - \lambda(|\partial_x U^N_{\rho_f}|)\partial_x U^N_{\rho_f}\|_{L^4(\mathbb{R}^3)} \\
&\qquad \leq C \||\partial_x U^N_{\rho_\epsilon} - \partial_x U^N_{\rho_f}|^{1/2}\|_{L^4(\mathbb{R}^3)} = C \|\partial_x U^N_{\rho_\epsilon} - \partial_x U^N_{\rho_f}\|^{1/2}_{L^2(\mathbb{R}^3)} \to 0
\end{aligned}$$

pointwise on $[0,T]$ for $\epsilon \to 0$. Since $j_\epsilon(t) \to j_f(t)$ in $L^{4/3}(\mathbb{R}^3)$ for $\epsilon \to 0$, $t \in [0,T]$, and $H : L^{4/3} \to L^{4/3}$ is continuous,

$$H(j_\epsilon(t)) \to H(j_f(t)) \quad \text{ in } L^{4/3}(\mathbb{R}^3) \text{ for } \epsilon \to 0.$$

Hence by Hölder

$$\begin{aligned}
\frac{\mathrm{d}}{\mathrm{d}t} E_{pot}(\rho_\epsilon) &= \int (\partial_x U^N_{\rho_\epsilon} + \lambda(|\partial_x U^N_{\rho_\epsilon}|)\partial_x U^N_{\rho_\epsilon}) \cdot H(j_\epsilon) \,\mathrm{d}x \\
&\to \int (\partial_x U^N_{\rho_f} + \lambda(|\partial_x U^N_{\rho_f}|)\partial_x U^N_{\rho_f}) \cdot H(j_f) \,\mathrm{d}x
\end{aligned}$$

pointwise on $[0,T]$ for $\epsilon \to 0$. Rewriting this convergence using Lemma 3.2.8 gives

$$\frac{\mathrm{d}}{\mathrm{d}t} E_{pot}(\rho_\epsilon) \to \int \partial_x U^M_{\rho_f} \cdot j_f \,\mathrm{d}x \qquad (4.14)$$

pointwise on $[0,T]$ for $\epsilon \to 0$.

Now we show that the pointwise convergences (4.13) and (4.14) are sufficient to prove the absolute continuity of $E_{pot}(\rho_f)$. Using the bounds on ρ_ϵ and j_ϵ from Proposition 4.4.9 gives

$$\begin{aligned}\left|\frac{\mathrm{d}}{\mathrm{d}t}E_{pot}(\rho_\epsilon)\right| &= \left|\int (\partial_x U^N_{\rho_\epsilon} + \lambda(|\partial_x U^N_{\rho_\epsilon}|)\partial_x U^N_{\rho_\epsilon}) \cdot H(j_\epsilon)\,\mathrm{d}x\right| \\ &\leq \left(\|\partial_x U^N_{\rho_\epsilon}\|_{L^4(\mathbb{R}^3)} + \Lambda_2 \|\partial_x U^N_{\rho_\epsilon}\|^{1/2}_{L^2(\mathbb{R}^3)}\right) \|H(j_\epsilon)\|_{L^{4/3}(\mathbb{R}^3)} \\ &\leq C\left(\|\rho_\epsilon\|_{L^{12/7}(\mathbb{R}^3)} + \|\rho_\epsilon\|^{1/2}_{L^{6/5}(\mathbb{R}^3)}\right) \|j_\epsilon\|_{L^{4/3}(\mathbb{R}^3)} \leq C\end{aligned}$$

with $C > 0$ independent of $\epsilon > 0$ small. This estimate allows us to use Lebesgue and together with (4.13) and (4.14) we get for $s, t \in [0, T]$

$$\begin{aligned}E_{pot}(\rho_f(t)) - E_{pot}(\rho_f(s)) &= \lim_{\epsilon\to 0}(E_{pot}(\rho_\epsilon(t)) - E_{pot}(\rho_\epsilon(s))) \\ &= \lim_{\epsilon\to 0}\int_s^t \frac{\mathrm{d}}{\mathrm{d}t}E_{pot}(\rho_\epsilon(\tau))\,\mathrm{d}\tau \\ &= \int_s^t \int \partial_x U^M_{\rho_f}(\tau) \cdot j_f(\tau)\,\mathrm{d}x\,\mathrm{d}\tau \\ &= -\int_s^t \frac{\mathrm{d}}{\mathrm{d}\tau}E_{kin}(f(\tau))\,\mathrm{d}\tau.\end{aligned}$$

Hence $E_{pot}(\rho_f)$ is continuous on $[0, T]$ and the total energy is conserved. □

4.5 The missing uniqueness problem

There are several proofs in the literature to prove uniqueness for the Vlasov-Poisson system. Unfortunately all these proofs cannot be transferred to the (VQMS).

Proofing uniqueness for the (VQMS) like in Theorem 1.1 of Rein (2007) does not work due to both ∇U^M_ρ being at most Hölder continuous instead of Lipschitz continuous and due to the non-linear nature of the estimates

$$\|\lambda(|\nabla U^M_\rho|)\nabla U^M_\rho\|_{2s} \leq \||\nabla U^M_\rho|^{1/2}\|_{2s} = \|\nabla U^M_\rho\|^{1/2}_s \leq \|\rho\|^{1/2}_p; \tag{4.15}$$

we assumed that (Λ2) holds and that $\frac{3}{2} < s < \infty$ and $1 < p < 3$ are as in Lemma 3.1.4. Further the uniqueness proofs in (Knopf, 2017, Proposition 18), (DiPerna & Lions, 1989b, Theorem II.2) and (Loeper, 2006, Section 3.2.) can also all three not be transferred to the (VQMS) due to the non-linear nature of the estimate (4.15).

The major problem is that all four proofs rely on a Gronwall-loop argument. They define some quantity $d(t)$ that resembles the difference between two different solutions with the same initial data. Then an estimate of the form

$$d'(t) \leq Cd(t)$$

is derived. Since the two solutions have the same initial data, $d(0) = 0$, and Gronwall's lemma yields $d(t) = 0$ for all $t > 0$. This yields uniqueness.

However, when the estimate for d' is derived, all four proofs have at some point to estimate the gradient of the potential by some norm of the density. If we consider now the (VQMS) then due to the estimate (4.15) a square root enters at this point and we end up with an estimate of the form

$$d'(t) \leq C\left(d(t) + \sqrt{d(t)}\right).$$

In the following we do a formal calculation and follow the ansatz of DiPerna & Lions and Knopf to illustrate this.

Consider $f, g \in C^1([0, T] \times \mathbb{R}^6)$, $T > 0$, with $f(0) = g(0)$ such that for all $t \in [0, T]$

$$\operatorname{supp} f(t), \operatorname{supp} g(t) \subset B_R$$

for an $R > 0$ and

$$\begin{aligned}\partial_t f + v \cdot \partial_x f - \partial_x U^M_f \cdot \partial_v f = 0, \\ \partial_t g + v \cdot \partial_x g - \partial_x U^M_g \cdot \partial_v g = 0.\end{aligned}$$

For $p > 3$ study

$$d(t) := \|f(t) - g(t)\|_p, \quad t \in [0, T].$$

Then - suppressing the time variable on the right side -

$$d'(t) = \|f - g\|_p^{1-p} \int |f - g|^{p-2}(f - g)\partial_t(f - g)\,\mathrm{d}z.$$

Using the Vlasov equation we get

$$\partial_t(f - g) = -v \cdot \partial_x(f - g) + \partial_x U_f^M \cdot \partial_v(f - g) + (\partial_x U_f^M - \partial_x U_g^M) \cdot \partial_v g.$$

Using the compact support the theorem of Gauss gives

$$p \int |f - g|^{p-2}(f - g)\partial_x(f - g) \cdot v\,\mathrm{d}z = \int \mathrm{div}_x(|f - g|^p v)\,\mathrm{d}z = 0$$

and

$$p \int |f - g|^{p-2}(f - g)\partial_v(f - g) \cdot \partial_x U_f^M\,\mathrm{d}z = \int \mathrm{div}_v(|f - g|^p \partial_x U_f^M)\,\mathrm{d}z = 0.$$

Hence

$$d'(t) \le C\|f - g\|_p^{1-p} \int |f - g|^{p-1} \left|\partial_x U_f^M - \partial_x U_g^M\right| \mathrm{d}z.$$

Assuming that ($\Lambda 3$) holds, Lemma 3.3.1 gives

$$\begin{aligned}\int |f - g|^{p-1} \left|\partial_x U_f^M - \partial_x U_g^M\right| \mathrm{d}z & \\ &\le \int |f - g|^{p-1} \left(\left|\partial_x U_{f-g}^N\right| + \left|\partial_x U_{f-g}^N\right|^{1/2}\right) \mathrm{d}z \\ &\le C\|f - g\|_p^{p-1} \left(\left\|\partial_x U_{f-g}^N\right\|_p + \left\|\partial_x U_{f-g}^N\right\|_{p/2}^{1/2}\right).\end{aligned}$$

Thus

$$d'(t) \le C \left(\left\|\partial_x U_{f-g}^N\right\|_p + \left\|\partial_x U_{f-g}^N\right\|_{p/2}^{1/2}\right).$$

For $s > 3/2$ and $1 < q < 3$ with

$$\frac{2}{3} + \frac{1}{q} = 1 + \frac{1}{s}$$

Lemma 3.1.4 gives

$$\left\|\partial_x U_{f-g}^N\right\|_s \le C\|\rho_{f-g}\|_q.$$

Since $q < 3 < p$ and the support of f and g is compact, we can estimate this further and get

$$\left\|\partial_x U_{f-g}^N\right\|_s \le C\|\rho_{f-g}\|_p \le C\|f - g\|_p.$$

Thus

$$d'(t) \le C(\|f - g\|_p + \|f - g\|_p^{1/2}) = C(d(t) + \sqrt{d(t)}).$$

Unfortunately this estimate is useless to prove uniqueness for the (VQMS).

5 Stationary solutions of the (VQMS) and their stability

In the following subsections we prove that there is a large class of stationary solutions to the (VQMS) that are stable against small, spherically symmetric perturbations. The solutions are of the form

$$f_0(x,v) = \phi(E) \tag{5.1}$$

where ϕ is a suitable chosen function and

$$E = E(x,v) = \frac{1}{2}|v|^2 + U^M_{f_0}(x), \quad x,v \in \mathbb{R}^3,$$

is the local energy. Since the local energy is conserved along solutions of

$$\begin{aligned}\dot{X} &= V,\\ \dot{V} &= -\partial_x U^M_{f_0}(X),\end{aligned}$$

f_0 is constant along such solutions, too. This enables us to prove that f_0 is a weak Eulerian solution of the (VQMS). The difficulty in constructing such an f_0 is that the right side of (5.1) depends on f_0 itself due to the term $U^M_{f_0}$, which appears in E. We construct f_0 as the minimizer of an energy-Casimir functional under a mass constraint. The corresponding Euler-Lagrange equation ensures that f_0 is of the form (5.1) and the fact that f_0 is a minimizer grants the desired stability.

5.1 The reduced energy-Casimir functional

Instead of finding f_0 directly it is convenient to construct first its density

$$\rho_0 = \rho_{f_0}$$

as the minimizer of a reduced energy-Casimir functional. For this purpose we introduce the Casimir functional on the space of densities first. For a suitable ansatz function Ψ and a measurable density $\rho : \mathbb{R}^3 \to [0,\infty)$ we define the Casimir functional

$$\mathcal{C}(\rho) := \int \Psi(\rho)\,\mathrm{d}x.$$

We demand that Ψ satisfies the following assumptions:

Assumptions on Ψ. $\Psi \in C^1([0,\infty))$, $\Psi(0) = \Psi'(0) = 0$ *and it holds:*

(Ψ1) Ψ *is strictly convex,*

(Ψ2) $\Psi(\rho) \geq C\rho^{1+1/n}$ *for* $\rho > 0$ *large, where* $0 < n < 3$.

In the following sections we use for a sufficiently regular density ρ the notation

$$E_{pot}(\rho) = E^N_{pot}(\rho) + E^Q_{pot}(\rho)$$

where

$$E^N_{pot}(\rho) := -\frac{1}{8\pi}\int \left|\nabla U^N_\rho\right|^2 \mathrm{d}x$$

is the "Newtonian" part of the potential energy and

$$E^Q_{pot}(\rho) := -\frac{1}{4\pi}\int \left(\mathcal{Q}\left(\left|\nabla U^N_\rho\right|\right) - \mathcal{Q}\left(\left|\nabla \bar{U}^N\right|\right)\right)\mathrm{d}x$$

is the part of the potential energy that makes Mondian physics different from Newtonian physics - we refer to it as the "Mondian" part of the potential energy. As discussed earlier for $E^Q_{pot}(\rho)$ to be finite it is important to fix a reference density $\bar{\rho}$ that has the same mass as ρ.

Let $M > 0$. Fix $\bar{\rho} \in C_c(\mathbb{R}^3)$, ≥ 0, spherically symmetric with $\|\bar{\rho}\|_1 = M$. Let $\bar{R} > 0$ be such that

$$\operatorname{supp}\bar{\rho} = B_{\bar{R}}.$$

In the following we use the notation

$$\nabla \bar{U}^N = \nabla U^N_{\bar{\rho}}.$$

For a sufficiently regular density ρ with the same mass $M > 0$ as $\bar{\rho}$ we define the reduced energy-Casimir functional

$$\mathcal{H}_r(\rho) := E_{pot}(\rho) + \mathcal{C}(\rho).$$

We search a minimizer of $\mathcal{H}_r$ over the set

$$\mathcal{R}_M := \left\{ \rho \in L^1_+(\mathbb{R}^3) \text{ sph. sym.} \middle| \|\rho\|_1 = M, |E^Q_{pot}(\rho)| + \mathcal{C}(\rho) < \infty \right\}.$$

Since we will see in the following section that $\mathcal{R}_M \subset L^{6/5}(\mathbb{R}^3)$, it follows from the Hardy-Littlewood-Sobolev inequality that for all $\rho \in \mathcal{R}_M$ also the Newtonian part of the potential energy is finite.

Note that the minimizer of the above variational problem does not depend on the choice of $\bar{\rho}$. To see this take another reference density $\tilde{\rho} \in C_c(\mathbb{R}^3)$, ≥ 0, spherically symmetric with $\|\tilde{\rho}\|_1 = M$. For $\rho \in \mathcal{R}_M$ denote by $\tilde{E}^Q_{pot}(\rho)$ the Mondian part of the potential energy of ρ with respect to the reference density $\tilde{\rho}$. Then

$$E^Q_{pot}(\rho) = \tilde{E}^Q_{pot}(\rho) + C$$

with

$$C = -\frac{1}{4\pi} \int \left(\mathcal{Q}\left(\left|\nabla U^N_{\tilde{\rho}}\right|\right) - \mathcal{Q}\left(\left|\nabla U^N_{\tilde{\rho}}\right|\right) \right) \mathrm{d}x \in \mathbb{R}$$

independent of $\rho \in \mathcal{R}_M$.

In the next section we prove the existence of a minimizer $\rho_0 \in \mathcal{R}_M$ of the reduced energy-Casimir functional $\mathcal{H}_r$. In Section 5.3 we deduce the corresponding Euler-Lagrange equation and analyse the regularity of ρ_0. Finally in Section 5.4 we define the full energy-Casimir functional on the space of distribution functions f and construct from ρ_0 a minimizer f_0 of the full functional. Using the fact that f_0 is a minimizer, we prove that f_0 is stable against small, spherically symmetric perturbations.

5.2 Minimizers of the reduced Energy-Casimir functional under a mass constraint

General assumptions. *Throughout this section we assume that (Λ1) and (Λ2) hold.*

Proposition 5.2.1. *$\mathcal{Q} \in C([0,\infty))$ and monotonic increasing. If $u \geq v \geq 0$, it holds that*

$$\mathcal{Q}(u) \leq \frac{2\Lambda_2}{3} u^{3/2}$$

and

$$\mathcal{Q}(u) - \mathcal{Q}(v) \leq \frac{2\Lambda_2}{3}(u^{3/2} - v^{3/2}).$$

If $u \geq v \geq 0$ are small, it holds additionally that

$$\mathcal{Q}(u) \geq \frac{2\Lambda_1}{3} u^{3/2}$$

and

$$\mathcal{Q}(u) - \mathcal{Q}(v) \geq \frac{2\Lambda_1}{3}(u^{3/2} - v^{3/2}).$$

Proof. Follows directly from the definition of $\mathcal{Q}$, (Λ1) and (Λ2). Compare the proof of Lemma 4.4.2. □

First we have to find bounds for the potential energy. Here we use the spherical symmetry to get also good bounds for the Mondian part of the potential energy.

Lemma 5.2.2. *There are $C_0 > 0$ and $C_1 = C_1(\bar{R}, \Lambda_2) > 0$ such that for all $\rho \in \mathcal{R}_M$*

$$-E^N_{pot}(\rho) \leq C_0 \|\rho\|^2_{6/5}$$

and

$$-E^Q_{pot}(\rho) \leq \frac{1}{4\pi} \int_{|x|\leq \bar{R}} \mathcal{Q}\left(\left|\nabla U^N_\rho\right|\right) \mathrm{d}x \leq -C_1 E^N_{pot}(\rho)^{3/4} \leq C_1 C_0 \|\rho\|^{3/2}_{6/5}.$$

Proof. The inequality for E^N_{pot} is a direct consequence of the Hardy-Littlewood-Sobolev inequality (Lieb & Loss, 2010, Theorem 4.3) since for $\rho \in L^{6/5}(\mathbb{R}^3)$

$$-E_{pot}(\rho) = \frac{1}{2} \iint \frac{\rho(x)\rho(y)}{|x-y|} \,\mathrm{d}x \,\mathrm{d}y;$$

see Lemma 3.1.6. So let us study the inequality for E^Q_{pot}: $\mathcal{Q}$ is monotonic. Thanks to spherical symmetry we have further for $|x| \geq \bar{R}$

$$|\nabla \bar{U}^N(x)| = \frac{M}{|x|^2} \geq |\nabla U^N_\rho(x)|.$$

Thus

$$\begin{aligned} -E^Q_{pot}(\rho) &= \frac{1}{4\pi} \int_{|x|\leq \bar{R}} \left(\mathcal{Q}\left(\left|\nabla U^N_\rho\right|\right) - \mathcal{Q}\left(\left|\nabla \bar{U}^N\right|\right)\right) \mathrm{d}x + \int_{|x|>\bar{R}} \dots \mathrm{d}x \\ &\leq \frac{1}{4\pi} \int_{|x|\leq \bar{R}} \mathcal{Q}\left(\left|\nabla U^N_\rho\right|\right) \mathrm{d}x. \end{aligned}$$

Further Hölder and Proposition 5.2.1 imply

$$\begin{aligned} \frac{1}{4\pi} \int_{|x|\leq \bar{R}} \mathcal{Q}\left(\left|\nabla U^N_\rho\right|\right) \mathrm{d}x &\leq \frac{\Lambda_2}{6\pi} \left(\int_{|x|\leq \bar{R}} |\nabla U^N_\rho|^2 \,\mathrm{d}x \right)^{3/4} \left(\frac{4\pi}{3} \bar{R}^3 \right)^{1/4} \\ &\leq -\Lambda_2 C(\bar{R}) E^N_{pot}(\rho)^{3/4}. \end{aligned}$$

Applying the inequality for $E^N_{pot}(\rho)$ closes the proof. □

Next we prove that $\mathcal{H}$ is bounded from below on $\mathcal{R}_M$ and several bounds along minimizing sequences.

Lemma 5.2.3. $\inf_{\mathcal{R}_M} \mathcal{H}_r > -\infty$ *and along every minimizing sequence* $(\rho_j) \subset \mathcal{R}_M$ *of* $\mathcal{H}_r$

$$\|\rho_j\|_{6/5},\ \|\rho_j\|_{1+1/n} \text{ and } \int \Psi(\rho_j) \,\mathrm{d}x$$

remain bounded.

Proof. Let $\rho \in \mathcal{R}_M$. From (Ψ2) and the definition of $\mathcal{R}_M$ we can deduce

$$\begin{aligned} \|\rho\|^{1+1/n}_{1+1/n} &= \int_{\{\rho\leq 1\}} \rho^{1+1/n} \,\mathrm{d}x + \int_{\{\rho>1\}} \rho^{1+1/n} \,\mathrm{d}x \\ &\leq M + C \int \Psi(\rho) \,\mathrm{d}x. \end{aligned} \tag{5.2}$$

Let either $\beta = 2$ or $\beta = 3/2$. Since for $\alpha = (n+1)/6$

$$\frac{1-\alpha}{1} + \frac{\alpha}{1+1/n} = \frac{5-n}{6} + \frac{n}{6} = \frac{5}{6},$$

the interpolation formula yields

$$\begin{aligned} \|\rho\|^\beta_{6/5} &\leq \|\rho\|_1^{(1-\alpha)\beta} \|\rho\|^{\alpha\beta}_{1+1/n} \\ &\leq C \left(1 + \int \Psi(\rho) \,\mathrm{d}x \right)^{n\beta/6} \\ &\leq C + C \left(\int \Psi(\rho) \,\mathrm{d}x \right)^{n\beta/6}; \end{aligned} \tag{5.3}$$

in the last inequality we used that $n\beta/6 < 1$. Using now Lemma 5.2.2, we can estimate $\mathcal{H}_r$ from below:

$$\begin{aligned} \mathcal{H}_r(\rho) &\geq \int \Psi(\rho) \,\mathrm{d}x - C\|\rho\|^2_{6/5} - C\|\rho\|^{3/2}_{6/5} \\ &\geq \int \Psi(\rho) \,\mathrm{d}x - C - C \left(\int \Psi(\rho) \,\mathrm{d}x \right)^{n/3} - C \left(\int \Psi(\rho) \,\mathrm{d}x \right)^{n/4}. \end{aligned} \tag{5.4}$$

Since $n < 3$, this implies that $\mathcal{H}_r$ is bounded from below on $\mathcal{R}_M$:

$$\inf_{\mathcal{R}_M} \mathcal{H}_r \geq \min_{a \geq 0}(a - C - Ca^{n/3} - Ca^{n/4}) > -\infty.$$

Let now $(\rho_j) \subset \mathcal{R}_M$ be a minimizing sequence of $\mathcal{H}_r$. Then (5.4) implies that $\int \Psi(\rho_j)\,\mathrm{d}x$ is bounded. (5.2) and (5.3) give the bounds for $\|\rho_j\|_{1+1/n}$ and $\|\rho_j\|_{6/5}$. □

Lemma 5.2.3 enables us to extract from minimizing sequences (ρ_j) a subsequence that converges weakly to a $\rho_0 \in L^{1+1/n}$. This ρ_0 is our candidate for the minimizer of $\mathcal{H}_r$. To prove that it is a minimizer we have in particular to show that

$$E_{pot}(\rho_j) \to E_{pot}(\rho_0) \quad \text{for } j \to \infty.$$

For this the following compactness result from Rein (2007) is helpful.

Lemma 5.2.4. *Let $(\rho_j) \subset L^{1+1/n}_+(\mathbb{R}^3)$ be such that*

$$\rho_j \rightharpoonup \rho_0 \quad \textit{weakly in } L^{1+1/n}(\mathbb{R}^3),$$
$$\forall \epsilon > 0\, \exists R > 0 : \quad \limsup_{j\to\infty} \int_{|x|\geq R} \rho_j\,\mathrm{d}x < \epsilon.$$

Then $\nabla U^N_{\rho_j} \to \nabla U^N_{\rho_0}$ strongly in L^2.

Proof. See Lemma 2.5. in Rein (2007). □

Thus in order to pass with E_{pot} to the limit we have to show that the mass along a minimizing sequence remains concentrated. In the Mondian situation this is even easier to prove than in the Newtonian situation. Far away from the centre of mass Mondian forces are much higher than their Newtonian counterpart, hence they should also confine mass much more efficiently. And since E^Q_{pot} is the term that makes the difference between Newtonian and Mondian physics, this effect should be hidden there. This turns out to be true as the following lemma shows.

Lemma 5.2.5. *If $(\rho_j) \subset \mathcal{R}_M$ is a minimizing sequence of $\mathcal{H}_r$, then there is a $C > 0$ such that for all $R > \bar{R}$ large enough and $j \in \mathbb{N}$*

$$\int_{|x|>R} \rho_j\,\mathrm{d}x \leq C\left(\log R - \log \bar{R}\right)^{-2/3} \tag{5.5}$$

Proof. For $r \geq 0$ let

$$M(\rho_j, r) := \int_{|x|\leq r} \rho_j\,\mathrm{d}x.$$

For $R > \bar{R}$ sufficiently large we can use Proposition 5.2.1 and get

$$-\frac{1}{4\pi}\int_{|x|\geq\bar{R}} \left(\mathcal{Q}\left(\left|\nabla U^N_{\rho_j}\right|\right) - \mathcal{Q}\left(\left|\nabla \bar{U}^N\right|\right)\right)\mathrm{d}x \geq \frac{\Lambda_1}{6\pi}\int_{|x|\geq\bar{R}} \left(|\nabla \bar{U}^N|^{3/2} - |\nabla U^N_{\rho_j}|^{3/2}\right)\mathrm{d}x.$$

Introducing polar coordinates and using that $M(\rho_j, r)$ takes values between 0 and M and is monotonic increasing, we can estimate further

$$\begin{aligned}
-\frac{1}{4\pi}\int_{|x|\geq\bar{R}} \left(\mathcal{Q}\left(\left|\nabla U^N_{\rho_j}\right|\right) - \mathcal{Q}\left(\left|\nabla \bar{U}^N\right|\right)\right)\mathrm{d}x &\geq \frac{2\Lambda_1}{3}\int_{\bar{R}}^{\infty} \frac{M^{3/2} - M(\rho_j, r)^{3/2}}{r}\,\mathrm{d}r \\
&\geq \frac{2\Lambda_1}{3}\int_{\bar{R}}^{\infty} \frac{(M - M(\rho_j, r))^{3/2}}{r}\,\mathrm{d}r \\
&\geq \frac{2\Lambda_1}{3}\left(M - M(\rho_j, R)\right)^{3/2}\int_{\bar{R}}^{R} \frac{\mathrm{d}r}{r}.
\end{aligned}$$

Additionally, Lemma 5.2.2 and 5.2.3 imply that $\mathcal{C}(\rho_j) + E^N_{pot}(\rho_j)$ is bounded. Hence $E^Q_{pot}(\rho_j)$ is bounded and

$$-\frac{1}{4\pi}\int_{|x|\geq\bar{R}} \left(\mathcal{Q}\left(\left|\nabla U^N_{\rho_j}\right|\right) - \mathcal{Q}\left(\left|\nabla \bar{U}^N\right|\right)\right)\mathrm{d}x \leq E^Q_{pot}(\rho_j) + \frac{1}{4\pi}\int_{|x|<\bar{R}} \mathcal{Q}\left(\left|\nabla U^N_{\rho_j}\right|\right)\mathrm{d}x \leq C$$

independent of $j \in \mathbb{N}$. Now we have only to use that

$$M - M(\rho_j, R) = \int_{|x|>R} \rho_j \, \mathrm{d}x$$

and we can close the proof. □

Now we can prove that there are minimizers of $\mathcal{H}_r$ over $\mathcal{R}_M$. To prove later that these minimizers are also stable against small perturbations, it is important that we prove further several convergences along minimizing sequences.

Theorem 5.2.6. *Let $(\rho_j) \subset \mathcal{R}_M$ be a minimizing sequence of $\mathcal{H}_r$. Then there exists a subsequence, again denoted by (ρ_j), such that*

$$\rho_j \rightharpoonup \rho_0 \quad \textit{weakly in } L^{1+1/n}(\mathbb{R}^3).$$

$\rho_0 \in \mathcal{R}_M$ is a minimizer of $\mathcal{H}_r$ and

$$\nabla U^N_{\rho_j} \to \nabla U^N_{\rho_0} \quad \textit{strongly in } L^2(\mathbb{R}^3).$$

If additionally ρ_0 is compactly supported,

$$\nabla U^N_{\rho_j} - \nabla U^N_{\rho_0} \to 0 \quad \textit{strongly in } L^{3/2}(\mathbb{R}^3).$$

Remark. Observe that

$$\nabla U^N_{\rho_0}, \, \nabla U^N_{\rho_j} \notin L^{3/2}(\mathbb{R}^3)$$

but

$$\nabla U^N_{\rho_j} - \nabla U^N_{\rho_0} \in L^{3/2}(\mathbb{R}^3).$$

Proof. Let $(\rho_j) \subset \mathcal{R}_M$ be a minimizing sequence of $\mathcal{H}_r$. Since by Lemma 5.2.3 $(\rho_j) \subset L^{1+1/n}(\mathbb{R}^3)$ is bounded, there exists a subsequence, again denoted by (ρ_j), such that

$$\rho_j \rightharpoonup \rho_0 \quad \text{weakly in } L^{1+1/n}(\mathbb{R}^3).$$

First we want to prove that $\rho_0 \in \mathcal{R}_M$. Obviously ρ_0 is spherically symmetric and non-negative. Due to the weak convergence and Lemma 5.2.5, there is for every $\epsilon > 0$ an $R > 0$ such that

$$\int_{B_R} \rho_0 \, \mathrm{d}x = \lim_{j\to\infty} \int_{B_R} \rho_j \, \mathrm{d}x \in [M - \epsilon, M].$$

Thus by monotone convergence

$$\int \rho_0 \, \mathrm{d}x = M.$$

Now we extract from (ρ_j) a subsequence $(\hat{\rho}_j)$ such that

$$\lim_{j\to\infty} \int \Psi(\hat{\rho}_j) \, \mathrm{d}x = \liminf_{j\to\infty} \int \Psi(\rho_j) \, \mathrm{d}x.$$

From Mazur's lemma we know that

$$\forall j \in \mathbb{N} \, \exists N_j \geq j \text{ and } c^{(j)}_j, \ldots, c^{(j)}_{N_j} \geq 0 \text{ with } \sum_{i=j}^{N_j} c^{(j)}_i = 1$$

such that

$$\tilde{\rho}_j := \sum_{i=j}^{N_j} c^{(j)}_i \hat{\rho}_i \to \rho_0 \quad \text{strongly in } L^{1+1/n}(\mathbb{R}^3).$$

We extract a subsequence $(\tilde{\rho}_{j_k})$ of $(\tilde{\rho}_j)$ such that $\tilde{\rho}_{j_k}$ converges to ρ_0 pointwise a.e.. Since Ψ is continuous, $\Psi(\tilde{\rho}_{j_k})$ converges pointwise a.e., too. Using Fatou's lemma and the convexity of Ψ we conclude that

$$\begin{aligned}
\int \Psi(\rho_0) \, \mathrm{d}x &\leq \liminf_{k\to\infty} \int \Psi(\tilde{\rho}_{j_k}) \, \mathrm{d}x = \liminf_{k\to\infty} \int \Psi\left(\sum_{i=j_k}^{N_{j_k}} c^{(j_k)}_i \hat{\rho}_i \right) \mathrm{d}x \\
&\leq \liminf_{k\to\infty} \sup_{l \geq j_k} \int \Psi(\hat{\rho}_l) \, \mathrm{d}x = \limsup_{j\to\infty} \int \Psi(\hat{\rho}_j) \, \mathrm{d}x \\
&= \lim_{j\to\infty} \int \Psi(\hat{\rho}_j) \, \mathrm{d}x = \liminf_{j\to\infty} \int \Psi(\rho_j) \, \mathrm{d}x. \qquad (5.6)
\end{aligned}$$

Lemma 5.2.3 implies that $\liminf \int \Psi(\rho_j)\,\mathrm{d}x < \infty$. Hence $\int \Psi(\rho_0) < \infty$. It remains to prove that $|E^Q_{pot}(\rho_0)| < \infty$. Then $\rho_0 \in \mathcal{R}_M$. We know that $\rho_0 \in L^1 \cap L^{1+1/n}(\mathbb{R}^3)$. In particular $\rho_0 \in L^{6/5}(\mathbb{R}^3)$. Thus Lemma 5.2.2 implies

$$E^Q_{pot}(\rho_0) > -\infty.$$

Before we can show that $E^Q_{pot}(\rho_0) < \infty$ we have to pass to the limit with the potential energy.

For the Newtonian part this is straightforward: Lemma 5.2.4 together with Lemma 5.2.5 imply that

$$\nabla U^N_{\rho_j} \to \nabla U^N_{\rho_0} \quad \text{strongly in } L^2(\mathbb{R}^3) \text{ for } j \to \infty.$$

In particular,

$$E^N_{pot}(\rho_j) \to E^N_{pot}(\rho_0) \quad \text{for } j \to \infty. \tag{5.7}$$

Now we treat the Mondian part of the potential energy: Thanks to spherical symmetry for every $\rho \in \mathcal{R}_M$ and $x \in \mathbb{R}^3$ with $|x| > \bar{R}$ holds

$$\mathcal{Q}(|\nabla U^N_\rho(x)|) \le \mathcal{Q}(|\nabla \bar{U}^N(x)|). \tag{5.8}$$

Thus for every $R > \bar{R}$ and $j \in \mathbb{N}$

$$E^Q_{pot}(\rho_j) \ge -\frac{1}{4\pi} \int_{|x|\le R} \Big(\mathcal{Q}(|\nabla U^N_{\rho_j}|) - \mathcal{Q}(|\nabla \bar{U}^N|) \Big)\,\mathrm{d}x. \tag{5.9}$$

Now we extract a subsequence of $(\nabla U^N_{\rho_j})$, which we denote again by $(\nabla U^N_{\rho_j})$, such that

$$\nabla U^N_{\rho_j} \to \nabla U^N_{\rho_0} \quad \text{pointwise a.e. for } j \to \infty.$$

Since $\mathcal{Q}$ is continuous, $\mathcal{Q}(|\nabla U^N_{\rho_j}|)$ converges pointwise a.e., too. From Proposition 5.2.1 and Lemma 5.2.3 we know further that

$$\mathcal{Q}(|\nabla U^N_{\rho_j}|) \le C\frac{M(\rho_j, r)^{3/2}}{r^3} \le C\|\rho_j\|^{3/2}_{6/5}\frac{\mathcal{L}(B_r)^{1/4}}{r^3} \le Cr^{-9/4}, \quad r > 0,$$

with $C > 0$ independent of $j \in \mathbb{N}$. Hence we can apply the theorem of dominated convergence in (5.9) and it follows

$$\begin{aligned}\liminf_{j\to\infty} E^Q_{pot}(\rho_j) &\ge -\lim_{j\to\infty} \frac{1}{4\pi}\int_{|x|\le R} \mathcal{Q}(|\nabla U^N_{\rho_j}|)\,\mathrm{d}x + \frac{1}{4\pi}\int_{|x|\le R} \mathcal{Q}(|\nabla \bar{U}^N|)\,\mathrm{d}x \\ &= -\frac{1}{4\pi}\int_{|x|\le R} \big(\mathcal{Q}(|\nabla U^N_{\rho_0}|) - \mathcal{Q}(|\nabla \bar{U}^N|)\big)\,\mathrm{d}x.\end{aligned}$$

(5.8) holds for ρ_0, too. Thus, when we send $R \to \infty$, monotone convergence yields

$$\liminf_{j\to\infty} E^Q_{pot}(\rho_j) \ge E^Q_{pot}(\rho_0). \tag{5.10}$$

In particular, $E^Q_{pot}(\rho_0) < \infty$ and thus $\rho_0 \in \mathcal{R}_M$.

Taking into account (5.6), (5.7) and (5.10) it follows

$$\begin{aligned}\mathcal{H}_r(\rho_0) &= \int \Psi(\rho_0)\,\mathrm{d}x + E^N_{pot}(\rho_0) + E^Q_{pot}(\rho_0) \\ &\le \liminf_{j\to\infty} \int \Psi(\rho_j)\,\mathrm{d}x + \lim_{j\to\infty} E^N_{pot}(\rho_j) + \liminf_{j\to\infty} E^Q_{pot}(\rho_j) \\ &\le \lim_{j\to\infty} \mathcal{H}_r(\rho_j) = \min_{\mathcal{R}_M} \mathcal{H}_r.\end{aligned} \tag{5.11}$$

Since $\rho_0 \in \mathcal{R}_M$,

$$\mathcal{H}_r(\rho_0) = \min_{\mathcal{R}_M} \mathcal{H}_r$$

and ρ_0 is indeed a minimizer of $\mathcal{H}_r$ over $\mathcal{R}_M$.

Now it proves important that, when we derived the estimate (5.6), we extracted first the subsequence $(\hat{\rho}_j)$. This way in the inequality (5.11) appears twice a $\liminf$. This actually implies that both $(\int \Psi(\rho_j)\,\mathrm{d}x)$ and $(E^Q_{pot}(\rho_j))$ are convergent and

$$\begin{aligned}\int \Psi(\rho_j)\,\mathrm{d}x &\to \int \Psi(\rho_0)\,\mathrm{d}x, \\ E^Q_{pot}(\rho_j) &\to E^Q_{pot}(\rho_0)\end{aligned} \tag{5.12}$$

for $j \to \infty$. This we need when we prove next that

$$\nabla U^N_{\rho_j} - \nabla U^N_{\rho_0} \to 0 \quad \text{strongly in } L^{3/2}(\mathbb{R}^3)$$

provided the support of ρ_0 is compact.

Let us assume in the following that ρ_0 has compact support and let $R_0 > 0$ be sufficiently large such that

$$\operatorname{supp} \rho_0 \subset B_{R_0}.$$

We have already seen above that

$$\nabla U^N_{\rho_j} \to \nabla U^N_{\rho_0} \quad \text{strongly in } L^2(\mathbb{R}^3) \text{ for } j \to \infty.$$

Hence

$$\nabla U^N_{\rho_j} \to \nabla U^N_{\rho_0} \quad \text{strongly in } L^{3/2}(B_{R_0}) \text{ for } j \to \infty.$$

Using spherical symmetry and the compact support of ρ_0 we derive the estimate

$$\begin{aligned}
\left\|\nabla U^N_{\rho_0} - \nabla U^N_{\rho_j}\right\|^{3/2}_{L^{3/2}(\{|x|\geq R_0\})} &= \int_{|x|\geq R_0} \left|\nabla U^N_{\rho_0} - \nabla U^N_{\rho_j}\right|^{3/2} \mathrm{d}x \\
&= \int_{|x|\geq R_0} \frac{(M - M(\rho_j, |x|))^{3/2}}{|x|^3}\, \mathrm{d}x \\
&\leq \int_{|x|\geq R_0} \frac{M^{3/2} - M(\rho_j, |x|)^{3/2}}{|x|^3}\, \mathrm{d}x \\
&= \int_{|x|\geq R_0} \left(|\nabla U^N_{\rho_0}|^{3/2} - |\nabla U^N_{\rho_j}|^{3/2}\right) \mathrm{d}x.
\end{aligned}$$

For R_0 sufficiently large we can use Proposition 5.2.1 and estimate further

$$\begin{aligned}
\left\|\nabla U^N_{\rho_0} - \nabla U^N_{\rho_j}\right\|^{3/2}_{L^{3/2}(\{|x|\geq R_0\})} &\leq \frac{3}{2\Lambda_1} \int_{|x|\geq R_0} \left(\mathcal{Q}(|\nabla U^N_{\rho_0}|) - \mathcal{Q}(|\nabla U^N_{\rho_j}|)\right) \mathrm{d}x \\
&= -\frac{6\pi}{\Lambda_1} \left(E^Q_{pot}(\rho_0) - E^Q_{pot}(\rho_j)\right) \\
&\quad - \frac{3}{2\Lambda_1} \int_{|x|<R_0} \left(\mathcal{Q}(|\nabla U^N_{\rho_0}|) - \mathcal{Q}(|\nabla U^N_{\rho_j}|)\right) \mathrm{d}x. \qquad (5.13)
\end{aligned}$$

Using Proposition 5.2.1, the mean value theorem and Hölder

$$\begin{aligned}
\frac{3}{2\Lambda_1} \int_{|x|<R_0} \left|\mathcal{Q}(|\nabla U^N_{\rho_0}|) - \mathcal{Q}(|\nabla U^N_{\rho_j}|)\right| \mathrm{d}x &\leq \frac{\Lambda_2}{\Lambda_1} \int_{|x|<R_0} \left||\nabla U^N_{\rho_0}|^{3/2} - |\nabla U^N_{\rho_j}|^{3/2}\right| \mathrm{d}x \\
&\leq \frac{\Lambda_2}{\Lambda_1} \int_{|x|<R_0} \frac{3}{2} \left(|\nabla U^N_{\rho_0}| + |\nabla U^N_{\rho_j}|\right)^{1/2} \left|\nabla U^N_{\rho_0} - \nabla U^N_{\rho_j}\right| \mathrm{d}x \\
&\leq C \left\|\nabla U^N_{\rho_0} - \nabla U^N_{\rho_j}\right\|_{L^{3/2}(B_{R_0})}
\end{aligned}$$

and this converges to zero for $j \to \infty$. Together with (5.12) and (5.13) this implies

$$\left\|\nabla U^N_{\rho_0} - \nabla U^N_{\rho_j}\right\|_{L^{3/2}(\{|x|\geq R_0\})} \to 0 \quad \text{for } j \to \infty.$$

So

$$\nabla U^N_{\rho_0} - \nabla U^N_{\rho_j} \to 0 \quad \text{in } L^{3/2}(\mathbb{R}^3) \text{ for } j \to \infty$$

provided that ρ_0 has compact support. □

5.3 The Euler-Lagrange equation for the reduced variational problem

Next we want to derive the Euler-Lagrange equation that belongs to the minimizer ρ_0. It will be important that $\lambda(|u|)u$, $u \in \mathbb{R}^3$, is Hölder continuous. Therefore we strengthen the general assumptions of the previous section.

General assumptions. *Throughout this section we assume that (Λ1) and (Λ3) hold.*

First a technical proposition:

Proposition 5.3.1. *Let $\phi \in L^\infty(\mathbb{R}^3)$ with compact support and $\int \phi \,\mathrm{d}x = 0$. Then*

$$\nabla U_\phi^N \in L^p(\mathbb{R}^3)$$

for every $1 < p \leq \infty$.

Proof. Let $\operatorname{supp}\phi \subset B_R$ and $x \in \mathbb{R}^3$, then

$$|\nabla U_\phi^N(x)| \leq \|\phi\|_\infty \int_{|y|\leq R} \frac{\mathrm{d}y}{|x-y|^2} \leq 4\pi R \|\phi\|_\infty < \infty.$$

Thus $\nabla U_\phi^N \in L^\infty(\mathbb{R}^3)$. Let now $|x| > 2R$. W.l.g. we may assume that

$$x = (x_1, 0, 0) \in \mathbb{R}^3 \text{ with } x_1 > 2R.$$

Then

$$\begin{aligned} |\partial_{x_2} U_\phi^N(x)| &= \left| \int \frac{-y_2}{|x-y|^3} \phi(y)\,\mathrm{d}y \right| \leq \|\phi\|_\infty R \int_{|y|<R} \frac{\mathrm{d}y}{|x-y|^3} \\ &\leq \|\phi\|_\infty R \mathcal{L}(B_R) \left(\frac{2}{|x|}\right)^3. \end{aligned}$$

And with the same calculation for $|\partial_{x_3} U_\phi(x)|$ we get that both

$$\partial_{x_2} U_\phi^N(x),\ \partial_{x_3} U_\phi^N(x) = O(|x|^{-3})$$

for $x_1 \to \infty$. Now let

$$\alpha := \phi 1_{\{\phi > 0\}}$$

and

$$\beta := -\phi 1_{\{\phi < 0\}}.$$

Then $\alpha, \beta \geq 0$, $\|\alpha\|_1 = \|\beta\|_1 = \|\phi\|_1/2$ and

$$\partial_{x_1} U_\phi^N(x) = \int_{|y|<R} \frac{x_1 - y_1}{|x-y|^3} \alpha(y)\,\mathrm{d}y - \int_{|y|<R} \frac{x_1 - y_1}{|x-y|^3} \beta(y)\,\mathrm{d}y$$

where both integrands on the right side are non-negative. With the same argumentation as in Proposition 4.4.1 we get

$$\begin{aligned} \frac{|\partial_{x_1} U_\phi^N(x)|}{\|\alpha\|_1} &\leq \frac{1}{(|x|-R)^2} - \frac{\sqrt{1-R^2/|x|^2}}{(|x|+R)^2} = \\ &= \frac{1 - \sqrt{1-R^2/|x|^2}}{(|x|-R)^2} \\ &\quad + \sqrt{1-R^2/|x|^2} \left(\frac{1}{(|x|-R)^2} - \frac{1}{(|x|+R)^2} \right). \end{aligned} \tag{5.14}$$

Since

$$\frac{\mathrm{d}}{\mathrm{d}\sigma} \sqrt{1-\sigma} = -\frac{1}{2}(1-\sigma)^{-1/2}, \quad \sigma < 1,$$

we have

$$1 - \sqrt{1 - \frac{R^2}{|x|^2}} \leq \frac{1}{2} \left(1 - \frac{R^2}{|x|^2}\right)^{-1/2} \frac{R^2}{|x|^2} = \frac{1}{2}(|x|^2 - R^2)^{-1/2} \frac{R^2}{|x|} \leq \frac{C}{|x|}.$$

Further

$$\frac{1}{(|x|-R)^2} - \frac{1}{(|x|+R)^2} \leq \frac{2}{(|x|-R)^3}(|x|+R-|x|+R) = \frac{4R}{(|x|-R)^3}.$$

Thus (5.14) implies that

$$\partial_{x_1} U_\phi^N(x) = O(|x|^{-3})$$

for $x_1 \to \infty$. Thus in general

$$\nabla U_\phi^N(x) = O(|x|^{-3})$$

for $|x| \to \infty$. And since ∇U_ϕ^N is bounded, this implies that

$$\nabla U_\phi^N \in L^p(\mathbb{R}^3)$$

for every $1 < p \leq \infty$.

□

The most delicate part in deriving the Euler-Lagrange equation belonging to ρ_0 is the derivative of $E_{pot}^Q(\rho)$. This derivative we study in the next lemma.

Lemma 5.3.2. *Let $\rho \in L^1 \cap L^p(\mathbb{R}^3)$ for a $1 < p < 3$ and let $\phi \in L^\infty(\mathbb{R}^3)$ with compact support and $\int \phi \, \mathrm{d}x = 0$. Then*

$$\int \left| \mathcal{Q}\left(|\nabla U_{\rho+\tau\phi}^N|\right) - \mathcal{Q}\left(|\nabla U_\rho^N|\right) \right| \mathrm{d}x < \infty$$

and

$$\lim_{\tau \to 0} -\frac{1}{\tau} \frac{1}{4\pi} \int \left(\mathcal{Q}\left(|\nabla U_{\rho+\tau\phi}^N|\right) - \mathcal{Q}\left(|\nabla U_\rho^N|\right) \right) \mathrm{d}x = \int U_\rho^\lambda \phi \, \mathrm{d}x.$$

Remark 5.3.3. Observe that in Lemma 5.3.2 we did neither assume that ρ is spherically symmetric (like in Lemma 5.2.2) nor that the support of ρ is compact (like in Lemma 4.4.4). Nevertheless the difference between the Mondian part of the potential energy of ρ and $\rho + \tau\phi$ is finite. The reason is that the difference between the two densities under consideration is given by $\tau\phi$ and we have made several regularity assumptions on ϕ.

Proof of Lemma 5.3.2. We prove first the intermediate assertion

$$\lim_{\tau \to 0} -\frac{1}{\tau} \frac{1}{4\pi} \int \left(\mathcal{Q}\left(|\nabla U_{\rho+\tau\phi}^N|\right) - \mathcal{Q}\left(|\nabla U_\rho^N|\right) \right) \mathrm{d}x = -\frac{1}{4\pi} \int \lambda(|\nabla U_\rho^N|) \nabla U_\rho^N \cdot \nabla U_\phi^N \, \mathrm{d}x. \tag{5.15}$$

To avoid lengthy equations we use the abbreviation

$$F(v) := \lambda(|v|)v, \quad v \in \mathbb{R}^3.$$

Since we assume that (Λ3) holds, we have more regularity for $\mathcal{Q}$ and λ than in the previous section. From Lemma 4.4.2 follows

$$\mathcal{Q} \in C^1([0, \infty))$$

with

$$\mathcal{Q}'(\sigma) = \lambda(\sigma)\sigma, \quad \sigma \geq 0.$$

Since $\mathcal{Q}'(0) = 0$,

$$\mathcal{Q}(|\cdot|) \in C^1(\mathbb{R}^3)$$

with

$$\nabla \mathcal{Q}(|v|) = F(v), \quad v \in \mathbb{R}^3.$$

For $u, v \in \mathbb{R}^3$ set

$$f_{u,v}(t) := \mathcal{Q}(|tu + (1-t)v|), \quad 0 \leq t \leq 1.$$

From the mean value theorem follows that for every $u, v \in \mathbb{R}^3$ exists $s \in [0, 1]$ such that

$$\begin{aligned} \mathcal{Q}(|u|) - \mathcal{Q}(|v|) &= f_{u,v}(1) - f_{u,v}(0) = f'_{u,v}(s) \\ &= F(su + (1-s)v) \cdot (u - v). \end{aligned}$$

Treat $\nabla U_{\rho+\tau\phi}^N$ and ∇U_ρ^N as pointwise defined functions and interpret $\nabla U_{\rho+\tau s(y)\phi}^N$ and ∇U_ϕ^N as linear combinations of the two. Then for every $y \in \mathbb{R}^3$ there is $0 \leq s(y) \leq 1$ such that

$$\mathcal{Q}\left(|\nabla U_{\rho+\tau\phi}^N(y)|\right) - \mathcal{Q}\left(|\nabla U_\rho^N(y)|\right) = \tau F\left(\nabla U_{\rho+\tau s(y)\phi}^N(y)\right) \cdot \nabla U_\phi^N(y).$$

In view of the intermediate assertion 5.15, which we want to prove, we estimate (suppressing the y-argument)

$$\begin{aligned}\left|\mathcal{Q}\left(|\nabla U^N_{\rho+\tau\phi}|\right)-\mathcal{Q}\left(|\nabla U^N_\rho|\right)-\tau F(\nabla U^N_\rho)\cdot\nabla U^N_\phi\right| &\le \tau\left|F\left(\nabla U^N_{\rho+\tau s\phi}\right)-F(\nabla U^N_\rho)\right||\nabla U^N_\phi| \\ &\le C\tau\left|\nabla U^N_{\rho+\tau s\phi}-\nabla U^N_\rho\right|^{1/2}|\nabla U^N_\phi| \\ &\le C\tau^2|\nabla U^N_\phi|^{3/2};\end{aligned}$$

we have used the Hölder continuity of $F(u)=\lambda(|u|)u$ (Lemma 3.3.1). Thus

$$\frac{1}{4\pi}\frac{1}{\tau}\int\left|\mathcal{Q}\left(|\nabla U^N_{\rho+\tau\phi}|\right)-\mathcal{Q}\left(|\nabla U^N_\rho|\right)-\tau F(\nabla U^N_\rho)\cdot\nabla U^N_\phi\right|\mathrm{d}y\le C\tau\int|\nabla U^N_\phi|^{3/2}\,\mathrm{d}y.$$

With Proposition 5.3.1 this yields the intermediate assertion (5.15). Further this guarantees that the integral

$$\int\left|\mathcal{Q}\left(|\nabla U^N_{\rho+\tau\phi}|\right)-\mathcal{Q}\left(|\nabla U^N_\rho|\right)\right|\mathrm{d}x<\infty$$

for all $\tau\ge 0$. Using the estimates from the proof of Lemma 3.3.3 allows us to use Fubini in the following calculation:

$$\begin{aligned}-\frac{1}{4\pi}\int\lambda(|\nabla U^N_\rho|)\nabla U^N_\rho\cdot\nabla U^N_\phi\,\mathrm{d}x &= -\frac{1}{4\pi}\int\lambda(|\nabla U^N_\rho(y)|)\nabla U^N_\rho(y)\cdot\int\frac{y-x}{|y-x|^3}\phi(x)\,\mathrm{d}x\,\mathrm{d}y \\ &= \frac{1}{4\pi}\iint\lambda(|\nabla U^N_\rho(y)|)\nabla U^N_\rho(y)\cdot\left(\frac{x-y}{|x-y|^3}+\frac{y}{|y|^3}\right)\phi(x)\,\mathrm{d}y\,\mathrm{d}x \\ &= \int U^\lambda_\rho(x)\phi(x)\,\mathrm{d}x.\end{aligned}$$

□

We prove that minimizers ρ_0 of $\mathcal{H}_r$ satisfy the following Euler-Lagrange equation.

Lemma 5.3.4. *Let $\rho_0\in\mathcal{R}_M$ be a minimizer of $\mathcal{H}_r$ over $\mathcal{R}_M$. Then there is an $E_0\in\mathbb{R}$ such that for a.e. $x\in\mathbb{R}^3$*

$$\rho_0(x)=\begin{cases}(\Psi')^{-1}(E_0-U^M_{\rho_0}(x)), & \text{if } U^M_{\rho_0}<E_0,\\ 0, & \text{if } U^M_{\rho_0}\ge E_0.\end{cases}$$

Proof. Consider ρ_0 as a pointwise defined function. Let $\epsilon>0$ and set

$$S_\epsilon:=\{x\in B_{1/\epsilon}|\epsilon\le\rho_0(x)\le 1/\epsilon\}.$$

For $\epsilon>0$ small enough

$$\mathcal{L}(S_\epsilon)>0.$$

Let $w\in L^\infty(\mathbb{R}^3)$ be spherically symmetric and compactly supported such that

$$w\ge 0 \text{ on } \{\rho=0\} \tag{5.16}$$

and

$$w \text{ vanishes on } \operatorname{supp}\rho_0\backslash S_\epsilon. \tag{5.17}$$

Define

$$\phi:=w-\frac{\int w\,\mathrm{d}x}{\mathcal{L}(S_\epsilon)}1_{S_\epsilon}$$

and

$$\rho_\tau:=\rho_0+\tau\phi,\quad \tau>0.$$

Observe that $\phi\in L^\infty(\mathbb{R}^3)$, $\operatorname{supp}\phi\subset S_\epsilon\cup\operatorname{supp}w$ is compact and $\int\phi\,\mathrm{d}x=0$.

We show that $\rho_\tau\in\mathcal{R}_M$ for $\tau>0$ small: Obviously ρ_τ is spherically symmetric. If $\tau\ge 0$ is small, then $\rho_\tau\ge 0$ due to (5.16), (5.17) and the boundedness of ϕ on S_ϵ. Since $\int\phi\,\mathrm{d}x=0$, $\int\rho_\tau\,\mathrm{d}x=M$. Further

$$\begin{aligned}\int\Psi(\rho_\tau)\,\mathrm{d}x &\le \int\Psi(\rho_0)\,\mathrm{d}x+\int_{S_\epsilon}\Psi(\rho_0+\tau\phi)\,\mathrm{d}x+\int_{\operatorname{supp}w\setminus\operatorname{supp}\rho_0}\Psi(w)\,\mathrm{d}x \\ &\le \int\Psi(\rho_0)\,\mathrm{d}x+\Psi(1/\epsilon+\tau\|\phi\|_\infty)\mathcal{L}(B_{1/\epsilon})+\Psi(\|w\|_\infty)\mathcal{L}(\operatorname{supp}w)<\infty.\end{aligned}$$

And last, $\rho_0 \in \mathcal{R}_M$ and Lemma 5.3.2 imply

$$\int \left|\mathcal{Q}(|\nabla U^N_{\rho_\tau}|) - \mathcal{Q}(|\nabla \bar{U}^N|)\right| \mathrm{d}x \le \int \left|\mathcal{Q}(|\nabla U^N_{\rho_\tau}|) - \mathcal{Q}(|\nabla U^N_{\rho_0}|)\right| \mathrm{d}x + \int \left|\mathcal{Q}(|\nabla U^N_{\rho_0}|) - \mathcal{Q}(|\nabla \bar{U}^N|)\right| \mathrm{d}x < \infty.$$

Thus $\rho_\tau \in \mathcal{R}_M$.

Lemma 5.3.2 implies further

$$\frac{1}{\tau}(E^Q_{pot}(\rho_\tau) - E^Q_{pot}(\rho_0)) \to \int U^\lambda_{\rho_0}\phi \,\mathrm{d}x \quad \text{for } \tau \to 0.$$

Since

$$\frac{1}{\tau}(\Psi(\rho_\tau) - \Psi(\rho_0)) \to \Psi'(\rho_0)\phi \quad \text{pointwise for } \tau \to 0$$

and

$$\frac{1}{\tau}|\Psi(\rho_\tau) - \Psi(\rho_0)| \le \Psi'(1/\epsilon + \|\phi\|_\infty)|\phi|, \quad 0 \le \tau \le 1,$$

dominated convergence implies

$$\frac{1}{\tau}\int (\Psi(\rho_\tau) - \Psi(\rho_0)) \,\mathrm{d}x \to \int \Psi'(\rho_0)\phi \,\mathrm{d}x \quad \text{for } \tau \to 0.$$

Since both $\rho_\tau, \rho_0 \in \mathcal{R}_M \subset L^{6/5}(\mathbb{R}^3)$, we have thanks to Lemma 3.1.6

$$\begin{aligned}
&\frac{1}{\tau}(E^N_{pot}(\rho_\tau) - E^N_{pot}(\rho_0)) \\
&\qquad = -\frac{1}{2\tau}\iint \frac{\rho_\tau(x)\rho_\tau(y)}{|x-y|}\,\mathrm{d}x\,\mathrm{d}y + \frac{1}{2\tau}\iint \frac{\rho_0(x)\rho_0(y)}{|x-y|}\,\mathrm{d}x\,\mathrm{d}y \\
&\qquad = -\iint \frac{\phi(x)\rho(y)}{|x-y|}\,\mathrm{d}x\,\mathrm{d}y - \frac{\tau}{2}\iint \frac{\phi(x)\phi(y)}{|x-y|}\,\mathrm{d}x\,\mathrm{d}y.
\end{aligned}$$

Thus

$$\frac{1}{\tau}(E^N_{pot}(\rho_\tau) - E^N_{pot}(\rho_0)) \to \int U^N_{\rho_0}\phi \,\mathrm{d}x \quad \text{for } \tau \to 0.$$

Since $\rho_0, \rho_\tau \in \mathcal{R}_M$ and ρ_0 is a minimizer of $\mathcal{H}_r$ over $\mathcal{R}_M$, we have

$$\begin{aligned}
0 &\le \lim_{\tau \searrow 0} \frac{1}{\tau}(\mathcal{H}_r(\rho_\tau) - \mathcal{H}_r(\rho_0)) \\
&= \int (U^M_{\rho_0} + \Psi'(\rho_0))\phi \,\mathrm{d}x \\
&= \int (U^M_{\rho_0} + \Psi'(\rho_0))w \,\mathrm{d}x - \int_{S_\epsilon} (U^M_{\rho_0} + \Psi'(\rho_0))\frac{\int w \,\mathrm{d}x}{\mathcal{L}(S_\epsilon)} \,\mathrm{d}y \\
&= \int \left[U^M_{\rho_0} + \Psi'(\rho_0) - \frac{\int_{S_\epsilon}(U^M_{\rho_0} + \Psi'(\rho_0))\,\mathrm{d}y}{\mathcal{L}(S_\epsilon)}\right] w \,\mathrm{d}x \\
&= \int \left[U^M_{\rho_0} + \Psi'(\rho_0) - E_\epsilon\right] w \,\mathrm{d}x
\end{aligned}$$

with

$$E_\epsilon := \frac{\int_{S_\epsilon}(U^M_{\rho_0} + \Psi'(\rho_0))\,\mathrm{d}y}{\mathcal{L}(S_\epsilon)}.$$

w was arbitrary. In view of (5.16) and (5.17) the above inequality implies

$$\begin{aligned}
U^M_{\rho_0} + \Psi'(\rho_0) &\ge E_\epsilon && \text{a.e. on } \{\rho_0 = 0\}, \\
U^M_{\rho_0} + \Psi'(\rho_0) &= E_\epsilon && \text{a.e. on } S_\epsilon.
\end{aligned}$$

Since $\epsilon > 0$ was arbitrary, too, $E_\epsilon = E_0$ is independent of ϵ and

$$\begin{aligned}
U^M_{\rho_0} + \Psi'(\rho_0) &\ge E_0 && \text{a.e. on } \{\rho_0 = 0\}, \\
U^M_{\rho_0} + \Psi'(\rho_0) &= E_0 && \text{a.e. on } \{\rho_0 > 0\}.
\end{aligned}$$

Since $\Psi'(0) = 0$ and $\Psi'(\sigma) > 0$ if $\sigma > 0$, it holds for a.e. $x \in \mathbb{R}^3$

$$\rho_0(x) = 0 \iff U^M_{\rho_0}(x) \geq E_0$$

and

$$\rho_0(x) > 0 \iff U^M_{\rho_0} < E_0.$$

If $U^M_{\rho_0} < E_0$ the convexity of Ψ gives

$$\rho_0(x) = (\Psi')^{-1}(E_0 - U^M_{\rho_0}(x)).$$

□

Since for a suitable density ρ $\nabla U^M_\rho(x) = O(|x|^{-1})$ for $|x| \to \infty$, the potential $U^M_\rho(x)$ diverges logarithmically when $|x| \to \infty$. Combining this with the just proven Euler-Lagrange equation yields that minimizers of $\mathcal{H}_r$ are compactly supported.

Lemma 5.3.5. *Let $\rho_0 \in \mathcal{R}_M$ be a minimizer of $\mathcal{H}_r$ over $\mathcal{R}_M$. Then ρ_0 is compactly supported.*

Proof. Since ρ_0 is spherically symmetric and $\rho_0 \in \mathcal{R}_M \subset L^{6/5}(\mathbb{R}^3)$, Lemma 3.3.4 states that $U^M_{\rho_0} \in C^1(\mathbb{R}^3\backslash\{0\})$ and

$$U^M_{\rho_0}(r) = U^M_{\rho_0}(1) + \int_1^r \left(1 + \lambda\left(\frac{M(s)}{s^2}\right)\right)\frac{M(s)}{s^2}\,\mathrm{d}s, \quad r = |x|,\, x \in \mathbb{R}^3\backslash\{0\}.$$

Let $R > 1$ be sufficiently large such that we can use $(\Lambda 1)$ in the following estimate and such that $M(r) \geq M/2$ for every $r > R$. Then we get

$$U^M_{\rho_0}(r) \geq U^M_{\rho_0}(1) + \Lambda_1\sqrt{\frac{M}{2}}\int_R^r \frac{\mathrm{d}s}{s} \geq C' + C\log r, \quad r > R,$$

with $C' \in \mathbb{R}$ and $C > 0$. In particular $U^M_{\rho_0}(r) > E_0$ for $r > R$ sufficiently large. Thus ρ_0 is compactly supported. □

Last in this section we use the Euler-Lagrange equation to prove that minimizers are continuous.

Lemma 5.3.6. *Let $\rho_0 \in \mathcal{R}_M$ be a minimizer of $\mathcal{H}_r$ over $\mathcal{R}_M$. Then*

$$\rho_0 \in C_c(\mathbb{R}^3)$$

and

$$U^M_{\rho_0} \in C^1(\mathbb{R}^3).$$

Proof. As in the proof of Lemma 5.2.3

$$\rho_0 \in L^{1+1/n}(\mathbb{R}^3).$$

Hence

$$M(r) \leq \|\rho_0\|_{1+1/n}\|1_{B_r}\|_{n+1} \leq Cr^{3/(n+1)}, \quad r \geq 0. \tag{5.18}$$

Since $0 < n < 3$, we have in particular

$$M(r) \leq Cr^{3/4}, \quad 0 \leq r \leq R_0, \tag{5.19}$$

where $R_0 > 0$ is such that

$$\operatorname{supp}\rho_0 = B_{R_0}.$$

(5.19) and $(\Lambda 2)$ imply

$$|\nabla U^\lambda_{\rho_0}(x)| = \lambda\left(\frac{M(r)}{r^2}\right)\frac{M(r)}{r^2} \leq \frac{\sqrt{M(r)}}{r} \leq Cr^{-5/8}, \quad 0 < r = |x| < R_0.$$

Thus $(U^\lambda_{\rho_0}(r))'$ is in $L^1([0, R_0])$ and hence

$$U^\lambda_{\rho_0} \in C(B_{R_0}).$$

and with Lemma 3.3.4

$$U^{\lambda}_{\rho_0} \in C(\mathbb{R}^3).$$

(5.18) implies

$$|\nabla U^N(x)| = \frac{M(r)}{r^2} \leq Cr^{3/(n+1)-2}, \quad r = |x| > 0.$$

If $0 < n < 2$, $(U^N_{\rho_0}(r))' \in L^1([0, R_0])$ and hence

$$U^N_{\rho} \in C(\mathbb{R}^3).$$

Then $\rho \in C_c(\mathbb{R}^3)$. Since ($\Lambda$3) holds, $\nabla U^M_{\rho_0} \in C(\mathbb{R}^3)$ and $U^M_{\rho_0} \in C^1(\mathbb{R}^3)$.

If however $2 \leq n < 3$, some more arguments are necessary to get the same regularity for ρ_0 and $U^M_{\rho_0}$. Let us employ again (5.19). Then we have for $0 < r \leq R_0$

$$|U^N_{\rho_0}(r)| \leq |U^N_{\rho_0}(R_0)| + C \int_r^{R_0} s^{-5/4} \, \mathrm{d}s \leq Cr^{-1/4}. \tag{5.20}$$

Observe that due to the mean value theorem, the convexity of Ψ and (Ψ2) holds:

$$\Psi'(\rho) \geq \Psi'(\tau) = \frac{\Psi(\rho) - \Psi(0)}{\rho - 0} = \frac{\Psi(\rho)}{\rho} \geq C\rho^{1/n}$$

for every $\rho > 0$ large with an intermediate value $0 < \tau < \rho$. Thus

$$(\Psi')^{-1}(\eta) \leq C\eta^n \quad \text{for } \eta > 0 \text{ large.}$$

Thus

$$\begin{aligned} \int \rho_0^4 \, \mathrm{d}x &\leq \int_{\{\rho_0 \text{ small}\}} \rho_0^4 \, \mathrm{d}x + C \int_{\{\rho_0 \text{ large}\}} (E_0 - U^{\lambda}_{\rho_0} - U^N_{\rho_0})^{4n} \, \mathrm{d}x \\ &\leq C \int \rho_0 \, \mathrm{d}x + C \int_{B_{R_0}} (1 + |U^N_{\rho_0}(x)|)^{4n} \, \mathrm{d}x. \end{aligned}$$

Using (5.20) gives

$$\int \rho_0^4 \, \mathrm{d}x \leq C \left(1 + \int_{B_{R_0}} |x|^{-n} \, \mathrm{d}x \right) < \infty$$

since $0 < n < 3$. Hence

$$M(r) \leq \|\rho_0\|_4 \|1_{B_r}\|_{4/3} \leq Cr^{9/4}$$

and

$$|\nabla U^N_{\rho_0}| = \frac{M(r)}{r^2} \leq Cr^{1/4}, \quad x \in \mathbb{R}^3, \, r = |x|.$$

Thus

$$\nabla U^N_{\rho_0}, \, \nabla U^{\lambda}_{\rho_0} \in C(\mathbb{R}^3).$$

Hence

$$U^M_{\rho_0} \in C^1(\mathbb{R}^3)$$

and

$$\rho_0 \in C_c(\mathbb{R}^3).$$

□

5.4 Minimizers of the full energy-Casimir functional and their stability

General assumptions. *As in the previous section we assume throughout this section that (Λ1) and (Λ3) hold.*

For a suitable ansatz function Φ and a distribution function $f : \mathbb{R}^6 \to [0, \infty)$ measurable we define the Casimir functional

$$\mathcal{C}(f) := \iint \Phi(f) \, \mathrm{d}x \, \mathrm{d}v.$$

We demand that Φ satisfies the following assumptions:

Assumptions on Φ. $\Phi \in C^1([0,\infty))$, $\Phi(0) = \Phi'(0) = 0$ *and it holds:*

(Φ1) Φ *is strictly convex,*

(Φ2) $\Phi(f) \geq Cf^{1+1/k}$ *for* $f \geq 0$ *large, where* $0 < k < 3/2$.

In the following we use for a sufficiently regular distribution function f the notations

$$E_{pot}(f) := E_{pot}(\rho_f)$$

with $E_{pot}(\rho_f)$ as before and

$$E_{kin}(f) := \frac{1}{2} \iint |v|^2 f(x,v)\,\mathrm{d}x\,\mathrm{d}v$$

as in Section 4.4. We define the full energy-Casimir functional

$$\mathcal{H}_C(f) := E_{pot}(f) + E_{kin}(f) + \mathcal{C}(f).$$

Fix $M > 0$. We search a minimizer f_0 of $\mathcal{H}_C$ over the set

$$\mathcal{F}_M := \left\{ f \in L^1_+(\mathbb{R}^6) \text{ sph. sym} \middle| \|f\|_1 = M,\ |E^Q_{pot}(f)| + E_{kin}(f) + \mathcal{C}(f) < \infty \right\};$$

recall that a distribution function f is called spherically symmetric if for all $A \in SO(3)$

$$f(Ax, Av) = f(x,v) \quad \text{for a.e. } x, v \in \mathbb{R}^3.$$

We want to construct minimizers of $\mathcal{H}_C$ from the minimizers of $\mathcal{H}_r$. For this purpose we 'reduce' the full functional by factoring out the v-dependence. This we do exactly in the same manner as Rein (2007):

For $r \geq 0$ define

$$\mathcal{G}_r := \left\{ g \in L^1_+(\mathbb{R}^3) \text{ sph. sym} \middle| \int g(v)\,\mathrm{d}v = r,\ \int \left(\frac{1}{2}|v|^2 g(v) + \Phi(g(v)) \right) \mathrm{d}v < \infty \right\}$$

and

$$\Psi(r) := \inf_{g \in \mathcal{G}_r} \int \left(\frac{1}{2}|v|^2 g(v) + \Phi(g(v)) \right) \mathrm{d}v.$$

The relation between Φ and Ψ arises in a natural way. More details on that can be found in Rein (2007). But the relation between Φ and Ψ can also be made more explicit using Legendre transformations. This is done in Lemma 2.3. of Rein (2007). From this relation one deduces the following properties of Ψ:

Lemma 5.4.1. $\Psi \in C^1([0,\infty))$, $\Psi(0) = \Psi'(0) = 0$ *and it holds:*

(Ψ1) Ψ *is strictly convex,*

(Ψ2) $\Psi(\rho) \geq C\rho^{1+1/n}$ *for* $\rho > 0$ *large, where* $n := k + \frac{3}{2}$.

Proof. The proof of this lemma is identical with the proof of Lemma 2.3. in Rein (2007). □

Thus Ψ satisfies all assumptions that we used in the sections 5.1, 5.2 and 5.3. So we know that with the just defined Ψ there exists a minimizer $\rho_0 \in \mathcal{R}_M$ of $\mathcal{H}_r$ over $\mathcal{R}_M$, which satisfies in particular the Euler-Lagrange equation

$$\rho_0(x) = \begin{cases} (\Psi')^{-1}(E_0 - U^M_{\rho_0}(x)), & \text{if } U^M_{\rho_0} < E_0, \\ 0, & \text{if } U^M_{\rho_0} \geq E_0, \end{cases}$$

for an $E_0 \in \mathbb{R}$. Making use of this equation we can construct a minimizer f_0 of the full functional $\mathcal{H}_C$:

Lemma 5.4.2. *For every* $f \in \mathcal{F}_M$

$$\mathcal{H}_C(f) \geq \mathcal{H}_r(\rho_f).$$

Let $\rho_0 \in \mathcal{R}_M$ *be a minimizer of* $\mathcal{H}_r$ *over* $\mathcal{R}_M$ *and set*

$$f_0(x) := \begin{cases} (\Phi')^{-1}(E_0 - E), & \text{if } E < E_0, \\ 0, & \text{if } E \geq E_0, \end{cases}$$

with $E(x,v) = |v|^2/2 + U^M_{\rho_0}(x)$, $x, v \in \mathbb{R}^3$. *Then* $\rho_{f_0} = \rho_0$,

$$\mathcal{H}_C(f_0) = \mathcal{H}_r(\rho_0)$$

and $f_0 \in \mathcal{F}_M$ *is a minimizer of* $\mathcal{H}_C$ *over* $\mathcal{F}_M$. *We have further*

$$f_0 \in C_c(\mathbb{R}^6).$$

Proof. Inequality (2.11) from Rein (2007) states that for every $f \in \mathcal{F}_M$

$$\mathcal{C}(f) + E_{kin}(f) \geq \int \Psi(\rho_f)\,\mathrm{d}x.$$

Thus $\rho_f \in \mathcal{R}_M$ and

$$\mathcal{H}_C(f) \geq \mathcal{H}_r(\rho_f). \tag{5.21}$$

With exactly the same proof as for Theorem 2.2. in Rein (2007) if follows that

$$\mathcal{H}_C(f_0) = \mathcal{H}_r(\rho_0) \tag{5.22}$$

and

$$\rho_{f_0} = \rho_0;$$

one has only to replace U – which represents the Newtonian potential in Rein (2007) – by U^M everywhere. (5.21), (5.22) and that ρ_0 is a minimizer of $\mathcal{H}_r$ over $\mathcal{R}_M$ imply that f_0 is a minimizer of $\mathcal{H}_C$ over $\mathcal{F}_M$. By Lemma 5.3.6 $U^M_{\rho_0} \in C^1(\mathbb{R}^3)$. Thus $f_0 \in C(\mathbb{R}^6)$. By Lemma 5.3.5

$$\operatorname{supp}\rho_0 = B_{R_0}$$

for an $R_0 > 0$. Thus there is a $C_0 > 0$ such that

$$|U^M_{\rho_0}| \leq C_0 \text{ on } \operatorname{supp}\rho_0.$$

By the definition of f_0, for all $(x,v) \in \operatorname{supp} f_0$ holds

$$|v| \leq \sqrt{2(E_0 - U^M_{\rho_0}(x))} \leq \sqrt{2(|E_0| + C_0)} =: R_1.$$

Hence

$$\operatorname{supp} f_0 \subset B_{R_0} \times B_{R_1}$$

is compact. □

In the following let f_0, ρ_0 and $U^M_0 := U^M_{\rho_0}$ be as in Lemma 5.4.2. Since f_0 is a function of the local energy E, f_0 is constant along solutions of

$$\begin{aligned}\dot{X} &= V,\\ \dot{V} &= -\nabla U^M_0,\end{aligned}$$

and in this sense it is a solution of the (VQMS). However we can make this statement more explicit in the notions that we used previously in this thesis.

Lemma 5.4.3. *For every $\phi \in C^\infty_c(\mathbb{R}^6)$ holds*

$$\iint \left(v \cdot \partial_x\phi - \nabla U^M_0 \cdot \partial_v\phi\right) f_0\,\mathrm{d}x\,\mathrm{d}v = 0.$$

In particular $f(t) := f_0$, $t \geq 0$, is a static, weak Eulerian solution of the (VQMS).

Proof. We know from Lemma 5.3.6 that $U^M_0 \in C^1(\mathbb{R}^3)$ and from the previous lemma that f_0 has compact support. Thus there is a $C_0 > 0$ such that

$$E_0 - \frac{1}{2}|v|^2 - U^M_0(x) \leq C_0 \quad \text{for } (x,v) \in \operatorname{supp} f_0.$$

Further

$$E_0 - \frac{1}{2}|v|^2 - U^M_0(x) \leq 0 \quad \text{for } (x,v) \notin \operatorname{supp} f_0.$$

Extend $(\Phi')^{-1}$ by 0 to $(-\infty, 0)$. Then $(\Phi')^{-1} \in C(\mathbb{R})$. By smoothening $(\Phi')^{-1}$ we find a sequence $(\varphi_k) \subset C^1(\mathbb{R})$ such that

$$\varphi_k \to (\Phi')^{-1} \quad \text{uniformly on } [-1, C_0] \text{ for } k \to \infty$$

and for all $k \in \mathbb{N}$

$$\operatorname{supp} \varphi_k \subset [-1, C_0 + 1].$$

Set

$$f_k(x,v) := \varphi_k(E_0 - \frac{1}{2}|v|^2 - U_0^M(x)), \quad x, v \in \mathbb{R}^3.$$

In the proof of Lemma 5.3.5 we have seen that $U_0^M(x)$ diverges logarithmically for $|x| \to \infty$. Hence the uniform boundedness of $\operatorname{supp} \varphi_k$ implies that there is an $R' > 0$ such that

$$\operatorname{supp} f_k \subset B_{R'} \subset \mathbb{R}^6$$

for all $k \in \mathbb{N}$. Further the uniform convergence of the φ_k implies that also

$$f_k \to f_0 \quad \text{uniformly on } \mathbb{R}^6.$$

Thus for every $\phi \in C_c^\infty(\mathbb{R}^6)$

$$\iint \left(v \cdot \partial_x \phi - \nabla U_0^M \cdot \partial_v \phi\right) f_k \,\mathrm{d}x \,\mathrm{d}v \to \iint \left(v \cdot \partial_x \phi - \nabla U_0^M \cdot \partial_v \phi\right) f_0 \,\mathrm{d}x \,\mathrm{d}v$$

for $k \to \infty$. Since the theorem of Gauss gives

$$\begin{aligned}
&\iint \left(v \cdot \partial_x \phi - \nabla U_0^M \cdot \partial_v \phi\right) f_k \,\mathrm{d}x \,\mathrm{d}v \\
&\qquad = \iint \left(\operatorname{div}_x(\phi v) - \operatorname{div}_v(\phi \nabla U_0^M)\right) f_k \,\mathrm{d}x \,\mathrm{d}v \\
&\qquad = \iint \phi \varphi_k'(E_0 - E) \left(-v \cdot \nabla U_0^M + \nabla U_0^M \cdot v\right) \mathrm{d}x \,\mathrm{d}v = 0,
\end{aligned}$$

this implies

$$\iint \left(v \cdot \partial_x \phi - \nabla U_0^M \cdot \partial_v \phi\right) f_0 \,\mathrm{d}x \,\mathrm{d}v = 0.$$

In particular for $f(t) := f_0$, $t \geq 0$, and for every $\phi \in C_c^\infty([0,\infty) \times \mathbb{R}^6)$

$$\int_0^T \iint \left(\partial_t \phi + v \cdot \partial_x \phi - \nabla U_0^M \cdot \partial_v \phi\right) f_0 \,\mathrm{d}x \,\mathrm{d}v \,\mathrm{d}t + \iint \phi(0,x,v) f_0 \,\mathrm{d}x \,\mathrm{d}v = 0.$$

Thus f is a static, weak Eulerian solution of the (VQMS). □

Last we use the fact that f_0 is a minimizer to prove that f_0 is stable against small, spherically symmetric perturbations. For this purpose we need suitable tools to measure the distance between f_0 and another distribution function $f \in \mathcal{F}_M$. A first order Taylor expansion of E_{pot} under the integral sign gives for $f \in \mathcal{F}_M$

$$\mathcal{H}_C(f) - \mathcal{H}_C(f_0) = d(f, f_0) + \text{ remainder terms}$$

where

$$d(f, f_0) := \iint (\Phi(f) - \Phi(f_0) + E(f - f_0)) \,\mathrm{d}x \,\mathrm{d}v;$$

as before $E = |v|^2/2 + U_0^M(x)$, $x, v \in \mathbb{R}^3$. It holds

Lemma 5.4.4. *For every $f \in \mathcal{F}_M$ $d(f, f_0) \geq 0$ and $d(f, f_0) = 0$ iff $f = f_0$.*

Proof. Since $\iint f \,\mathrm{d}x \,\mathrm{d}v = \iint f_0 \,\mathrm{d}x \,\mathrm{d}v = M$ and Φ is convex,

$$\begin{aligned}
d(f, f_0) &= \iint (\Phi(f) - \Phi(f_0) + (E - E_0)(f - f_0)) \,\mathrm{d}x \,\mathrm{d}v \\
&\geq \iint \left[\Phi'(f_0) + E - E_0\right] (f - f_0) \,\mathrm{d}x \,\mathrm{d}v.
\end{aligned}$$

Due to the definition of f_0 the term in the brackets vanishes if $f_0 > 0$. Hence

$$d(f, f_0) \geq 0.$$

Moreover, since Φ is strictly convex, there is for every $f \in \mathcal{F}_M$ with $f \neq f_0$ a set of positive measure where

$$\Phi(f) - \Phi(f_0) > \Phi'(f_0)(f - f_0).$$

Hence $d(f, f_0) = 0$ iff $f = f_0$. □

Thus d is an appropriate tool to measure distances between f_0 and $f \in \mathcal{F}_M$. We have to take care of the remainder terms. Since

$$E^N_{pot}(f) = -\frac{1}{8\pi}\int |\nabla U^N_f|^2 \,\mathrm{d}x = -\frac{1}{2}\iint \frac{\rho_f(x)\rho_f(y)}{|x-y|}\,\mathrm{d}x\,\mathrm{d}y$$

is quadratic in f, its Taylor expansion stops after the second term and the corresponding remainder term is simple. For E^Q_{pot} the Taylor expansion does not stop and we have to estimate the corresponding remainder term using Lemma 4.4.3. This leads to the following lemma.

Lemma 5.4.5. *Let $f \in \mathcal{F}_M \cap L^\infty(\mathbb{R}^6)$ be compactly supported, then*

$$|\mathcal{H}_C(f) - \mathcal{H}_C(f_0) - d(f,f_0)| \le C\left(\|\nabla U^N_f - \nabla U^N_0\|_2^2 + \|\nabla U^N_f - \nabla U^N_0\|_{3/2}^{3/2}\right).$$

Proof. We have

$$\mathcal{H}_C(f) - \mathcal{H}_C(f_0) - d(f,f_0) = E_{pot}(f) - E_{pot}(f_0) - \iint U^M_0(f-f_0)\,\mathrm{d}x\,\mathrm{d}v. \tag{5.23}$$

A second order Taylor expansion under the integral sign gives

$$\begin{aligned} E^N_{pot}(f) - E^N_{pot}(f_0) &= -\frac{1}{8\pi}\int \left(|\nabla U^N_f|^2 - |\nabla U_0|^2\right)\mathrm{d}x \\ &= -\frac{1}{4\pi}\int \nabla U^N_0 \cdot (\nabla U^N_f - \nabla U^N_0)\,\mathrm{d}x - \frac{1}{8\pi}\int |\nabla U^N_f - \nabla U^N_0|^2\,\mathrm{d}x. \end{aligned}$$

Since $\rho_f, \rho_0 \in \mathcal{R}_M \subset L^{6/5}(\mathbb{R}^3)$, Lemma 3.1.6 gives

$$-\frac{1}{4\pi}\int \nabla U^N_0 \cdot (\nabla U^N_f - \nabla U^N_0)\,\mathrm{d}x = \iint U^N_0(f-f_0)\,\mathrm{d}x\,\mathrm{d}v.$$

Thus we have

$$E^N_{pot}(f) - E^N_{pot}(f_0) - \iint U^N_0(f-f_0)\,\mathrm{d}x\,\mathrm{d}v = -\frac{1}{8\pi}\|\nabla U^N_f - \nabla U^N_0\|_2^2. \tag{5.24}$$

Further Lemma 4.4.3 implies

$$\left|E^Q_{pot}(f) - E^Q_{pot}(f_0) + \frac{1}{4\pi}\int \lambda(|\nabla U^N_0|)\nabla U^N_0 \cdot (\nabla U^N_f - \nabla U^N_0)\,\mathrm{d}x\right| \le C\|\nabla U^N_f - \nabla U^N_0\|_{3/2}^{3/2}.$$

Since $\operatorname{supp}\rho_f, \operatorname{supp}\rho_0$ are compact, $\|\rho_f\|_\infty, \|\rho_0\|_\infty < \infty$ and $\int \rho_f\,\mathrm{d}x = \int \rho_0\,\mathrm{d}x = M$, we get as in the proof of Lemma 5.3.2

$$\frac{1}{4\pi}\int \lambda(|\nabla U^N_0|)\nabla U^N_0 \cdot (\nabla U^N_f - \nabla U^N_0)\,\mathrm{d}x = -\iint U^\lambda_0(f-f_0)\,\mathrm{d}x\,\mathrm{d}v.$$

Thus

$$\left|E^Q_{pot}(f) - E^Q_{pot}(f_0) - \iint U^\lambda_0(f-f_0)\,\mathrm{d}x\,\mathrm{d}v\right| \le C\|\nabla U^N_f - \nabla U^N_0\|_{3/2}^{3/2}. \tag{5.25}$$

Taking (5.23), (5.24) and (5.25) together implies

$$|\mathcal{H}_C(f) - \mathcal{H}_C(f_0) - d(f,f_0)| \le C\left(\|\nabla U^N_f - \nabla U^N_0\|_2^2 + \|\nabla U^N_f - \nabla U^N_0\|_{3/2}^{3/2}\right).$$

□

Now we can prove the following stability result.

Theorem 5.4.6. *Assume that λ is as in Lemma 3.3.2 and that the minimizer $f_0 \in \mathcal{F}_M$ of $\mathcal{H}_C$ over $\mathcal{F}_M$ is unique. Then for every $\epsilon > 0$ there is a $\delta > 0$ such that for every $\mathring{f} \in \mathcal{F}_M \cap C^1_c(\mathbb{R}^3)$ spherically symmetric with*

$$d(\mathring{f}, f_0) + \|\nabla U^N_{\mathring{f}} - \nabla U^N_0\|_2 + \|\nabla U^N_{\mathring{f}} - \nabla U^N_0\|_{3/2} < \delta$$

holds

$$d(f(t), f_0) + \|\partial_x U^N_f(t) - \nabla U^N_0\|_2 + \|\partial_x U^N_f(t) - \nabla U^N_0\|_{3/2} < \epsilon, \quad 0 \le t < \infty,$$

where f is the weak Eulerian solution of the (VQMS) with initial condition $\mathring{f}$ from Theorem 4.2.1.

Proof. Assume that there exist $\epsilon > 0$, $(\mathring{f}_j) \subset \mathcal{F}_M \cap C_c^1(\mathbb{R}^3)$ spherically symmetric, $(t_j) \subset [0, \infty)$ such that

$$d(\mathring{f}_j, f_0) + \|\nabla U^N_{\mathring{f}_j} - \nabla U^N_0\|_2 + \|\nabla U^N_{\mathring{f}_j} - \nabla U^N_0\|_{3/2} < \frac{1}{j} \tag{5.26}$$

but

$$d(f_j(t_j), f_0) + \|\partial_x U^N_{f_j}(t_j) - \nabla U^N_0\|_2 + \|\partial_x U^N_{f_j}(t_j) - \nabla U^N_0\|_{3/2} > \epsilon; \tag{5.27}$$

f_j is the weak Eulerian solution of the (VQMS) with initial condition $\mathring{f}_j$ from Theorem 4.2.1. First we check that $f_j(t_j) \in \mathcal{F}_M$ for every $j \in \mathbb{N}$. From Theorem 4.3.3 we know that f_j is also a weak Lagrangian solution. Thus it is in particular non-negative and by Lemma 4.1.3 it preserves L^p-norms. Thus

$$\iint f_j(t_j)\,\mathrm{d}x\,\mathrm{d}v = \|f_j(t_j)\|_1 = \|\mathring{f}_j\|_1 = M$$

and

$$\|f_j(t_j)\|_\infty = \|\mathring{f}_j\|_\infty < \infty.$$

As we have argued in the proof of Theorem 4.4.7 we see that $f_j(t_j)$ has compact support. Thus

$$|E^Q_{pot}(f_j(t_j))| + E_{kin}(f_j(t_j)) + \mathcal{C}(f_j(t_j)) < \infty.$$

Since $f_j(t_j)$ is also spherically symmetric, $f_j(t_j) \in \mathcal{F}_M$.

Now (5.26) and Lemma 5.4.5 imply that

$$\mathcal{H}_C(\mathring{f}_j) \to \mathcal{H}_C(f_0) \quad \text{for } j \to \infty.$$

By Theorem 4.4.7 f_j conserves energy and thus

$$E(f_j(t_j)) = E(\mathring{f}_j).$$

Further the flow Z_j corresponding to f_j conserves also phase space volume and by (Z5)

$$\begin{aligned}\mathcal{C}(f_j(t_j)) &= \int \Psi(f_j(t_j, z))\,\mathrm{d}z = \int \Psi(\mathring{f}_j(Z_j(0, t, z)))\,\mathrm{d}z \\ &= \int \Psi(\mathring{f}_j(z))\,\mathrm{d}z = \mathcal{C}(\mathring{f}_j).\end{aligned}$$

Hence

$$\mathcal{H}_C(f_j(t_j)) = \mathcal{H}_C(\mathring{f}_j) \to \mathcal{H}_C(f_0) \quad \text{for } j \to \infty. \tag{5.28}$$

Thus $(f_j(t_j)) \subset \mathcal{F}_M$ is a minimizing sequence of $\mathcal{H}_C$ over $\mathcal{F}_M$. Lemma 5.4.2 implies that $(\rho_{f_j}(t_j)) \subset \mathcal{R}_M$ is also a minimizing sequence of $\mathcal{H}_r$ over $\mathcal{R}_M$. Hence Theorem 5.2.6 implies

$$\|\partial_x U^N_{f_j}(t_j) - \nabla U^N_0\|_2 + \|\partial_x U^N_{f_j}(t_j) - \nabla U^N_0\|_{3/2} \to 0 \quad \text{for } j \to \infty.$$

Together with (5.28) and Lemma 5.4.5 this implies

$$d(f_j(t_j), f_0) \to 0 \quad \text{for } j \to \infty.$$

Thus for j sufficiently large

$$d(f_j(t_j), f_0) + \|\partial_x U^N_{f_j}(t_j) - \nabla U^N_0\|_2 + \|\partial_x U^N_{f_j}(t_j) - \nabla U^N_0\|_{3/2} < \epsilon,$$

which contradicts the assumption (5.27).

□

6 Discussion about the assumption of spherical symmetry

In many theorems in Sections 4 and 5 we made the assumption that the distribution function f must be spherically symmetric. We discuss where one can easily get rid of this assumption and where it was much more crucial.

In Theorem 4.2.1 we summarized the result of Keller (2016) that the initial value problem for the (VQMS) has global, weak Eulerian solutions under the assumption of spherical symmetry. In her proof Keller constructed first classical solutions f_k for a smoothed MOND field $\partial_x U_k^M$. Then the main ingredient in her proof is to guarantee that on every time interval $[0,T]$, $T>0$, the support of the f_k remains uniformly bounded. This enables her to pass to the limit and construct a weak Eulerian solution f of the (VQMS). The following formal calculation shows that at least on time intervals $[0,\delta]$ with $\delta>0$ sufficiently small we can guarantee that the support of a Lagrangian solution $f(t)$ remains bounded also without the assumption of spherical symmetry:

Let $T>0$ and assume that $f(t)$ is a weak Lagrangian solution of the (VQMS) on $[0,T]$ such that $\operatorname{supp} f(t)\subset B_R$ for a an $R>0$ and for every $t\in[0,T]$. Set

$$P(t):=\sup\left\{|v|\,|(x,v)\in\operatorname{supp} f(s),\,0\le s\le t\right\},\quad t\in[0,T].$$

Since f is a Lagrangian solution $\|f(t)\|_1$ and $\|f(t)\|_\infty$ are conserved and like in the exploratory calculation on page 395 in Rein (2007)

$$\|\partial_x U_f^N(t)\|_\infty\le C\|\rho_f(t)\|_\infty^{2/3}\le CP(t)^2,\quad t\in[0,T].$$

Let $(X(t),V(t))$ be an absolutely continuous characteristic with $(X(0),V(0))\in\operatorname{supp} f(0)$. Then

$$V(t)=V(0)-\int_0^t\partial_x U_f^M(s,X(s))\,\mathrm{d}s.$$

Assuming here in this formal calculation for simplicity[10] that

$$\partial_x U_f^M=\partial_x U_f^N+|\partial_x U_f^N|^{-1/2}\partial_x U_f^N,$$

we get the estimate

$$P(t)\le P(0)+C\int_0^t(P(s)^2+P(s))\,\mathrm{d}s.$$

Denote by $Q(t)$ the solution of

$$\dot Q=C(Q^2+Q),\quad Q(0)=P(0).$$

Then

$$P(t)\le Q(t)=\frac{1}{1-q_0e^{Ct}}-1$$

with $0<q_0=P(0)/(P(0)+1)<1$ and $t>0$ sufficiently small. Thus the v-support of f remains bounded on small time intervals and thus also the x-support remains bounded.

Marrying the idea of this formal calculation with the proof of Keller (2016) makes it possible to prove that on small timescales the initial value problem for the (VQMS) has weak Eulerian solutions also without symmetry assumptions.

Is it also possible to prove the existence of global, weak Eulerian solutions for the (VQMS) without symmetry assumptions? For the Vlasov-Poisson system this is possible (Pfaffelmoser, 1992; Lions & Perthame, 1991). In these proofs one shows that on every time interval $[0,T]$, $T>0$, the support of a solution f remains bounded. The main difficulty is to guarantee that the forces do not become so strong that they can accelerate mass in finite time to infinite velocities. When trying to prove the existence of global solutions of the (VQMS), we will have to deal with the same difficulty. But when the forces are strong Mondian and Newtonian physics are very similar. Hence one might suspect that it should be possible to prove the existence of global solutions of the (VQMS) by using similar techniques as in the situation of the Vlasov-Poisson system. However this is only a philosophical answer and a rigorous treatment of this question is left open.

As discussed in Section 4.3 we doubt that it is possible to prove that every weak Eulerian solution of the (VQMS) is also a Lagrangian one when we drop the assumption of spherical symmetry. But while

[10] Without symmetry assumptions $\partial_x U_f^M$ is then no longer a gradient but for this formal calculation we do not worry about that. For a precise argument we must employ that not only $\partial_x U_f^N\in L^\infty$ but that also $\partial_x U_f^N\in C^{0,\alpha}$, $\alpha>0$. Then

$$\partial_x U_f^M=H\left(\partial_x U_f^N+|\partial_x U_f^N|^{-1/2}\partial_x U_f^N\right)\in C^{0,\alpha/2}$$

since H maps Hölder continuous functions on Hölder continuous functions. From this connection between the regularity of $\partial_x U_f^N$ and $\partial_x U_f^M$ we get also L^∞-bounds for $\partial_x U_f^M$. This is a fact that we have not used here in this thesis.

we have proved conservation of energy in Section 4.4 without symmetry assumptions, we have done so only for weak Lagrangian solutions. So the question arises: Do weak Eulerian solutions conserve energy if we do not assume that they are spherically symmetric? Weak solutions for the Vlaosv-Poisson system (Horst et al., 1984) or for the Vlasov-Maxwell system (DiPerna & Lions, 1989a) are not known to conserve energy. So why should weak solutions for the (VQMS) do so? There is a difference why one considers weak solutions for these systems: For the above cited weak solutions of the Vlasov-Poisson and the Vlasov-Maxwell system the authors used the concept of weak solutions because they could not control L^∞-norms of the force term effectively enough. This is not the reason why we consider weak solutions for the (VQMS). We consider weak solutions for the (VQMS) because we cannot control the regularity of the force term. In particular the derivatives of the force term cause problems. But as shown and discussed above one can control L^∞-norms of the force term in MOND efficiently enough to guarantee that on finite time intervals the support of a solution f remains bounded. When now one constructs a weak Eulerian solution with the technique from Keller (2016) by approximating it with solutions f_k for a smoothed version of the Vlasov-QUMOND system, we can apply Theorem 4.4.6 to the f_k and get that these smooth solutions conserve energy. We can do so because the necessary smoothing applies only to the MOND function λ and we have proven Theorem 4.4.6 for very general λ. Since the support of the f_k remains uniformly bounded, we can pass to the limit also in the energy-integrals and we will get that the resulting weak Eulerian solution f conserves energy, too.

Is it also possible to prove the stability result from Section 5 without symmetry assumptions? Here the discussion becomes more tricky. The first point where we used the assumption of spherical symmetry was Lemma 5.2.2 where we proved bounds for the potential energy. For the Mondian part of the potential energy this proof relied very much on the assumption of spherical symmetry. In order to get a similar bound also without symmetry assumption we suspect that one has to prove first a confining property like the one from Lemma 5.2.5 where $E^Q_{pot}(\rho)$ controls how far apart the mass of ρ can be scattered. But also this proof used spherical symmetry and a new idea is necessary to prove such a confining property without symmetry assumptions. The next problem that one faces is that for a minimizing sequence (ρ_j) that converges weakly to a minimizer ρ_0 we must prove

$$\nabla U^N_{\rho_j} - \nabla U^N_{\rho_0} \to 0 \quad \text{strongly in } L^{3/2}(\mathbb{R}^3).$$

This is an essential ingredient in the proof of the stability statement in Theorem 5.4.6. Proofing that $\nabla U^N_{\rho_j} - \nabla U^N_{\rho_0}$ converges strongly to zero in $L^{3/2}(\mathbb{R}^3)$ relied on the assumption of spherical symmetry, too, and it did so in a somewhat sophisticated way. So also there we need a new proof.

If we manage to prove that without the assumption of spherical symmetry there are minimizers for the variational problem from Section 5, it is easy to get the corresponding Euler-Lagrange equation since our proof from Section 5.3 did not depend on the assumption of spherical symmetry. Further we would expect that the minimizers are still spherically symmetric. This holds in the Newtonian situation of the Vlasov-Poisson system and there is no reason why this should be different in the Mondian situation of the (VQMS). In the Newtonian situation we are aware of two proofs to show that minimizers are still spherically symmetric but both proofs fail in the Mondian situation:

The first proof uses that under the symmetric rearrangement of a density ρ the corresponding potential energy $E^N_{pot}(\rho)$ decreases (Lieb & Loss, 2010, Theorem 3.7). But this argument relies on the fact that the potential energy can be written in the form

$$E^N_{pot}(\rho) = -\frac{1}{2} \iint \frac{\rho(x)\rho(y)}{|x-y|} \,\mathrm{d}x \,\mathrm{d}y.$$

We do not have such a representation for $E^Q_{pot}(\rho)$ and therefore this proof cannot be applied in the Mondian situation.

The second proof relies on a symmetry result for solutions of elliptic equations (Gidas et al., 1979). In the Newtonian situation we can deduce from the Poisson equation and from the Euler-Lagrange equation that the potential U^N of a minimizer ρ_0 solves an equation of the form

$$\Delta U^N = 4\pi\rho_0 = 4\pi g(U^N)$$

with a suitable function g. For such an equation one can deduce from Theorem 4 of Gidas et al. (1979) that U^N must be spherically symmetric. Now we consider again the Mondian situation and we switch from the QUMOND formulation to the AQUAL[11] formulation of the MOND theory. This enables us to

[11] AQUAL is an acronym for aquadratic Lagrangian. Compare footnote 6 on Page 19.

see more directly why the result of Gidas et al. cannot be applied in the Mondian situation. In AQUAL the Mondian potential U^M is derived as the solution of the PDE

$$\operatorname{div}\left(\mu(|\nabla U^M|)\nabla U^M\right) = 4\pi\rho_0, \quad \lim_{|x|\to\infty} |\nabla U^M(x)| = 0.$$

In spherical symmetry the potentials U^M derived from the AQUAL and the QUMOND theory are identical, but without the assumption of spherical symmetry these potentials are in general different. Let μ be as in Lemma 3.3.2. We have

$$\begin{aligned}
&\operatorname{div}\left(\mu(|\nabla U^M|)\nabla U^M\right) - 4\pi g(U^M) \\
&\quad = \mu(|\nabla U^M|)\sum_{i=1}^{3}\partial_{x_i}^2 U^M + \frac{\mu'(|\nabla U^M|)}{|\nabla U^M|}\sum_{i,j=1}^{3}\partial_{x_i}U^M\partial_{x_j}U^M\partial_{x_i}\partial_{x_j}U^M - 4\pi g(U^M) \\
&\quad = G(U^M, \partial_{x_i}U^M, \partial_{x_i}\partial_{x_j}U^M)
\end{aligned}$$

with a suitable function $G = G(a, x, H)$, $a \in \mathbb{R}$, $x \in \mathbb{R}^3$, $H = (h_{ij}) \in \mathbb{R}^3 \times \mathbb{R}^3$. To apply Theorem 4 of Gidas et al. (1979) we need that for all $a \in \mathbb{R}$, $x \in \mathbb{R}^3$ the matrix

$$(\partial_{h_{ij}}G)_{1\le i,j\le 3} = \mu(|x|)E_3 + \frac{\mu'(|x|)}{|x|}xx^T$$

is positive definite; E_3 denotes the identity matrix with dimension 3. If $|x|$ is small, $\mu(|x|) = |x|$ and

$$(\partial_{h_{ij}}G)_{1\le i,j\le 3} = |x|\left(E_3 + \frac{xx^T}{|x|^2}\right).$$

Thus

$$(\partial_{h_{ij}}G)_{1\le i,j\le 3} \to 0 \quad \text{for } |x| \to 0.$$

Hence $(\partial_{h_{ij}}G)$ is not positive definite for $x = 0$ and the symmetry result of Gidas et al. (1979) cannot be applied in the Mondian situation.

Summarizing we can say, that it is possible to remove the assumption of spherical symmetry from the treatment of the time-dependent solutions in Section 4 and still get almost the same results – except for the link between Eulerian and Lagrangian solutions, which we discussed in detail in Section 4.3. In contrast, removing the assumption of spherical symmetry from the treatment of the variational problem in Section 5 will be quite a challenging task.

Part II: Modelling the Milky Way

Now we leave MOND and the equations that govern the evolution of globular clusters and emerge ourselves in the modelling of spiral galaxies:

7 Introduction Part II

The Milky Way - and spiral galaxies in general - still ask us many a riddle. To three of them we develop new answers here in this thesis:

> Where does the four armed spiral pattern in the Milky Way's ISM originate from (Steiman-Cameron et al., 2010)?
>
> Why does atomic hydrogen have in most spiral galaxies the same velocity dispersion well above the value expected from thermal considerations (Tamburro et al., 2009)?
>
> Is a halo of non-baryonic, dark matter necessary to explain the Milky Way's flat circular velocity curve?

The key in answering these questions is a model for our galaxy where the interstellar medium (ISM) is equipped with self-consistent dynamics. These dynamics are difficult to model because the ISM's mass is moving on almost circular orbits around the galactic centre. This 'almost' makes things difficult; how to implement it in a self-consistent model? But we cannot ignore it because it is important for stability. We solved this mathematical problem and this enables us to shed a new light on the three questions above.

The distribution function in our model is a function of the third component of the angular momentum and the energy only and our technique can easily be extended to construct a self-consistent, multi-phase model for the whole galaxy; a task that was elusive up to now (Binney, 2020). Our technique is based on a fixed-point like algorithm, which is an improved version of the algorithm from Andréasson & Rein (2015), plus a good understanding of how distribution functions, which match observations, must look like. The resulting distribution function is comparable with the one of a cut-out Mestel disc like it is, e.g., studied in Zang (1976), Toomre (1981) or Sellwood & Carlberg (2019). But here in this thesis our distribution function is embedded in a realistic model for our galaxy; not in an infinitely extended Mestel disc with infinite mass, like in the papers just cited.

How do we model the Milky Way in this thesis? The Milky Way has three baryonic components, a bulge, a stellar disc[12] and the interstellar medium (ISM). We include the bulge and the stellar disc as rigid components and model the ISM dynamically. In the Milky Way, the ISM's gaseous mass is confined to a very thin disc, which exhibits spiral patterns and where all mass is moving on almost circular orbits around the galactic centre. Simplifying, we assume in our model that the disc is razor-thin, i.e., all mass is restricted to live in the plain, and - at first - we ignore the spiral patterns and assume that the disc is axially symmetric. One could be tempted to simplify further and assume that all mass is on purely circular orbits. However, this would be a bad idea, because such a disc destroys itself very fast (Binney & Tremaine, 2008, §6.2.3). It is therefore important that we have at each position a dispersion of the velocities – and this makes things complicated. In total we will search for a rigid bulge, a rigid stellar disc and an axisymmetric distribution function $f(x,v) \geq 0$ on position-velocity space with $x, v \in \mathbb{R}^2$ that models the ISM.

Since most of the mass in our galaxy is on almost circular orbits, one can deduct from the observational data how the circular velocity curve looks like (Eilers et al., 2019). From this, one can calculate the axisymmetric gravitational potential U_{Gal} of our galaxy. In our model we assume that the potential is time-independent and we demand that the distribution function f is time-independent, too. This is the case if f is constant along each particle orbit, i.e., if for a given test particle with orbit $(x(t), v(t))$, where

$$\begin{aligned} \dot{x} &= v, \\ \dot{v} &= -\nabla U_{Gal}(x), \end{aligned}$$

it holds that

$$\frac{\mathrm{d}}{\mathrm{d}t} f(x(t), v(t)) = 0.$$

[12] In fact the Milky Way has two stellar discs but they have similar properties and so we include only one stellar disc with averaged parameters.

This is the case if and only if f is a solution of the (time-independent) Vlasov equation[13]

$$v \cdot \partial_x f - \nabla U_{Gal} \cdot \partial_v f = 0. \tag{7.1}$$

We use Newton's law of gravitation[14] and thus the gradient of the gravitational potential that corresponds to f is given by

$$\nabla U_f(x) := G \int_{\mathbb{R}^2} \frac{x-y}{|x-y|^3} \Sigma_f(y)\,\mathrm{d}y, \quad x \in \mathbb{R}^2, \tag{7.2}$$

where

$$\Sigma_f(x) := \int_{\mathbb{R}^2} f(x,v)\,\mathrm{d}v \tag{7.3}$$

is the (flat) density on position space $\mathbb{R}^2$ that corresponds to f, and G is the constant of gravitation. We search for a model for the Milky Way, so we demand that the gravitational potential generated by our model must equal the gravitational potential U_{Gal} of our galaxy, i.e.,

$$\nabla U_{Gal} = \nabla U_{bulge} + \nabla U_{st.disc} + \nabla U_f. \tag{7.4}$$

We call f a self-consistent model for the Milky Way's ISM if it satisfies (7.1) - (7.4).

Mathematically the problem of finding such models is challenging because we have to find models that are compactly supported, fast rotating and reasonable stable. Every model that one finds in the literature fails at least at one aspect. The infinitely extended Mestel disk mentioned above is not compactly support and has infinite mass. A cold disk where all mass is on purely circular orbits is highly unstable. And while the models from Andréasson & Rein (2015), Firt & Rein (2006) or Frenkler (2016) are compactly supported and stable, they are not fast rotating. Here in this thesis we present for the first time a model that succeeds in all three aspects.

The outline of Part II is as follows: In Section 8 we study a new class of self-consistent models for the Mestel disc, analyse their inner structure and construct from this understanding our model for the Milky Way. We describe how multiphase models can be constructed with our technique. In Section 9 we compare our model with other models from the literature and classify our model as a typical example for the Bosma effect. In Section 10 we study numerically the stability of our model. There are two instabilities and they correctly predict the spiral structure in the Milky Way's ISM and the velocity dispersion of atomic hydrogen. This explanations would fail if we included non-baryonic, dark matter. In Section 11 we summarize our results and identify the tasks that should be tackled next.

8 From the Mestel disc to a realistic model of the Milky Way

8.1 The Mestel disc

As starting point we analyse first the so called Mestel disc (Mestel, 1963). This disc has the flat, axially symmetric density

$$\Sigma_0(r) := \frac{v_0^2}{2\pi G r}, \quad r > 0,$$

where $v_0 > 0$ is a constant with dimension of velocity. The derivative of the axisymmetric gravitational potential generated by this flat mass distribution can be approximated using the well known formula for a spherically symmetric mass distribution

$$U_0'(r) \approx \frac{GM(r)}{r^2} = \frac{v_0^2}{r}$$

where $M(r)$ denotes the mass inside the radius r (compare Lemma 3.1.5 from Part I). In general this is only a rough approximation for a flat mass distribution but in the special case of the Mestel disc, this approximation gives indeed the correct values (Binney & Tremaine, 2008, §2.6.1a) and we have for every $r > 0$

$$U_0'(r) = \frac{v_0^2}{r}. \tag{8.1}$$

[13] In astrophysics this equation is often called the collisionless Boltzmann equation.

[14] In Part I it was necessary to distinguish between the Newtonian potential U^N and the Mondian potential U^M. Here in Part II there is only the Newtonian potential. Thus we drop the superscript ^{N} and write shortly U for the Newtonian potential.

The velocity on a circular orbit is related to the derivative of the potential at radius r via the simple formula

$$v_c(r) = \sqrt{rU_0'(r)}. \tag{8.2}$$

Hence the Mestel disc has an everywhere flat circular velocity curve with $v_c(r) = v_0$. For the understanding of galaxies like the Milky Way, which exhibit an almost flat circular velocity curve, it is therefore useful to analyse first the analytically accessible Mestel disc. In the following theorem we equip this disc with dynamics:

Theorem 8.1.1. *Let $v_0 > 0$ and let $U_0(r) = v_0^2 \log r$, $r > 0$, be the potential of the Mestel disc. Take a function $\Phi_0 : [0, \infty) \to [0, \infty)$ measurable such that*

$$0 < I := \int_0^\infty \int_{-\infty}^\infty \frac{1}{v_2} \Phi_0 \left(\frac{v_1^2 + v_2^2}{2} - v_0^2 \log \frac{v_2}{v_0} - \frac{v_0^2}{2} \right) \mathrm{d}v_1 \, \mathrm{d}v_2 < \infty.$$

Set

$$C_0 := \frac{v_0^2}{2\pi G I}$$

and

$$f_0(L_z, E) := \frac{C_0}{L_z} \Phi_0 \left(E - v_0^2 \log \frac{L_z}{v_0} - \frac{v_0^2}{2} \right) \mathbf{1}_{\{L_z > 0\}}$$

where

$$L_z(x, v) := x_1 v_2 - x_2 v_1$$

is the third component of the angular momentum and

$$E(x, v) := \frac{1}{2}|v|^2 + U_0(x)$$

is the local energy. This f_0 is a self-consistent model for the Mestel disc in the following sense:

The density that belongs to f_0 equals the density of the Mestel disc:

$$\Sigma_{f_0} = \Sigma_0.$$

Further along every solution of

$$\begin{aligned} \dot{x} &= v, \\ \dot{v} &= -\nabla U_0(x) \end{aligned} \tag{8.3}$$

L_z and E are conserved, because U_0 is axisymmetric and time-independent. Thus f_0 is constant along every solution of the ODE (8.3) and in this sense it solves the Vlasov equation (7.1) with ∇U_{Gal} replaced by ∇U_0.

Remark. In the following we refer to L_z as the angular momentum because the other two components of the angular momentum are zero.

A sufficient condition for $0 < I < \infty$ is for example that $\Phi_0 \in L_+^\infty([0, \infty))$, has compact support and does not vanish everywhere.

Proof of the Theorem. For $x \in \mathbb{R}^3 \backslash \{0\}$ and $r = |x|$ we use the transformation

$$(v_r, v_t) := \left(\frac{x \cdot v}{r}, \frac{L_z}{r} \right).$$

v_r denotes the velocity in radial direction and v_t the velocity in tangential direction. Using this transformation we get

$$\begin{aligned} E - v_0^2 \log \frac{L_z}{v_0} - \frac{v_0}{2} &= \frac{v_r^2 + v_t^2}{2} + v_0^2 \log r - v_0^2 \log \frac{r v_t}{v_0} - \frac{v_0}{2} \\ &= \frac{v_r^2 + v_t^2}{2} - v_0^2 \log \frac{v_t}{v_0} - \frac{v_0}{2}. \end{aligned} \tag{8.4}$$

Since $\log s \leq s - 1$ for all $s > 0$,

$$\begin{aligned} E - v_0^2 \log \frac{L_z}{v_0} - \frac{v_0}{2} &\geq \frac{v_r^2 + v_t^2}{2} - v_0(v_t - v_0) - \frac{v_0}{2} \\ &= \frac{v_r^2}{2} + \frac{(v_t - v_0)^2}{2} \geq 0. \end{aligned} \tag{8.5}$$

Thus the argument of Φ_0 is everywhere non-negative and f_0 is well defined. Further (8.4) implies

$$\begin{aligned} \Sigma_{f_0}(r) &= \int f_0(L_z, E)\, \mathrm{d}v \\ &= \frac{C_0}{r} \int_0^\infty \int_{-\infty}^\infty \frac{1}{v_t} \Phi_0 \left(\frac{v_r^2 + v_t^2}{2} - v_0^2 \log \frac{v_t}{v_0} - \frac{v_0}{2} \right) \mathrm{d}v_r\, \mathrm{d}v_t \\ &= \frac{v_0^2}{2\pi G r} = \Sigma_0(r). \end{aligned}$$

Thus f_0 is a self-consistent model for the Mestel disc in the above sense. □

There are two choices for Φ_0 where f_0 resembles known distributions functions for the Mestel disc: The first choice is to set Φ_0 as the δ-distribution. In this case we have a cold disc were all mass is on purely circular orbits. This is because the argument of Φ_0 is zero if and only if the radial component of the velocity $v_r = 0$ and the tangential component of the velocity $v_t = v_0$ (see inequation (8.5)). The second choice is $\Phi_0(\eta) = \exp(-C\eta)$ with $C > 0$. In this case we get Toomres model for the Mestel disc that was studied extensively in Zang (1976).

At a first glance f_0 might look a bit complicated and unmotivated, but with the help of the next Lemma we are able to write it down in a simpler form that is more intuitive.

Lemma 8.1.2. *Let $v_0 > 0$ and let $U_0(r) = v_0^2 \log r$, $r > 0$, be the potential of the Mestel disc. Every orbit in the potential U_0 can be characterized uniquely – up to rotations and shifts in time – by its values for L_z and E. Let us study orbits with $(L_z, E) \in (0, \infty) \times \mathbb{R}$; we call this half-plane the L_z-E-plane. All these orbits are moving counter-clock wise around the origin. The angular momentum-energy curve of circular orbits*

$$\begin{aligned} (L_c(r), E_c(r)) &= \left(r v_0, v_0^2 \log r + \frac{v_0^2}{2} \right) \\ &= \left(L_c, v_0^2 \log \frac{L_c}{v_0} + \frac{v_0^2}{2} \right) = \left(L_c, E_c \left(\frac{L_c}{v_0} \right) \right) \end{aligned}$$

can either be characterized by $r \in (0, \infty)$ or by $L_c \in (0, \infty)$. It divides the L_z-E-plane into two parts. All admissible orbits have an L_z-E-coordinate above the angular momentum-curve, there are no orbits below. The orbits that are almost circular are those that are close to the angular momentum curve.

Proof. We only consider orbits with $L_z \neq 0$ since these are the orbits that do not pass through the origin. Let $L_z \neq 0$ and let

$$U_{\text{eff}}(s) := v_0^2 \log s + \frac{L_z^2}{2s^2}, \quad s > 0,$$

be the corresponding effective potential. We have

$$U'_{\text{eff}}(s) = \frac{1}{s} \left(v_0^2 - \frac{L_z^2}{s^2} \right).$$

Hence U_{eff} is decreasing for $0 < s < r_c = L_z / v_0$. It is increasing for $s > r_c$ and it takes its minimum at $s = r_c$. Further

$$\lim_{s \searrow 0} U_{\text{eff}}(s) = \lim_{s \to \infty} U_{\text{eff}}(s) = \infty.$$

Let $(x(t), v(t))$ be an orbit in the potential U_0 with angular momentum $L_z \neq 0$. Set $r := |x|$ and $v_r := x \cdot v / r$. Then

$$\begin{aligned} \dot{r} &= v_r, \\ \dot{v}_r &= -U'_{\text{eff}}(r). \end{aligned} \tag{8.6}$$

The energy E along this orbit is constant and we have

$$E = \frac{1}{2}|v_r|^2 + U_{\text{eff}}(r) \geq U_{\text{eff}}(r_c).$$

Thus there are uniquely determined $0 < r_1 < r_c < r_2$ such that

$$E = U_{\text{eff}}(r_1) = U_{\text{eff}}(r_2).$$

The right side $(v_r, -U'_{\text{eff}}(r))$ of the ODE (8.6) is locally Lipschitz continuous for $(r, v_r) \in (0, \infty) \times \mathbb{R}$. Thus uniqueness implies that there are $t_1, t_2 \in \mathbb{R}$ such that $r(t_1) = r_1$ and $r(t_2) = r_2$, and that every orbit with the same values L_z and E is identical to $(x(t), v(t))$ up to rotations and shifts in time. If we consider another orbit $(\tilde{x}, \tilde{v})$ with angular momentum $\tilde{L}_z \neq L_z$ then obviously the orbit is different from (x, v) because at the same position the orbits will have different tangential velocities. If $\tilde{L}_z = L_z$ but the energy $\tilde{E} \neq E$, then $\tilde{r}_1 \neq r_1$ and $\tilde{r}_2 \neq r_2$ and hence the orbits are different, too; $\tilde{r}_1$ and $\tilde{r}_2$ are defined in the same manner as r_1 and r_2. Thus every orbit in the potential U_0 of the Mestel disc is uniquely characterized by its values for L_z and E.

Consider now two test particles with the same angular momentum $L_z > 0$. Assume that the first particle is moving on a circular orbit ar radius $r_c = L_z/v_0$ and that the second particle is moving on an eccentric orbit. A short look at the effective potential tells us that at some time $t \in \mathbb{R}$ the second particle has to appear at the radius r_c, too. Then the energy of the first particle is

$$E_1 = U_{\text{eff}}(r_c)$$

and the energy of the second particle is

$$E_2 = U_{\text{eff}}(r_c) + \frac{1}{2}|v_r(t)|^2 > U_{\text{eff}}(r_c) = E_1.$$

Hence the L_z-E-coordinate of every orbit is located above the angular momentum-energy curve of circular orbits. Further a particle is on an almost circular orbit if the radial component of its velocity is small, i.e., if it has an L_z-E-coordinate close to the angular momentum-energy curve. □

Now let us write down f_0 a second time:

$$f_0(L_z, E) = \frac{C_0}{L_z}\Phi_0\left(E - E_c\left(\frac{L_z}{v_0}\right)\right)\mathbf{1}_{\{L_z>0\}}. \tag{8.7}$$

For the rest of this thesis we use the following simple form for Φ_0:

$$\Phi_0(\eta) := \begin{cases} 1 & \text{if } \eta < (2\sigma)^2, \\ 0 & \text{else,} \end{cases} \tag{8.8}$$

where $\sigma > 0$ is a parameter with the dimension of velocity. Now we can explain the structure of f_0 in a much more intuitive way: We take a narrow stripe along the angular momentum-energy curve of circular orbits in the potential U_0, namely of thickness $(2\sigma)^2$, and define f_0 on it. This is the part $\Phi_0(E - E_c)$. For self-consistency the density generated by f_0 must be Σ_0, for this purpose we need also the prefactor C_0/L_z. Since we want only orbits that rotate counter-clockwise, we exclude all orbits with $L_z < 0$.

We are interested in models where all mass is on almost circular orbits. Thus we need a narrow stripe and a small parameter σ. We see in the next Lemma that the parameter σ gives the dispersion of the tangential velocities:

Lemma 8.1.3. *When $\sigma \searrow 0$ the average tangential velocity in the model f_0 for the Mestel disc is*

$$v_{t,avg} = v_0 + o(\sigma)$$

independent of radius. The dispersion of the tangential velocities is

$$\sigma + o(\sigma)$$

and also independent of radius; in the rest of this thesis we refer to σ as the velocity dispersion. Further the dispersion of the radial velocities is $\sqrt{2}\sigma + o(\sigma)$ and

$$C_0 = \frac{v_0^3}{8\sqrt{2}\pi^2 G\sigma^2} + o(\sigma^{-2}). \tag{8.9}$$

Remark 8.1.4. We can calculate the minimal and the maximal appearing tangential velocities $v_{t,min}$ and $v_{t,max}$ in the model f_0 explicitly:

$$v_{t,min/max} = v_0\sqrt{-W_{0/-1}\left[-\exp\left(-\frac{8\sigma^2}{v_0^2}-1\right)\right]}$$

where W_0 and W_{-1} denote the two real branches of the Lambert W function. We postpone the proof of this fact to the appendix.

Proof of Lemma 8.1.3. All $o(\sigma^m)$ and $O(\sigma^m)$ terms in this proof are with respect to $\sigma \searrow 0$. Let $\sigma, v_0 > 0$. At radius $r > 0$ the radial and the tangential component v_r and v_t of the velocity are distributed according to the law

$$(v_r, v_t) \sim p(v_r, v_t) := \frac{1}{\Sigma_0(r)} f_0\left(r, 0, v_r, v_t\right)$$

where we have written f_0 in Cartesian coordinates; $x = (r, 0)$ and $v = (v_1, v_2) = (v_r, v_t)$. $\int p \,\mathrm{d}v = 1$ and we treat p as a probability density function. Thank to (8.4) we have

$$p(v_r, v_t) = \begin{cases} 1/(Iv_t), & \text{if } (v_r^2 + v_t^2 - v_0^2)/2 - v_0^2 \log(v_t/v_0) \le (2\sigma)^2 \text{ and } v_t \ge 0 \\ 0, & \text{else.} \end{cases}$$

We see that p does not depend on the radius. The average tangential velocity is the expected value $\mathrm{E}(v_t)$ and the square of the velocity dispersion is the Variance $\mathrm{Var}(v_t)$. We are interested in the behaviour of $\mathrm{E}(v_t)$ and $\mathrm{Var}(v_t)$ when $\sigma \searrow 0$. Then the support of p shrinks more and more. Since the point $(0, v_0)$ is always located inside the support of p it is convenient to introduce coordinates that zoom onto that point while $\sigma \searrow 0$. We use the coordinate transformation

$$\begin{aligned} v_r &= \sigma w_r, \\ v_t &= v_0 + \sigma(w_t - v_0). \end{aligned}$$

Then $\mathrm{d}v = \sigma^2 \,\mathrm{d}w$,

$$(w_r, w_t) \sim q(w_r, w_t) = \sigma^2 p(\sigma w_r, v_0 + \sigma(w_t - v_0))$$

and

$$\mathrm{E}(v_t) = \mathrm{E}(v_0 + \sigma(w_t - v_0)).$$

For $\sigma > 0$ we denote the support of q by

$$\begin{aligned} W_\sigma &:= \left\{ (w_r, w_t) \middle| w_t \ge v_0 - \frac{v_0}{\sigma},\, \sigma^2 \frac{w_r^2 + (w_t - v_0)^2}{2} + \sigma v_0 (w_t - v_0) - v_0^2 \log\left(1 + \sigma \frac{w_t - v_0}{v_0}\right) \le 4\sigma^2 \right\} \\ &= \left\{ (w_r, w_t) \middle| w_t \ge v_0 - \frac{v_0}{\sigma},\, \frac{w_r^2 + (w_t - v_0)^2}{2} + \frac{v_0 (w_t - v_0)}{\sigma} - \frac{v_0^2}{\sigma^2} \log\left(1 + \sigma \frac{w_t - v_0}{v_0}\right) \le 4 \right\}. \end{aligned}$$

Thus

$$q(w_r, w_t) = \begin{cases} \sigma^2/(I(v_0 + \sigma(w_t - v_0))), & \text{if } (w_r, w_t) \in W_\sigma, \\ 0, & \text{else.} \end{cases}$$

We set

$$W_0 := \left\{ (w_r, w_t) \middle| \frac{w_r^2}{2} + (w_t - v_0)^2 \le 4 \right\}.$$

Using that there is a compactum $K \subset \mathbb{R}^2$ such that

$$W_\sigma \subset K$$

for all $\sigma > 0$ sufficiently small, a second order Taylor approximation gives

$$\begin{aligned} \frac{v_0^2}{\sigma^2} \log\left(1 + \sigma \frac{w_t - v_0}{v_0}\right) &= \frac{v_0^2}{\sigma^2} \left(\sigma \frac{w_t - v_0}{v_0} - \frac{1}{2} \sigma^2 \frac{(w_t - v_0)^2}{v_0^2} + O(\sigma^3) \right) \\ &= \frac{v_0 (w_t - v_0)}{\sigma} - \frac{1}{2} (w_t - v_0)^2 + O(\sigma). \end{aligned}$$

Thus for $\sigma \searrow 0$ the envelope of W_σ converges uniformly to the envelope of W_0. This fact we will employ frequently below. We have

$$\begin{aligned}\mathrm{E}(v_t) &= \mathrm{E}(v_0 + \sigma(w_t - v_0)) \\ &= \int (v_0 + \sigma(w_t - v_0)) q(v_r, v_t)\,\mathrm{d}w \\ &= \frac{\sigma^2}{I} \int_{W_\sigma} \mathrm{d}w. \end{aligned} \tag{8.10}$$

We have

$$I = \int_{\{(v_r^2+v_t^2-v_0^2)/2 - v_0^2 \log(v_t/v_0) \le (2\sigma)^2,\, v_t \ge 0\}} \frac{\mathrm{d}v}{v_t} = \sigma^2 \int_{W_\sigma} \frac{\mathrm{d}w}{v_0 + \sigma(w_t - v_0)}$$

and hence

$$\frac{\sigma^2}{I} \to \frac{v_0}{\mathcal{L}(W_0)} \quad \text{for } \sigma \to 0. \tag{8.11}$$

If we would pass to the limit in (8.10) now, we would only get

$$\mathrm{E}(v_t) = v_0 + o(1).$$

This result makes only use of the fact that $(0, v_0)$ lies inside of W_σ and is too weak to analyse $\mathrm{Var}(v_t)$. We must elaborate that $(0, v_0)$ marks the centre of W_0 to get better convergences:

$$\begin{aligned}\mathrm{E}(v_t) &= v_0 + \frac{\sigma^2}{I} \int_{W_\sigma} \mathrm{d}w - v_0 \frac{\sigma^2}{I} \int_{W_\sigma} \frac{\mathrm{d}w}{v_0 + \sigma(w_t - v_0)} \\ &= v_0 + \frac{\sigma^2}{I} \int_{W_\sigma} \left(1 - \frac{v_0}{v_0 + \sigma(w_t - v_0)}\right) \mathrm{d}w \\ &= v_0 + \frac{\sigma^3}{I} \int_{W_\sigma} \frac{w_t - v_0}{v_0 + \sigma(w_t - v_0)}\,\mathrm{d}w. \end{aligned}$$

Using (8.11) and that

$$\int_{W_\sigma} \frac{w_t - v_0}{v_0 + \sigma(w_t - v_0)}\,\mathrm{d}w \to \int_{W_0} \frac{w_t - v_0}{v_0}\,\mathrm{d}w = 0 \quad \text{for } \sigma \searrow 0,$$

we get

$$\mathrm{E}(v_t) = v_0 + o(\sigma). \tag{8.12}$$

We have

$$\begin{aligned}\mathrm{Var}(v_t) &= \int |v_t - \mathrm{E}(v_t)|^2 p(v_r, v_t)\,\mathrm{d}v \\ &= \int |v_t - v_0 + v_0 - E(v_t)|^2 p(v_r, v_t)\,\mathrm{d}v \\ &= \int |v_t - v_0|^2 p\,\mathrm{d}v + 2\int (v_t - v_0)(v_0 - \mathrm{E}(v_t)) p\,\mathrm{d}v + |v_0 - \mathrm{E}(v_t)|^2. \end{aligned}$$

(8.12) and

$$\|v_t - v_0\|_{L^\infty(\operatorname{supp} p)} = O(\sigma)$$

imply

$$\mathrm{Var}(v_t) = \int |v_t - v_0|^2 p\,\mathrm{d}v + o(\sigma^2).$$

Since

$$\int |v_t - v_0|^2 p\,\mathrm{d}v = \frac{\sigma^4}{I} \int_{W_\sigma} \frac{|w_t - v_0|^2}{v_0 + \sigma(w_t - v_0)}\,\mathrm{d}w$$

and

$$\int_{W_\sigma} \frac{|w_t - v_0|^2}{v_0 + \sigma(w_t - v_0)}\,\mathrm{d}w \to \int_{W_0} \frac{|w_t - v_0|^2}{v_0}\,\mathrm{d}w \quad \text{for } \sigma \searrow 0,$$

we have

$$\int |v_t - v_0|^2 p \, \mathrm{d}v - \sigma^2 \frac{\sigma^2}{I} \int_{W_0} \frac{|w_t - v_0|^2}{v_0} \, \mathrm{d}w = o(\sigma^2)$$

and

$$\mathrm{Var}(v_t) = \sigma^2 \frac{\sigma^2}{I v_0} \int_{W_0} |w_t - v_0|^2 \, \mathrm{d}w + o(\sigma^2).$$

With the transformation $w_t - v_0 = 2s$

$$\begin{aligned}
\int_{W_0} |w_t - v_0|^2 \, \mathrm{d}w &= \int_{v_0-2}^{v_0+2} \int_{-\sqrt{8-2(w_t-v_0)^2}}^{\sqrt{8-2(w_t-v_0)^2}} \mathrm{d}w_r \, |w_t - v_0|^2 \, \mathrm{d}w_t \\
&= 2\sqrt{8} \int_{v_0-2}^{v_0+2} \sqrt{1 - \frac{(w_t - v_0)^2}{4}} |w_t - v_0|^2 \, \mathrm{d}w_t \\
&= 32\sqrt{2} \int_{-1}^{1} \sqrt{1 - s^2} s^2 \, \mathrm{d}s.
\end{aligned}$$

Using the transformation $s^2 = t$, $\mathrm{d}t = 2s \, \mathrm{d}s$ and the Beta-function B

$$\begin{aligned}
\int_{W_0} |w_t - v_0|^2 \, \mathrm{d}w &= 64\sqrt{2} \int_0^1 \sqrt{1 - s^2} s^2 \, \mathrm{d}s = 32\sqrt{2} \int_0^1 \sqrt{1 - t} \sqrt{t} \, \mathrm{d}t \\
&= 32\sqrt{2} B(3/2, 3/2) = 4\sqrt{2}\pi = \mathcal{L}(W_0).
\end{aligned}$$

Since

$$\frac{\sigma^2}{I v_0} \to \mathcal{L}(W_0)^{-1} \quad \text{for } \sigma \searrow 0,$$

this implies that

$$\mathrm{Var}(v_t) = \sigma^2 + o(\sigma^2).$$

Due to symmetry the average radial velocity is zero. $\mathrm{Var}(v_r)$ can be calculated with the same techniques as above and one gets that the dispersion of the radial velocities is given by $\sqrt{2}\sigma + o(\sigma)$. Further

$$C_0 = \frac{v_0^2}{2\pi G I} = \frac{v_0^2}{2\pi G \sigma^2} \frac{\sigma^2}{I}$$

and

$$\left| C_0 - \frac{v_0^3}{8\sqrt{2}\pi^2 G \sigma^2} \right| = \frac{v_0^2}{2\pi G \sigma^2} \left| \frac{\sigma^2}{I} - \frac{v_0}{4\sqrt{2}\pi} \right|.$$

By (8.11)

$$C_0 = \frac{v_0^3}{8\sqrt{2}\pi^2 G \sigma^2} + o(\sigma^{-2}).$$

□

8.2 A cut-out Mestel disc resembling the Milky Way's ISM

This is the point where we leave the Mestel disc and start to construct from it a self-consistent model with finite mass and extension. It is plausible to assume that the dynamics of a galaxy should be similar to (8.7) in a region where the circular velocity curve is almost flat. The Milky Way has such a flat curve between 5 kpc and 25 kpc from the galactic centre (Eilers et al., 2019). Luckily the Milky Way belongs also to the minority of galaxies that have a central depression of their hydrogen distribution, which makes up about 70 per cent of the Milky Way's interstellar medium (ISM). Thus for the Milky Way we are in the situation that most mass of the ISM is located in the region where the circular velocity curve is flat. This makes it an ideal candidate to be modelled with a distribution function similar to (8.7). This is somewhat a fortunate coincidence since on the one hand this is the easiest situation where we can deduct a finitely extended, self-consistent model from (8.7) and on the other hand the ISM is the part of the visible galaxy that asks us most riddles.

To get from the Mestel disc to a model with finite extension, we will now drop several orbits from f_0. First we cut a hole into the central region. By choosing only orbits with

$$L_z > v_0 R_1$$

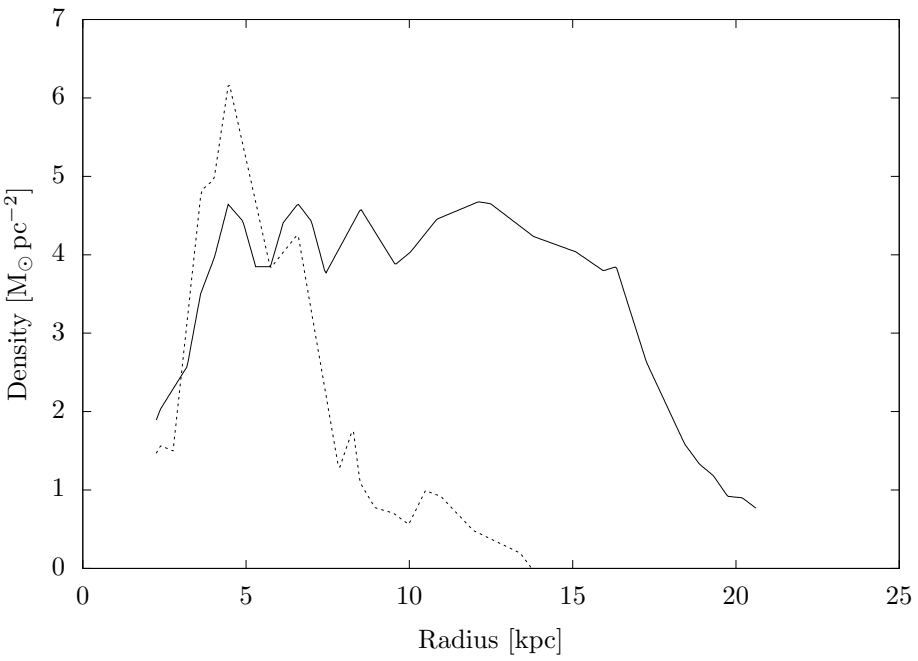

Figure 6: The average density of atomic hydrogen HI (solid line) and of molecular hydrogen H2 (dashed line) in an annulus around the galactic centre, versus radius of the annulus. The density is low for radii smaller than 4 kpc or larger than 21 kpc. After Figure 9.19 of Binney & Merrifield (1998).

for some $R_1 > 0$, we drop most orbits that live within the region $0 < r < R_1$. Further we want a finitely extended model, so we demand

$$L_z < v_0 R_2$$

for some $R_2 > R_1$, thus dropping most orbits that live beyond R_2. In what follows the cut out central hole will do just fine, but at the border R_2 it will we necessary to further cut out every orbit that crosses R_2. This is achieved by demanding

$$E < U_0(R_2) + \frac{L_z^2}{2R_2^2}.$$

With these three cut-offs most orbits live beyond R_1, but there is no orbit beyond R_2. Our new distribution function in orbital form reads as follows:

$$f_1(L_z, E) := \frac{C}{L_z}\Phi_0\left(E - E_c\left(\frac{L_z}{v_0}\right)\right)\mathbf{1}_{\{v_0 R_1 < L_z < v_0 R_2\}} \times \mathbf{1}_{\{E < U_0(R_2) + L_z^2/(2R_2^2)\}} \tag{8.13}$$

where $C > 0$ will be determined below.

We want to model the Milky Way's ISM with this distribution function. In view of the Milky Way's hydrogen distribution (Figure 6) and its circular velocity curve (Eilers et al., 2019) we choose

$$R_1 = 4\,\text{kpc}, R_2 = 21\,\text{kpc and } v_0 = 230\,\text{km}\,\text{s}^{-1}. \tag{8.14}$$

For simplicity we had already chosen $\Phi_0 = \mathbf{1}_{[0,(2\sigma)^2]}$ in (8.8). As shown in Lemma 8.1.3, with this choice the velocity dispersion of the model is equal to σ. Leroy et al. (2008) calculated the velocity dispersion of atomic hydrogen in the outer regions of several nearby spiral galaxies. Atomic hydrogen is an abundant gas in the ISM which dominates the outer parts of spiral galaxies like the Milky Way. They found that most galaxies have a dispersion of $(11 \pm 3)\,\text{km}\,\text{s}^{-1}$. The concrete value, that we choose for σ, affects only little the resulting mass model, but it is important for the stability that we study in more detail in Section 10. There we vary σ and look at the different behaviour of the resulting dynamical models. For the present we fix $\sigma = 11\,\text{km}\,\text{s}^{-1}$, and thus choose a dispersion in the middle of the measurements of Leroy et al.

Further we will in the following smooth out the integral kernel of the gradient of the gravitational potential to take into account the observed thickness of the ISM's disc. We assume a constant scale

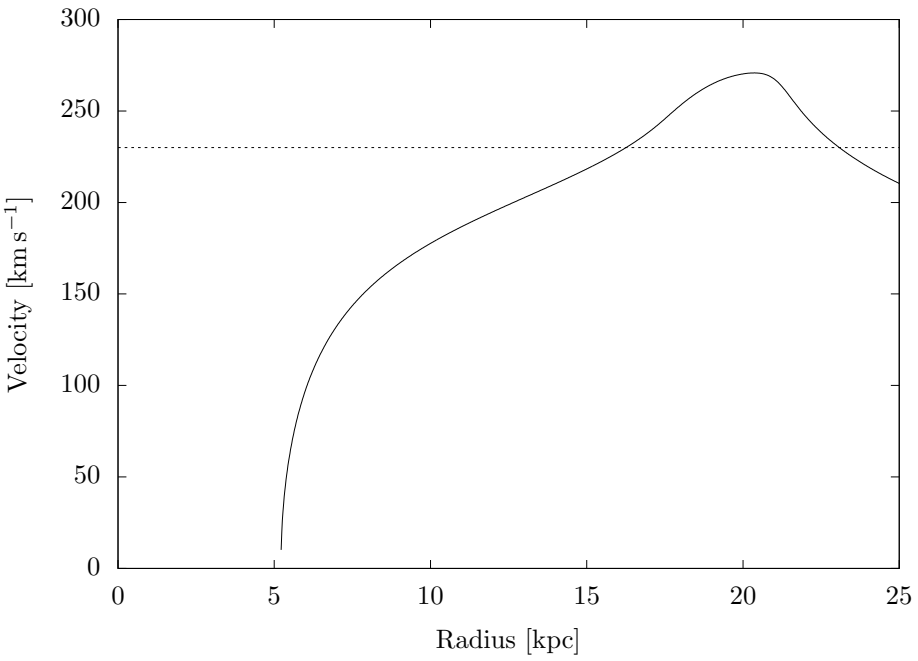

Figure 7: The circular velocity curve (solid line) that corresponds to the cut-out model f_1 if we choose the weight $C \approx C_0$, and the original, constant circular velocity curve (dashed line) that corresponds to the Mestel disc. The circular velocity curve of the cut-out model is no longer flat. To make it flat again, we need to include bulge and stellar disc in our model, too, and reduce the mass of our cut-out Mestel disc, which represents the ISM.

height[15] $z_g = 300\,\mathrm{pc}$ for the ISM. Nevertheless, we still define the density Σ_f on the planar space $\mathbb{R}^2$, but we replace the gradient of the gravitational potential (7.2) by

$$\nabla U_f(x) := G \int_{\mathbb{R}^2} \Sigma_f(y) \frac{x-y}{(|x-y|^2 + \delta_z^2)^{3/2}}; \tag{8.15}$$

here $\delta_z = 1.5 z_g$ is the average distance in z-direction when we draw two test particles at random from the spatial density

$$\Sigma_f(x_1, x_2) \exp\left(-|z|/z_g\right).$$

We give a proof of the relation $\delta_z = 1.5 z_g$ in the appendix.

Let us continue with the above parameters. From $f_1(L_z, E)$ we get $f_1(x, v)$ in Cartesian coordinates by replacing

$$E = U_0(r) + \frac{|v|^2}{2} \quad \text{and} \quad L_z = x_1 v_2 - x_2 v_1.$$

Then we can calculate numerically the density $\Sigma_1(r) = \int f_1 \, \mathrm{d}v$. Further, we calculate the corresponding potential and the circular velocity curve. The circular velocity curve that corresponds to f_1 is shown in Figure 7, where we set

$$C = 6.6 \times 10^{24}\,\mathrm{M}_\odot\,\mathrm{s}^{-1} \approx C_0$$

according to the approximation (8.9). Obviously the circular velocity curve is no longer flat. Mainly the force generated by the central mass is missing to support a flat circular velocity curve in the region between R_1 and R_2. This missing mass has to be 'replaced' by the bulge and the stellar disc which we implement as rigid components. We implement the bulge as spherically symmetric and since it only extends out to approximately $1.9\,\mathrm{kpc} < R_1$ (Binney & Tremaine, 2008, §2.7) its actual shape does not affect our model and we take for simplicity

$$\rho_b(x) := A\left(1 - \frac{|x|}{1.9\,\mathrm{kpc}}\right) \quad \text{for } x \in \mathbb{R}^3 \text{ and } |x| \leq 1.9\,\mathrm{kpc}.$$

[15] According to Ferrière (2001) most gas of the ISM is cold and warm atomic hydrogen with scale heights between 100 pc and 400 pc, followed by molecular hydrogen with scale heights between 120 pc and 140 pc. If we choose another scale height, e.g., $z_g = 100\,\mathrm{pc}$ this does hardly change the properties of the resulting model.

For the stellar disc we assume a scale length $R_d = 3.2\,\mathrm{kpc}$ and define the density

$$\Sigma_d(r) = B \exp\left(-\frac{r}{R_d}\right) \quad \text{for } r > 0.$$

For the stellar disc we assume a disc thickness of $500\,\mathrm{pc}$[16] and smooth out the gradient of its gravitational potential as in (8.15).

We have now three components, namely bulge, stellar disc and ISM with the free parameters $A, B, C > 0$. We fit these parts together such that our model reproduces the observed circular velocity curve of the Milky Way as closely as possible. This curve was measured in Eilers et al. (2019) and we refer to it as $v_{c,MW}$. We choose $A_1, B_1, C_1 > 0$ such that

$$\int_{5\,\mathrm{kpc}}^{25\,\mathrm{kpc}} \left(v_{c,MW}^2 - v_{b,1}^2 - v_{d,1}^2 - v_{g,1}^2\right)^2 \mathrm{d}r \tag{8.16}$$

becomes minimal; here $v_{b,1}$, $v_{d,1}$ and $v_{g,1}$ denote the circular velocity curve of the bulge, the stellar disc and the gaseous component ISM respectively where we have replaced A, B, C by A_1, B_1, C_1. The integral borders $5\,\mathrm{kpc}$ and $25\,\mathrm{kpc}$ are the lower and upper border of the range covered by Eilers et al. and we treat $v_{c,MW}$ as a piece-wise linear function. Calculating numerically the optimal parameters we get

$$\begin{aligned} A_1 &= 2.7\,\mathrm{M}_\odot\,\mathrm{pc}^{-3} \\ B_1 &= 1300\,\mathrm{M}_\odot\,\mathrm{pc}^{-2} \\ C_1 &= 1.7 \times 10^{24}\,\mathrm{M}_\odot\,\mathrm{s}^{-1} \approx 0.26 C_0. \end{aligned}$$

With these parameters fixed we can calculate the circular velocity curve of our model

$$v_{c,1} = \sqrt{v_{b,1}^2 + v_{d,1}^2 + v_{g,1}^2}.$$

In Figure 8 both $v_{c,1}$ and the measured curve of the Milky Way $v_{c,MW}$ are shown. As can be seen, this is already quite a good fit. Nevertheless the model is not self-consistent yet, because the potential that belongs to the mass model is different from the potential that we assumed for the dynamics.

8.3 A Model of the Milky Way with self-consistent dynamics for the ISM

Before we continue, recall how in the previous section the dynamical part of our model, the ISM, was constructed. The ISM is located mostly between R_1 and R_2 where the circular velocity curve is almost flat. We thought about how a distribution function in such a region should look like and in (8.13) we defined f_1 under the assumption of a logarithmic potential that gives rise to an exactly flat rotation curve everywhere. After adding a bulge and a stellar disc to the model, the resulting circular velocity curve has now some bumps and is slightly decaying in the relevant region between R_1 and R_2 (Figure 8). But it is almost flat. So the initially assumed logarithmic potential is close to the resulting potential, and thus f_1 is also close to a self-consistent model. We want to iterate what we have done so far and use the following algorithm to construct a self-consistent model:

Algorithm for the construction of a model of the Milky Way where the ISM is equipped with self-consistent dynamics

1. Given a gravitational potential $U_i(r)$. Calculate

$$\begin{aligned} v_{c,i}(r) &= \sqrt{rU_i'(r)}, \\ L_{c,i}(r) &= r v_{c,i}(r), \\ E_{c,i}(r) &= U_i(r) + v_{c,i}^2(r)/2 \end{aligned}$$

   for $R_1 < r < R_2$

[16] Binney & Tremaine (2008) included two stellar discs that have similar properties. One has a scale height 300 pc and the other 1000 pc. We consider one disc with average parameters and set the scale height to 500 pc

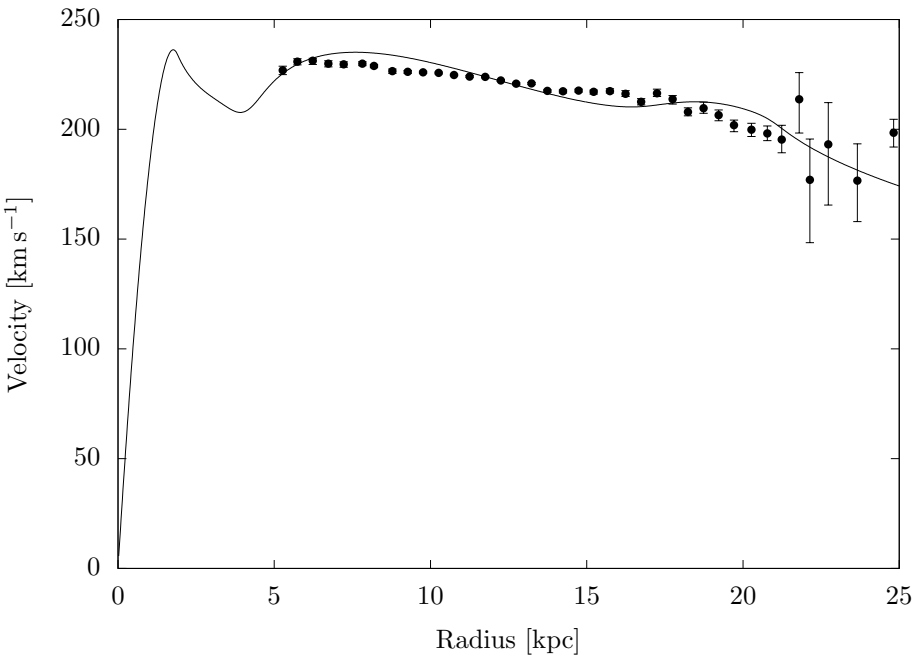

Figure 8: The resulting circular velocity curve (solid line) after we have also included a bulge and a stellar disc and after we have weighted the three baryonic components optimally. In this model the ISM is represented by f_1 with $C = C_1 \approx 0.26 C_0$. Its dynamics are not self-consistent yet. The dots mark the circular velocity curve of the Milky Way as measured by Eilers et al. (2019), which we try to approximate with our model.

2. Choose $R_2' < R_2$ maximal such that $L_{c,i}$ is strictly increasing on $[R_1, R_2']$ [17] and define the inverse map of $L_{c,i}(r)$:
$$[L_{c,i}(R_1), L_{c,i}(R_2')] \ni L_z \mapsto r_c(L_z)$$
(hence $r_c(L_z)$ is the radius where a test particle with angular momentum L_z is on a circular orbit)

3. Define
$$f_{i+1}(L_z, E) := \frac{C}{L_z}\Phi_0\left(E - E_c(r_c(L_z))\right)\mathbf{1}_{\{L_{c,i}(R_1) < L_z < L_{c,i}(R_2')\}} \times \mathbf{1}_{\{E < U_0(R_2') + L_z^2/(2R_2'^2)\}}$$

4. Replace
$$E = U_i(x) + \frac{|v|^2}{2} \text{ and } L_z = x_1 v_2 - x_2 v_1$$
and calculate the flat density $\Sigma_{i+1} = \int f_{i+1}\,\mathrm{d}v$ and the corresponding potential and circular velocity curve $v_{g,i+1}$

5. Replace A, B, C by $A_{i+1}, B_{i+1}, C_{i+1}$ and choose them such that
$$\int_{5kpc}^{25kpc} \left(v_{c,MW}^2 - v_{b,i+1}^2 - v_{d,i+1}^2 - v_{g,i+1}^2\right)^2 \mathrm{d}r$$
is minimal

6. Calculate the total potential $U_{i+1}(r)$ of all three baryonic components and return to the first step

To measure the convergence of our algorithm we look at
$$\delta_i := \frac{||\Sigma_{i+1} - \Sigma_i||_2}{||\Sigma_i||_2}$$

[17] This is necessary because the disc of the ISM is truncated at R_2. As a result $v_{c,i}$ is decaying very rapidly near R_2. This is an effect due to the flatness of the disc. As a result $L_{c,i}$ is not monotonous in this region.

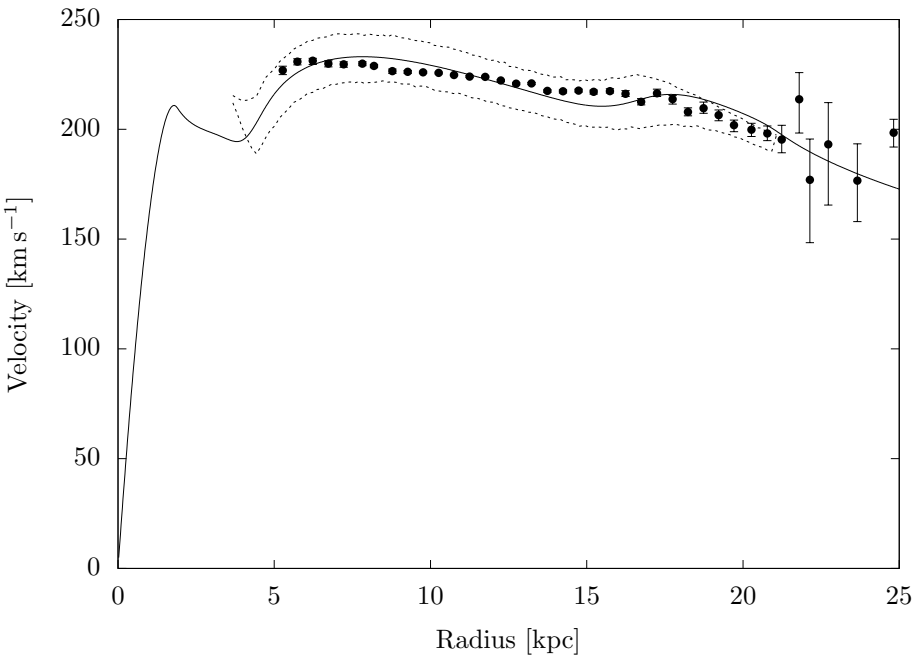

Figure 9: The circular velocity curve (solid line) of our final model. For comparison we show also the circular velocity curve of the Milky Way (thick dots) measured by Eilers et al. (2019). The velocity dispersion (dashed lines) is shown. In our model now the ISM is equipped with self-consistent dynamics.

where $||\cdot||_2$ denotes the L^2-Norm on $\mathbb{R}^2$. With the parameters chosen in (8.14), $\delta_1 \approx 0.10$, δ_i decreases in each iteration step roughly by a factor between 0.5 and 0.7, and we stop the algorithm after twelve iterations when $\delta_i < 0.001$. The resulting distribution function f is a self-consistent model for the Milky Way's ISM where the bulge and the stellar disc are rigid components. Or more precisely, it is as close to a self-consistent model as possible: We cannot distinguish it anymore from a self-consistent model on a computer.

The circular velocity curve and the velocity dispersion in our model are shown in Figure 9. The densities of the baryonic components in our model are shown in Figure 10. The circular velocity curve and the low velocity dispersion resemble quiet well the properties of the Milky Way. This is very nice, but with this observation alone we can not be satisfied yet. We have to cover two more very relevant topics: First how do the densities in our model compare to the densities in present models and observations (Section 9), and second what about the stability of the dynamical part in our model (Section 10)? These two question are closely coupled.

8.4 A self-consistent, multiphase model of the entire galaxy

Before in the next sections we compare our model with other models and study the stability of our model, let us take a closer look on the algorithm itself. The algorithm of the previous section is very powerful since it is highly customizable. It can easily be extended to create a multiphase, self-consistent model of the entire galaxy. This is a task that was elusive up to now; see, e.g., the review from Binney (2020).

How can the algorithm from Section 8.3 be extended to construct a multiphase, self-consistent model for the entire galaxy? Look for this on Step 3 in the algorithm where we define our distribution function. In this definition we have a prefactor C/L_z. This prefactor was motivated from the Mestel disc where it was necessary for self-consistency (see equation (8.7)). But in our finitely extended model this is no longer necessary. There the algorithm takes care that the dynamics become self-consistent. So we can replace C/L_z by any suitable function $\psi(L_z)$. Further we can add to our model as many different distribution functions as we want and choose for every one a different prefactor ψ. Each of these new distribution functions has to be updated in Step 3 of the algorithm.

It could for example be convenient to decompose the ISM into atomic hydrogen HI and molecular hydrogen H2. This can easily be achieved by including two distribution function f_{HI} and f_{H2} with suitable prefactors ψ_{HI} and ψ_{H2}.

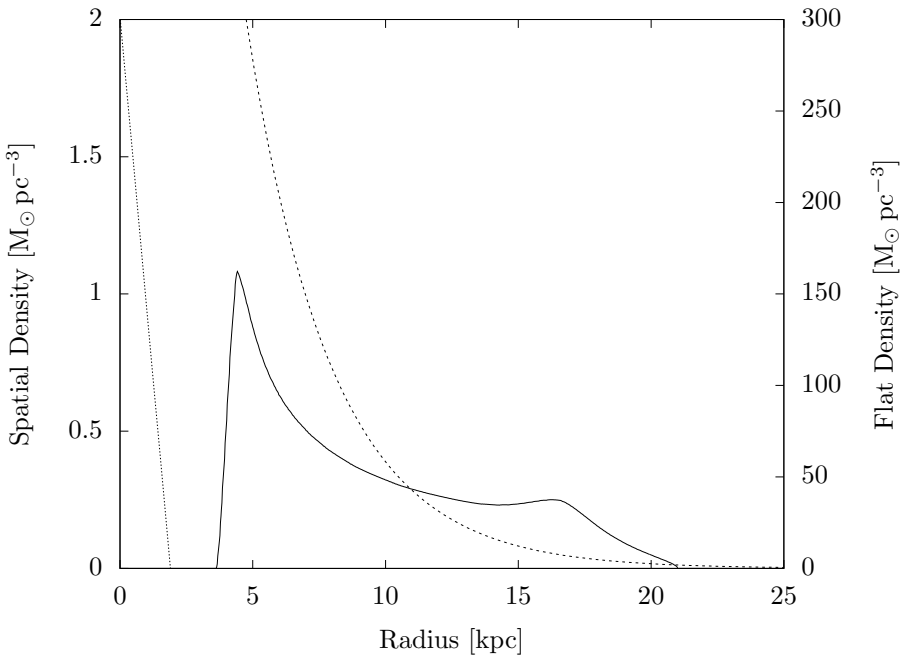

Figure 10: The densities of the ISM (solid line), the stellar disc (dashed line) and the bulge (dotted line) of our model for the Milky Way.

In the same way we can equip a stellar disc with dynamics. But it is important to note that a stellar disc must be defined also in regions where the circular velocity curve is not flat but rising. So one has to study first how a suitable ansatz in these regions looks like.

Obviously also a dark matter halo (dynamical or not) can easily be added to the model. We have not done this because we wanted to analyse on the basis of a dynamical, purely baryonic model whether a halo of non-baryonic dark matter is necessary or not to explain the dynamics of spiral galaxies. And this leads to interesting results that we discuss in the Sections 9 and 10.

9 Comparing our mass model with observational data

In the introduction we posed the question:

> Is a halo of non-baryonic, dark matter necessary to explain the Milky Way's flat circular velocity curve?

In the previous section we have constructed a model that explains the Milky Way's flat circular velocity curve out to 25 kpc. The disc of this model has an extension of only 21 kpc, there is no large halo of non-baryonic, dark matter involved and the densities of bulge, stellar disc and ISM conform to observations up to a prefactor. Nevertheless, to explain the circular velocity curve a certain amount of mass is needed that creates the necessary gravitational potential. Since most current models make use of a dark matter halo, while our model does not, our model needs more baryonic mass than current models and a mass gap occurs. In this section we study how large this mass gap is by comparing our model with our models from the literature.

A short side note: We have read that it should not be possible to explain a flat circular velocity curve with a finitely extended gaseous disc like we did with our model (Rubin et al. (1980) and Sparke & Gallagher (2000)). However, this statement is based on the simple formula that can be used in spherical symmetry to calculate the gradient of a gravitational potential. There one has

$$U'(r) = GM(r)/r^2$$

where $M(r)$ denotes the mass in the interior of a ball with radius $r > 0$. One can use this formula also in the situation of a spiral galaxy to approximate the mass function $M(r)$. But a flat circular velocity curve, which is related to $U'(r)$ via formula (8.2), would imply that the mass function does not converge

	BT08 $10^{10}\,M_\odot$	Here $10^{10}\,M_\odot$	Factor
Total	21.5	15.0	0.7
Total baryonic	4.3	15.0	3.5
Bulge	0.36	1.4	3.9
Stellar disc	3.0	8.5	2.8
ISM	1.0	5.1	5.1
Dark matter	17.1	-	-

Table 1: Masses of the different components of the Milky Way. The first column contains the masses of Model 2 in Binney and Tremaine (BT08), the second one the masses of our self-consistent model (Here), and the third column (Factor) states by how much the mass of BT08 must be multiplied to match the mass of our model. Only masses within 25 kpc were included. In our model all mass lies within 25 kpc. In BT08 a high amount of mass, in particular dark matter, lies beyond 25 kpc; this mass we ignore in our comparison. (The masses from BT08 were calculated using central surface densities of $463\,M_\odot\,pc^{-2}$ and $73\,M_\odot\,pc^{-2}$ for the stellar disc and the ISM respectively)

to a limit at the edge of the observable galactic disc. However, in a flat, axially symmetric situation the above formula is only a rough approximation. To understand the main difference between the spherical and the flat case consider an infinitesimally thin sphere and an infinitesimally thin ring and distribute over both the same amount of mass. If we approach the sphere with a test particle, the forces, which pull the test particle to the sphere, are bounded. In contrast, if we approach the ring with a test particle, the forces become infinitely strong. This effect is responsible that a flat density that is rapidly decaying can create strong forces near the region where this rapid decay occurs. This effect can very nicely be observed in Figure 7 where the cut-off of our disc at $R_2 = 21$ kpc causes the circular velocity curve to peak there. The Milky Way has such a rapid decay in the outskirts of its HI disc (Figure 6). By mimicking this decay our model with an extension of only 21 kpc can explain the Milky Way's flat circular velocity curve out to 25 kpc.

9.1 Comparing our mass model with the one in Binney & Tremaine (2008)

In §2.7 of Binney & Tremaine (2008) (hereafter referenced as BT08) two mass models for the Milky Way were constructed. Their Model 2 assumes a stellar disc with a scale length $R_d = 3.2$ kpc as we did in Section 8. Therefore we compare this model with ours.

The masses of the Milky Way's components in the model of BT08 and in our model are listed in Table 1. All mass in our model is confined to a disc with radius 21 kpc and we explain with this mass the circular velocity curve of the Milky Way out to 25 kpc. In the model of BT08 much mass (mostly dark matter) lies beyond the edge of the visible galaxy. To compare the two models properly, we list therefore in the table only masses within a ball with radius 25 kpc.

We see that the total mass of our model and the one of the model in BT08 take similar values. This is to be expected because both models must explain the same circular velocity curve and for this similar amounts of mass are necessary. Nevertheless, the total mass of our model is about 30 per cent lower than the mass in BT08. Since in the model of BT08 only one quarter of the mass is baryonic while in our model all mass is baryonic, necessarily a mass gap arises. Our model needs 3.5 times as much baryonic mass as the model in BT08. The missing mass distributes almost uniformly over the three baryonic components of our model. We have to multiply the masses of the three baryonic components in our model by factors between 2.8 and 5.1 to reproduce the masses in BT08.

9.2 Our model for the Milky Way as an example for the Bosma effect

That it is possible to explain circular velocity curves of spiral galaxies by scaling the gaseous content of these galaxies was already noticed by Bosma (1981). When he measured the densities and dynamics in the outer parts of spiral galaxies, he calculated the disc density necessary to explain the observed circular velocity curve and compared it to the observed density of the gas. He noticed that as a rule the ratio of the two is roughly constant in the outer parts of the galaxies in his sample. This phenomenon is called the Bosma effect. Hessman & Ziebart (2011) used this phenomenon to explain the circular velocity curves of 17 galaxies from The Nearby HI Galaxy Survey (THINGS) without invoking non-baryonic, dark matter. They scaled the observed densities of both the stellar and the gaseous discs like we did for the

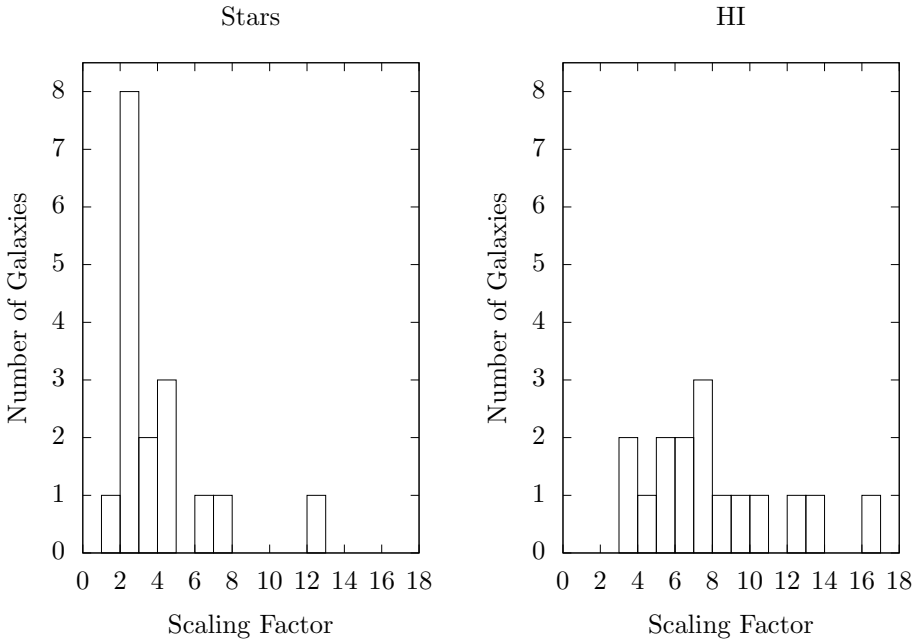

Figure 11: Scaling factors used by Hessman & Ziebart (2011) for the stellar and the HI discs of 17 spiral galaxies from the THINGS sample. One outlier (scaling factor 28.0 for the HI content) is not displayed in the right histogram. With the such scaled discs Hessman & Ziebart can explain the circular velocity curves of the respective galaxies without invoking non-baryonic, dark matter. Our factors 2.8 for the stellar and 5.1 for the gaseous disc of the Milky Way fall in the midst of their factors.

Milky Way in Sections 8.2 and 8.3. They interpreted the scaled stellar and the scaled gaseous discs as proxies for other – presumedly non-stellar – mass components that reside in the disc and have not been observed, yet. They found good agreement between observed and predicted circular velocity curves. We have summarized their scaling factors for the gaseous and the stellar discs[18] in Figure 11.

Both BT08 and we (Section 8.2) took a functional form for the ISM that is similar to the observed density of atomic plus molecular hydrogen reported by Binney & Merrifield (1998). Further both BT08 and we took the same functional form for the stellar disc. In our model the ISM is 5.1 times and the stellar disc 2.8 times more massive than the corresponding discs from BT08. These two factors fall in the midst of the factors from Hessman & Ziebart (2011) making our model for the Milky Way a typical example for the Bosma effect.

9.3 Higher densities of the ISM measured by the Voyager probes

An argument that the density of the ISM could indeed be higher than currently assumed is provided by the Voyager 1 and 2 probes which in 2012 and 2018 left the heliosphere and entered the interstellar medium. They are the first artificial objects to do so. Inside the heliosphere the electron density is very low (about 0.001 particles per cm^3). In the interstellar medium current models predict a higher value of about 0.04 particles per cm^3 (Gurnett et al., 1993). Measurements carried out by the space probes motivated Gurnett et al. already in 1993 to postulate that there must be a 'pill up' region in front of the heliospheric nose where the electron density is higher than the predicted value. The Voyager 1 and 2 probes entered the ISM far off the region where the pile up was expected to be (Kurth & Gurnett, 2020). First they measured an electron density of $0.04\,cm^{-3}$ and $0.05\,cm^{-3}$ close to the estimate mentioned above. But after travelling 20 AU more this density rose to $0.13\,cm^{-3}$ and $0.12\,cm^{-3}$. Roughly three

[18] In Hessman & Ziebart (2011) the scaling factors for the stellar discs are given by $1 + f_{\rm disc}$ and the scaling factors for the gaseous discs by $1 + f_{\rm HI}$. The values for $f_{\rm disc}$ and $f_{\rm HI}$ are tabulated in their paper. Since the gaseous discs of Hessman & Ziebart contained only atomic hydrogen HI, Hessman & Ziebart multiplied their gaseous discs with an additional factor of 1.39 to correct the disc densities for the presence of Helium and heavier elements. We have not invoked such an additional factor since the model for the ISM from Binney & Tremaine (2008) includes already similar corrections.

times higher than expected. Since the two space probes entered the interstellar medium at different positions, Gurnett and Kurth expect that this high electron density is a large scale feature that can be found everywhere in the direction of the heliospheric nose.

Gurnett and Kurth discussed some possible explanations for this high density but concluded that the question of its origin cannot be answered satisfactory. We would like to add another possible explanation to their list: Could it be that this high electron density is not just a local phenomenon near the heliospheric nose, but that is is real? Meaning that the electron density is indeed higher than expected everywhere in the Milky Way and that this points toward a higher density of the whole interstellar medium, consistent with our model?

10 Stability, Spiral Structure and Velocity Dispersion

Let us pose the question: Is our model stable? The answer to this question is: No, it is unstable. It can suffer from two instabilities. And this good. Because these instabilities take care that our model offers simple answers to the two questions from the introduction:

> Where does the four armed spiral pattern in the Milky Way's ISM originate from?[19]
>
> Why does atomic hydrogen have in most spiral galaxies the same velocity dispersion well above the value expected from thermal considerations?

For these answers it is important that the ISM mass in our model is as high as we have seen in the previous section. Models that use an ISM disc with a lower mass embedded in a halo of non-baryonic, dark matter cannot answer these questions as easily as our model does.

In this section we show several simulations where the initial particles were drawn at random from the distribution function constructed in Section 8.3 and where the equations of motion were integrated numerically. In Section 10.1, where we study the spiral activity, we choose in our model $\sigma = 11\,\mathrm{km\,s^{-1}}$ and in Section 10.3, where we study the Jeans instability, we look on a model with $\sigma = 9\,\mathrm{km\,s^{-1}}$. Details on our numerical methods can be found in the appendix.

10.1 Spiral structure in our model and in the Milky Way

The first instability our model suffers from offers a simple explanation for the observed four armed spiral pattern in the Milky Way's ISM (see Figure 12). To understand what happens there, let us take a look on the tangential accelerations. In axial symmetry, these accelerations would be zero. However, in our simulation the particles were drawn at random from the distribution function and hence these accelerations are different from zero although they are very small initially. If now we run the simulation, these tangential accelerations grow exponentially. This can be seen very well in Figure 13 where we have plotted the root mean square (RMS) of the tangential accelerations as a function of time:

$$RMS(a_{tan}) = \sqrt{\sum_i \left(\frac{x_{i,1} a_{i,2} - x_{i,2} a_{i,1}}{r_i} \right)^2},$$

where $a = \dot{v}$ and the sum ranges over all particles in the simulation. These growing tangential accelerations correspond to local overdensities which become denser and denser and result in a spiral structure with four large spiral arms that match the observed spiral arms in the Milky Way's ISM to a high degree; in Figure 12 we have overlaid the spiral structure of our model with the four armed spiral structure that was observed by Steiman-Cameron et al. (2010). Given that the spiral structure in our model forms spontaneously, the similarity is astonishing. We are not aware of any other simulation that can reproduce the spiral structure in the Milky Way's ISM as well as our model does.

Steiman-Cameron et al. discuss several possible explanations why the Milky Way's ISM has a four armed spiral structure – in contrast to a two armed spiral structure that can be observed in the stellar disc. Our model gives the most simple explanation: Assuming the mass of the ISM is as high as in our model, then spiral activity is self-excited, it is independent from the dynamical properties of the rest of the galaxy and it gives rise to exactly the spiral pattern that is observed in the Milky Way.

[19] In this thesis we consider only the four armed spiral structure reported by Steiman-Cameron et al. (2010). It should be noted that the exact structure of the spiral arms in the Milky Way is still debated (see, e.g., the discussion in the introduction of Poggio et al. (2021)). But nevertheless a four armed spiral structure in the Milky Way's ISM similar to the one reported by Steiman-Cameron et al. (2010) is at the moment the most accurate visualization of what the Milky Way looks like (Shen & Zheng, 2020).

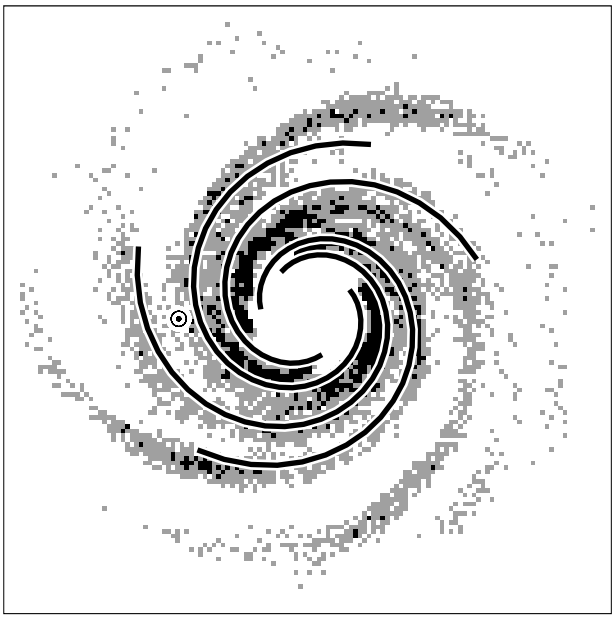

Figure 12: Spiral structure (Background image) that has formed in our model within 400 Myr out of the initially axially symmetric disc, overlaid with the four spiral arms that were calculated from observational data by Steiman-Cameron et al. (2010) (solid lines); the position of the sun is marked by $\odot$. Given that the spiral arms in our model form spontaneously, the similarity between them and the observed arms is astonishing. The plate covers 40 kpc x 40 kpc. In the background image black corresponds to densities above $120\,M_\odot\,pc^{-2}$, gray to densities above $60\,M_\odot\,pc^{-2}$, and white to densities below.

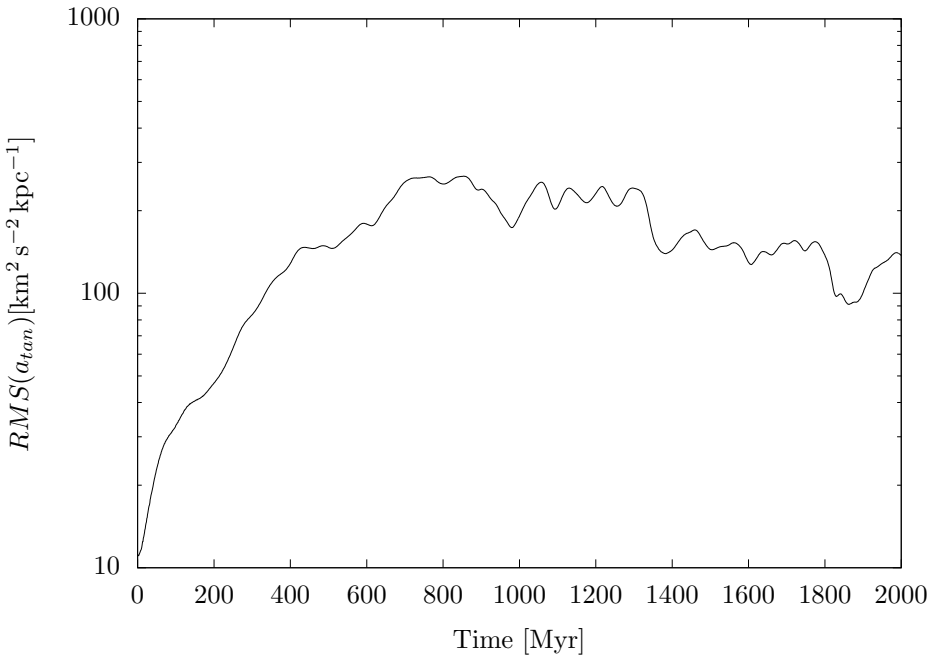

Figure 13: The RMS of the tangential accelerations is very low initially but grows exponentially for about 400 Myr (take note of the logarithmic scale for the y-axis). It still continues to grow for 300 Myr more at a slower pace and then it decays gradually. The growth of the tangential accelerations corresponds to local overdensities which become denser and denser. These overdensities result in a spiral structure that resembles very well the observed spiral structure of the Milky Way's ISM (see Figure 12).

10.2 Prolonging spiral activity

The spiral activity in our simulation does not last forever, it is only strong for about 1 Gyr. When we continue the simulation (see Figure 14) the arms move and permanently disrupt and merge with each other. In the simulation the velocity dispersion σ has initially a low and realistic value of $11\,\mathrm{km\,s^{-1}}$. Since the mass moves faster than the spiral arms, the mass passes through the spiral arms and gets deviated. Within the 1 Gyr of strong spiral activity the velocity dispersion rises to a value that is about four times as high as the initial one (Figure 15). This higher velocity dispersion stabilizes the disc, suppresses the spiral activity and the simulation converges to a new axially symmetric state.

In the Milky Way this seems not to happen - and in other spiral galaxies neither. For comparison the Milky Way's stellar disc is assumed to be (8.8 ± 1.7) Gyr old (del Peloso et al., 2005). Nevertheless, we can observe nearly everywhere in the Milky Way's ISM the same low dispersion of velocities (Marasco et al., 2017) and also the spiral activity seems to last forever. Why?

In the real galaxy the velocity dispersion of the gas becomes permanently reduced. The Milky Way's gaseous mass in the ISM is not distributed homogeneously but it is concentrated in large clouds. As long as these clouds would move on circular orbits, everything would be fine. But when they become deviated and the velocity dispersion rises, the orbits of these clouds intersect and they collide. In these collisions they loose the radial component of their velocity and continue on on circular orbits. Thus the velocity dispersion decreases again. This keeps the velocity dispersion low and enables a long lasting spiral activity (Sellwood & Masters, 2021, §6.1.).

10.3 Velocity dispersion and the Jeans instability

The dissipative process just describe must be strong because everywhere in the Milky Way atomic hydrogen has a low velocity dispersion slightly below $10\,\mathrm{km\,s^{-1}}$ (see, e.g., Marasco et al. (2017) where they have measured the velocity dispersion in the inner regions of our galaxy). So in the Milky Way the spiral activity does not manage to increase this dispersion like in our simulation. The observed velocity dispersion of atomic hydrogen in the Milky Way is typical for other spiral galaxies, too. In the sample of twenty nearby spiral galaxies from Leroy et al. (2008) most spiral galaxies have a dispersion close to $10\,\mathrm{km\,s^{-1}}$ (see Figure 16). This is higher than the value one would expect from thermal considerations (Tamburro et al., 2009). In spiral galaxies most hydrogen can be found either in a cold ($\sim 100\,\mathrm{K}$) or in a warm ($\sim 8000\,\mathrm{K}$) thermal equilibrium. Cold atomic hydrogen has a line width of $\sim 1\,\mathrm{km/s}$, while warm atomic hydrogen has a line width of $\sim 8\,\mathrm{km\,s^{-1}}$. But if the dissipative process of cloud-cloud collisions is strong, why does it not reduce the velocity dispersion to the minimal thermal value somewhere between $1\,\mathrm{km\,s^{-1}}$ and $8\,\mathrm{km\,s^{-1}}$?

Our model offers an answer to this question, again in the form of an instability. If in our model we choose $\sigma \gtrapprox 10\,\mathrm{km\,s^{-1}}$ only the instability from Section 10.1, which causes the spiral arms, is active. If, however, we choose $\sigma \lessapprox 10\,\mathrm{km\,s^{-1}}$ a second instability enters the model: The Jeans instability. This instability rearranges the masses and increases the velocity dispersion. In Figure 17 we show this instability in action in our model with $\sigma = 9\,\mathrm{km\,s^{-1}}$. The threshold between stability and the Jeans instability coincides with the observed velocity dispersion of atomic hydrogen in the Milky Way and in most other spiral galaxies. A dissipative process – however strong it may by – cannot reduce the velocity dispersion below this threshold because if it does so, the Jeans instability starts to work against it. Thus – assuming that other spiral galaxies are comparable to the Milky Way – the Jeans instability can explain why most spiral galaxies share the same velocity dispersion of atomic hydrogen well above the value expected from thermal considerations.

Interestingly, the Jeans instability in our model triggers only in the outskirts of the galactic disc. And it is good that it does not trigger in the inner regions, too, because there the mass contained in our stellar disc dominates (see Figure 10). But at the present the dynamics of this component are missing in our model (see the discussion in Section 8.4 how we plan to include the dynamics of this component in future models). Obviously these dynamics will affect the Jeans instability in the inner regions of our model. On the contrary in the outskirts of our model the ISM disc, which we have modelled dynamically, dominates the mass. So there our model has to predict the velocity dispersion correctly; and this it does.

10.4 What about non-baryonic, dark matter

Let us pose a last question here in this thesis: Do models that use a halo of non-baryonic, dark matter have similar easy explanations for the spiral structure in the Milky Way's ISM and the velocity dispersion

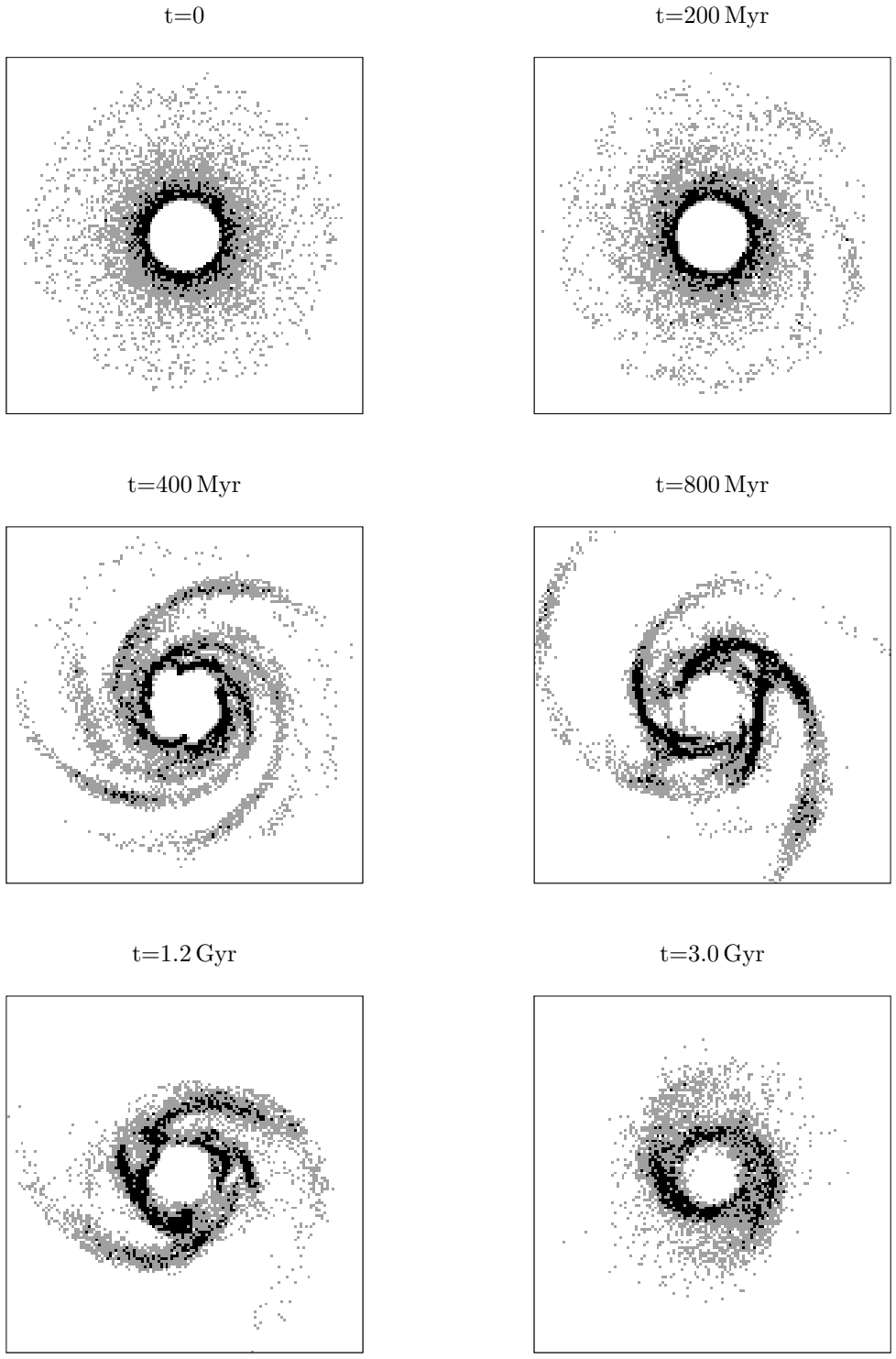

Figure 14: A simulation of our self-consistent model where the initial particles are drawn at random. After about 200 Myr we can make out a faint multi-armed spiral structure. These spiral arms merge and after 400 Myr form four large spiral arms, which resemble the Milky Way's spiral arms very well. As time continues these arms move, become elongated due to the differential rotation and disrupt and merge with each other. After 800 Myr we still see a three-armed, and after 1.2 Gyr a two-armed spiral structure. Afterwards the spiral activity calms down. After 3 Gyr still a weak, bi-symmetric structure is visible. As the simulation continues, the system converges more and more to a new axially symmetric state. Each plate covers 40 kpc x 40 kpc and the colour scheme is the same as in Figure 12. A more detailed video of this simulation can be found on the project homepage: `https://www.diffgleichg.uni-bayreuth.de/en/research/spiral-galaxies/index.html`

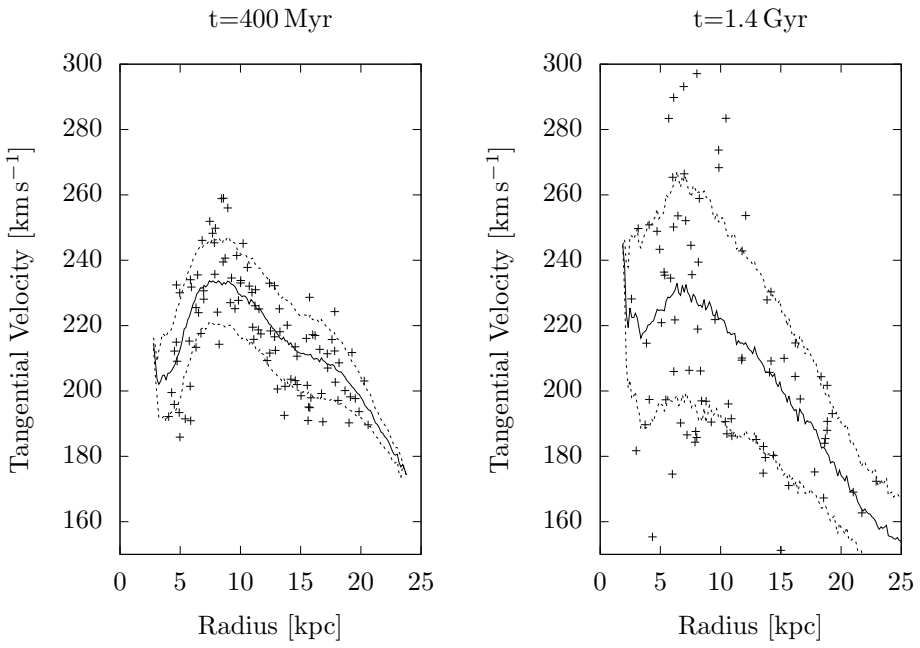

Figure 15: Scatter plot of the tangential velocity versus distance from the galactic centre for a random sample of 100 particles after 400 Myr (left) and after 1.4 Gyr (right). The solid line shows the mean tangential velocity and the dashed line the velocity dispersion (calculated for all particles in the simulation). During the first 400 Myr the dynamical properties of the model have hardly changed. Afterwards the spiral activity dominates the evolution of the model and increases the velocity dispersion. At time 1.4 Gyr the velocity dispersion has risen to a value about four times as high as initially. This stabilizes the model and suppresses further spiral activity. When we stop the simulation after 10 Gyr the plot on the right hand side has not changed much any more. Observe that the vertical axis shows only velocities between 150 km s^{-1} and 300 km s^{-1}

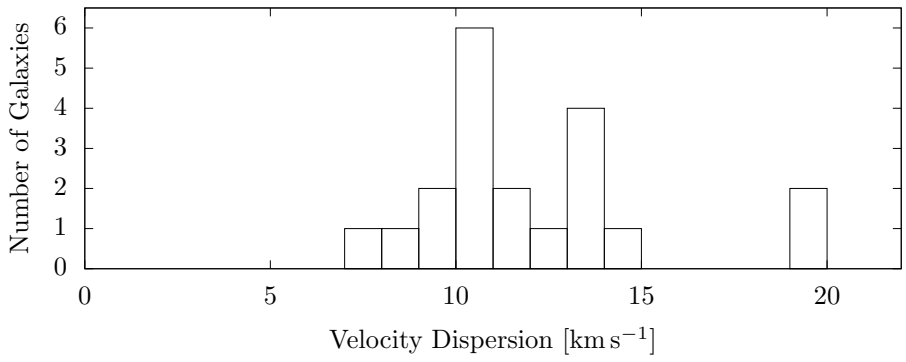

Figure 16: Histogram of the velocity dispersion of atomic hydrogen in the outer parts of the galactic discs of 20 nearby spiral galaxies. The sample is taken from Leroy et al. (2008) and only galaxies with an inclination below 60° were included. Above an inclination of 60° the calculated velocity dispersion is affected by projection errors. We see that most spiral galaxies have a velocity dispersion around 10 km s^{-1} or 11 km s^{-1} and there is a gap between dispersion zero and the observed velocity dispersions.

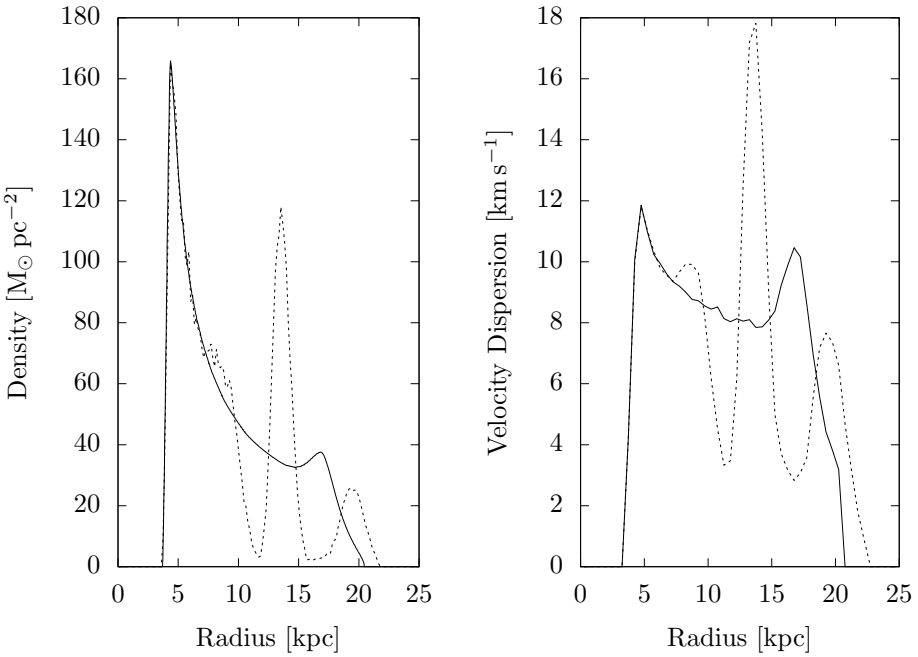

Figure 17: The two figures show the Jeans instability in action if we choose in our model $\sigma = 9\,\mathrm{km\,s^{-1}}$. The left plot shows the density as a function of the radius at time zero (solid line) and after 800 Myr (dashed line). The right plot shows the velocity dispersion as a function of the radius at time zero (solid line) and after 800 Myr (dashed line). After 800 Myr the Jeans instability has rearranged the mass beyond 10 kpc. This mass is now concentrated in two rings around the galactic centre. The velocity dispersion in these rings is higher than initially. In the simulation that was run to create these plots axial symmetry was enforced to suppress the formation of spiral arms so that we can study the Jeans instability isolated. If in this simulation we choose $\sigma = 11\,\mathrm{km\,s^{-1}}$, like in Section 10.1 above, the model just remains stable.

of atomic hydrogen? The answers is No, at least not ad hoc. The problem is that a dark matter halo provides too much stability.

In our baryonic model we can freeze four fifths of the ISM mass and study only the dynamical rest. Then the frozen mass is kind of a rigid dark matter component and the remaining dynamical disc resembles an ISM disc like it is predicted by Model II of Binney & Tremaine (2008) (see Section 9.1). In such a disc neither the instability that causes the spiral structure (Section 10.1) nor the Jeans instability, which explains the velocity dispersion (Section 10.3), is active. So models that make use of dark matter have to search for more complicated answers to explain the two dynamical phenomenons spiral activity and velocity dispersion.

Looking into the literature, one sees that models that make use of dark matter indeed struggle to reproduce the spiral structures observed in spiral galaxies (see the review of Sellwood & Masters (2021) and the references therein). Also it is difficult for these models to explain the observed velocity dispersion of atomic hydrogen exactly (Tamburro et al., 2009).

10.5 Spiral Arms and Bar-Shaped Bulges result from the same instability

We want to close this section with a short note, which is independent of the previous discussions. When we started this work, we had at first self-consistent models, too, but these lacked many properties of the models presented here in this thesis. Almost all of these first models degenerated into bars or lop-sided discs. In this context it is noteworthy that the formation of a bar, of a lop-sided disc or of large scale spiral structures is always preceded by an exponential growth of the tangential accelerations as shown in Figure 13. So these three phenomena are all due to the same instability. This instability always is triggered if sufficient mass is in sufficiently rotational motion. But to which result this instability leads, depends on the concrete distribution of the mass and its dynamical properties. We have not examined this instability any further, but it is obvious that a good understanding of it would prove very useful since it is both responsible for the formation of large scale spiral structures and relevant for how bulges are shaped.

11 Conclusion Part II

Let us summarize the answers our model for the Milky Way gives to the three questions from the introduction:

> Where does the four armed spiral pattern in the Milky Way's ISM originate from?

In our model the origin of this spiral pattern lies in the dynamical properties of the ISM itself. Our self-consistent, axisymmetric model for the ISM suffers from an instability that transforms the ISM disc into a disc with four large spiral arms that resemble very well the spiral arms observed in the Milky Way's ISM (Section 10.1).

> Why does atomic hydrogen have in most spiral galaxies the same velocity dispersion well above the value expected from thermal considerations?

In the outer regions of the galactic disc the Jeans instability is active in our model if we choose a velocity dispersion that is below $10\,\mathrm{km\,s^{-1}}$ (Section 10.3). Thus if we would include in our model the dissipative process of cloud-cloud collisions (Section 10.2), this dissipative process can only reduce the velocity dispersion to the threshold between stability and the Jeans instability. Then the Jeans instability starts to work against it and stops the further reduction of the velocity dispersion. This threshold between stability and the Jeans instability coincides with the observed values of the velocity dispersion of atomic hydrogen in the outer regions of spiral galaxies (Figure 17). Assuming that the structure of most spiral galaxies is comparable to the Milky Way's, the Jeans instability offers an explanation why in most spiral galaxies the velocity dispersion of atomic hydrogen gets reduced to the same value somewhere around $10\,\mathrm{km\,s^{-1}}$, which is well above the value expected from thermal considerations.

> Is a halo of non-baryonic, dark matter necessary to explain the Milky Way's flat circular velocity curve?

Our model explains the Milky Way's flat circular velocity curve out to 25 kpc without relying on non-baryonic, dark matter (Section 8.3). Our model has an extension of 21 kpc and is made up only of baryonic matter. The densities of the three baryonic components bulge, stellar disc and ISM match the

densities derived from observations up to a prefactor. The three prefactors take values between three and five making our model a typical example for the Bosma effect (Section 9.2). Following the interpretation of the Bosma effect from Hessman & Ziebart (2011), a baryonic, yet unobserved mass component that resides in the disc and traces the known baryonic components can explain the Milky Way's flat circular velocity curve. Then a halo of non-baryonic dark matter is no longer necessary. An argument in favour of an ISM density as high as in our model is provided by the measurements of the two voyager probes, the first artificial objects to reach the ISM. Both probes measure a three times higher density than was expected a priori (Section 9.3). But perhaps an even stronger evidence for the existence of a baryonic, yet unobserved matter component, which shares the same dynamical properties as the HI gas, is given by the answers to the other two questions: Both answers would fail if we included a stabilizing, non-baryonic dark matter component and reduced the ISM mass, so that it matches current assumptions (Section 10.4). In particular it is surprising that the Jeans instability vanishes completely from the outer parts of our model if we include a dark matter component. In the outer parts of the galaxy the gaseous mass that we have modelled dynamically dominates and other mass components like stars are of minor importance. Thus there our model should predict the dynamical properties correctly. Without non-baryonic, dark matter that works, but with it it does not work.

What should be done next? In a future project we plan to discuss the above questions using models that are superior to the present model in several aspects: First we should leave the Milky Way and construct dynamical models for spiral galaxies, which we can observe from outside. There the HI content and the spiral structure can be observed with much less uncertainty than it is the case for the Milky Way[20]. It is then important that these models contain also a dynamical stellar disc. For this purpose we have to model dynamics also in the central regions of spiral galaxies where the circular velocity curve is rising. Here in this thesis we have constructed a self-consistent model for the Milky Way in the region where the circular velocity curve is flat. Using similar techniques we are confident that we can construct self-consistent galaxy models also in regions where the circular velocity curve is rising. When we construct such models and analyse their structure and stability, we should have an open mind for all three answers to the missing mass problem that we have summarized in the introduction to this thesis. An excellent sample for such a study are the spiral galaxies contained in The Nearby HI Galaxy Survey (THINGS). For these galaxies high quality HI maps and circular velocity curves exist. Further the stellar content of these galaxies can be determined using data from the SIRTF Nearby galaxy survey (SINGS). These data already enabled several authors to construct mass models for these galaxies that explain the respective circular velocity curves by either using non-baryonic, dark matter (de Blok et al., 2008), MOND (Gentile et al., 2011) or the Bosma effect (Hessman & Ziebart, 2011). Equipping these models with self-consistent dynamics will allow us to undertake a good stability analysis and compare the different outcomes in all three settings. We are particularly interested in answers to the following questions regarding spiral structure and the Jeans instability:

Is spiral structure in such galaxy models self-excited? And does it lead to the observed spiral structure? There are some spiral galaxies where an external effect like a closer encounter with another galaxy or a rotating bar in the centre of the galaxy can account for the observed spiral pattern. But there are many spiral galaxies were no such explanation exists and a self-excitation mechanism like the one we have described in Section 10.1 is necessary to explain the observed spiral structure (Sellwood & Masters, 2021, §3). We have seen in Section 10.4 that a certain amount of mass in rotational motion is necessary for spiral structure to be self-excited. Will the dynamical mass in galaxies embedded in a non-baryonic, dark matter halo suffices?

What about the Jeans instability? Does it serve as an explanation for the observed velocity dispersion of the gas like we suspected in Section 10.3 and like it is claimed by Meurer et al. (2013)? We plan to dig deeper into this question than we have done in Section 10.3. For the Jeans instability it is important that axisymmetric waves can propagate through the disc and aggravate themselves. But spiral patterns break the symmetry of an initially axisymmetric disc. How does this affect the Jeans instability? To examine this question in more detail we can use what we have learned in this thesis: The growth of a spiral structure relies on the growth of the forces in the tangential direction (Section 10.1). The Jeans instability relies on the evolution of forces in radial direction (see Figure 17). By suppressing the evolution

[20] While writing Part II of this thesis the author – as a mathematician – had to learn astrophysics by studying on his own. Since in the textbook Galactic Dynamics from Binney & Tremaine, which the author considered a lot in the early phase of this thesis, much information about the Milky Way can be found, we constructed in Part II a model for the Milky Way, too. But perhaps it was not the wisest decision to consider the Milky Way, since there information about the HI content or the spiral structure is affected by many uncertainties due to our position inside the Milky Way's disc. See for example the review of Lockman (2002) about HI in the Milky Way or the comparison of different models with different parameters for the Milky Way's spiral arms in Poggio et al. (2021).

of the radial forces we can suppress the Jeans instability and wait for a spiral pattern to emerge from an initially self-consistent, axisymmetric model that would otherwise have been destroyed by the Jeans instability. Will the resulting disc with its spiral pattern and the broken axisymmetry still be affected by the Jeans instability? How efficiently will the spiral structure stabilize the disc?

Answering the above questions in all three settings (dark matter, MOND, Bosma effect) can enable us to decide which of the three answers to the missing mass problem from the introduction is the most plausible one.

We have one last question that deserve our attention: What is the very nature of the instability that causes the spiral arms to form? In Figure 13 we have seen that this instability shows up as an exponential growth of the forces in tangential direction. It must be possible to track down the nature of this instability with rigorous mathematical methods. Since this instability is not only responsibly for the formation of spiral structures but also for the formation of bar-shaped bulges (Section 10.5), a better understanding of this instability would enhance our understanding of both: Spirals in the disc and bulges in the centre of spiral galaxies.

A Appendix

A.1 Tangential velocity in our model for the Mestel disc

In Remark 8.1.4 we had left open the proof that the minimal and the maximal appearing tangential velocity in our self-consistent model f_0 for the Mestel disc are given by

$$v_{t,min/max} = v_0\sqrt{-W_{0/-1}\left[-\exp\left(-\frac{8\sigma^2}{v_0^2}-1\right)\right]}. \tag{A.1}$$

Let us prove this.

Proposition A.1.1. *Let $a \in \mathbb{R}$, then*

$$x^2 + a = \log x, \quad x > 0,$$

has

two solutions iff $a < -\log\sqrt{2} - 1/2$,

one solution iff $a = -\log\sqrt{2} - 1/2$,

no solution iff $a > -\log\sqrt{2} - 1/2$.

The solutions are

$$x_i = \sqrt{-\frac{1}{2}W_i(-2e^{2a})}$$

with $i = 0, -1$ and W_i denoting the i-th branch of the Lambert W function.

Remark A.1.2. The two Lambert W functions $W_{-1} : [-1/e, 0) \to (-\infty, -1]$ and $W_0 : [-1/e, \infty) \to [-1, \infty)$ are the two branches of the inverse function of

$$(-\infty, \infty) \ni z \mapsto ze^z \in [-1/e, \infty).$$

In particular for all admissible $\zeta \geq -1/e$ and $i = 0, -1$

$$\zeta = W_i(\zeta)\exp(W_i(\zeta)).$$

Proof of the Proposition. Use the transformation

$$x = \exp\left(-\frac{y}{2} + a\right), \quad y \in \mathbb{R}.$$

Then

$$\begin{aligned} x^2 + a = \log x &\iff \exp(-y + 2a) = -\frac{y}{2} \\ &\iff -2e^{2a} = ye^y. \end{aligned} \tag{A.2}$$

Since

$$(ye^y)' = (y+1)e^y = 0 \iff y = -1$$

we see that ye^y takes its global minimum at $y = -1$ and hence

$$ye^y \geq -\frac{1}{e}$$

for all $y \in \mathbb{R}$. Thus (A.2) can hold iff

$$2e^{2a} \leq \frac{1}{e} \iff a \leq -\log\sqrt{2} - \frac{1}{2}.$$

In this case we have the two solutions

$$y_i = W_i(-2e^{2a})$$

with $i = 0$ or $i = -1$. Thus

$$x_i = \exp\left(-\frac{y_i}{2} + a\right) = \exp\left(-\frac{1}{2}W_i(-2e^{2a}) + a\right)$$

are the solutions of $x^2 + a = \log x$. We want to simplify this formula further. For this purpose let $b \in \mathbb{R}$. With $\zeta = -e^b$ we get as in Remark A.1.2

$$-e^b = W_i(-e^b)\exp(W_i(-e^b)).$$

Thus

$$\frac{-1}{W_i(-e^b)} = \exp(W_i(-e^b) - b)$$

Taking the logarithm on both sides of the equation gives

$$-\log(-W_i(-e^b)) = W_i(-e^b) - b, \quad b \in \mathbb{R}.$$

Applying this equality with $b = 2a + \log 2$ gives

$$\begin{aligned}
\exp\left(-\frac{1}{2}W_i(-2e^{2a}) + a\right) &= \exp\left[-\frac{1}{2}\left[W_i(-e^{2a+\log 2}) - (2a + \log 2)\right]\right]\exp\left[-\frac{1}{2}\log 2\right] \\
&= \frac{1}{\sqrt{2}}\exp\left[\frac{1}{2}\log\left(-W_i(-e^{2a+\log 2})\right)\right] \\
&= \sqrt{-\frac{1}{2}W_i(-2e^{2a})}.
\end{aligned}$$

□

Lemma A.1.3. *For $v_0, \sigma > 0$ and f_0 as in Lemma 8.1.3 the minimal and the maximal appearing tangential velocity at every position $x \in \mathbb{R}^2\backslash\{0\}$ are given by*

$$v_{t,min/max} = v_0\sqrt{-W_{0/-1}\left[-\exp\left(-\frac{8\sigma^2}{v_0^2} - 1\right)\right]}$$

Proof. Denote by v_r, v_t the radial and the tangential component of the velocity. For every $x \in \mathbb{R}^2\backslash\{0\}$

$$\begin{aligned}
(v_r, v_t) \in \operatorname{supp} f_0(x, \cdot) &\iff \frac{v_r^2 + v_t^2}{2} - v_0^2 \log\frac{v_t}{v_0} - \frac{v_0^2}{2} \le (2\sigma)^2 \\
&\iff \frac{1}{2}\left(\frac{v_t}{v_0}\right)^2 - \log\frac{v_t}{v_0} - \frac{1}{2} \le \left(\frac{2\sigma}{v_0}\right)^2 - \frac{1}{2}\left(\frac{v_r}{v_0}\right)^2.
\end{aligned}$$

Since the left side of the last inequality is strictly convex and diverges to infinity for $v_t \to 0$ and $v_t \to \infty$, the minimal and maximal tangential velocity are the two solutions of

$$\frac{1}{2}\left(\frac{v_t}{v_0}\right)^2 - \log\frac{v_t}{v_0} - \frac{1}{2} = \left(\frac{2\sigma}{v_0}\right)^2$$

With

$$x^2 = \frac{1}{2}\left(\frac{v_t}{v_0}\right)^2$$

this holds iff

$$\begin{aligned}
&x^2 - \log\sqrt{2} - \log x - \frac{1}{2} = \left(\frac{2\sigma}{v_0}\right)^2 \\
\iff\ &x^2 - \left(\log\sqrt{2} + \frac{1}{2} + \left(\frac{2\sigma}{v_0}\right)^2\right) = \log x.
\end{aligned}$$

This has the two solutions

$$\begin{aligned} x_i &= \sqrt{-\frac{1}{2}W_i\left[-2\exp\left(-2\log\sqrt{2}-1-\frac{8\sigma^2}{v_0^2}\right)\right]} \\ &= \sqrt{-\frac{1}{2}W_i\left[-\exp\left(-\frac{8\sigma^2}{v_0^2}-1\right)\right]}. \end{aligned}$$

Thus

$$v_{t,min} = \sqrt{2}v_0x_0 = v_0\sqrt{-W_0\left[-\exp\left(-\frac{8\sigma^2}{v_0^2}-1\right)\right]}$$

and

$$v_{t,max} = \sqrt{2}v_0x_{-1} = v_0\sqrt{-W_{-1}\left[-\exp\left(-\frac{8\sigma^2}{v_0^2}-1\right)\right]}$$

□

A.2 Average z-distance in a disk with constant scale height

We claimed in Section 8.2 that for a disc with the spatial density

$$\Sigma(x_1,x_2)\exp\left(-|z|/z_g\right)$$

the expected value of the distance in z-direction between two particles that we draw at random from this density is $1.5z_g$. We give a short derivation of this. W.l.g. we set $z_g = 1$ in the following calculations. Then the z-coordinates Z_1 and Z_2 of the two particles are distributed according to the law

$$Z_1, Z_2 \sim \frac{1}{2}e^{-|z|}.$$

The probability that the distance between the two particles is lower than $\delta > 0$ is

$$P(|Z_1 - Z_2| < \delta) = \frac{1}{4}\int_{-\infty}^{\infty}\int_{z-\delta}^{z+\delta} e^{-|z|}e^{-|z'|}\,\mathrm{d}z'\,\mathrm{d}z.$$

The probability distribution function $p(\delta)$ that corresponds to the random variable $|Z_1 - Z_2|$ is given by

$$\begin{aligned} p(\delta) &= \frac{\mathrm{d}}{\mathrm{d}\delta}P(|Z_1 - Z_2| < \delta) \\ &= \frac{1}{4}\int_{-\infty}^{\infty} e^{-|z|}\left(e^{-|z+\delta|} + e^{-|z-\delta|}\right)\mathrm{d}z \\ &= \frac{1}{2}\int_{-\infty}^{\infty} e^{-|z|}e^{-|z+\delta|}\,\mathrm{d}z \\ &= \frac{1}{2}\int_{-\infty}^{-\delta} e^{z}e^{z+\delta}\,\mathrm{d}z + \frac{1}{2}\int_{-\delta}^{0} e^{z}e^{-z-\delta}\,\mathrm{d}z + \frac{1}{2}\int_{0}^{\infty} e^{-z}e^{-z-\delta}\,\mathrm{d}z \\ &= \frac{e^{\delta}}{2}\int_{-\infty}^{-\delta} e^{2z}\,\mathrm{d}z + \frac{e^{-\delta}}{2}\int_{-\delta}^{0}\mathrm{d}z + \frac{e^{-\delta}}{2}\int_{0}^{\infty} e^{-2z}\,\mathrm{d}z \\ &= \frac{e^{\delta}e^{-2\delta}}{4} + \frac{\delta e^{-\delta}}{2} + \frac{e^{-\delta}}{4} \\ &= \frac{1}{2}(1+\delta)e^{-\delta} \end{aligned}$$

if $\delta > 0$, and $p(\delta) = 0$ if $\delta \le 0$. Since

$$\int_0^{\infty}\delta e^{-\delta}\,\mathrm{d}\delta = \int_0^{\infty}\delta(-e^{-\delta})'\,\mathrm{d}\delta = \int_0^{\infty} e^{-\delta}\,\mathrm{d}\delta = 1$$

and

$$\int_0^{\infty}\delta^2 e^{-\delta}\,\mathrm{d}\delta = 2\int_0^{\infty}\delta e^{-\delta}\,\mathrm{d}\delta = 2,$$

we have for the expected value

$$\begin{aligned} EV(|Z_1 - Z_2|) &= \int_0^\infty \frac{\delta}{2}(1+\delta)e^{-\delta}\,\mathrm{d}\delta \\ &= \frac{1}{2}\int_0^\infty \delta e^{-\delta}\,\mathrm{d}\delta + \frac{1}{2}\int_0^\infty \delta^2 e^{-\delta}\,\mathrm{d}\delta = \frac{3}{2}. \end{aligned}$$

These calculations show that for a disc with scale height z_g the distance in z-direction between two randomly determined particles is at average $1.5z_g$.

A.3 Integrating the equations of motions in Section 10

In Section 10 we discuss several simulations. We want to describe the numerical methods used in these simulations.

For every simulation we use a distribution function $f(x, v)$ that was generated with the algorithm from Section 8.3. From this distribution function we draw at random particles with initial coordinates $(x_i(0), v_i(0))$ and integrate the equations of motion

$$\dot{x_i} = v_i, \quad \dot{v_i} = G\sum_{j\neq i} \frac{x_j - x_i}{\left(|x_j - x_i|^2 + \delta_z^2\right)^{3/2}}.$$

We have modified Newton's law of gravitation to take into account the disc thickness as we have done already in Section 8.2. As previously $\delta_z = 1.5z_g$ with $z_g = 300\,\mathrm{pc}$.

We integrate the equations of motion numerically using a Velocity Verlet algorithm and we have implemented two ways to calculate the force efficiently. The first method uses a polar grid where the disc is divided in 100 uniform angles and along each radial line 400 meshpoints are distributed out to 100 kpc. Particles that move beyond 100 kpc are dropped from the simulation. To distribute the meshpoints radially, we approximate the density of our initial data by a continuous, piecewise function which is linearly increasing to 4.3 kpc and exponentially decreasing beyond. The meshpoints are distributed such that to each meshpoint the same mass of the approximate density would be assigned. In the simulation we use bi-linear interpolation to assign the mass of each particle to the four adjacent meshpoints, calculate the force between the meshpoints and get the force on the particles by again using bi-linear interpolation. For simulations with this polar mesh, we created 1 Million particles from $f(x, v)$. The second method enforces axial symmetry. This is achieved by calculating in each time step a histogram of the radial positions of the particles. This histogram is transformed into an axially symmetric density and from this density the forces on the particles are calculated. For simulations with enforced axial symmetry we used 100.000 particles.

References

Andréasson H., Rein G., 2015, MNRAS, 446, 3932

Bekenstein J., Milgrom M., 1984, ApJ, 286, 7

Binney J., 2020, in Valluri M., Sellwood J. A., eds, Vol. 353, Galactic Dynamics in the Era of Large Surveys. pp 101–108, doi:10.1017/S1743921319008214

Binney J., Merrifield M., 1998, Galactic Astronomy. Princeton University Press, Princeton, NJ

Binney J., Tremaine S., 2008, Galactic Dynamics, 2nd edn. Princeton University Press, Princeton, NJ

Bosma A., 1981, AJ, 86, 1825

Deutscher Rundfunk 2021, Hubble-Konstante: Was stimmt nicht mit der Expansion des Universums? Last access: 2022-07-15, `https://www.deutschlandfunk.de/hubble-konstante-was-stimmt-nicht-mit-der-expansion-des-100.html`, `https://articles.adsabs.harvard.edu/pdf/1981seng.proc..111T`

DiPerna R. J., Lions P. L., 1989a, Communications on Pure and Applied Mathematics, 42, 729

DiPerna R. J., Lions P. L., 1989b, Invent. math., 98, 511

Dietz S., 2001, PhD thesis, University of Munich, Germany, `https://edoc.ub.uni-muenchen.de/1/1/Dietz_Svetlana.pdf`

Eilers A.-C., Hogg D. W., Rix H.-W., Ness M. K., 2019, ApJ, 871, 120

Evans L. C., 2010, Partial differential equations, 2nd edn. Graduate studies in mathematics, American Mathematical Society, Providence, RI

Famaey B., McGaugh S. S., 2012, Living Reviews in Relativity, 15, 10

Ferrière K. M., 2001, Reviews of Modern Physics, 73, 1031

Firt R., Rein G., 2006, Analysis, 26, 507

Frenkler J., 2016, Master thesis, University of Bayreuth, Germany

Galdi G. P., 2011, An Introduction to the Mathematical Theory of the Navier-Stokes Equations, 2nd edn. Springer Monographs in Mathematics, Springer, New York, NY

Gentile G., Famaey B., de Blok W. J. G., 2011, A&A, 527, A76

Gidas B., Ni W.-M., Nirenberg L., 1979, Communications in Mathematical Physics, 68, 209

Gilbarg D., Trudinger N. S., 1977, Elliptic Partial Differential Equations of Second Order. Grundlehren der mathematischen Wissenschaften, Springer, Berlin, DE

Gurnett D. A., Kurth W. S., Allendorf S. C., Poynter R. L., 1993, Science, 262, 199

Hessman F. V., Ziebart M., 2011, A&A, 532, A121

Horst E., Hunze R., Neunzert H., 1984, Mathematical Methods in the Applied Sciences, 6, 262

Ibata R., Sollima A., Nipoti C., Bellazzini M., Chapman S. C., Dalessandro E., 2011, ApJ, 743, 43

Keller C., 2016, Master thesis, University of Bayreuth, Germany

Knopf P., 2017, PhD thesis, University of Bayreuth, Germany, `https://epub.uni-bayreuth.de/3387/`

Kurth W. S., Gurnett D. A., 2020, ApJL, 900, L1

Leroy A. K., Walter F., Brinks E., Bigiel F., de Blok W. J. G., Madore B., Thornley M. D., 2008, AJ, 136, 2782

Lieb E., Loss M., 2010, Analysis, 2nd edn. Graduate studies in mathematics, American Mathematical Society, Providence, RI

Lions P. L., Perthame B., 1991, Inventiones Mathematicae, 105, 415

Lockman F. J., 2002, in Taylor A. R., Landecker T. L., Willis A. G., eds, Astronomical Society of the Pacific Conference Series Vol. 276, Seeing Through the Dust: The Detection of HI and the Exploration of the ISM in Galaxies. p. 107 (arXiv:astro-ph/0203210)

Loeper G., 2006, Journal de Mathématiques Pures et Appliquées, 86, 68

Marasco A., Fraternali F., van der Hulst J. M., Oosterloo T., 2017, A&A, 607, A106

Mestel L., 1963, MNRAS, 126, 553

Meurer G. R., Zheng Z., de Blok W. J. G., 2013, MNRAS, 429, 2537

Milgrom M., 1983, ApJ, 270, 365

Milgrom M., 2010, MNRAS, 403, 886

Peano 1890, Mathesis, pp 153–154

Pfaffelmoser K., 1992, Journal of Differential Equations, 95, 281

Poggio E., et al., 2021, A&A, 651, A104

Rein G., 2007, Handbook of Differential Equations: Evolutionary Equations, pp 383–476

Rein G., 2015, Kinetic and Related Models, 8, 381

Rubin V. C., Ford W. K. J., Thonnard N., 1980, ApJ, 238, 471

Rudin W., 1976, Principles of Mathematical Analysis, 3rd edn. International series in pure and applied mathematics, McGraw-Hill, New York, NY

Rudin W., 1999, Reelle und Komplexe Analysis, translation of 3rd edn. Oldenburg, München, DE

Sanders R. H., 2012, MNRAS, 422, L21

Sellwood J. A., Carlberg R. G., 2019, MNRAS, 489, 116

Sellwood J. A., Masters K. L., 2021, arXiv e-prints, p. arXiv:2110.05615

Shen J., Zheng X.-W., 2020, Research in Astronomy and Astrophysics, 20, 159

Sparke L. S., Gallagher J. S., 2000, Galaxies in the universe. Cambridge University Press, Cambridge, UK

Steiman-Cameron T. Y., Wolfire M., Hollenbach D., 2010, ApJ, 722, 1460

Stein E. M., 1970, Singular Integrals and Differentiability Properties of Functions. Princton University Press, Princton, NJ

Tamburro D., Rix H. W., Leroy A. K., Mac Low M. M., Walter F., Kennicutt R. C., Brinks E., de Blok W. J. G., 2009, AJ, 137, 4424

Toomre A., 1981, in Fall S. M., Lynden-Bell D., eds, Structure and Evolution of Normal Galaxies. pp 111–136, https://ui.adsabs.harvard.edu/abs/1981seng.proc..111T

Zang T. A., 1976, PhD thesis, Massachusetts Institute of Technology, United States, https://dspace.mit.edu/handle/1721.1/27444

de Blok W. J. G., Walter F., Brinks E., Trachternach C., Oh S. H., Kennicutt R. C. J., 2008, AJ, 136, 2648

del Peloso E. F., da Silva L., Porto de Mello G. F., Arany-Prado L. I., 2005, A&A, 440, 1153

Eidesstattliche Versicherung

Hiermit versichere ich an Eides statt, dass ich die vorliegende Arbeit selbstständig verfasst und keine anderen als die von mir angegebenen Quellen und Hilfsmittel verwendet habe.

Weiterhin erkläre ich, dass ich die Hilfe von gewerblichen Promotionsberatern bzw. -vermittlern oder ähnlichen Dienstleistern weder bisher in Anspruch genommen habe, noch künftig in Anspruch nehmen werde.

Zusätzlich erkläre ich hiermit, dass ich keinerlei frühere Promotionsversuche unternommen habe.

Bayreuth, den

Joachim Frenkler